



# MONASH University

**microRNA-21 in Diabetic Nephropathy and a Cross-Sectional Analysis of  
the Role of TGF $\beta$  in Proximal Tubule Epithelial Cells and Mesangial Cells**

*Aaron David McClelland*

*Bachelor of Biotechnology & Cell Biology  
Science (Honours)*

A thesis submitted for the degree of Doctor of Philosophy at  
Monash University in 2016  
Department of Medicine, Nursing & Health Care (Central Clinical School)  
Baker IDI Heart & Diabetes Institute



## **Copyright notice**

© The author 2016. Except as provided in the Copyright Act 1968, this thesis may not be reproduced in any form without the written permission of the author.

## Abstract

Diabetic nephropathy (DN) is the leading cause of renal failure in much of the world. It is a complex disease resulting in pathological changes in various cell types and ultimately culminating in end-stage renal disease. Specifically, mesangial cells (MC) undergo hyperplasia and hypertrophy leading to destruction of the glomerular ultrastructure while also contributing to podocytes loss. Proximal tubule epithelial cells (PTC) undergo similar processes leading to tubulointerstitial fibrosis and also interstitial inflammation. Although these changes are initially propagated by chronic hyperglycaemia, the changes in cellular physiology are elicited via activation and modulation of a wide range of pathways and their products. A central and potent mediator cellular pathophysiology in diabetic nephropathy is TGF $\beta$  which is itself upregulated by hyperglycaemia.

TGF $\beta$  influences many cellular processes and signalling networks. It has becoming increasingly clear that TGF $\beta$  mediates its effects in the diabetic kidney through dysregulation of microRNA particularly in MC and PTC, although the extent of these relationships has not been investigated. Despite this, there is still a lack of system biology approaches available for the study of microRNA. Also gaining attention in recent years is the role of mitochondrial dysfunction in the propagation of DN. Although links have been made between TGF $\beta$  and mitochondrial function or microRNA expression and mitochondrial function, little has been reported on the influence of TGF $\beta$ -mediated microRNA dysregulation on mitochondria.

To this end, this thesis has demonstrates and explores the wide reaching effects of TGF $\beta$  upon both PTC and MC. The genome wide effect of TGF $\beta$ -mediated miRNA dysregulation of the cell wide signalling landscape is also explored. miR-21 is highly dysregulated in PTC and its role in TGF $\beta$ -mediated fibrotic signalling is clarified. This effect is clearly defined in regard to the relative contribution of SMAD7 and PTEN. The significance of miR-21 in human DN is also demonstrated. Finally, the role of miR-21 in mitochondrial dysfunction in PTC is proposed to occur at least in part through ACAT1 and AK2. This work adds valuable knowledge to the growing recognition of the importance of microRNA in DN. Furthermore, the development of *in silico* pipelines may aid those who endeavour to undertake similar projects with the data garnered from such experiments providing an important reference for future investigations. The findings from this thesis are likely to aid in the development of future therapies focusing on retarding the development and progression of DN, not least of all in the rectification of mitochondrial dysfunction and preventing the relentless cycle of fibrotic tissue damage that ultimately results in renal failure.

## **Declaration**

This thesis contains no material which has been accepted for the award of any other degree or diploma at any university or equivalent institution and that, to the best of my knowledge and belief, this thesis contains no material previously published or written by another person, except where due reference is made in the text of the thesis.

## **Publications and presentations**

### **Published Manuscripts**

McClelland AD, Herman-Edelstein M, Komers R, Jha JC, Winbanks CE, Hagiwara S, et al. miR-21 promotes renal fibrosis in diabetic nephropathy by targeting PTEN and SMAD7. *Clin Sci*. 2015;129(12):1237-49.

McClelland AD, Kantharidis P. MicroRNAs as Biomarkers of Diabetic Nephropathy. In: Patel BV, editor. *Biomarkers in Kidney Disease*. Dordrecht: Springer Netherlands; 2015. p. 1-29.

Kantharidis P, Hagiwara S, Brennan E, McClelland AD. Study of microRNA in diabetic nephropathy: isolation, quantification and biological function. *Nephrology (Carlton, Vic)*. 2015;20(3):132-9.

Wang B, Jha JC, Hagiwara S, McClelland AD, Jandeleit-Dahm K, Thomas MC, et al. Transforming growth factor-beta1-mediated renal fibrosis is dependent on the regulation of transforming growth factor receptor 1 expression by let-7b. *Kidney international*. 2014;85(2):352-61

McClelland A, Hagiwara S, Kantharidis P. Where are we in diabetic nephropathy: microRNAs and biomarkers? *Current opinion in nephrology and hypertension*. 2014;23(1):80-6.

McClelland AD, Kantharidis P. microRNA in the development of diabetic complications. *Clinical Science*. 2014;126(2):95-110.

Komers R, Xu B, Fu Y, McClelland A, Kantharidis P, Mittal A, et al. Transcriptome-based analysis of kidney gene expression changes associated with diabetes in OVE26 mice, in the presence and absence of losartan treatment. *PLoS One*. 2014;9(5):e96987.

Hagiwara S, McClelland A, Kantharidis P. MicroRNA in diabetic nephropathy: renin angiotensin, AGE/RAGE, and oxidative stress pathway. *Journal of diabetes research*. 2013;2013:173783.

### **Poster abstracts**

McClelland AD, Kantharidis P, Cooper ME. miR-21 contributes to PTC dysfunction in DN via augmentation of TGF $\beta$ -induced changes in mitochondrial metabolism. *American Society of Nephrology Kidney Week in Philadelphia, America, 2014.*

Aaron D. McClelland, Michal Herman, Shinji Hagiwara, Jay C. Jha, Radko Komers, Mark E. Cooper, Phillip Kantharidis. miR-21 regulates fibrosis in the development of diabetic nephropathy. *Asia Pacific Congress of Nephrology in Tokyo, Japan, 2014.*

Aaron D. McClelland, Michal Herman, Shinji Hagiwara, Jay C. Jha, Radko Komers, Mark E. Cooper, Phillip Kantharidis. Cooperative repression of SMAD7 and PTEN by miR-21 mediate overlapping and unique changes in renal fibrogenesis. *International Diabetes Federation (IDF), World Diabetes Congress, Melbourne, Australia, 2013.*

Aaron D. McClelland, Michal Herman, Shinji Hagiwara, Jay C. Jha, Radko Komers, Mark E. Cooper, Phillip Kantharidis. Cooperative Repression of SMAD7 and PTEN by miR-21 Mediate Pathological Gene Expression Changes in Renal Fibrogenesis. *Alfred Medical Research and Education Precinct (AMREP) Alfred Week, Melbourne, Australia, 2013. (Award winning poster)*

### **Oral abstracts**

Brooke E. Harcourt, Aaron McClelland, Sally A. Penfold, Angelika Bierhaus, P Kantharidis, Josephine M. Forbes. Nuclear RAGE self-promotes its own expression via Sp-1, AP-1 and NF-kB in diabetic nephropathy. *Japanese Society of Nephrology, Tokyo, Japan, 2013.*

Harcourt B, McClelland AD, Yamamoto H, Bierhaus A, Kantharidis P, Forbes JM. The DNA Binding Capacity of RAGE and its Consequences in the Development of Diabetic Nephropathy. *Australian Diabetes Society and Australian Diabetes Educators Association ASM in Sydney, Australia, 2013.*

Mark Ziemann, Aaron McClelland, Alba Fricke, Karlheinz Peter, Assam El-Osta, Phillip Kantharidis. Illumina TruSeq small RNA sequencing: method validation and strategies for data analysis. *Illumina community presentation, Melbourne, Australia, 2012.*

Brooke E. Harcourt, Aaron McClelland, Sally A. Penfold, Angelika Bierhaus, Phillip Kantharidis, Josephine M. Forbes. Nuclear RAGE self-promotes its own expression via Sp-1, AP-1 and NF-kB in diabetic nephropathy. *International Maillard Society in Nancy, France, 2012.*

## Thesis including published works General Declaration

I hereby declare that this thesis contains no material which has been accepted for the award of any other degree or diploma at any university or equivalent institution and that, to the best of my knowledge and belief, this thesis contains no material previously published or written by another person, except where due reference is made in the text of the thesis.

This thesis includes 1 original papers and 2 review papers published in peer reviewed journals. The core theme of the thesis is the role of miRNA and more specifically miR-21 in TGF $\beta$  mediated gene dysregulation in diabetic nephropathy, specifically in mesangial cells and proximal tubule epithelial cells. The ideas, development and writing up of all the papers in the thesis were the principal responsibility of myself, the candidate, working within the Doctor of Philosophy under the supervision of Dr. Phillip Kantharidis and Professor Mark Cooper.

In the case of chapter 1 my contribution to the work involved the following: In regard to the first manuscript in this chapter, I researched, wrote and edited the manuscript. Co-authors revised and edited the manuscript. In regard to the second manuscript in this chapter, all authors equally shared researching, writing and editing of the manuscript.

In the case of chapter 3 my contribution to the work involved the following: design of the project, execution of all RNA and protein based *in vitro* studies, RNA analysis of animal tissues in addition to researching, writing and editing the manuscript. Co-authors Dr. Michal Herman and Dr. Radko Komers provided human histological analysis and clinical data and rat renal samples respectively. Co-authors Dr. Catherine Winbanks and Dr. Paul Gregorevic provided technical assistance with SMAD western blots. All co-authors contributed to editing the manuscript.

Thesis chapter	Publication title	Publication status*	Nature and extent (%) of students contribution
1	microRNA in the development of diabetic complications	Published	95
1	Where are we in diabetic nephropathy: microRNAs and biomarkers	Published	55
3	miR-21 promotes renal fibrosis in diabetic nephropathy by targeting PTEN and SMAD7	Published	90

\* e.g. 'published' / 'in press' / 'accepted' / 'returned for revision'

I have renumbered sections of submitted or published papers in order to generate a consistent presentation within the thesis, however figures and tables from publications are not included the list of figures and tables.

**Student signature:**



**Date:** 04/04/2016

The undersigned hereby certify that the above declaration correctly reflects the nature and extent of the student and co-authors' contributions to this work.

**Main Supervisor signature:**



**Date:** 04/04/2016

## **Acknowledgements**

Thank you to both of my supervisors, Dr. Phillip Kantharidis and Prof Mark Cooper who with much patience, knowledge and support provided an excellent environment in which to undertake postgraduate studies.

Thanks also go to Dr. Mark Ziemann for the RNA sequencing and data assembly which provided a platform for much of this thesis.

Last but not least, thank you to all my friends and family (both near and far) for your love and encouragement. You keep me grounded and reminded me of the value of my work.

## Table of Contents

Copyright notice.....	i
Abstract.....	ii
Declaration.....	iii
Publications and presentations.....	iv
Thesis including published works General Declaration .....	vii
Acknowledgements.....	ix
Table of Contents.....	x
List of Tables .....	xiv
List of Figures.....	xvi
List of Abbreviations .....	xix
1. Literature Review.....	1
1.1. Introduction.....	3
1.2. Introduction to diabetic nephropathy .....	4
1.3. Cellular contributions in the diabetic kidney .....	7
1.3.1. The role of mesangial cells in diabetic nephropathy .....	7
1.3.2. The role of proximal tubule epithelial cells in diabetic nephropathy .....	9
1.4. Effectors of diabetic nephropathy .....	12
1.4.1. TGF $\beta$ in glomerulosclerosis.....	13
1.4.2. TGF $\beta$ in tubulointerstitial fibrosis .....	15
1.5. microRNA in diabetic nephropathy .....	19
1.5.1. microRNA in the development of diabetic complications.....	19
1.5.2. Where are we in diabetic nephropathy: microRNAs and biomarkers .....	36
1.6. Mitochondria in diabetic nephropathy .....	44
1.6.1. Mitochondrial role in cellular metabolism.....	44
1.6.2. Mitochondrial dysfunction in proximal tubule epithelial cells .....	47
1.6.3. Interactions among mitochondria, TGF $\beta$ and miRNA .....	49
1.7. Conclusion.....	52
1.8. Hypothesis and specific aims .....	52
2. Methods and Materials.....	54
2.1. Cell culture .....	54
2.1.1. Cell lines (maintenance and passaging).....	54
2.1.2. Cryopreservation of cells .....	55
2.1.3. Cell quantitation.....	55
2.2. Cell seeding density .....	55
2.2.1. 6-well plates.....	55

2.2.2.	12-well plates .....	56
2.2.3.	Seahorse XF24 plates.....	56
2.3.	Treatments.....	56
2.3.1.	TGF $\beta$ treatment.....	56
2.3.2.	LY294002 treatment .....	56
2.4.	Transfection.....	57
2.4.1.	Transfection concentration of oligonucleotides and vectors .....	57
2.4.2.	6-well transfection complexes .....	58
2.4.3.	12-well transfection complexes .....	58
2.4.4.	XF24 plate transfection complexes.....	59
2.4.5.	Post transfection.....	59
2.5.	RNA preparation .....	60
2.5.1.	Harvesting cells and RNA extraction .....	60
2.5.2.	RNA quantitation/quality control .....	60
2.5.3.	DNase treatment.....	60
2.6.	cDNA synthesis.....	61
2.6.1.	Total cDNA.....	61
2.6.2.	miRNA specific cDNA .....	61
2.7.	qRT-PCR.....	62
2.7.1.	mRNA qRT-PCR.....	62
2.7.2.	miRNA qRT-PCR.....	65
2.8.	Amplification of reporter constructs .....	66
2.8.1.	Bacterial transformation.....	66
2.8.2.	Mini prep.....	66
2.8.3.	3'UTR luciferase vector quality control .....	67
2.8.4.	Maxi prep.....	67
2.9.	Reporter assays.....	67
2.9.1.	$\beta$ -galactosidase assay .....	67
2.9.2.	Luciferase assay .....	68
2.10.	Protein expression analysis.....	68
2.10.1.	Cell harvest for protein.....	68
2.10.2.	BCA assay .....	69
2.10.3.	SDS-PAGE.....	69
2.10.4.	Western blotting .....	69
2.10.5.	Membrane stripping/reprobing.....	71

2.11.	FACS assays .....	72
2.11.1.	Staining procedures .....	72
2.11.2.	Gating and acquisition procedures .....	73
2.11.3.	ATP assay.....	74
2.12.	Confocal microscopy .....	74
2.13.	Next-Generation sequencing .....	75
2.13.1.	Sample Isolation .....	75
2.13.2.	Library Preparation .....	75
2.13.3.	Sequencing .....	75
2.13.4.	Read data pre-processing .....	76
2.13.5.	Read assembly and processing.....	76
2.13.6.	Differential gene expression analysis.....	76
2.14.	In silico analysis .....	76
2.14.1.	Online databases utilised.....	76
2.14.2.	R Packages utilised.....	77
2.14.3.	List of custom functions, scripts and workflow files .....	78
2.15.	Statistical analysis.....	78
3.	Results I – miR-21 promotes renal fibrosis in diabetic nephropathy by targeting PTEN and SMAD7 .....	80
3.1.	Introduction .....	82
3.2.	Conclusion.....	96
4.	Results II - Genome wide effects of TGF $\beta$ on proximal tubule epithelial cells and mesangial cells .....	97
4.1.	Introduction .....	97
4.2.	TGF $\beta$ induces gross disturbances to cellular function and signalling through genome wide mRNA dysregulation.....	98
4.2.1.	Suitability of normalisation methods and treatment effectiveness .....	98
4.2.2.	Overview of common and cell-specific TGF $\beta$ -induced mRNA gene dysregulation in PTC and MC .....	103
4.3.	Potential functional consequences of TGF $\beta$ induced gene dysregulation .....	107
4.3.1.	An ontological perspective of common and cell specific effects of TGF $\beta$ .....	107
4.3.2.	A pathway orientated perspective of common and cell-specific effects of TGF $\beta$	113
4.4.	Discussion .....	126
5.	Results III – Contribution of TGF $\beta$ -mediated miRNA dysregulation to transcriptional topography .....	132
5.1.	Introduction .....	132

5.2.	TGFβ induced dysregulation of miRNA coding genes is both general and cell-specific .....	133
5.2.1.	Suitability of normalisation methods and treatment effectiveness .....	133
5.2.2.	Overview of common and cell-specific TGFβ-induced miRNA gene dysregulation in PTC and MC .....	138
5.3.	Contribution of TGFβ-mediated miRNA dysregulation to signalling pathway enrichment.....	144
5.3.1.	Naïve miRNA-augmentation reveals core TGFβ-miRNA network pathways and highlights important pathway topology .....	144
5.3.2.	Biased augmentation reveals novel roles for established and unestablished DN-associated miRNA .....	149
5.4.	Discussion .....	154
6.	Results IV – miR-21 regulates mitochondrial function by targeting of ACAT1 and AK2 . .....	159
6.1.	Introduction .....	159
6.2.	miR-21 alters mitochondrial function and morphology .....	160
6.3.	Integrative analysis of RNA-seq data and public databases identifies novel, mitochondrially relevant targets of miR-21 .....	165
6.3.1.	Identification of novel mitochondrially associated miR-21 targets.....	165
6.3.2.	AK2 and ACAT1 are downregulated <i>in vitro</i> and <i>in vivo</i> .....	167
6.4.	Repression of ACAT1 and AK2 is associated with changes in mitochondrial function.....	169
6.4.1.	ACAT1 and AK2 are targeted and repressed by miR-21 .....	169
6.4.2.	siRNA-mediated repression of ACAT1 and AK2 alter mitochondrial function similarly to miR-21 .....	172
6.5.	Fibrotic effects of miR-21/TGFβ may be partially mediated through dysregulation of novel mitochondrially associated targets of miR-21 .....	176
6.6.	Discussion .....	179
7.	General Discussion .....	186
7.1.	Introduction .....	186
7.2.	GAGE-mediated analysis of the TGFβ-induced transcriptional landscape .....	187
7.3.	Impact factor analysis of TGFβ-mediated miRNA dysregulation of signalling topology.....	189
7.4.	The link between miR-21, TGFβ and tubulointerstitial fibrosis .....	192
7.5.	The link between miR-21, TGFβ and mitochondrial dysfunction .....	193
7.6.	Conclusion.....	195
8.	Reference List .....	197

## List of Tables

Table 1-1 Summary of clinical signs of DN. ....	5
Table 2-1 List of miRNA, siRNA and expression vectors utilised.....	57
Table 2-2 miRNA-specific reverse transcription primer mixes as supplied by Applied Biosciences. ....	62
Table 2-3 Sequences of qRT-PCR primer/probe sets. ....	62
Table 2-4 TaqMan miRNA probes utilised. ....	65
Table 2-5 Primary antibodies used in western blot immunodetection during the course of this study.....	70
Table 2-6 HRP-conjugated secondary antibodies used in western blot.....	71
Table 2-7 Infra-red secondary antibodies used in western blot immunodetection. ....	71
Table 4-1 Summary data for mRNA-seq in PTC and MC.....	98
Table 4-2 Genes commonly dysregulated in PTC and MC were enriched for a number of <i>molecular function</i> ontology terms. ....	108
Table 4-3 Genes commonly dysregulated in PTC and MC were enriched for a number of <i>biological process</i> ontology terms. ....	109
Table 4-4 Genes uniquely dysregulated in MC were uniquely enriched for a number of <i>molecular function</i> ontology terms. ....	110
Table 4-5 Genes uniquely dysregulated in either PTC or MC were uniquely enriched for a number of <i>biological process</i> ontology terms. ....	111
Table 4-6 Genes inversely expressed between PTC and MC were uniquely enriched for a number of <i>molecular function</i> ontology terms.....	112
Table 4-7 Genes inversely expressed between PTC and MC were uniquely enriched for a number of biological process ontology terms.....	112
Table 4-8 Results of KEGG pathway analysis on proximal tubule epithelial cells and mesangial cells.....	116
Table 4-9 Top 5 ranking pathways for different enrichment classes in proximal tubule epithelial cells and mesangial cells.....	124
Table 5-1 Summary data for miRNA-seq in PTC and MC. ....	134
Table 5-2 logFC and adjusted <i>p</i> -values of miRNA involved in DN.....	143
Table 5-5 Top 10 hits from impact factor analysis on augmented rat KEGG signalling pathways. ....	145

Table 5-6 Top 10 hits from impact factor analysis on augmented mouse KEGG signalling pathways. ....	146
Table 5-7 Top 10 results from impact factor analysis of rat KEGG pathways augmented with DN-associated miRNA .....	151
Table 5-8 Top 10 results from impact factor analysis of mouse KEGG pathways augmented with DN-associated miRNA .....	151
Table 6-1 Significantly dysregulated genes identified following integration of PTC DGE data with MitoCarta and <i>microRNA.org</i> miR-21-target list. ....	167

## List of Figures

Figure 1-1 Histological changes in diabetic nephropathy.....	6
Figure 1-2 Structure of the Bowmans capsule.....	7
Figure 1-3 The role of mesangial cells in glomerulosclerosis. ....	8
Figure 1-4 The role of proximal tubule epithelial cells tubulointerstitial fibrosis. ....	10
Figure 1-5 The roles of TGF $\beta$ in glomerulosclerosis. ....	14
Figure 1-6 The role of TGF $\beta$ in tubulointerstitial fibrosis. ....	17
Figure 1-7 Summary of the effects of TGF $\beta$ in the diabetic kidney .....	18
Figure 1-8 Inter-relationship between glycolysis, beta-oxidation and ATP production.....	45
Figure 1-9 Role of hyperglycaemia in ROS generation and its effects in proximal tubule epithelial cells. ....	48
Figure 4-1 Negative binomial models effectively estimated normalised read counts in mRNA-seq data from proximal tubule epithelial cells and mesangial cells.....	100
Figure 4-2 TGF $\beta$ treatment induces significant gene dysregulation in both proximal tubule epithelial cells and mesangial cells. ....	102
Figure 4-3 Summary of TGF $\beta$ -induced gene dysregulation in proximal tubule epithelial cells and mesangial cells .....	103
Figure 4-4 Top 100 significantly dysregulated genes in proximal tubule epithelial cells. ....	105
Figure 4-5 Top 100 significantly dysregulated genes in mesangial cells. ....	106
Figure 4-6: Comparative summary of TGF $\beta$ -induced gene dysregulation in proximal tubule epithelial cells and mesangial cells .....	107
Figure 4-7 TGF $\beta$ preferentially downregulates pathways in proximal tubule epithelial cells. ....	114
Figure 4-8 TGF $\beta$ preferentially upregulates pathways in mesangial cells. ....	115
Figure 4-9 Focal adhesion pathway is positively enriched by TGF $\beta$ in both proximal tubule epithelial cells and mesangial cells. ....	117
Figure 4-10 ECM-receptor interaction pathway is positively enriched by TGF $\beta$ in proximal tubule epithelial cells and mesangial cells. ....	118
Figure 4-11 Genes essential to statistical enrichment in pathways between cells types exhibit cell specific responses to TGF $\beta$ . ....	119
Figure 4-12 TGF directly dysregulates oxidative phosphorylation by targeting components of the electron transport chain. ....	121

Figure 4-13 Adherens junctions pathway is bidirectionally enriched by TGF $\beta$ in a cell specific manner. ....	122
Figure 4-14 GAGE analysis does not evade false-positives. ....	123
Figure 4-15 Pathways pertaining to cell specific biology were uniquely enriched in proximal tubule epithelial cells and mesangial cells by TGF $\beta$ . ....	125
Figure 5-1 Negative binomial models effectively estimated normalised read counts in miRNA-seq data from proximal tubule epithelial cells and mesangial cells. ....	135
Figure 5-2 TGF $\beta$ treatment induces significant short RNA dysregulation in both proximal tubule epithelial cells and mesangial cells. ....	137
Figure 5-3 Summary of TGF $\beta$ -induced gene dysregulation in proximal tubule epithelial cells and mesangial cells. ....	139
Figure 5-4 Top 100 significantly dysregulated short RNA in proximal tubule epithelial cells. ....	140
Figure 5-5 Top 100 significantly dysregulated genes in mesangial cells. ....	141
Figure 5-6 Comparative summary of TGF $\beta$ -induced miRNA dysregulation in proximal tubule epithelial cells and mesangial cells ....	142
Figure 5-7 Rat TGF $\beta$ signalling pathway (KEGG ID: 04350) augmented with miRNA-gene interactions. ....	147
Figure 5-8 Mouse TGF $\beta$ signalling pathway (KEGG ID: 04350) augmented with predicted miRNA-gene interactions. ....	148
Figure 5-9 Rat TGF $\beta$ signalling pathway (KEGG ID: 04350) augmented with predicted miRNA- gene interactions for DN-associated miRNA. ....	150
Figure 5-10 TGF $\beta$ induces specific pathway topologies in PTC and MC. ....	153
Figure 6-1 TGF $\beta$ and miR-21 impact important mitochondrial parameters. ....	161
Figure 6-2 Mitochondrial respiration parameters under TGF $\beta$ or miR-21 are mostly unaffected. ....	163
Figure 6-3 miR-21 and TGF $\beta$ induce changes in mitochondrial morphology but not cellular mitochondrial content. ....	164
Figure 6-4 miR-21 alters protein levels of mitochondrial dynamics machinery. ....	165
Figure 6-5 Summary data from integration of mRNA-seq data with various resources. ....	166
Figure 6-6 Mitochondrially associated genes are downregulated by both TGF $\beta$ and miR-21. ....	168
Figure 6-7 ACAT1 and AK2 mRNA levels are decreased in experimental diabetic models. ....	169

Figure 6-8 miR-21 decreases luciferase expression from 3' UTR expression vectors..... 171

Figure 6-9 Protein levels of ACAT1 and AK2 are decreased by miR-21. .... 172

Figure 6-10 siRNA sufficiently represses ACAT1 and AK2 gene expression..... 173

Figure 6-11 Repression of ACAT1 or AK2 alter mitochondrial function..... 175

Figure 6-12 ACAT1 and AK2 repression alter fibrotic gene expression. .... 177

Figure 6-13 ACAT1 and AK2 repression impact TGFβ-mediated expression of growth factors..... 178

## List of Abbreviations

·OH	hydroxyl radical
αSMA	smooth muscle actin, alpha
ACACB	acetyl-CoA carboxylase B
ACADM	acyl-CoA dehydrogenase C-4 To C-12 straight chain
ACAT1	acetyl-CoA acetyltransferase
ADP	adenosine diphosphate
AIF	apoptosis inducing factor
AK2	adenylate kinase 2
AKT	v-akt murine thymoma viral oncogene homolog 1
AGE	advanced glycation end-product
AN	Alport nephropathy
AngII	angiotensin II
APOL6	apolipoprotein l-6
ATP	adenosine triphosphate
ATPAF1	ATP synthase mitochondrial F <sub>1</sub> complex assembly factor 1
BAK	BCL2-antagonist/killer 2
BAX	BCL2-associated X protein
BCL2	B-cell CCL/lymphoma 2
BCV	biological coefficient of variance
BECN	beclin 1
BIM	BCL-2 interacting mediator of cell death
BMP	bone morphogenetic protein
BP	biological process gene ontology
CDKN1A	cyclin dependent kinase inhibitor 1a
CMV	cytomegalovirus
CPM	counts per million
CPT	carnitine palmitoyltransferase 1
COL4A3	collagen 4 alpha 3
COL5A2	collagen 5 alpha 2
COLI	collagen I
COLIII	collagen III
COLIV	collagen IV

contig	contiguous sequence
COX	cytochrome C oxidase
CTGF	connective tissue growth factor
cytC	cytochrome C
DCT	distal convoluted tubule
DGE	differential gene expression
DM	diabetes mellitus
DN	diabetic nephropathy
DNA	deoxyribonucleic acid
DRP1	dynamain-related protein 1
ECM	extra-cellular matrix
eGFR	estimated glomerular filtration rate
EMT	epithelial-mesenchymal transition
EndMT	endothelial-mesenchymal transition
ErbB	epidermal growth factor receptor
ERK	extracellular signal-regulated kinase 2
ESRD	end-stage renal disease
ETC	electron transport chain
FA	fatty acids
FACS	fluorescence-activated cell sorting
FADH <sub>2</sub>	reduced flavin adenine dinucleotide
FCS	functional class scoring
FDR	false discovery rate
FN1	fibronectin
FSP1	fibroblast specific protein 1
GBM	glomerular basement membrane
GLUT1	glucose transporter type 1
GLUT4	glucose transporter type 4
GS	glomerulosclerosis
GSK3 $\beta$	glycogen synthase kinase 3 beta
GAGE	generally applicable gene set analysis
GSEA	gene set enrichment analysis
H <sub>2</sub> O <sub>2</sub>	hydrogen peroxide
IFA	impact factor analysis

IL-1	interleukin 1
IL-11	interleukin 11
IL-23a	interleukin 23 alpha subunit
IL-6	interleukin 6
IL21R	interleukin 21 receptor
JAK	janus kinase
KEGG	Kyoto encyclopaedia of genes and genomes
LC3	microtubule-associated protein 1 light chain 3
logFC	log <sub>2</sub> fold-change
MAPK	mitogen activated protein kinase
MC	mesangial cell/s
MCP1	monocyte chemotactic protein 1
MD	macula densa
MDS	multi-dimensional scaling
MF	molecular function gene ontology
MFN2	mitofusin 2
miR-NC	negative control miRNA
miRNA/miR	micro ribonucleic acid
miRNA-seq	microRNA sequencing
MMP9	matrix metalloproteinase 9
MPV17L	MPV17 mitochondrial membrane protein-like
mRNA	messenger ribonucleic acid
mRNA-seq	mRNA sequencing
NADH	reduced nicotinamide adenine dinucleotide
NE	norepinephrine
NFκB	nuclear factor of kappa light polypeptide gene enhancer in B-cells
NOX4	NADPH oxidase 4
O <sub>2</sub> <sup>-</sup>	superoxide
ODC	ornithine decarboxylase
OPA1	optic atrophy 1
ORA	over representation analysis
p27 <sup>Kip1</sup>	cyclin-dependant kinase inhibitor 1B
p38	mitogen-activated protein kinase 14
PAGE	parametric analysis of gene set enrichment

PARP2	poly ADP-ribose polymerase 2
PCT	proximal convoluted tubule
PDC	pyruvate dehydrogenase complex
PDCD4	programmed cell death 4
PDGF	platelet derived growth factor
PDHA1	pyruvate dehydrogenase alpha 1
PDP1	pyruvate dehydrogenase phosphatase 1
Pert	perturbation factor
PGC-1 $\alpha$	peroxisome proliferator-activated receptor gamma coactivator 1 alpha
PGE2	prostaglandin E2
PGI <sub>2</sub>	prostacyclin
PI3K	phosphatidylinositol-4,5-bisphosphate 3-kinase
PINK1	PTEN-induced putative kinase 1
PKC	protein kinase C
PKC $\beta$ 1	protein kinase C, beta
PPAR	peroxisome proliferator-activated receptor
PTC	proximal tubule epithelial cell/s
QQ	quantile-quantile
RISP	rieske iron-sulphur protein
RNA	ribonucleic acid
ROS	reactive oxygen species
SGLT1	sodium-glucose cotransporter 1
SGLT2	sodium-glucose cotransporter 2
SHC	SRC homology 2 domain containing transforming protein 1
SiC	negative control siRNA
siRNA	short interfering RNA
SLC25A25	solute carrier family 25 member 25
SLC27A1	solute carrier family 27 member 1
SMAD7	mothers against decapentaplegic homolog 7
SNAIL1	snail family zinc finger 1
SOD2	superoxide dismutase 2
SPRY2	sprouty RTK signalling antagonist 2
STAT	signal transducer and activator of transcription
STZ	streptozotocin

T1D	type 1 diabetes
T2D	type 2 diabetes
TBM	tubule basement membrane
TCA	tricarboxylic acid cycle
TGF $\beta$	transforming growth factor beta
TGF $\beta$ RI	TGF $\beta$ receptor 1
TIF	tubulointerstitial fibrosis
TNF $\alpha$	tumour necrosis factor alpha
TXNRD1	thioredoxin reductase 1
UCP2	uncoupling protein 2
UNx	uninephrectomised
UTR	untranslated region
UO	unilateral ureteral obstruction
VEGF	vascular endothelial growth factor
WNT	wingless-type MMTV integration site family
ZO-1	zona occludins 1

## Declaration for Thesis Chapter

Monash University

### Declaration for Thesis Chapter 1: microRNA in the development of diabetic complications

#### Declaration by candidate

In the case of Chapter 1, the nature and extent of my contribution to the work was the following:

Nature of contribution	Extent of contribution (%)
Researched, wrote and edited the manuscript	95

The following co-authors contributed to the work. If co-authors are students at Monash University, the extent of their contribution in percentage terms must be stated:

Name	Nature of contribution	Extent of contribution (%) for student co-authors only
Phillip Kantharidis	Edited manuscript	

The undersigned hereby certify that the above declaration correctly reflects the nature and extent of the candidate's and co-authors' contributions to this work\*.

Candidate's  
Signature

	Date 04/04/2016
---	--------------------

Main  
Supervisor's  
Signature

	Date 04/04/2016
---	--------------------

\*Note: Where the responsible author is not the candidate's main supervisor, the main supervisor should consult with the responsible author to agree on the respective contributions of the authors.

## Declaration for Thesis Chapter

Monash University

### Declaration for Thesis Chapter 1: Where are we in diabetic nephropathy: microRNA and biomarkers.

#### Declaration by candidate

In the case of Chapter 1, the nature and extent of my contribution to the work was the following:

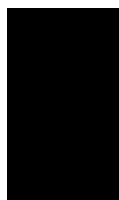
Nature of contribution	Extent of contribution (%)
Researched, wrote and edited the manuscript	55

The following co-authors contributed to the work. If co-authors are students at Monash University, the extent of their contribution in percentage terms must be stated:

Name	Nature of contribution	Extent of contribution (%) for student co-authors only
<b>Shinji Hagiwara</b>	Wrote and edited manuscript	
<b>Phillip Kantharidis</b>	Wrote and edited manuscript	

The undersigned hereby certify that the above declaration correctly reflects the nature and extent of the candidate's and co-authors' contributions to this work\*.

**Candidate's  
Signature**

	<b>Date</b> 04/04/2016
---	---------------------------

**Main  
Supervisor's  
Signature**

	<b>Date</b> 04/04/2016
---	---------------------------

\*Note: Where the responsible author is not the candidate's main supervisor, the main supervisor should consult with the responsible author to agree on the respective contributions of the authors.

## 1. Literature Review

### 1.1. Introduction

Diabetes mellitus (DM) is essentially a group of metabolic disorders which is the result of either loss or death of pancreatic  $\beta$ -cells and therefore loss of insulin production (Type I diabetes, T1D) or an inability to respond to insulin (Type II diabetes, T2D), also termed insulin resistance (1). Regardless, the major physiological characteristic of DM is an inability to regulate blood glucose levels resulting in chronic systemic hyperglycaemia. In Australia, DM is listed in the top six national health priorities with more than 6% of all people aged between 20 and 79 years (up to 1.3 million people) currently considered to have some form of diabetes (2). Although this is below the world wide incidence of DM of almost 9%, health care spending in Australia is the highest in the Western Pacific region equating to between 7652 and 14498 USD per person and accounts for approximately 10% of the country's health care spending. Therefore, DM represents a significant health care burden in Australia and one which is predicted to significantly worsen in the coming years.

Both T1D and T2D are linked to either insulin reduced production or insulin response. T1D subjects lack the ability to produce insulin due to an autoimmune attack on pancreatic  $\beta$ -cells or in some cases an idiopathic loss of  $\beta$ -cell mass and/or function (3). This lack of insulin renders metabolic tissues unable to control systemic glucose levels resulting in characteristic hyperglycaemia. However, since T1D is primarily an inability to produce insulin, T1D subjects are readily treated with self-administered insulin (4). Conversely, T2D involves a decreased insulin response by metabolic tissues and/or decreased glucose response by  $\beta$ -cells again resulting in poor glucose control (5). The complex pathophysiology of T2D is inherently more difficult to treat and often requires combination therapy aimed at increasing insulin sensitivity and production in addition to regulating glucose uptake and secretion as well as influencing gluconeogenesis predominately, but not exclusively, by the liver (6).

Despite the overarching theme of systemic hyperglycaemia, the prognosis for T2D subjects is often worse than that of T1D subjects due other co-morbid conditions such as obesity, hypertension and dyslipidaemia in addition to a greatly increased disease onset-diagnosis window (7). These factors place T2D subjects at greater risk of macrovascular complications such as cardiomyopathy, atherosclerosis and stroke in addition to microvascular complications including retinopathy, neuropathy, peripheral vascular disease and nephropathy (8).

Diabetic nephropathy (DN) is of particular interest being the leading cause of renal failure in Australia accounting for 36% of all non-indigenous cases and 79% of all indigenous cases of end-stage renal disease (ESRD) (9). Therefore, DN represents a significant health burden which is only poised to worsen with the predicted increases in the incidence of DM and increasing number of subjects with early onset T2D. Therefore, this devastating complication of diabetes needs further attention from academic, medical and government sectors.

## **1.2. Introduction to diabetic nephropathy**

DN is the leading cause of renal failure in much of the world and is the product of both metabolic and haemodynamic factors (2, 10). The condition progresses through various stages, all of which are detectable at the ultrastructural level (Table 1-1). Clinical manifestation of DN is predominately the result of changes that occur in the glomerulus such as glomerular basement thickening, mesangial expansion and podocyte effacement/loss as well as tubular dysfunction (Figure 1-1) (11). These phenotypic changes result in clinically measurable increases in urinary albumin excretion and typically can progress to ESRD. Overt ESRD is marked by failure of the glomerular apparatus to filter metabolites from the blood for tubular reabsorption. Histologically ESRD is often associated with severe mesangial expansion, glomerulosclerosis (GS) and tubulointerstitial fibrosis (TIF) (12). The contribution of various cell types to DN pathology has been well studied although the molecular mechanisms behind these contributions are still being elucidated.

**Table 1-1 Summary of clinical signs of DN.**

eGFR, serum creatinine, blood pressure and albuminuria all worsen with DN progression toward ESRD. \*, classified as microalbuminuria; \*\*, patients may pass up to 15 g/day albumin/protein; \*\*\*, urinary albumin/protein may fall as a result of severe glomerulosclerosis. Adapted from Halt *et al.* (2010).

		<u>Disease Aspect</u>				
		<b>Albuminuria (mg/24hr)</b>	<b>eGFR (ml/min)</b>	<b>Serum Creatinine (<math>\mu</math>mol/l)</b>	<b>Blood Pressure (mm/Hg)</b>	<b>Clinical Signs</b>
<b>Stages</b>	<b>Normal</b>	< 20	+ / ++	60 - 100 (normal)	+	None
	<b>Developing</b>	20 – 300 *	+ / ++	60 - 120 (normal)	++	None
	<b>Persistent</b>	$\geq$ 300 **	+ / -	80 - 120 (high normal)	+++	May be absent or may include anaemia $\pm$ oedema and symptoms of increased blood pressure
	<b>Clinical</b>	$\geq$ 300 **	-	120 – 400 (high)	+++	As above
	<b>End stage</b>	$\geq$ 300 ***	--	> 400 (very high)	+++	As above with symptoms of uraemia

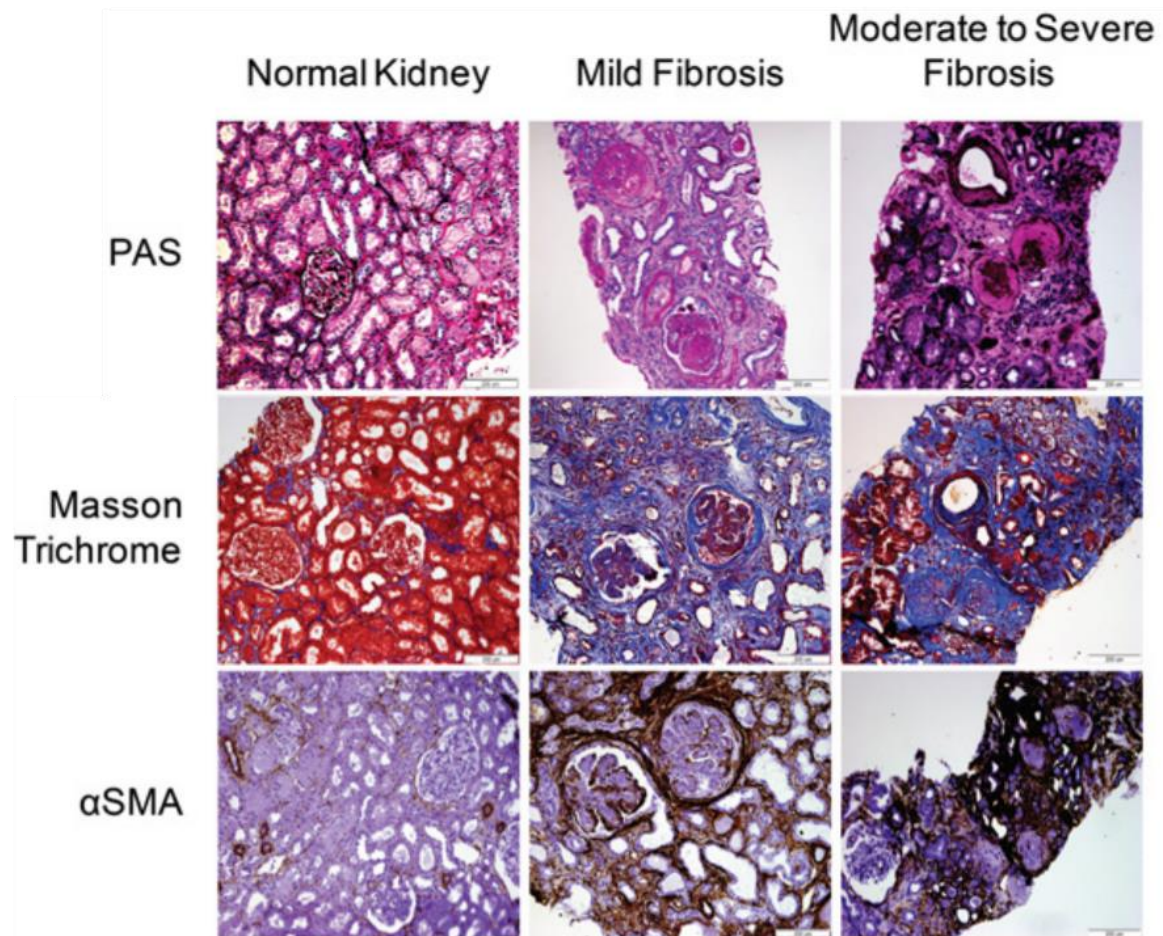


**Figure 1-1 Histological changes in diabetic nephropathy.**

Both glomerular and tubular region of the renal cortex undergo severe structural changes as a result of the diabetic milieu. As the renal architecture declines into mildly fibrotic to moderately to severely fibrotic there are increasing levels of collagen (Masson Trichrome) and alpha smooth muscle actin ( $\alpha$ SMA) deposition in the tubular and glomerular basement membranes and in the interstitial and glomerular spaces. This ultimately results in glomerular hyalinosis and tubular loss followed by ESRD. Adapted from McClelland et al. (2015)

### 1.3. Cellular contributions in the diabetic kidney

The kidney's major functional components are comprised of the glomerulus and renal tubule (Figure 1-2). The glomerulus contains a microvascular network which is wrapped in podocytes and supported by mesangial cells (MC) (13). It is this part of the kidney which is responsible for primary filtration (14). The tubule is comprised of various segments and epithelial cell types with each segment performing different roles in metabolite, electrolyte and water reclamation and is broadly divided into the proximal, loop of Henle and distal tubule. Despite the importance of podocytes forming an essential part of the filtration component of the glomerulus, this cell population was not utilised in the present study and therefore will not be specifically addressed. Excellent reviews on podocyte biology have been previously written (15, 16).

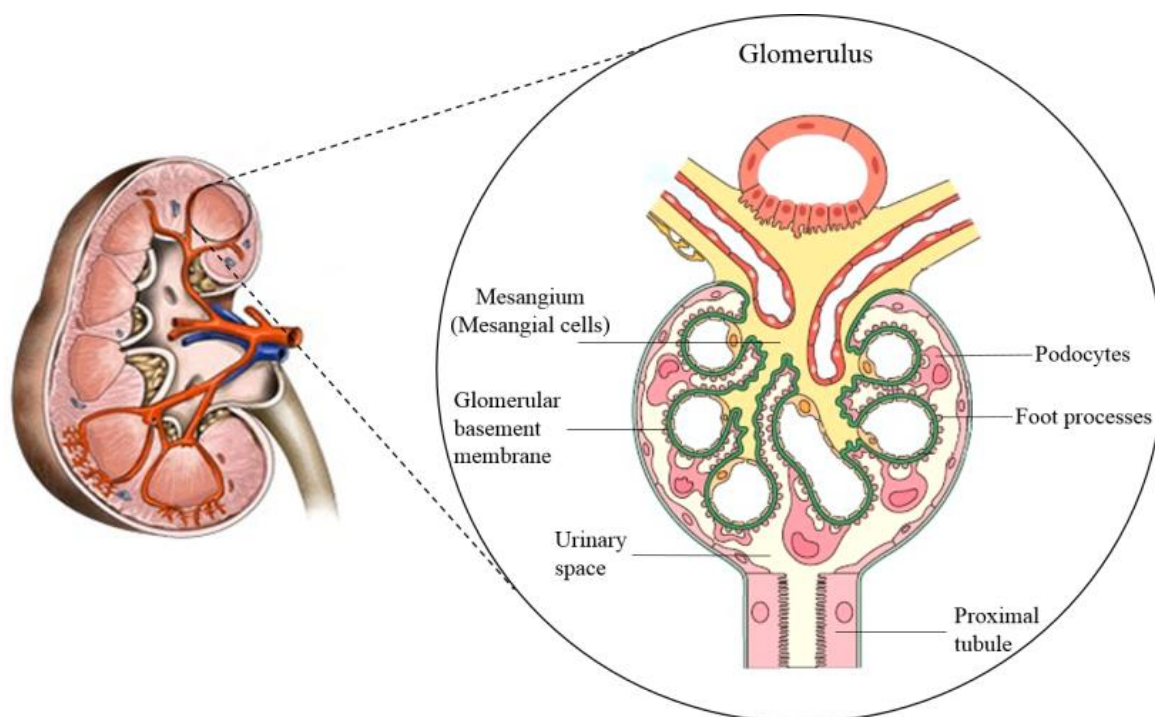


**Figure 1-2 Structure of the Bowmans capsule.**

The Bowmans capsule houses the glomerulus, the filtration unit of the kidney. Immediately downstream of the glomerulus is the proximal tubule. Indicated are the primary effector cells in diabetic nephropathy. Adapted from Feehally et al. (2010).

#### 1.3.1. The role of mesangial cells in diabetic nephropathy

Mesangial cells (MC) are located on the non-urinary side of the glomerular basement membrane (GBM) and are irregularly shaped cells rich in pseudopodia (17). These

pseudopodia connect individual cells to each other and also to GBM regions containing podocyte foot processes affording structural integrity and organisation to the capillary tuft (18). Intracellularly, inter-mesangial and GBM connections are attached to a disorganised 3-dimensional mesh of tropomyosin and actinomyosin contractile fibrils (19). Through expression of receptors for various vasoactive agents such as angiotensin II, prostaglandins and norepinephrin, MC are able to fine-tune intra-glomerular pressure through cellular contraction and dilation (Figure 1-3) (18). By exerting control over intra-glomerular pressure, mesangial cells also regulate glomerular filtration rate and by extension, podocyte and microvascular endothelial cell workload.

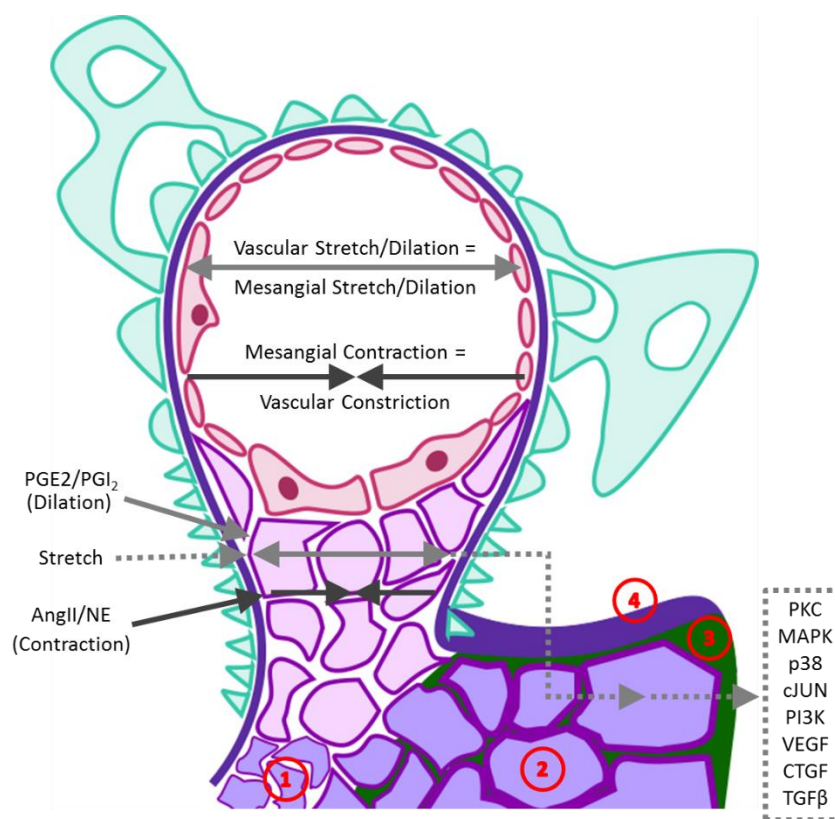


**Figure 1-3 The role of mesangial cells in glomerulosclerosis.**

A) Changes in intravascular pressure can result in mechanosensory feedback to mesangial cells (purple) via the glomerular basement membrane (dark purple) with increased haemodynamic pressure inducing mesangial cell stress responses and pathway activation. Hyperglycaemic cells (violet) undergo (1) proliferation and (2) hypertrophy and also (3) increase ECM synthesis (green) leading to loss of mesangial elasticity and (4) basement membrane thickening. Adapted from M. Komorniczak, Wikimedia Commons (2009).

Gross regulation of intraglomerular pressure is however regulated by the afferent and efferent arterioles and it is this hydrostatic regulation that is a major driving force in MC pathology in DN (20). MC possess mechanosensory properties and are sensitive to the microvascular stretch that occurs with increased plasma flow and pressure. This mechanosensory property is especially important in DM where hypertension is typically present. Vascular stretch activates numerous pathways in MC including protein kinase C (PKC), mitogen activated protein kinase (MAPK), p38, cJun and phosphatidylinositol-4,5-bisphosphate 3-kinase (PI3K) signalling pathways in addition to inducing expression of growth factors important in DN including vascular endothelial growth factor (VEGF), connective tissue growth factor (CTGF) and transforming growth factor beta (TGF $\beta$ ) (21-26).

MC also express low levels of insulin receptor and the insulin receptive glucose transporter type 4 (GLUT4) and instead predominately express the insulin independent glucose transporter, GLUT1 (27). This renders MC directly susceptible to the hyperglycaemic environment of the diabetic kidney with intracellular glucose levels approaching that of the plasma. Glucose can directly induce expression of fibronectin (FN1) as demonstrated by decreased FN1 expression by antisense GLUT1 under high glucose conditions (28). Glucose also promotes the expression of GLUT1 thereby increasing the free passage of glucose into MC (29). Furthermore, hyperglycaemic conditions increase TGF $\beta$  production in MC which in turn increases GLUT1 production creating a positive feed-forward loop which allows increasingly free passage of glucose into MC and TGF $\beta$  production and activity (30).

Glucose stimulated TGF $\beta$  production is of particular importance as it may act locally in a positive feedback loop reinforcing its own expression, and also act on adjacent MC increasing extra-cellular matrix (ECM) production whilst also decreasing production of ECM turnover proteins and inducing mesangial cell growth and proliferation (31). This collectively results in increased ECM deposition and mesangial expansion and also GBM thickening, all these processes are important in glomerulosclerosis. These processes are a core component of the progressive nature of DN due to the resultant increases in TGF $\beta$  production as this impacts directly upon podocyte effacement and loss (32, 33). Importantly, TGF $\beta$  is also passed to downstream segments of the nephron, in particular the proximal tubule.

### **1.3.2. The role of proximal tubule epithelial cells in diabetic nephropathy**

The renal tubule is comprised of numerous epithelial cell types all of which have specialised functions (11). The proximal tubule, or proximal convoluted tubule (PCT), lies immediately downstream of the glomerulus and is responsible for the reabsorption of a broad range of

compounds ranging from peptides and amino acids to electrolytes and bicarbonate (34). Importantly, this section of the nephron is responsible for almost all glucose reabsorption from the glomerular filtrate which is achieved through the actions of two sodium ( $\text{Na}^+$ )-glucose transporters, SGLT1 and SGLT2. Each isoform being expressed in a different region of the PCT (35). SGLT2, which is expressed in the S1 region of the proximal tubule, is responsible for 97% of all glucose uptake along the length of the PCT. However, SGLT1, predominantly in the S3 segment can absorb up to 40% of urinary glucose in the case of SGLT2 inhibition. These insulin-independent glucose transporters place PTC at risk of intracellular hyperglycaemia (Figure 1-4).

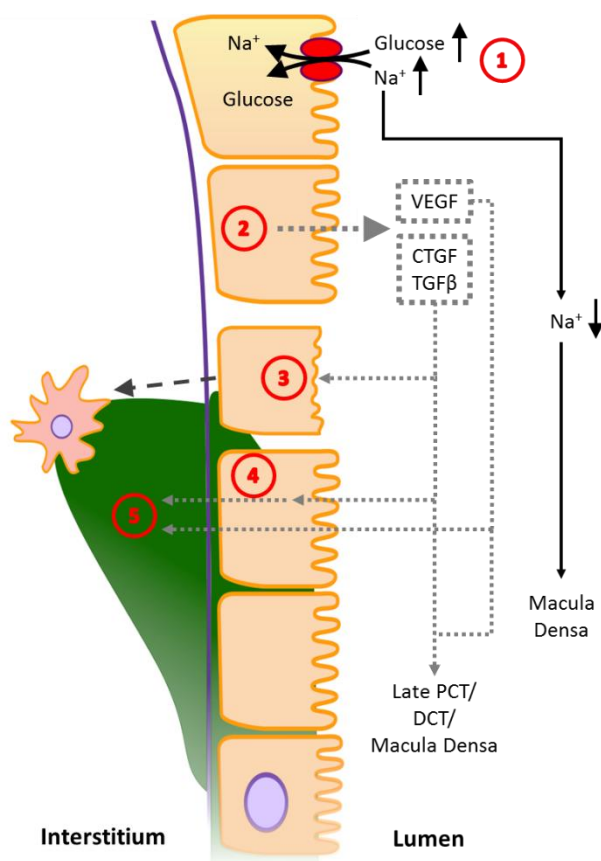


**Figure 1-4 The role of proximal tubule epithelial cells tubulointerstitial fibrosis.**

PTC pathology is instigated by (1) increased glucose uptake through via SGLT2 which also increases  $\text{Na}^+$  reabsorption and decreases  $\text{Na}^+$  delivery to the macula densa. Intracellular hyperglycaemia (2) induces expression of a number of nephropathic growth factors. In the case of (2) CTGF and  $\text{TGF}\beta$ , these may act in a paracrine or autocrine fashion to (3) induce EMT in PTC resulting in fibroblast generation and ECM synthesis or (4) may act on distal cells to induce ECM synthesis. All three growth factors may be (5) transferred to the interstitium where they may act on interstitial fibroblasts

or leukocytes or may enter the peritubular vasculature where they may be systemically delivered or act on local vascular endothelial cells. Adapted from M. Komorniczac, Wikimedia Commons (2009). As SGLT1/2 are Na<sup>+</sup>/glucose symporters, PTC will exhibit Na<sup>+</sup> hyperreabsorption under hyperglycaemic conditions. Whilst this is of no direct consequence to PTC, hyperreabsorption does have knock on effects which affect both downstream and upstream regions of the nephron. Plasma filtrate Na<sup>+</sup> levels are detected at the macula densa (MD) located downstream of the PCT at the junction of thick ascending limb of the loop of Henle and the distal convoluted tubule (36). Decreased Na<sup>+</sup> levels at the MD activate tubuloglomerular feedback pathways leading to increased GFR of the adjacent nephron. PTC hyperreabsorption also acts to increase GFR through reduction of hydrostatic pressure in the Bowmans capsule which also increases effective glomerular pressure (37). Increased flow and pressure in the glomerulus not only results in greater glucose delivery to PTC, but also increased production and glomerular leakage of growth factors by MC as discussed above.

As in MC, high intracellular glucose in PTC elicits a number of pathological changes in cellular biology such as increased ECM production thereby contributing directly to tubulointerstitial fibrosis (38). Hyperglycaemia also triggers expression of growth factors including VEGF, CTGF and TGFβ (39-41). These may then act on adjacent PTC, cells further downstream in the distal convoluted tubule or collecting ducts or can be secreted from the basolateral surface of the PTC to either the peritubular vasculature or into the renal interstitium. Secretion of growth factors into the interstitium can lead to fibroblast activation resulting in increased fibrosis and production of factors that impact upon PTC (42, 43). This again creates a feed-forward loop leading to increased growth factor production/secretion, interstitial cell activation and PTC-mediated ECM production.

Finally, PTC can undergo processes reminiscent of embryonic epithelial-mesenchymal transition (EMT) in response to growth factors such as TGFβ (44). During EMT, epithelial cells take on a mesenchymal phenotype which *in vitro*, affords them some degree of motility and is essential to metastasis of epithelial cancers (45). In the diabetic kidney, cell lineage studies proposed that 36% of fibroblasts are born from proximal tubule epithelial cells undergoing EMT (46). However subsequent studies were unable to identify epithelial cells in the interstitium thereby confounding these findings particularly that of cellular migration (47, 48). Regardless, in the diabetic kidney PTC may still develop other characteristics of EMT such as apoptotic evasion, loss of E-cadherin, increased ECM production and decreased production of ECM turnover genes in addition to changes in cytokine and growth factor

production (49). While these changes are readily measured *in vitro*, PTC migration has not been observed *in situ* thus rendering the use of the term ‘EMT’ a controversial concept (50). However, many of the pathophysiological processes associated with EMT are observed in PTC *in vivo* therefore supporting an EMT-like process existing in the diabetic PCT (51). Indeed, snail family zinc finger 1 (SNAIL1), an embryonic regulator of EMT, was recently reported to be essential to induction of an EMT-like phenotype in PTC *in vivo* and that this phenotype was required for the development of renal fibrosis and inflammation in the unilateral ureteral obstruction (UUO) model of kidney disease (52). This study also demonstrated that the EMT-like phenotype increased renal myofibroblast content not by cellular migration and transformation but by SNAIL1-dependent secretion of TGF $\beta$  from the PCT leading to transformation of bone marrow-derived mesenchymal cell to myofibroblasts. Additionally, F4/80 macrophage content was reduced in SNAIL1 knockout UUO mice compared to wild-type UUO mice in addition to reduction in other inflammatory markers and cytokines including nuclear factor of kappa light polypeptide gene enhancer in B-cells (NF $\kappa$ B), tumour necrosis factor alpha (TNF $\alpha$ ), various interleukins, chemokine (C-C motif) ligands and chemokine (C-X-C motif) ligands. This study clarifies the long standing debate over the relevance of EMT-like processes in PTC and their significance to myofibroblast content in the diabetic kidney.

Although PTC are well regarded as progenitors of TIF, their role in glomerulosclerosis is less understood nor are the underlying transcriptional mechanisms which lead to the phenotypes described above (53, 54). For this reason, it is imperative to gain a better understanding of PTC pathophysiology in order to interrupt the feed-forward loops which seem to arise from PTC dysfunction in DM.

#### **1.4. Effectors of diabetic nephropathy**

DM is the consequence of both genetic and lifestyle factors and results in a wide range of physiological changes in a great number of tissues and systems. The resultant cytokine and growth factor cocktail that emerges from each affected tissue has the potential to induce changes in distal tissues. This makes study of any of the major diabetic complications somewhat more complex than similar tissue pathologies in non-diabetic conditions. Furthermore, many of the effector compounds have wide knock-on effects in regards to intracellular signalling as is the case with angiotensin II (AngII), advanced glycation end products (AGE), reactive oxygen species (ROS) along with myriad of inflammatory

cytokines and growth factors (44, 55-58). Amongst these, TGF $\beta$  is considered to be a particularly important growth factors as one of the most potent mediators of the pathological changes occurring in DN (59).

#### **1.4.1. TGF $\beta$ in glomerulosclerosis**

Glomerulosclerosis is the progressive scarring with a consequent functional loss of the glomerular function. It is often associated with glomerular and mesangial hypertrophy, podocyte loss and effacement and endothelial apoptosis leading to collapse or loss of glomerular capillaries (60). Although these characteristics are predominantly propagated by mesangial cells, podocytes and microvascular endothelial cells respectively there is considerable cross-talk among these cells (61, 62). Furthermore, despite each cell type possessing unique biology, they all respond and are susceptible to a number of factors common to the diabetic milieu. Amongst these, TGF $\beta$  mediates the more dramatic changes observed in these cell types leading to gross changes in cellular function and physiology (Figure 1-5).

One of the most prominent changes induced by TGF $\beta$  in the glomerulus is that of ECM accumulation as a result of increased ECM production and decreased production or activity of ECM turnover genes (63, 64). This process is a major contributor to glomerular hypertrophy and also GBM thickening. In response to TGF $\beta$ , MC increase production of collagen 1 (COL1), collagen 3 (COL3) and collagen 4 (COL4) in addition to laminins and FN1 and also decrease production of ECM degradation enzymes including matrix metalloproteases (65). This collectively results in expansion of the mesangium along with stiffening of the matrix which prevents MC from fine-tuning glomerular pressure.

Podocytes also increase ECM production and decrease ECM turnover in response to TGF $\beta$  leading to GBM thickening (66). In addition to changes in ECM structures, TGF $\beta$  also induces podocytes loss by increasing production of SMAD7 leading to decreased expression of the survival factor NF $\kappa$ B (67). Alternatively, TGF $\beta$  induced podocyte apoptosis may be elicited via ROS production and mitochondrial depolarisation as a result of TGF $\beta$ -mediated upregulation of NADPH oxidase 4 (NOX4) (68). Podocytes constitutively express VEGF and their loss may also be linked with endothelial loss as VEGF signalling promotes endothelial cell survival (69, 70).

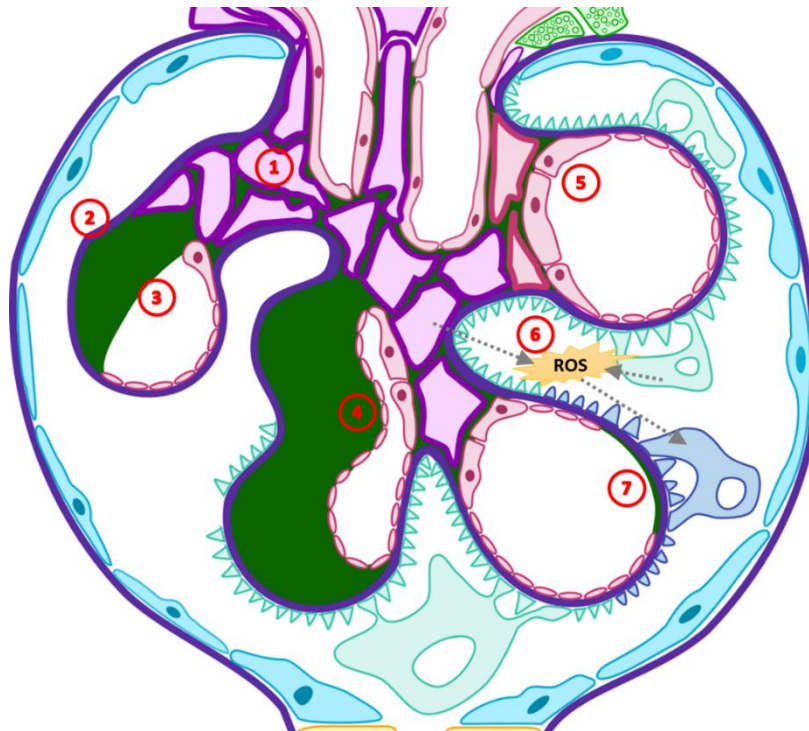


**Figure 1-5 The roles of TGF $\beta$  in glomerulosclerosis.**

(1) TGF $\beta$  induces proliferation and hypertrophy in MC. Podocytes undergo foot process effacement or (2) become detached from the GBM and excreted. Through TGF $\beta$ -stimulated MC, (3) ECM synthesis may result in detachment and loss of microvascular endothelial cells from the thickening GBM or (4) in vascular collapse. Microvascular endothelial cells (5) may undergo EndMT in response to TGF $\beta$ , migrate to the mesangial space and contribute to pathological ECM deposition. (6) TGF $\beta$  induced ROS production in both MC and podocytes can lead to podocytes apoptosis or loss; a process which can also be mediated by TGF-mediated increases in SMAD7 expression (not shown). Podocytes are important for endothelial cell survival and their loss decreases VEGF levels resulting in (7) endothelial cell loss and vascular leakage. Adapted from M. Komorniczak, Wikimedia Commons (2009).

Finally, TGF $\beta$  induces gross phenotypic transformations in all three cell types. Podocytes, being of an epithelial developmental lineage, may undergo EMT-like transformations thereby decreasing expression of podocyte specific proteins such as nephrin and zona occludins 1 (ZO1) and increasing mesenchymal markers such as desmin and fibroblast specific protein 1 (FSP1) (71, 72). Podocyte effacement occurs in response to TGF $\beta$  which involves gross intracellular reorganisation and loss of foot processes and is likely part of the EMT-like process. Conversely, endothelial cells can undergo endothelial-mesenchymal transition (EndMT)

which similarly results in the fibrotic, migratory phenotype observed in EMT ultimately adding to the increased fibroblast population observed in DN (73).

Whilst MC do not exhibit cellular transformation *per se*, they do undergo cellular hypertrophy after an initial period of proliferation (18). MC hypertrophy is attributable to maintenance of G<sub>1</sub> cell cycle arrest due to induction of the cyclin-dependent kinase inhibitors such as cyclin-dependant kinase inhibitor 1B (p27<sup>Kip1</sup>) (74). Although increased p27<sup>Kip1</sup> is the result of prolonged exposure to high glucose, blockade of TGFβ signalling prevents high glucose induced p27<sup>Kip1</sup> expression indicating TGFβ signalling directly is responsible for MC hypertrophy and not high glucose (75). Regardless, mesangial expansion and hypertrophy are essential to glomerulosclerosis and place excessive biochemical and mechanical strain on podocytes and glomerular microvascular endothelial cells (76).

#### **1.4.2. TGFβ in tubulointerstitial fibrosis**

Similarly to glomerulosclerosis, TIF is a hallmark histopathological characteristic of DN. Collectively, TIF is marked by PTC hyperplasia and hypertrophy, ECM accumulation, activation and production of fibroblasts and interstitial inflammation (42). The process is contributed to in the early phases by PTC with fibroblasts, monocytes and peritubular vascular endothelial cells becoming involved in later stages as damage increases (77, 78). As with glomerulosclerosis, there are a number of factors that contribute to TIF, however TGFβ is considered to be the most potent and has been widely examined in many studies. However, due to its roles in mediating and regulating inflammatory cells and production of inflammatory cytokines TGFβ has proven to not be a suitable therapeutic target (79, 80).

Even in the early stages of DN, the kidney can be seen to increase in size which is in part due to tubular growth through hyperplasia (81). This is proposed to occur through ornithine decarboxylase (ODC) mediated polyamine synthesis in the DCT acting in a paracrine manner on the PCT (Figure 1-6) (82). In streptozotocin-induced diabetic rats, tubular hypertrophy takes over in response to TGFβ in a process that appears dependent on protein kinase C beta (PKCβ1), extracellular signal-regulated kinase 2 (ERK) or mitogen activated protein kinase 14 (p38) (83, 84). Hypertrophy may also occur in a p27<sup>Kip1</sup> dependent manner as that described for MC above. Regardless, PTC from TGFβ knockout mice do not enter a hypertrophic growth phase in response to high glucose (85).

In its most basic form, TIF is defined as a progressive accumulation of ECM material ultimately leading to destruction of tissue architecture in the tubulointerstitium (86). Under this definition, TGFβ is considered a central mediator of TIF (87). PTC may be exposed to

TGF $\beta$  from a number of sources with the most immediate being that secreted from MC and podocytes in addition to TGF $\beta$  produced by PTC in response to high glucose (88). TGF $\beta$  is a strong inducer of ECM genes in PTC upregulating various collagens, alpha smooth muscle actin ( $\alpha$ SMA) and FN1 (89). Various growth factors such as platelet derived growth factor (PDGF) and CTGF are also induced by TGF $\beta$  further exacerbating the fibrotic phenotype (90). Importantly, TGF $\beta$  also potently induces EMT in PTC leading to loss of epithelial markers and acquisition of a mesenchymal-like phenotype (44). This phenotype may include degradation of the tubule basement membrane (TBM) and cellular migration into the interstitium however as outlined earlier, this has been difficult to observe *in vivo*.

Despite lack of evidence of EMT-mediated cellular migration leading to myofibroblast formation, recent evidence has emerged demonstrating fibroblast formation without PTC migration (52). Here, the EMT-like phenotype displayed by PTC was found to be dependent upon Snail1 expression and that Snail1-mediated EMT was required for renal fibrosis. Furthermore, increased fibroblast content in the fibrotic kidney is attributed to transformation of bone marrow-derived mesenchymal cells and not PTC transdifferentiation. In addition to EMT-mediated fibroblast formation, the FN1 isoform ED-A FN, which arises from an alternative splicing event of the FN1 mRNA, may also be produced by PTC and secreted into the TBM (91). This FN1 isoform acts as an anchorage for fibroblasts upon the TBM (92). Furthermore, anti-ED-A FN antibodies blocked fibroblast mediated production of  $\alpha$ SMA and COL1 (93). Regardless of the source of renal fibroblasts, it is clear that TGF $\beta$  is involved in their recruitment to and activation at the TBM therefore contributing to TIF.

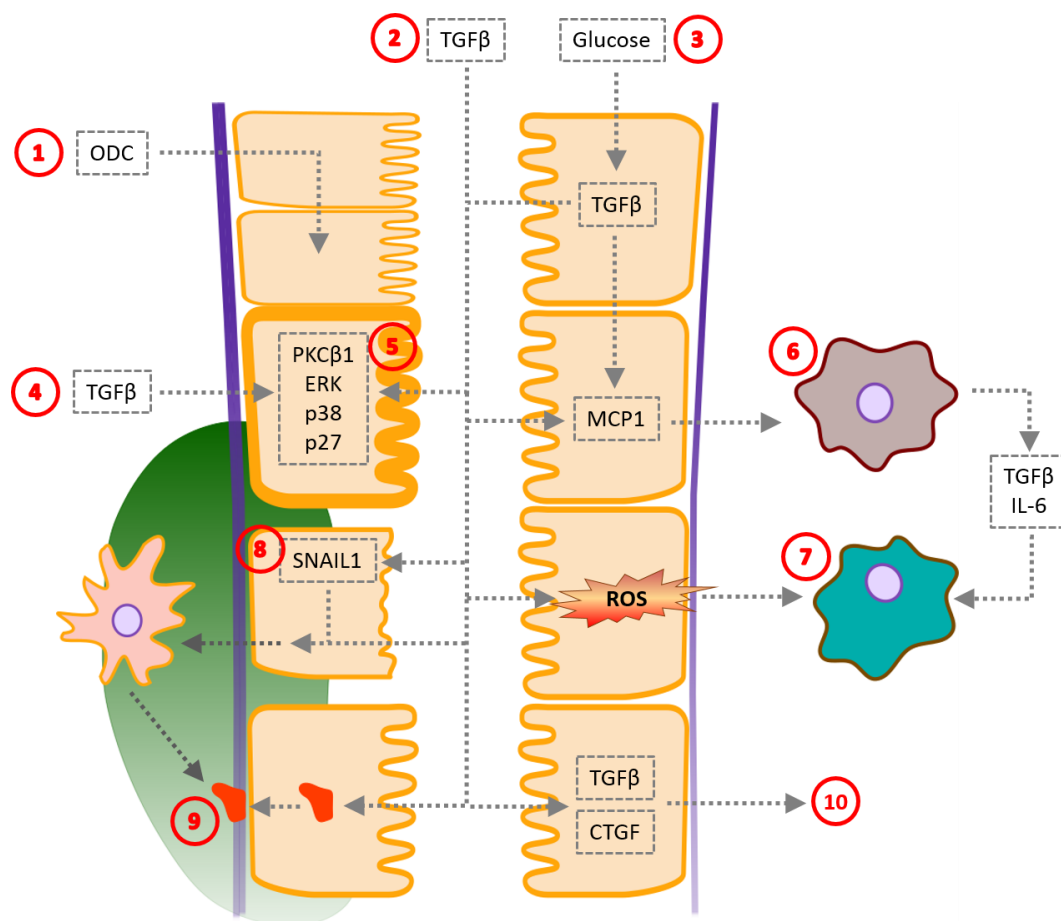


**Figure 1-6 The role of TGF $\beta$  in tubulointerstitial fibrosis.**

Following (1) ODC induced hyperplasia, TGF $\beta$  from a number of sources including (2) the glomerulus, (3) intracellular hyperglycaemia or (4) the interstitium, triggers a (5) hypertrophic switch via a number of possible pathways. MCP1 induction (6) can lead to the recruitment and activation of macrophage which secrete TGF $\beta$  and IL-6 resulting in differentiation of T-cells which (7) may be recruited by TGF $\beta$ -induced PTC oxidative stress. (8) EMT-like phenotypes are also induced by TGF $\beta$  and ROS resulting in increased ECM and TBM production in addition to fibroblast generation through SNAIL1-mediated TGF $\beta$  production. New and resident fibroblasts may localise to the TBM (9) through binding the ED-A FN1 isoform. Finally, TGF $\beta$  induces its own expression, and that of CTGF, both of which may be secreted to the interstitium to act on fibroblasts, various leukocytes and the peritubular vasculature. Adapted from M. Komorniczac, Wikimedia Commons (2009).

TGF $\beta$  also plays a role in renal inflammation from the early stages of DN. *In vitro*, TGF $\beta$  has been demonstrated to increase monocyte chemotactic protein 1 (MCP1) in PTC possibly accounting for increased macrophage content in the diabetic kidney (94). Macrophage recruitment and activation forms another important aspect of the progressive nature of DN as activated macrophage secrete TGF $\beta$  and interleukin 1 (IL-1) which then promote further

fibroblast activation and proliferation respectively (95). Naïve T cells may also be differentiated into inflammatory helper T cells by macrophage produced interleukin-6 (IL-6) (96). Furthermore, TGF $\beta$  signalling was found to recruit F4/80 macrophages in association with increased ROS production in a non-diabetic model of acute kidney injury induced by constitutive TGF $\beta$  receptor 1 (TGF $\beta$ RI) expression (97). Blockade of ROS with mitochondrial ROS scavengers was found to attenuate this recruitment.

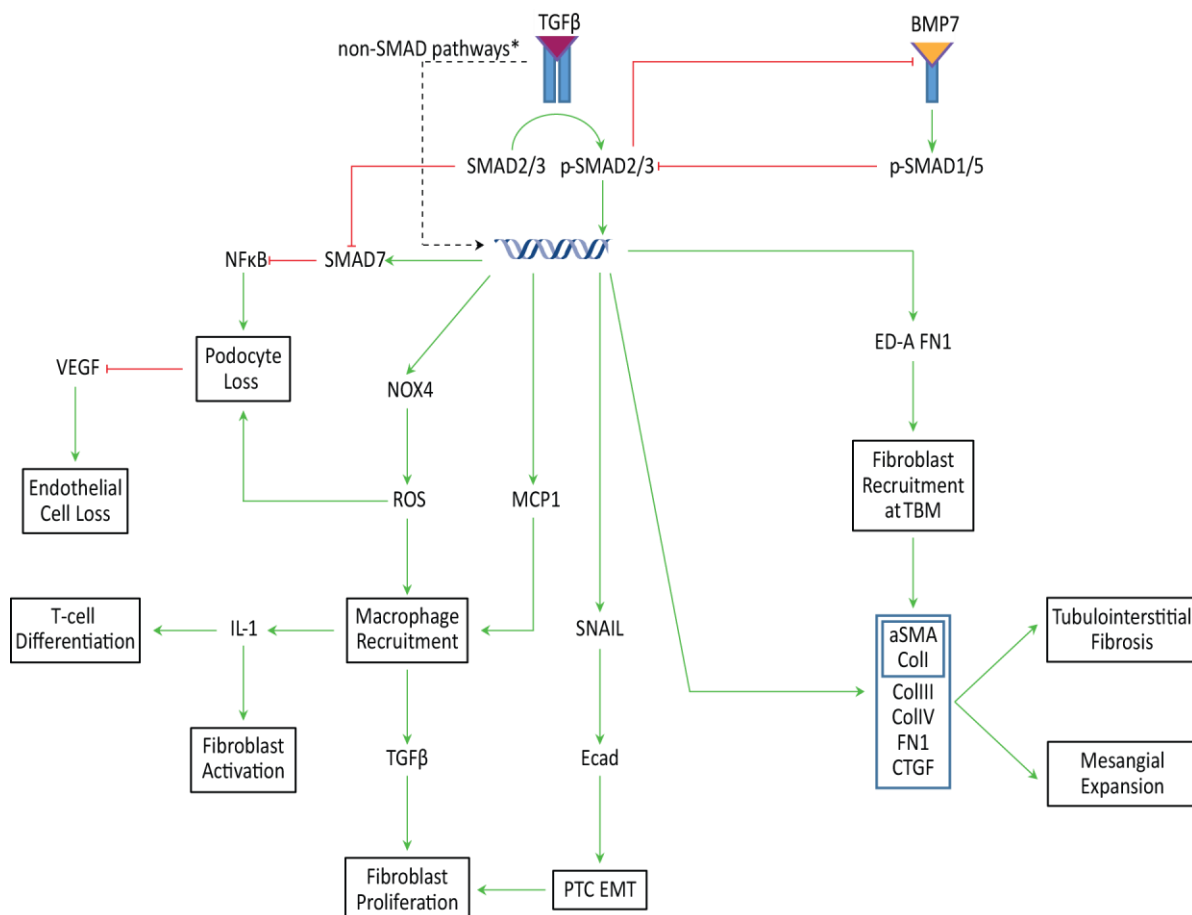


**Figure 1-7 Summary of the effects of TGF $\beta$  in the diabetic kidney**

A number of aspects of TGF $\beta$  biology in diabetic nephropathy have been discussed and are summarised here. Additionally, BMP7 has emerged as an important TGF-family member for its role in negative regulation of SMAD-dependent TGF $\beta$ -mediated signalling and is therefore indicated in the figure to highlight the some of the complexities extant in signalling within the TGF-family.

It is clear that TGF $\beta$  is a major player in DN and is involved in numerous processes in various renal cell types and these effects are summarised in Figure 1-7. It should be noted however, that a number of the roles of TGF $\beta$  in DN, including EMT and cellular hypertrophy, are also mediated by TGF $\beta$  in malignant and metastatic cancers leading to cancer growth and spread respectively (98-100). However, these and many other roles are secondary to the primary role of TGF $\beta$  as a wound healing cytokine and result from continued activation of the wound healing process through the extended cellular stress and damage observed in the diabetic kidney. Incidentally, another TGF-family member, bone morphogenic protein 7 (BMP7) acts to repress pathogenic TGF $\beta$  signalling and has shown promise as a therapeutic agent *in vitro* and in experimental animal models which adds another level of complexity to TGF $\beta$  signalling (101-103). It is therefore necessary to gain a better understanding of the pathomechanisms of TGF $\beta$  signalling and its sustained activation in order to effectively intervene in these processes.

## **1.5. microRNA in diabetic nephropathy**

Just over 15 years ago, a seminal report on microRNA (miRNA; miR) was published highlighting the discovery of 19 miRNA in humans. These small, non-coding RNA molecules were reported in *C.elegans* 35 years ago and were considered to be an anomaly of worm biology at the time. Since the report by Lagos-Quintana *et al.* in 2001, miRNA have rapidly emerged as important players in development and disease and have gained much interest from both academic and industrial research communities alike.

### **1.5.1. microRNA in the development of diabetic complications**

#### **1.5.1.1. Introduction**

The following review highlights the current state of knowledge regarding miRNA in the development and progression of diabetes and its complications. Furthermore, a brief introduction to miRNA as non-invasive biomarkers in addition to miRNA therapeutics currently under development is also presented.

# microRNA in the development of diabetic complications

Aaron D. McCLELLAND\* and Phillip KANTHARIDIS\*

\*JDRF Danielle Alberti Memorial Centre for Diabetes Complications, Diabetes Division, Baker IDI Heart and Diabetes Institute, 75 Commercial Road, Melbourne, Victoria 3004, Australia

## Abstract

Today's world population is currently faced with a new type of non-transmissible pandemic: obesity. This lifestyle-related condition is driving the emergence of the diabetes pandemic through the development of low-level chronic inflammation. In recent years, a novel class of non-coding RNA, microRNA (miRNA), have emerged as being important regulators of numerous biological functions. Among these functions are basic maintenance of cell signalling and tissue architecture. Disruption of miRNA levels can contribute not only to the development of the chronic inflammation observed in obese diabetics, but also the development of both pancreatic  $\beta$ -cell dysfunction and loss, along with insulin resistance in metabolic tissues. These primary events set the scene for dysfunction of other tissues, including the retina, kidney, peripheral nerves, heart and the vasculature as a whole. Here, miRNAs again play a deterministic role in the development of a range of diseases collectively termed diabetic complications. Disturbances in miRNA levels appear to be reflected in the serum of patients and this may prove to be diagnostic in patients prior to clinical manifestation of disease, thus improving management of diabetes and its associated complications. Not only are miRNAs displaying promise as an early biomarker for disease, but a number of these miRNAs are displaying therapeutic potential with several in pre-clinical development. The present review aims to highlight our current understanding of miRNAs and their interaction with inflammatory signalling in the development and progression of diabetes and its complications. Utilization of miRNAs as biomarkers and therapeutic targets will also be considered.

**Key words:** biomarker, diabetes, diabetic complication, microRNA (miRNA), non-coding RNA, obesity

## PAST AND PRESENT PANDEMICS

The human race has faced numerous health and disease challenges over the centuries with some of them such as the Black Death and 1918 influenza pandemic resulting in millions of deaths and crippling nations [1]. In more recent times, we have faced the AIDS pandemic, which has also killed millions and destroyed many more lives, and also the ominous looming threat of H5N1 influenza virus. These outbreaks, as with all of those recorded throughout history, have had their roots in transmissible agents such as bacteria, virus or protozoans.

Today, much of the world is facing a pandemic that is neither the cause of an infectious agent nor directly transmissible. The obesity pandemic is the result of increased living standards (particularly in relation to food 'quality') combined with increasing levels of sedentary behaviour [2]. According to the Organisation for Economic Co-operation and Development (OECD), much of the world is shown to be clinically obese with many countries, including Australia, U.K., U.S.A. and many possessing an adult population which exceeds 20% total obesity rates [3]. Disturbingly, in 2012, 5–10% of children under 5 years of age were overweight in a large number of WHO (World Health

**Abbreviations:** AGE, advanced-glycation end-product; Ago, Argonaute; BMI, body mass index; BMPR2, bone morphogenetic protein receptor 2; CTGF, connective tissue growth factor; DM, diabetes mellitus; DN, diabetic nephropathy; ECM, extracellular matrix; EMT, epithelial–mesenchymal transition; ERG, ether-à-go-go-related gene; ET, endothelin; FOXa2, forkhead box a2; HDL, high-density lipoprotein; Hsp60, heat-shock protein 60; IFN, interferon; IGF, insulin-like growth factor; IL, interleukin; IRF4, IFN regulatory factor 4; IRS, insulin receptor substrate; JNK, c-Jun N-terminal kinase; LDL, low-density lipoprotein; LNA, locked nucleic acid; MAPK, mitogen-activated protein kinase; MCP, monocyte chemoattractant protein; miRNA (miR), microRNA; Mtpn, myotrophin; MRE, miRNA recognition element; MyD88, myeloid differentiation factor 88; NEFA, non-esterified 'free' fatty acid; NF- $\kappa$ B, nuclear factor  $\kappa$ B; ORP9, oxysterol-binding-protein-related protein 9; oxLDL, oxidized LDL; PAK1, p21-activated kinase 1; PDCD4, programmed cell death protein 4; PDGF, platelet-derived growth factor; PTEN, phosphatase and tensin homologue deleted on chromosome 10; RISC, RNA-induced silencing complex; ROS, reactive oxygen species; T1DM, Type 1 DM; T2DM, Type 2 DM; TEC, tubular epithelial cell; TGF $\beta$ , transforming growth factor  $\beta$ ; TIF, tubulointerstitial fibrosis; TNF, tumour necrosis factor; TNFAIP3, TNF $\alpha$ -induced protein 3; T<sub>reg</sub> cell, regulatory T-cell; UTR, untranslated region; UUU, unilateral ureteral obstruction; VEGF, vascular endothelial growth factor; YB-1, Y-box-binding protein-1; VSMC, vascular smooth muscle cell; ZEB2, zinc finger E-box-binding homeobox 2.

**Correspondence:** Dr Phillip Kantharidis

Organization) member states [4]. Many of these member states have rates over 20%. Obese individuals have increased risk of a number of co-morbidities such as cardiovascular diseases, numerous cancers and stroke among others. Importantly, obesity is one of the primary drivers of another current lifestyle-related pandemic, namely that of T2DM [Type 2 DM (diabetes mellitus)].

## DIABETES

Like obesity, DM is increasingly common and was estimated to affect ~10% of the global adult 25+ year old population in 2008 [5]. This remains relatively constant across sexes and socio-economic groupings within individual countries, further implicating lifestyle as the major mitigating factor. The link between obesity and DM appears to be one of chronic inflammation [6]. However, a significant portion (~60%) of Asian diabetics have a BMI (body mass index) <25 kg/m<sup>2</sup> and are thus considered lean [7]. Although this phenomenon is perplexing, a report by Xue et al. [8] has demonstrated that deficiencies in adipose tissue development may be the underlying cause via stimulation of local inflammatory signalling. It is also possible that this lack of adipocyte maturation results in increased circulating fatty acids thus leading to the observed increases in inflammatory signalling and insulin resistance in other tissues. Regardless, inflammation has a contributing role in a number of microvascular complications of DM, including nephropathy, neuropathy and retinopathy [9]. Furthermore, inflammatory cells play a major role in macrovascular complications such as atherosclerosis. These conditions are also mediated by a number of other factors including sustained hyperglycaemia, cytokines, growth factors, AGEs (advanced-glycation end-products) and ROS (reactive oxygen species), which also play a role in the development of heart disease [10]. The complexity of each of these pathologies renders effective treatment difficult with many conditions becoming debilitating and potentially life threatening if left undiagnosed. Compounding the issue is the increased time between disease onset and clinical diagnosis due to the time required for patient-observed effects to be realized. The collective severity and complexity of diabetic complications thus require not only a greater understanding of the inherent molecular mechanisms, but also more specific therapies and better more sensitive detection systems.

In recent times, a novel class of non-coding RNA, miRNAs (microRNAs), have been found to be expressed in all tissues and play important roles in tissue homeostasis and disease progression [11,12]. Furthermore, these non-coding RNAs are found to circulate in most bodily fluids and thus have the potential to be utilized as biomarkers for disease susceptibility and onset. The aim of the present review is to illustrate the importance of miRNAs in diabetic complications along with current therapeutic developments and biomarker utilization.

## miRNA BIOGENESIS AND FUNCTION

miRNAs, in particular *lin-4*, were first reported by Chalfie et al. [13] 30 years ago as developmental regulators in *Caenorhabditis*

*elegans*, although their mechanistic nature was unknown at the time. Work concurrently published 10 years later by Wightman et al. [14] and Lee et al. [15] demonstrated that *lin-4* produced a small non-coding RNA molecule that bound and regulated the translational activity of a well-studied developmental gene, *lin-14*. Despite this, miRNAs were considered an anomaly of the worm until 2001 when Lagos-Quintana et al. [16] reported the presence of 19 miRNAs in humans and 14 in *Drosophila melanogaster*, indicating that miRNAs are indeed an evolutionarily conserved regulatory molecule. The proceeding years have seen a flurry of research regarding miRNA structure, function and biogenesis, which has also demonstrated solid evidence that miRNAs are important in developmental regulation, tissue maintenance and disease pathology.

Genomic organization and biology of miRNAs are rather complex and few clearly defined patterns have yet to emerge. Despite the possibility of being intergenic or intragenic, possessing their own promoter or being under transcriptional control of the gene they reside in, and being the sole miRNA in a primary transcript or one of many clustered miRNAs, it is known that all miRNAs are initially transcribed by RNA polymerase II and the initial primary miRNA transcript is 5'- and 3'-processed as conventional mRNA [17]. Transcript hairpins are recognized and recruited to the microprocessor complex by DGCR8 (DiGeorge syndrome critical region 8) where they are cleaved from the pri-miRNA by Drosha to form ~70 nt precursor-miRNA hairpin structures [18]. These are exported from the nucleus by the Ran-GTP/exportin 5 complex and the stem-loop structure cleaved by Dicer, forming a ~22 nt double-stranded RNA molecule. The thermodynamic stability of the duplex is responsible for mature strand selection and loading into the RISC (RNA-induced silencing complex) by Ago (Argonaute) proteins; however, the precise mechanisms of strand selection are still unclear as opposing strands may be loaded at different times in different tissues [19]. Regardless of which strand is loaded, it is the type of binding that determines the mechanism of translational repression.

Once loaded into RISC, miRNAs direct the complex to the target transcript via sequence complementarity between the miRNA seed sequence and the MRE (miRNA recognition element) in the target transcript [17]. MREs are predominately located in the 3'-UTRs (untranslated regions) of mammalian mRNA; however, there is evidence indicating that miRNAs can also mediate translational repression via binding 5'-UTRs or coding sequences [20,21]. However, for the purposes of the present review, only translational repression via 3'-UTR interaction will be considered. In this setting, during instances of complementary binding between the miRNA seed sequence and the MRE, Ago2 becomes activated cleaving the UTR and generating endonuclease entry points, thus decreasing transcript copy numbers [22]. In instances of incomplete complementarity between the miRNA seed sequence and MRE, Ago1 becomes activated and mediates translational repression via a number of different mechanisms. These may include binding of the 5' cap via a 7MeG motif in Ago1, disruption of the ribosomal complex formation, premature ribosomal drop-off, co-translational degradation of nascent peptides or even poly-A tail destabilization thus preventing Poly-A-binding protein interaction and therefore mRNA

**Table 1** miRNAs involved in pancreatic  $\beta$ -cell loss, damage and dysfunction

PDGFRA, PDGF receptor A; CDK6, cell division protein kinase 6; SHP2, Src homology 2 domain-containing protein tyrosine phosphatase 2; PTPN22, protein tyrosine phosphatase, non-receptor type 22; DUSP5/6, dual-specificity phosphatase 5/6.

miRNA	Change in diabetes	Target(s)	Net result	Reference(s)
<i>miR-342*</i>	Down	PDGFRA	T <sub>reg</sub> cell dysfunction and autoimmune development	[27], <a href="http://diana.cslab.ece.ntua.gr/">http://diana.cslab.ece.ntua.gr/</a>
		BMP2	T <sub>reg</sub> cell dysfunction and autoimmune development	
		EP300	Increased NF- $\kappa$ B signalling and inflammation	
<i>miR-510</i>	Up	?	~100-fold increase observed in diabetic T <sub>reg</sub> cell populations	[27]
<i>miR-191</i>	Down	CDK6	Increased T <sub>reg</sub> cell proliferation	[27], <a href="http://diana.cslab.ece.ntua.gr/">http://diana.cslab.ece.ntua.gr/</a>
<i>miR-181a</i>	Up	SHP2	Increased T-cell sensitivity and selection due to derepression of selection pathways	[28]
		PTPN22		
		DUSP5/6		
<i>miR-375</i>	Up	Mtpn	Decreased insulin vesicle trafficking and membrane fusion	[30]
		PDK1	Decreased glucose responsiveness	[31]
<i>miR-124a</i>	Up	FOxa2	Modulates inverse glucose/insulin responsiveness	[33]
<i>miR-9</i>	Up	Onecut2	Decreased insulin secretion via granulophilin	[33]
<i>miR-96</i>	Up	?	Increased granulophilin expression with decreased insulin secretion	[33]
<i>miR-200</i>	Down	EP300	Increased NF- $\kappa$ B signalling and inflammation	<a href="http://diana.cslab.ece.ntua.gr/">http://diana.cslab.ece.ntua.gr/</a>

\*Predicted targets belong to *miR-342-3p*, but the authors [27] do not specify which strand was altered in diabetes.

circularization. A number of these repressive mechanisms do not always result in transcript degradation thus explaining the observance of decreased protein in the presence of unaltered transcript levels.

Repressive mechanisms of miRNAs are clearly diverse as are their interactive patterns. Owing to the relatively short 8 nt seed regions present in miRNA, a single miRNA may have hundreds of targets [17]. Furthermore, a single mRNA may be targeted by multiple miRNAs, with some MREs being targeted by families of miRNAs that may be differentially regulated within cell types or tissues. There are currently over 2000 human miRNAs listed with miRBase, which are estimated to regulate up to 60% of known coding transcripts [23]. The sheer number of miRNAs combined with their vast target ranges has resulted in miRNAs being implicated in many diseases, including the complications of DM [24]. Despite the difficulties inherent in research of such complex regulatory networks, a number of miRNAs have emerged as important regulators of particular aspects of disease pathology in diabetic complications, with some exhibiting therapeutic potential or the possibility to act as biomarkers for non-invasive disease detection.

## miRNA IN INSULIN PRODUCTION AND SIGNALLING

The major defining manifestation of DM is either defective production of or response to insulin. Inflammation plays an important role in the development of these pathological states, which result in an inability to regulate serum glucose concentrations [6]. The resulting chronic hyperglycaemic state drives many of

the complications observed in patients with DM. Beyond hyperglycaemia, inflammatory signalling, in conjunction with cells mediating such signals, plays a role in the development and progression of these complications [25]. Although immune cells such as macrophages and T-cells generally act to maintain tissue health and architecture, in states of chronic activation, as seen in obesity-related diabetes, these cells become instigators of disease rather than preventers [9]. This occurs due to secretion of cytokines from cells directly and indirectly affected by elevated serum glucose. Furthermore, once activated, these cells secrete their own cocktail of chemokines and cytokines which act to recruit further inflammatory cells in addition to activating those extant in the tissue. This is prototypically seen in atherosclerosis [26]. The role of miRNAs in the events leading to inflammatory cell activation and signalling is discussed further in regard to specific diabetic complications in each section of the present review. With respect to insulin itself, in T1DM (Type 1 DM), loss of insulin production is rendered through modified secretion levels or via autoimmune destruction of pancreatic islet  $\beta$ -cells. Conversely, in T2DM, metabolic tissues are the drivers of decreased insulin sensitivity via systemic inflammatory signalling [27–29]. The complexity of these processes, combined with the array of cell types involved, provide ample opportunity for miRNA involvement (Table 1 and Table 2).

## miRNAs in $\beta$ -cell loss and insulin secretion

The destruction of  $\beta$ -cells is typically an event restricted to T1DM and is an event that occurs in early life and is mediated by T<sub>reg</sub> cells (regulatory T-cells) [30]. Interestingly, a subset of diagnosed T2DM is found to possess autoantibodies against the islet marker glutamic acid decarboxylase with the condition consequently

**Table 2** miRNAs involved in the development of insulin resistance, both systemically and locally, in metabolic tissues

miRNA	Change in diabetes	Target(s)	Net result	Reference(s)
<i>miR-103</i>	Up	?	Increased adipogenesis and adipose tissue expansion	[35]
<i>miR-107</i>	Up	?	Increased adipogenesis and adipose tissue expansion	[35]
<i>miR-181d</i>	–	See reference	Exogenous expression decreases intracellular lipid droplet formation in hepatocytes	[36]
<i>miR-24</i>	Down	p38	Up-regulation of TNF $\alpha$ -induced insulin resistance	[33,38]
<i>miR-125b</i>	Up	TNFAIP3	Increased NF- $\kappa$ B signalling and inflammation	[43]
	Up	IRF4	Increased M1 macrophage activation	[40]
<i>miR-144</i>	Up	IRS1	Decreased intracellular insulin signalling	[44]
<i>miR-181</i>	Up	IRS2	Decreased intracellular insulin signalling	<a href="http://diana.cslab.ece.ntua.gr/">http://diana.cslab.ece.ntua.gr/</a>
<i>miR-200a</i>	Down	?	Increased flux through p38 $\alpha$ and JNK pathways and decreased insulin signalling; c-Jun may be involved	[45,46]

labelled as latent autoimmune diabetes of adults [31]. miRNAs have been shown to be dysregulated in T<sub>reg</sub> cell populations in human T1DM and may play a role via a number of targets [32]. In particular, *miR-342* is down-regulated and is predicted to target the NF- $\kappa$ B (nuclear factor  $\kappa$ B) regulator EP300 in addition to BMPR2 (bone morphogenetic protein receptor 2) and the  $\alpha$ -peptide of PDGF (platelet-derived growth factor) receptor. The same study demonstrated decreased *miR-191* and increased *miR-510* expression, although the role of these miRNAs in T<sub>reg</sub> cell populations is unclear. Interestingly, the *miR-200* family, which is known to be down-regulated in a number of cell types in DM, also targets EP300. *miR-181a* has also been implicated in autoimmunity via regulation of a number of phosphatases known to negatively control T-cell sensitivity and thus clonal selection [33]. Although this role has not been shown to be relevant in autoimmune-mediated  $\beta$ -cell destruction, it is interesting to note that *miR-181a* is up-regulated in serum of diabetic patients [34].

There is little to link inflammation and insulin secretion itself aside from the processes mentioned above. However, insulin secretion may be altered by pancreas-specific miRNA such as *miR-375*, whose expression is inversely correlated with insulin levels [35]. This miRNA targets Mtpn (myotrophin), which is involved in vesicular transport in both neurons and  $\beta$ -cells. Regulation of PDK1 (phosphoinositide-dependent kinase 1) by this miRNA also alters glucose-mediated insulin secretion [36]. Indeed, *miR-375* is elevated in islets of obese diabetic mice [37]. This miRNA also appears to play a role in  $\beta$ -cell development as its deletion in the same model results in decreased  $\beta$ -cell mass and subsequent insulin deficiency. Further miRNAs involved in insulin secretion include *miR-124a*, *miR-9* and *miR-96* [38]. *miR-124a* plays an interesting role in that it greatly increases insulin secretion at low glucose concentrations yet results in decreased glucose-stimulated insulin release at higher concentrations. This is thought to occur via targeting of FOXa2 (forkhead box a2) which regulates PDX1 (pancreatic and duodenal homeobox 1) activity thereby modulating insulin signalling. Granulophilin, a negative regulator of insulin secretion, is derepressed by direct targeting of Onecut-2 by *miR-9*. *miR-96* also decreases insulin secretion by up-regulating granulophilin, albeit in an Onecut-2-independent manner.

### miRNA and insulin resistance

Insulin resistance is the mitigating factor in T2DM and is driven by the liver, skeletal muscle and adipose tissue: the major metabolic tissues of the body [6]. Circulating NEFAs (non-esterified 'free' fatty acids), at least in the case of obesity-induced DM, are the primary instigator of insulin resistance in all three tissues. NEFAs are taken up by adipocytes which swell and constrict blood supply, resulting in necrotic regions within adipose tissue [39]. *miR-103* and *miR-107*, which are up-regulated in obese individuals, accelerate adipocyte differentiation and growth, thus contributing to adipose growth [40]. These regions subsequently recruit and induce transformation of macrophages to the inflammatory M1 phenotype further, contributing to inflammation-mediated insulin resistance. In the liver, hepatocytes undergo steatosis in response to increased NEFAs and secrete cytokines responsible for the generation of the M1 phenotype of Kupffer cells. Importantly, *miR-181d* was identified in high-throughput screening of human hepatocytes as an miRNA that controls intracellular lipid droplet formation [41]. Although cytokine secretion was not analysed in that study, it is likely that hepatic delivery of *miR-181d* would improve systemic insulin responsiveness. Again, in skeletal muscle, increased NEFAs result in intramyocellular lipid accumulation. Here, lipid accumulation leads to increased ceramide production with subsequent activation of NF- $\kappa$ B pathways and secretion of inflammatory cytokines [42]. This leads to increased macrophage infiltration and activation, which, in conjunction with modifications to insulin signalling described below, contribute to insulin resistance. However, increases in macrophage activity as a result of circulating cytokines from the liver and adipose tissue, in particular TNF $\alpha$  (tumour necrosis factor  $\alpha$ ), may induce insulin resistance via p38 [43]. This MAPK (mitogen-activated protein kinase) is also increased by hyperglycaemia and is a direct target of *miR-24*, which is down-regulated in similar conditions [38]. This potentially leads to potent increases in p38 signalling and the vast array of processes it mediates. In addition to secondary activation due to changes in the local environment, macrophages can become classically activated by NEFAs directly binding TLR4 (Toll-like receptor 4) and inducing the signalling cascades described below [6]. Regardless, the inflammatory states of these tissues in obesity result in localized and

systemic insulin resistance via common intracellular signalling pathways.

Hyperglycaemia and ROS, leading to ER (endoplasmic reticulum) stress, NEFAs and hyperlipidaemia, along with local and circulating inflammatory cytokines, all activate JNK1 (c-Jun N-terminal kinase 1) and IKK $\beta$  (inhibitor of NF- $\kappa$ B kinase  $\beta$ ) and their signalling pathways [6]. These kinases potentially inhibit insulin activity, thus inducing insulin resistance, via serine phosphorylation of IRS (insulin receptor substrate) 1/2 and also activate AP-1 (activator protein-1) and NF- $\kappa$ B [44]. These transcription factors further induce the production and secretion of inflammatory cytokines from both immune and non-immune cells. The nature of miRNAs lends them to possible involvement in numerous stages of inflammation-mediated insulin resistance from M1 macrophage differentiation to modulation of the insulin signalling cascade. *miR-125b* seems to increase M1 macrophage polarization via direct targeting of IRF4 (interferon regulatory factor 4) thus increasing IFN (interferon)- $\gamma$  signalling [45]. Adipose tissue from obese individuals display elevated levels of *miR-125b* [46]. Owing to the role of IFN- $\gamma$  in regulating IL (interleukin)-1 $\beta$  expression and M1 activation, this miRNA may play an important role  $\beta$ -cell dysfunction, loss and inflammation [47]. Furthermore, this miRNA may promote the production of pro-inflammatory cytokines and thus insulin resistance in metabolic tissues through constitutive activation of NF- $\kappa$ B via direct targeting of TNFAIP3 (TNF $\alpha$ -induced protein 3) [48]. Additionally, *miR-125b* is up-regulated in VSMCs (vascular smooth muscle cells) from diabetic mice, thus potentially contributing to systemic insulin resistance.

*miR-144* has been shown to target IRS1 in diabetic rat models and the *miR-181* family is predicted to target IRS2, thus potentially generating co-ordinated repression of insulin signalling [49]. Decreased *miR-200a* has been shown to increase flux within the p38 $\alpha$  and JNK pathways in response to oxidative stress, which may further contribute to insulin resistance [50,51]. Furthermore, this miRNA is known to be down-regulated in a number of diabetic tissues. *miR-200a* is also predicted to target c-Jun, although this interaction is yet to be investigated. Regardless, it can be seen that miRNAs are involved in various stages of insulin secretion,  $\beta$ -cell destruction, macrophage-mediated inflammation and insulin resistance all of which contribute to the hallmark DM manifestation of chronic hyperglycaemia. It is this state, in conjunction with continued inflammatory signalling and activity, that results in a set of debilitating pathological conditions collectively known as diabetic complications.

## miRNA IN MICROVASCULAR COMPLICATIONS

### Retinopathy

A number of inflammatory markers have been identified within the vitreous and retinas of diabetic rats and patients, including TNF $\alpha$ , IL-1 $\beta$  and CXCL10 (CXC chemokine ligand 10) among others [52]. These indicate activation and a clear involvement of M1 macrophages. Indeed, Kovacs et al. [53] presented a set of

up-regulated NF- $\kappa$ B-responsive miRNAs in the retina of diabetic rats that may act as a biomarker profile, which included *miR-146a/b*, *miR-155*, *miR-132* and *miR-21* (Table 3). Of these, *miR-155* is known to be involved in immunomodulatory signalling, *miR-146a/b* and *miR-21* are involved in fibrotic responses and *miR-132* is involved in angiogenesis [54–56]. *miR-146a* has also been shown to regulate fibronectin production in retinal epithelial cells [57]. That study also demonstrated these changes in whole retina, kidney and heart. These processes collectively result in progressive vitreous haemorrhaging, protein leakage and scarring in conjunction with uncontrolled neovascularization within the retina, ultimately resulting in fibrosis driven detachment and blindness [52].

Despite this, little work has been produced on miRNA and inflammatory responses in the retina, although it is likely that miRNAs involved in inflammation in metabolic tissue will be important in the retina especially those involved in macrophage activation and recruitment. Indeed, *miR-200b* has been implicated in diabetic retinal pathology via direct targeting of VEGF (vascular endothelial growth factor) as proposed by Kantharidis et al. [24] and McArthur et al. [58]. This growth factor, although not immune-related, plays an important role in retinopathy and, indeed, all microvascular complications owing to stimulation of neovascularization. In the case of retinopathy, this results in vitreous haemorrhage [52].

VEGF is up-regulated in response to localized hypoxia which occurs under hyperglycaemia due to increased oxygen consumption and flux through the electron transport chain [59]. Kantharidis et al. [24] have also postulated the involvement of the *miR-29* family in the regulation of VEGF and, although this is yet to be shown, a recent report by Kovacs et al. [60] indicates that the *miR-29* family is down-regulated in retinal epithelial cells of diabetic rats. That report also indicated that *miR-126* was also down-regulated; *miR-126* has been shown to regulate a number of angiogenic factors in response to oxygen-induced retinopathy [61]. Other miRNAs decreased in the retina, as reported by Kovacs et al. [60], that are also involved in other tissues include *miR-181a* and *miR-125b* in addition to *miR-21*, which will be discussed in later sections and probably contributes to retinal detachment due to its role in fibrosis [34,45,46,54].

### Neuropathy

Neuropathy is another debilitating complication of DM often resulting in pain or numbness in the hands and feet [62]. Impaired wound healing and circulation can also result in ulceration and often in amputation. Much research has been conducted into neuropathy due to its high prevalence among diabetic patients. The condition primarily appears to be generated by hyperglycaemia, leading to vascular damage and subsequent ischaemia of surrounding tissues as seen in adipose tissue [63]. This inevitably results in secretion of immunomodulatory cytokines from the affected tissue with subsequent recruitment and activation of macrophages [64]. However, as with retinopathy, both immunological and post-transcriptional regulatory mechanisms of disease pathology have been somewhat neglected in peripheral nerve pathologies to the extent of a complete absence of publications on miRNAs outside entrapment neuropathies.

**Table 3** miRNAs involved in retinal damage during diabetic retinopathy

IRAK1, IL-1-receptor-associated kinase 1; TRAF6, TNF-receptor-associated factor 6; SOCS, suppressor of cytokine signalling; RASA1, RAS p21 protein activator 1.

miRNA	Change in diabetes	Target(s)	Net result	Reference(s)
<i>miR-146a/b</i>	Up	IRAK1 TRAF6	Ectopic expression inhibits NF- $\kappa$ B and IL-1 $\beta$ signalling	[48,49]
<i>miR-155</i>	Up	SOCS1	Collectively up-regulate cytokine production, including TNF $\alpha$	[50]
<i>miR-132</i>	Up	SHIP1 RASA1	Increased angiogenesis via derepressed MAPK signalling	[51]
<i>miR-21</i>	Up	PTEN	Up-regulation of Akt, resulting in increased matrix expansion	[49]
<i>miR-200b</i>	Down	VEGF	Increased angiogenesis and neovascularization	[52]
<i>miR-29</i>	Down	Collagens Lamins VEGF	Increased matrix deposition and retinal fibrosis Increased angiogenesis and neovascularization	[24,54], <a href="http://diana.cslab.ece.ntua.gr/">http://diana.cslab.ece.ntua.gr/</a>
<i>miR-126</i>	Down	VEGF IGF-2	Increased angiogenesis and neovascularization	[54,55]
<i>miR-181a</i>	Down	TNF $\alpha$	Increased macrophage maturation and inflammation	[54], <a href="http://diana.cslab.ece.ntua.gr/">http://diana.cslab.ece.ntua.gr/</a>
<i>miR-125b</i>	Down	?	Decreased expression may be protective (see insulin resistance)	[40,54]

Therefore the role of miRNA may only be postulated based upon what is known about inflammation in other microvascular complications, such as retinopathy and nephropathy. For example, any number of the NF- $\kappa$ B-responsive miRNAs identified by Kovacs et al. [53] may be of importance in neuropathic inflammation. Hyperglycaemia also induces secretion of IL-1 $\beta$ , MCP (monocyte chemoattractant protein)-1 and TNF $\alpha$  in neuropathic tissue lines, suggesting the involvement of M1 macrophage activation and consequentially the miRNAs involved in this process [64]. Furthermore, *miR-214*, along with *miR-21*, has been shown to target PTEN (phosphatase and tensin homologue deleted on chromosome 10) in the kidney and may therefore also drive inflammatory gene expression and signalling through the NF- $\kappa$ B pathways in diabetic neuropathies [65].

Vascular endothelial cells are also at risk of dysfunction due to hypoxia, as in retinopathy, which leads to nephropathic devascularization [63]. VEGF and its regulating miRNAs therefore are attractive targets for treatment. Indeed, a clinical trial for intramuscular VEGF gene delivery presented promising results, improving sensory and pain measurements in a significant number of subjects [66]. However, VEGF treatment also increased the number of adverse events such as epistaxis, excoriation and peripheral oedema. Importantly, no increases in extant retinopathy were observed. Owing to the 'softer' gene regulatory actions of miRNAs, VEGF-associated miRNAs may prove a novel therapeutic option with the potential to overcome the issues observed with VEGF gene delivery. Additionally, TGF $\beta$  (transforming growth factor  $\beta$ ) has been associated *in vivo* and *in vitro* in both neuronal function and growth respectively [67]. As will be discussed below, TGF $\beta$  mediates the expression of a large number of miRNAs, further expanding the potential therapeutic targets and molecular pathways involved in neuropathy [24]. Regardless, it is clear

that much work is needed to elucidate the role of miRNAs in the pathogenic mechanisms of diabetic neuropathy.

### Nephropathy

It is becoming clear that inflammatory cells, in particular macrophages, play an important role in diabetic nephropathy [68]. As seen in other tissues, macrophages are activated by a host of signals, including NEFAs, IFN- $\gamma$  and IL-1 $\beta$ . It is thus evident that many of the miRNAs discussed above potentially play a role in nephropathic inflammation. Once activated, M1 macrophages secrete a plethora of pathogenic factors, such as TNF $\alpha$ , IL-1 $\beta$ , ROS, PAI (plasminogen-activator inhibitor)-1, TGF $\beta$  and PDGF, which act upon various renal cell types to exacerbate inflammatory pathology via various signalling cascades. Furthermore, macrophage activation and accumulation have been associated with glomerular sclerosis in human biopsies and also correlated with proteinuria and elevated serum creatinine [69]. These predominantly glomerular dysfunctions are driven by a number of pathological processes such as podocyte effacement and mesangial expansion [70]. However, TIF (tubulointerstitial fibrosis) also contributes to glomerular dysfunction via tissue remodelling.

TIF may be driven by any number of factors, including AGes, ROS, various cytokines and growth factors, of which TGF $\beta$  is considered a major player [71]. Furthermore, TGF $\beta$  is considered a primary driving force in mesangial expansion, podocyte loss and effacement, all of which are also contributed to via TIF. This potent factor mediates EMT (epithelial-mesenchymal transition) in TECs (tubular epithelial cells), resulting in increased ECM (extracellular matrix) production, decreased ECM turnover, increased motility and invasive potential [72]. Of particular interest, TGF $\beta$  is known to regulate a number of miRNAs that have been shown to regulate various fibrotic processes [24]. Additionally,

**Table 4** miRNAs involved in dysfunction of various renal cell types contributing to diabetic nephropathy

miRNA	Change in diabetes	Target(s)	Net result	Reference(s)
<i>miR-200</i>	Down	ZEB2 TGF $\beta$ 2	Decreased E-cadherin expression, leading to increased EMT Feed-forward up-regulation of TGF- $\beta$ -mediated fibrotic signalling	[67, 68]
<i>miR-29</i>	Down	Collagen Lamins	Increased ECM deposition and fibrosis	[70], <a href="http://diana.cslab.ece.ntua.gr/">http://diana.cslab.ece.ntua.gr/</a>
<i>miR-192</i>	Up	ZEB2	Derepression of E-box elements in collagen promoters	[72,73]
	Down	ZEB2	E-cadherin repression and increased EMT	[71,74]
<i>miR-215</i>	Down	ZEB2	E-cadherin repression and increased EMT	
<i>miR-216a</i>	Up	YB-1	Increased Col1a2 expression via increased transcript maturation	[24]
<i>miR-216a</i>	Up	PTEN	Increased Akt signalling, mesangial cell survival and hypertrophy	[75]
<i>miR-217</i>				
<i>miR-21</i>	Up	SMAD7 PDCD4	Up-regulation of TGF- $\beta$ -mediated fibrotic events Enhancement of podocyte apoptosis and decreased TEC apoptosis	[77,79,80]
<i>miR-377</i>	Up	?	Decreased SOD1 expression, and increased ROS levels and fibronectin production	[81]
		PAK1	Increased cell motility, increased fibronectin production	
<i>miR-93</i>	Down	VEGF	Increased angiogenesis and neovascularization	[49]

some of these miRNAs are involved in feedback loops which regulate TGF $\beta$  itself.

A number of miRNAs have emerged as important members in the pathogenesis of T1F, some of which have already been discussed in the context of other tissues (Table 4). In particular, the *miR-200* family, which is involved in inflammatory signalling and angiogenesis, has been shown to be involved in EMT and consequential collagen deposition via the targeting of ZEB2 (zinc finger E-box-binding homeobox 2), a major regulator of E-cadherin expression [73]. This miRNA is down-regulated by TGF $\beta$ 1/2, of which TGF $\beta$ 2 is a direct target [74]. In times of transient TGF $\beta$ 2 up-regulation, this therefore creates the opportunity for a rapid and co-ordinated feed-forward up-regulation of TGF $\beta$ 2 signalling and fibrosis. Interestingly, exogenous *miR-200a* was able to down-regulate SMAD-dependent TGF $\beta$ -mediated ECM production in a previous study, which probably occurs via the repression of TGF $\beta$ 2 expression.

SMAD3, but not SMAD2, has been shown to mediate fibrotic signalling in the diabetic kidney [75]. Accordingly, in addition to regulation of the *miR-200* family, both the *miR-29* family and *miR-192* are also regulated by SMAD3 and regulate ECM production and ZEB1/2 translation respectively [76,77]. The *miR-29* family directly targets a long list of collagens, lamins and other ECM components and is itself down-regulated by TGF $\beta$  signalling, thus resulting in increased ECM accumulation. Findings on the role of *miR-192* in DN (diabetic nephropathy) vary depending on the animal model utilized or the cell type analysed. For example, streptozotocin-induced diabetic *db/db* mice displayed increased expression of *miR-192* with congruent increases in renal damage [78]. The proposed mechanism for this phenotype involves ZEB2 down-regulation in mesangial cells as a response to TGF $\beta$ , resulting in increases in collagen ex-

pression and mesangial expansion. In a rat 5/6 nephrectomy model, *miR-192* and renal damage were shown to be decreased by SMAD3, but not SMAD2 deletion, further supporting a role for increased *miR-192* via SMAD3 signalling in DN [79]. Conversely, decreased expression of *miR-192* has been observed in patients with advanced DN compared with those with early disease pathology [80]. Additionally, decreased expression of this miRNA, along with *miR-215*, has been demonstrated in TECs in response to TGF $\beta$ , resulting in decreased E-cadherin expression via increased ZEB2 [77]. These changes resulted in the progression of TECs to an EMT phenotype with increased fibrogenesis. Interestingly, CTGF (connective tissue growth factor) has also been shown to increase *miR-192* in TECs, therefore leading to decreased ZEB1/2 expression. Although this restored E-cadherin expression, fibrosis was not altered due to derepression of collagen expression. These confounding data further highlight cell-specific miRNA regulation and indicate that analysis of tissue lysates is not sufficient for characterization of miRNA function in disease.

Other miRNAs documented to play a role include *miR-216a*, *miR-377*, *miR-93* and *miR-21*. *miR-216a* is induced by TGF $\beta$  via *miR-192*, which also regulates *miR-217* [81]. *miR-216a* and *miR-217* directly target PTEN, leading to increases in Akt signalling which may result in increased inflammation, proliferation, cell survival and protein synthesis. Interestingly, *miR-21* targets PTEN and also leads to decreased mesangial expansion in *db/db* mice [82]. *miR-21* has also been implicated in the regulation of TGF $\beta$  signalling in a number of animals of T1F and associated renal dysfunction. In one such model, SMAD7 overexpression in the rat unilateral ureteral obstruction model has restored *miR-21* expression to normal levels with congruent improvements in renal pathology [83]. In line with a pro-fibrotic role for *miR-21*,

**Table 5** miRNAs involved in various cell types in the development and progression of diabetes-related atherosclerosis  
AT<sub>1</sub>R, angiotensin II type 1 receptor; LOX-1, lipoxigenase-1.

miRNA	Change in diabetes	Target(s)	Net result	Reference(s)
<i>miR-34a</i>	Up	Sirt1	Cell-cycle arrest in endothelial cells and atherogenic phenotype	[85,86]
<i>miR-155</i>	Down	AT <sub>1</sub> R	Increased angiotensin signalling, inflammation, vasoconstriction, vascular hypertrophy and decreased migration	[87,88]
		Ets-1	Increased macrophage infiltration and inflammation	
		MyD88	Increased macrophage activation	[88,89]
		CD36	Increased macrophage uptake of oxLDL via indirect derepression of scavenger receptors listed	[88,90]
		CD68		
		LOX-1		
<i>miR-125a/b</i>	Up	ET-1	Increased expression is protective and prevents vasoconstriction	[91]
<i>miR-125a</i>	Up	ORP9	Increased oxLDL uptake by macrophages and increased inflammation	[92]
<i>miR-125b</i>	Up	Suv39h1	Loss of H3K9 trimethylation and derepression at IL-6 and MCP-1 promoters, leading to increased inflammation	[93]
<i>miR-21</i>	Up	PTEN	Increased endothelial cell proliferation	[84,94]
		PDCD4	Increased endothelial cell survival	
		RhoB	Decreased endothelial cell migration	
<i>miR-27</i>	Up	See reference	Appears to be involved in all aspects of atherogenic disease	[95]
<i>miR-221</i>	Up	p27	Increased endothelial cell proliferation and angiogenesis	[84]
		p57		

up-regulation of this miRNA is inhibited by SMAD3 deletion in an obstructive nephropathy model [84]. Furthermore, regulation of PDCD4 (programmed cell death protein 4) by *miR-21* enhances podocyte apoptosis and loss in conjunction with increased TEC survival against growth arrest signals [85,86]. Collagen 1 $\alpha$ 2 is also regulated by *miR-216a* through regulation of YB-1 (Y-box-binding protein-1), which acts to sequester and decrease mRNA maturation [24]. VEGF is again regulated in DN by *miR-93*, which is decreased by TGF $\beta$ , possibly independently of SMAD3 [54]. Finally, oxidative stress may be increased in the kidney via the up-regulation of *miR-377*, which indirectly down-regulates SOD1 (superoxide dismutase 1), leading to increased ROS [87]. PAK1 (p21-activated kinase 1) is also down-regulated by *miR-377*, potentially regulating cell motility. Furthermore, down-regulation of these two proteins has also been associated with increased fibronectin expression, an important constituent of the ECM.

## miRNA IN MACROVASCULAR COMPLICATIONS

### Atherosclerosis

It is well accepted that atherosclerosis is predominately generated by immune responses mediated by macrophages and T-cells [88]. These cells infiltrate the arterial intima as a result of endothelial dysfunction induced by both high glucose and high levels of circulating LDL (low-density lipoprotein) infiltrating the sub-endothelial layer. Sub-intimal LDL subsequently is oxidized, generating further endothelial dysfunction. Macrophages are recruited in an attempt to clear oxLDL (oxidized LDL) and

restore tissue architecture [26]. However, the majority of these cells, due to excessive LDL loading, become foam cells, which eventually rupture depositing further cholesterol and fatty acids. This deposition becomes encased within a fibrotic cap, thus generating the atherosclerotic plaque which is incapable of repair [88]. Immune cells continue to infiltrate the plaque due to both endothelial and immune cell signalling, which eventually leads to aortic constriction, restenosis or thrombus. Not surprisingly, miRNAs have been shown to be involved in various stages of atherosclerotic plaque development (Table 5).

The number of miRNAs implicated in atherosclerosis and its various stages is staggering and has been recently reviewed extensively [89]. Of particular interest are those that are involved in initial endothelial cell dysfunction and those that regulate attraction and infiltration of macrophage and T-lymphocytes. Endothelial senescence is observed in advanced atherosclerotic plaques and is associated with increased levels of *miR-34a* [90]. Senescence is partially mediated by direct targeting of Sirt1 (sirtuin 1), a deacetylase whose restoration possesses therapeutic potential through modulation of cell-cycle control [91]. *miR-155*, which is decreased in serum of patients with coronary artery disease, is involved in vascular endothelial inflammation and cell migration by targeting the AngII (angiotensin II) receptor and Ets-1, resulting in decreased T-cell adhesion and vascular remodelling respectively [92,93]. This miRNA is also implicated in macrophage differentiation via MyD88 (myeloid differentiation factor 88) regulation [94]. Additionally, *miR-155* can also attenuate macrophage oxLDL uptake, thereby down-regulating the expression of inflammatory cytokines [95]. Collectively, this multifactorial miRNA presents itself as an attractive target for therapeutic targeting in atherosclerosis and microvascular diabetic complications.

**Table 6** miRNA involved in the symptoms and development of diabetic cardiomyopathy  
ERK, extracellular-signal-regulated protein kinase; IGFR, IGF-receptor.

miRNA	Change in diabetes	Target(s)	Net result	Reference(s)
<i>miR-133</i>	Down	CTGF	Increased myoblast-mediated interstitial fibrosis and hypertrophy	[100]
	Up	ERG	Long QT interval and contractile dysfunction	[24]
<i>miR-320</i>	Up	VEGF	These predicted targets may lead to decreased reparative capacity, ischaemic injury, reduced oxidative stress capabilities and increased fibrosis	[101,103]
		FGF		
		IGF-1		
<i>miR-29</i>	Down	Collagens Lamins	Increased myoblast-mediated ECM deposition and fibrosis	[99], <a href="http://diana.cslab.ece.ntua.gr/">http://diana.cslab.ece.ntua.gr/</a>
<i>miR-30</i>	Down	CTGF	Increased myoblast-mediated interstitial fibrosis and hypertrophy	[100]
<i>miR-21</i>	Up	Spry1	Increased ERK signalling, myoblast survival and activity	[98]
		PDCD4	Increased myocyte growth, proliferation and anti-apoptosis	
		PTEN	Cellular hypertrophy, cell survival and anti-apoptosis	
<i>miR-206</i>	Up	HSP60	Prevents cardiomyocyte apoptosis	[101]
<i>miR-1</i>	Up	IGF-1	Increased glucose-induced apoptosis	[102]
		IGFR	Increased apoptosis	
		Bcl-2		

*miR-125a/b* is also involved in inflammation via the regulation of oxLDL-induced ET (endothelin)-1 expression [96]. Macrophage lipid uptake is decreased by *miR-125a* targeting ORP9 (oxysterol-binding-protein-related protein 9), which also results in decreased cytokine secretion [97]. Additionally, *miR-125b* targets the histone methyltransferase Suv39h1 and is increased in VSMCs from *db/db* mice [98]. Decreased Suv39h1 results in a loss of repressive H3-Lys<sup>9</sup> (histone H3 at Lys<sup>9</sup>) trimethylation at certain promoters. Specifically, IL-6 and MCP-1 displayed increased expression in VSMCs as a result of increased *miR-125b*, potentially increasing aortic inflammation and thus atherosclerosis. Indeed, *in vitro* delivery of *miR-125b* resulted in increased MCP-1-mediated macrophage binding to cell monolayers. The *miR-125* isoforms thus generate macrophage dysfunction and invasion. Furthermore, the epigenetic mechanisms of histone modification and RNAi are linked in a novel mechanism involving *miR-125b*. In endothelial cells, the negative cell-cycle regulators p27 and p57 are targeted by increased levels of *miR-221*, resulting in increased cell proliferation and angiogenesis [89]. Endothelial cell proliferation and survival is increased further by up-regulated *miR-21* targeting PTEN and PDCD4 respectively. *miR-21* is also involved in cellular migration via RhoB repression [99]. *miR-27* has also been implicated in angiogenesis, NF- $\kappa$ B signalling, apoptosis, matrix deposition and PPAR (peroxisome-proliferator-activated receptor) signalling via a number of targets (see [100] for a recent review).

## Heart

Diabetic cardiac myopathy is generated by dysfunction of a number of cell types within the heart, including vascular endothelial cells, cardiomyocytes and myoblasts [101]. Additionally, increases in M1 macrophage recruitment have been detected in the myocardium, resulting in increased cytokine levels in the diabetic heart [102]. M1 activation in the heart results from cir-

culating NEFAs, resulting in TLR4 activation and thus increasing TNF $\alpha$ , IL-1 $\beta$ , IL-6 and NF- $\kappa$ B. These cytokines and transcription factors mediate the same effects as those seen in other tissues, which, in the case of the heart, results in cardiac hypertrophy, contractile dysfunction and fibrosis [101]. A number of miRNAs have been identified in these processes including *miR-133*, *miR-320*, *miR-29*, *miR-30*, *miR-1*, *miR-206* and *miR-21* (Table 6).

*miR-21* is dysregulated in a number of cardiac cell types, resulting in cardiac hypertrophy, fibrosis and heart disease in general [103]. The *miR-29* family has been shown to be dysregulated in *in vitro* myoblasts, resulting in increased collagen production thus contributing to cardiac hypertrophy and fibrosis [104]. Expression levels of these miRNAs have also been associated with interstitial fibrosis and myoblast-mediated collagen deposition *in vivo*. Another contributor to myopathy is CTGF which is subsequently derepressed by down-regulated levels of *miR-30* and *miR-133*, with *miR-133*-knockout animals exhibiting severe cardiac fibrosis [105]. Conversely, increased *miR-133* contributes to long QT syndrome, which is typically observed in diabetic patients, via direct targeting of ERG (ether-à-go-go-related gene) [24]. ERG regulates the potassium current rectifier whose perturbed expression results in the delayed repolarization of cardiomyocytes as observed in those with long QT intervals. This miRNA again highlights the complexities and challenges which need to be faced in order to resolve the true nature of miRNAs in disease pathology.

Survival of heart muscle itself is also mediated by miRNA dysregulation. Here, *miR-1*, which is increased under hyperglycaemic conditions, targets and decreases Pim1 and Hsp60 (heat-shock protein 60), leading to increased cardiomyocyte apoptosis in streptozotocin-induced diabetic mice [106]. Additionally, Hsp60 is also targeted by *miR-206*, another miRNA that is increased by hyperglycaemia. Interestingly, *miR-1* accounts for almost 40% of all reads in profiling of cardiac tissue and also

targets IGF (insulin-like growth factor)-1, IGF-receptor and Bcl-2, indicating that this miRNA and its regulation holds great importance for diabetic myopathy and cardiac stability in general [107]. Finally, *miR-320* may target a number of growth factors including VEGF, FGF (fibroblast growth factor) and IGF-1 which could lead to gross pathological signalling in the diabetic heart [106,108]. Decreases in IGF-1 and its receptor are prime candidates as mediators of decreased angiogenesis seen in the diabetic heart.

## miRNA AS BIOMARKERS FOR DIABETES AND ITS COMPLICATIONS

miRNAs have potential as non-invasive and sensitive biomarkers for various pathologies, such as heart failure and cancer [106,109]. This role is afforded by an inherent stability in biofluids such as urine and serum. It is now apparent that miRNAs are not just secreted by cells, but are chaperoned in bodily fluids by protein complexes, Argonaut proteins, lipid vesicles or HDL (high-density lipoprotein) [106]. Interestingly, HDL-miRNA secretosomes differ from that of exosome-packaged miRNA derived from serum of the same individual, suggesting that miRNA secretion is a selective and co-ordinated process [110]. Furthermore, miRNA-HDL complexes isolated from serum have predictable outcomes *in vitro*, indicating that the complexes are able to be functionally taken up by cells. It is therefore likely that miRNAs may act as a mode of communication between cells within tissues or between adjacent and distal tissues. Conversely, biofluid miRNAs may be the result of cellular death or dysfunction; however, the reproducibility of miRNA profiles from various conditions makes this unlikely. It follows that perturbation of healthy tissues, such as that seen in diabetic complications, may be identifiable via analysis of circulating miRNAs. As some miRNA changes are cell-type- or tissue-specific, serum and/or urine miRNA measurements may be able to indicate tissue dysfunction with a resolution much greater than that provided by conventional imaging techniques. Additionally, it may provide a means to determine those at risk of developing diabetic complications, enabling early intervention and subsequently improved outcomes for those with decreased insulin production or increased resistance.

To date, there have been a number of studies examining circulating miRNA profiles in patients with diabetes, comparing them with control and at-risk patients. In one of the largest of these, Zampetaki et al. [111] analysed the miRNA profiles of 80 patients with T2DM and 80 age- and gender-matched controls and revealed a defined signature that was also observed in *ob/ob* mice. This signature comprises a single overexpressed miRNA (*miR-28-3p*) and 12 underexpressed miRNAs (*miR-24*, *miR-21*, *miR-20b*, *miR-15a*, *miR-126*, *miR-191*, *miR-197*, *miR-223*, *miR-320*, *miR-486*, *miR-150* and *miR-29b*) and were able to predict development of diabetes in 70% of patients upon 10 years of follow-up. A separate study identified a different signature comprising seven up-regulated miRNAs, *miR-9*, *miR-29a*, *miR-34a*, *miR-30d*, *miR-124*, *miR-146a* and *miR-375*, in newly diagnosed

diabetic patients compared with control subjects [112]. A third group in that study comprising those deemed susceptible to diabetes by BMI, impaired glucose tolerance and a family history displayed no difference in these miRNAs compared with the control group, indicating that, at least in that study, the observed miRNAs are unsuitable for detection of the early stages of diabetes. Additionally, as that study did not utilize high-throughput methods to identify the dysregulated miRNAs, the efficacy of the suggested profile should be determined carefully.

The profile provided by Zampetaki et al. [111] raises some interesting and confounding questions. For example, decreased serum levels of *miR-21* are not in line with the expression of this miRNA in diabetic tissues [54,65,84,90,99,113]. Expression of this miRNA is increased in a number of cell types in diabetic tissues, resulting in increased inflammation, cell survival or anti-apoptosis, invasion and fibrogenic signalling. Conversely, *miR-29* family members have also been implicated in fibrotic and potentially angiogenic responses in diabetes and its decreased serum levels reflect that in studied tissues [24,60,124]. Paradoxically, increased *miR-29* expression leads to increased insulin resistance, decreased insulin secretion and signalling in metabolic tissues thereby contributing to the systemic diabetic milieu [114]. Thus maintaining insulin sensitivity may take a higher priority than that of preserving tissue architecture. The involvement of *miR-320* in angiogenic responses may also be pathogenic or protective depending on the tissue in question [106]. These discrepancies have dampened research into miRNAs as biomarkers for diabetic complications.

As with miRNA biomarkers for diabetes as a whole, present studies are also confounding when viewed in context of the tissue pathology they are detecting. For example, in urine, Neal et al. [115] measured *miR-16*, *miR-21*, *miR-155*, *miR-210* and *miR-638* with only *miR-368* displaying an increase in patients with stage 4 chronic kidney disease when compared with those with stage 3 kidney disease. Interestingly, in plasma, these miRNAs were all inversely correlated with the glomerular filtration rate compared with healthy individuals. Of these, decreases in *miR-155* have been observed in the serum of patients with coronary heart disease and therefore this miRNA may be unsuitable for specific detection of nephropathy [93]. Further complicating *miR-155* as a biomarker, this miRNA was shown to be elevated in the urine of patients with IgA nephropathy [116]. Recently, Argyropoulos et al. [117] presented numerous miRNAs which exhibited differential expression profiles dependent upon the presenting stage of albuminuria (microalbuminuria, intermittent albuminuria and persistent albuminuria). Unique miRNA profiles were also observed in those that developed nephropathy after a 25 year follow-up. A number of miRNAs were shown to be differentially expressed between the groups with the miRNA profile differing at various stages of disease. The study identified a number of miRNAs that have not previously been associated with renal pathology and represents the most comprehensive study of miRNA biomarkers in DN to date.

There have been a large number of studies investigating miRNA biomarkers in macrovascular complications and these have been reviewed recently [118]. However, as with studies aiming to identify profiles for other complications, very few studies

have utilized an unbiased analysis such as high-throughput parallel sequencing, possibly because of the difficulties inherent in the analysis of miRNAs in biofluids as conventional housekeeping non-coding RNAs are not secreted from cells. Nevertheless, a number of miRNAs appear in profiles for coronary artery disease, heart failure and myocardial infarction, and these are known to play a role in their respective pathology [119–122]. Of these miRNAs, *miR-1*, *miR-21*, *miR-27* and *miR-133* were increased and *miR-30* was decreased, observations that are consistent with tissue expression. Analysis of circulating microparticles by Deihl et al. [122] adds to the complications seen with *miR-155* as a miRNA biomarker as this miRNA was up-regulated in subjects with acute coronary syndrome compared with those with coronary artery disease [122]. With the exception of nephropathy, there is no work published examining circulating miRNAs for the purpose of generating early detection systems or biomarker profiles for diabetic complications.

## THERAPEUTIC POTENTIAL OF miRNAs

The present review has attempted to highlight not just the current state of knowledge in regard to miRNAs and disease progression, but also the complexity with which these post-transcriptional regulators carry out such functions. The number of targets a single miRNA has in conjunction with the number of miRNAs targeting a single gene transcript underscores this complexity. These complex interactions coupled with antagonizing roles of certain miRNAs in different tissues or even disease states forces one to realise that miRNA therapeutics are not something easily resolved. However, a number of miRNAs are seen to be tissue- or cell-type-specific, or are involved in regulating a central process common to pathological responses of a number of cell types. This glimmer of simplicity has resulted in a number of advances and trials targeting the modulation of miRNAs either through miRNA mimics or inhibitors which aim to prevent or at least dampen the progression of a number of pathologies. miRNA mimics are delivered as either a hairpin RNA similar to precursor miRNAs or a single-stranded oligonucleotide homologous to the miRNA of interest. These are processed by RNAi machinery and inhibit their targets in a manner akin to that of endogenous miRNAs [123]. They may also be delivered as an shRNA-style adenoviral vector or virus. Conversely, miRNA inhibition is achieved via the delivery of oligonucleotides which possess sequences complementary to their target miRNAs [124]. These inhibitors may possess any number of chemical modifications such as 2',4'-methylene bridging [LNA (locked nucleic acid)] or 3' cholesterol esterification and act to mask the target miRNA seed sequence thus removing its ability to bind target UTRs.

Both the chronic and complex nature of diabetes and its complications has hindered reasonable progression in recent years in the development of miRNA-based therapeutics. Despite this, there have been a number of studies demonstrating the ability of modulating specific miRNA to repress certain aspects of the complications experienced in particular tissues in response to diabetes. For example, delivery of LNA inhibitors targeting *miR-*

*192* via subcutaneous injection in streptozotocin-induced diabetic mice resulted in efficient decreases in the renal expression of the target miRNA [125,126]. This resulted in an increased expression of ZEB1/2 with concomitant decreases in collagen, fibronectin and, importantly, TGF $\beta$ , leading to improvements in renal function. *miR-21* has also been successfully repressed via LNA inhibitors albeit in a somewhat more artificial model of renal disease, the UUO (unilateral ureteral obstruction) model. Here, prevention of the UUO-induced up-regulation of *miR-21* resulted in improvements in the expression of a number of ECM proteins in addition to TGF $\beta$ . Furthermore, a large number of miRNAs have been repressed in a variety of cardiovascular complications. In particular, modulation of *miR-23* and *miR-27* have resulted in decreased neovascularization in response to laser-mediated injury to the choroid layer of the eye [127]. Improvements in glucose metabolism and control over plasma lipid content has been observed with *miR-208a* inhibition [128]. Reduction in this miRNA also reduced cardiac remodelling and increased survival after hypertension-induced heart failure [129]. Despite the promise of these studies, *miR-21* is the only miRNA in pre-clinical development which may be applicable to diabetic complications. Inhibition of the miRNA is being developed by Regulus against fibrosis of the kidney and heart. Conversely, there are a number of miRNAs undergoing pre-clinical and clinical development for non-diabetes-related pathologies.

As with much of the early work conducted with miRNAs was cancer-based, so too is cancer research leading the way for miRNA therapeutics. Indeed, both *let-7* and *miR-34* mimics are undergoing pre-clinical development by Mirna Therapeutics. Although *let-7* has multiple targets in cell-cycle and mitotic signalling, *miR-34* targets a number of apoptotic regulators downstream of p53 such as Bcl-2 [130,131]. Mimic-based therapeutics possess a number of problems, greatest of which is the short half-life of synthetic miRNAs *in vivo* after venous delivery [132]. This evidently requires increased treatments and cost for the patient, both physical and financial. Adenoviral delivery of miRNA mimic vectors provide a somewhat more stable expression, although an issue with tissue specificity exists despite a number of viral serotypes preferentially targeting some tissues [133]. Amendments to this have included the utilization of tissue-specific promoters. Despite these concerns, a number of miRNAs have been successfully utilized in animal studies to improve pathological states, including *miR-26a* in murine hepatic cancer [134]. Additionally, *miR-582* restoration via transurethral delivery effectively reduced bladder cancer in mouse models [135].

Repression of endogenous miRNAs, while possessing the same challenges as miRNA restoration, has had a somewhat greater success in both animal models and clinical development. This is partly attributable to developments in inhibitor chemistries such as LNA RNA, which possess reduced conformational changes and thus greater binding affinity in addition to greater half-lives *in vivo* [136]. Using LNA inhibitors, *miR-192* has been effectively repressed in mouse kidneys, resulting in a greatly improved pathology [126]. Additionally, *miR-208* and *miR-499* along with *miR-195* are all in pre-clinical development by Mirna Therapeutics for chronic heart failure and myocardial infarct remodelling respectively. This group also have

LNA-mediated repression of *miR-122* in Phase II clinical trials for the prevention of hepatitis C replication. Adenoviral delivery of miRNA ‘sponge’-expressing vectors has also had success in experimental models, although these are obviously plagued by the problems highlighted above. However, miRNA sponges allow less rigid inhibition of miRNA by ‘mopping up’ their target via multiple MREs along their length, thus affording the flexibility inherently seen in miRNA systems [137]. Additionally, sponges may repress multiple miRNAs with varying seed sequences providing the sponge is designed accordingly. In highlighting miRNA sponge efficacy, lentiviral delivery and genetic insertion of an miRNA sponge targeting *miR-326* resulted in the constitutive expression of the sponge and ameliorated experimental autoimmune encephalitis [138].

## CONCLUDING REMARKS

Since their initial discovery, miRNAs have rapidly emerged as important post-transcriptional regulators capable of exerting effects on development and disease. The complexity by which they perform this function, although perceived as relatively simple in early research, has just as rapidly been revealed to possess large-scale promiscuity of both individual miRNA species and the mRNA they target. Adding to this, miRNA expression profiles between cell types, tissues and disease states often differ dramatically with only a few miRNAs being discovered to date that are somewhat universal in these parameters. In spite of this, numerous research projects have delineated the complex nature of these molecules, in some cases only to raise further more challenging questions. However, although the tide of miRNA research quickly rises, the potential for miRNAs to act as non-invasive markers and even therapeutic targets is becoming apparent. Although the field of miRNA research is a relatively new one, exciting times lie ahead with much work still to be done. Who knows what the tide will leave behind in the coming years?

## REFERENCES

- Hays, J. N. (2005) Epidemics and Pandemics: Their Impacts on Human History. ABC-CLIO, Santa Barbara
- Swinburn, B. A., Sacks, G., Hall, K. D., McPherson, K., Finegood, D. T., Moodie, M. L. and Gortmaker, S. L. (2011) The global obesity pandemic: shaped by global drivers and local environments. *Lancet* **378**, 804–814
- Organisation for Economic Co-operation and Development (2012) OECD Health Data 2012, <http://www.oecd.org/health/health-systems/oecdhealthdata.htm>
- World Health Organization (2012) World Health Statistics. Report 2012, [http://www.who.int/gho/publications/world\\_health\\_statistics/2012/en/](http://www.who.int/gho/publications/world_health_statistics/2012/en/)
- World Health Organization (2011) Global status report on noncommunicable diseases 2010, [http://www.who.int/nmh/publications/ncd\\_report2010/en/](http://www.who.int/nmh/publications/ncd_report2010/en/)
- Odegaard, J. I. and Chawla, A. (2012) Connecting Type 1 and Type 2 diabetes through innate immunity. *Cold Spring Harbor Perspect. Med.* **2**, a007724
- Brunetti, P. (2007) The lean patient with type 2 diabetes: characteristics and therapy challenge. *Int. J. Clin. Pract. Suppl.* **153**, 3–9
- Xue, B., Sukumaran, S., Nie, J., Jusko, W. J., DuBois, D. C. and Almon, R. R. (2011) Adipose tissue deficiency and chronic inflammation in diabetic goto-kakizaki rats. *PLoS ONE* **6**, e17386
- Williams, M. and Nadler, J. (2007) Inflammatory mechanisms of diabetic complications. *Curr. Diabetes Rep.* **7**, 242–248
- Brownlee, M. (2001) Biochemistry and molecular cell biology of diabetic complications. *Nature* **414**, 813–820
- Soifer, H. S., Rossi, J. J. and Saetrom, P. (2007) MicroRNAs in disease and potential therapeutic applications. *Mol. Ther.* **15**, 2070–2079
- Stefani, G. and Slack, F. J. (2008) Small non-coding RNAs in animal development. *Nat. Rev. Mol. Cell Biol.* **9**, 219–230
- Chalfie, M., Horvitz, H. R. and Sulston, J. E. (1981) Mutations that lead to reiterations in the cell lineages of *C. elegans*. *Cell* **24**, 59–69
- Wightman, B., Ha, I. and Ruvkun, G. (1993) Posttranscriptional regulation of the heterochronic gene *lin-14* by *lin-4* mediates temporal pattern formation in *C. elegans*. *Cell* **75**, 855–862
- Lee, R. C., Feinbaum, R. L. and Ambros, V. (1993) The *C. elegans* heterochronic gene *lin-4* encodes small RNAs with antisense complementarity to *lin-14*. *Cell* **75**, 843–854
- Lagos-Quintana, M., Rauhut, R., Lendeckel, W. and Tuschl, T. (2001) Identification of novel genes coding for small expressed RNAs. *Science* **294**, 853–858
- Bartel, D. (2004) MicroRNAs: genomics, biogenesis, mechanism and function. *Cell* **116**, 281–297
- Olena, A. F. and Patton, J. G. (2010) Genomic organization of microRNAs. *J. Cell. Physiol.* **222**, 540–545
- Ro, S., Park, C., Young, D., Sanders, K. M. and Yan, W. (2007) Tissue-dependent paired expression of miRNAs. *Nucleic Acids Res.* **35**, 5944–5953
- Hausser, J., Syed, A. P., Bilen, B. and Zavolan, M. (2013) Analysis of CDS-located miRNA target sites suggests that they can effectively inhibit translation. *Genome Res.* **23**, 604–615
- Lee, I., Ajay, S. S., Yook, J. I., Kim, H. S., Hong, S. H., Kim, N. H., Dhanasekaran, S. M., Chinnaiyan, A. M. and Athey, B. D. (2009) New class of microRNA targets containing simultaneous 5'-UTR and 3'-UTR interaction sites. *Genome Res.* **19**, 1175–1183
- Wu, L. and Belasco, J. G. (2008) Let me count the ways: mechanisms of gene regulation by miRNAs and siRNAs. *Mol. Cell* **29**, 1–7
- Su, W. L., Kleinhanz, R. R. and Schadt, E. E. (2011) Characterizing the role of miRNAs within gene regulatory networks using integrative genomics techniques. *Mol. Syst. Biol.* **7**, 490
- Kantharidis, P., Wang, B., Carew, R. M. and Lan, H. Y. (2011) Diabetes complications: the microRNA perspective. *Diabetes* **60**, 1832–1837
- King, G. L. (2008) The role of inflammatory cytokines in diabetes and its complications. *J. Periodontol.* **79**, 1527–1534
- Weber, C. and Noels, H. (2011) Atherosclerosis: current pathogenesis and therapeutic options. *Nat. Med.* **17**, 1410–1422
- Clark, A., Jones, L. C., de Koning, E., Hansen, B. C. and Matthews, D. R. (2001) Decreased insulin secretion in type 2 diabetes: a problem of cellular mass or function? *Diabetes* **50**, S169
- Steele, C., Hagopian, W. A., Gitelman, S., Masharani, U., Cavaghan, M., Rother, K. I., Donaldson, D., Harlan, D. M., Bluestone, J. and Herold, K. C. (2004) Insulin secretion in type 1 diabetes. *Diabetes* **53**, 426–433
- Qatanani, M. and Lazar, M. A. (2007) Mechanisms of obesity-associated insulin resistance: many choices on the menu. *Genes Dev.* **21**, 1443–1455

- 30 Achenbach, P, Bonifacio, E., Koczwara, K. and Ziegler, A.-G. (2005) Natural history of Type 1 diabetes. *Diabetes* **54**, S25–S31
- 31 Atkinson, M. A. and Eisenbarth, G. S. (2001) Type 1 diabetes: new perspectives on disease pathogenesis and treatment. *Lancet* **358**, 221–229
- 32 Hezova, R., Slaby, O., Faltejskova, P, Mikulkova, Z., Buresova, I., Raja, K. R. M., Hodek, J., Ovesna, J. and Michalek, J. (2010) microRNA-342, microRNA-191 and microRNA-510 are differentially expressed in T regulatory cells of type 1 diabetic patients. *Cell. Immunol.* **260**, 70–74
- 33 Li, Q.-J., Chau, J., Ebert, P. J. R., Sylvester, G., Min, H., Liu, G., Braich, R., Manoharan, M., Soutschek, J., Skare, P et al. (2007) *miR-181a* is an intrinsic modulator of T cell sensitivity and selection. *Cell* **129**, 147–161
- 34 Zhou, B., Li, C., Qi, W., Zhang, Y., Zhang, F., Wu, J. X., Hu, Y. N., Wu, D. M., Liu, Y., Yan, T. T. et al. (2012) Downregulation of *miR-181a* upregulates sirtuin-1 (SIRT1) and improves hepatic insulin sensitivity. *Diabetologia* **55**, 2032–2043
- 35 Poy, M. N., Eliasson, L., Krutzfeldt, J., Kuwajima, S., Ma, X., MacDonald, P. E., Pfeffer, S., Tuschl, T., Rajewsky, N., Rorsman, P and Stoffel, M. (2004) A pancreatic islet-specific microRNA regulates insulin secretion. *Nature* **432**, 226–230
- 36 El Ouaamari, A., Baroukh, N., Martens, G. A., Lebrun, P, Pipeleers, D. and van Obberghen, E. (2008) *miR-375* targets 3'-phosphoinositide-dependent protein kinase-1 and regulates glucose-induced biological responses in pancreatic  $\beta$ -cells. *Diabetes* **57**, 2708–2717
- 37 Poy, M. N., Hausser, J., Trajkovski, M., Braun, M., Collins, S., Rorsman, P, Zavolan, M. and Stoffel, M. (2009) *miR-375* maintains normal pancreatic  $\alpha$ - and  $\beta$ -cell mass. *Proc. Natl. Acad. Sci. U.S.A.* **106**, 5813–5818
- 38 Karolina, D. S., Armugam, A., Sepramaniam, S. and Jeyaseelan, K. (2012) miRNAs and diabetes mellitus. *Expert Rev. Endocrinol. Metab.* **7**, 281–300
- 39 Tordjman, J., Guerre-Millo, M. and Clément, K. (2008) Adipose tissue inflammation and liver pathology in human obesity. *Diabetes Metab.* **34**, 658–663
- 40 Xie, H., Lim, B. and Lodish, H. F. (2009) MicroRNAs induced during adipogenesis that accelerate fat cell development are downregulated in obesity. *Diabetes* **58**, 1050–1057
- 41 Whittaker, R., Loy, P. A., Sisman, E., Suyama, E., Aza-Blanc, P, Ingermanson, R. S., Price, J. H. and McDonough, P. M. (2010) Identification of microRNAs that control lipid droplet formation and growth in hepatocytes via high-content screening. *J. Biomol. Screen.* **15**, 798–805
- 42 Eckardt, K., Taube, A. and Eckel, J. (2011) Obesity-associated insulin resistance in skeletal muscle: role of lipid accumulation and physical inactivity. *Rev. Endocr. Metab. Disord.* **12**, 163–172
- 43 de Alvaro, C., Teruel, T., Hernandez, R. and Lorenzo, M. (2004) Tumor necrosis factor  $\alpha$  produces insulin resistance in skeletal muscle by activation of inhibitor  $\kappa$ B kinase in a p38 MAPK-dependent manner. *J. Biol. Chem.* **279**, 17070–17078
- 44 Odegaard, J. I. and Chawla, A. (2011) Alternative macrophage activation and metabolism. *Annu. Rev. Pathol. Mech. Dis.* **6**, 275–297
- 45 Chaudhuri, A. A., So, A. Y.-L., Sinha, N., Gibson, W. S. J., Taganov, K. D., O'Connell, R. M. and Baltimore, D. (2011) MicroRNA-125b potentiates macrophage activation. *J. Immunol.* **187**, 5062–5068
- 46 Ortega, F. J., Moreno-Navarrete, J. M., Pardo, G., Sabater, M., Hummel, M., Ferrer, A., Rodriguez-Hermosa, J. I., Ruiz, B., Ricart, W. and Peral, B. (2010) miRNA expression profile of human subcutaneous adipose and during adipocyte differentiation. *PLoS ONE* **5**, e9022
- 47 Masters, S. L., Mielke, L. A., Cornish, A. L., Sutton, C. E., O'Donnell, J., Cengia, L. H., Roberts, A. W., Wicks, I. P, Mills, K. H. G. and Croker, B. A. (2010) Regulation of interleukin-1 $\beta$  by interferon- $\gamma$  is species specific, limited by suppressor of cytokine signalling 1 and influences interleukin-17 production. *EMBO Rep.* **11**, 640–646
- 48 Kim, S.-W., Ramasamy, K., Bouamar, H., Lin, A.-P, Jiang, D. and Aguiar, R. C. T. (2012) MicroRNAs miR-125a and miR-125b constitutively activate the NF- $\kappa$ B pathway by targeting the tumor necrosis factor  $\alpha$ -induced protein 3 (TNFAIP3, A20). *Proc. Natl. Acad. Sci. U.S.A.* **109**, 7865–7870
- 49 Karolina, D. S., Armugam, A., Tavintharan, S., Wong, M. T. K., Lim, S. C., Sum, C. F. and Jeyaseelan, K. (2011) MicroRNA 144 impairs insulin signaling by inhibiting the expression of insulin receptor substrate 1 in type 2 diabetes mellitus. *PLoS ONE* **6**, e22839
- 50 Mateescu, B., Batista, L., Cardon, M., Gruosso, T., de Feraudy, Y., Mariani, O., Nicolas, A., Meyniel, J.-P, Cottu, P, Sastre-Garau, X. and Mechta-Grigoriou, F. (2011) miR-141 and *miR-200a* act on ovarian tumorigenesis by controlling oxidative stress response. *Nat. Med.* **17**, 1627–1635
- 51 Liu, Z. and Cao, W. (2009) p38 mitogen-activated protein kinase: a critical node linking insulin resistance and cardiovascular diseases in type 2 diabetes mellitus. *Endocr. Metab. Immune Disord. Drug Targets* **9**, 38–46
- 52 Tang, J. and Kern, T. S. (2011) Inflammation in diabetic retinopathy. *Prog. Retin. Eye Res.* **30**, 343–358
- 53 Kovacs, B., Lumayag, S., Cowan, C. and Xu, S. (2011) microRNAs in early diabetic retinopathy in streptozotocin-induced diabetic rats. *Invest. Ophthalmol. Visual Sci.* **52**, 4402–4409
- 54 Natarajan, R., Putta, S. and Kato, M. (2012) MicroRNAs and Diabetic Complications. *J Cardiovasc. Transl. Res.* **5**, 413–422
- 55 O'Connell, R. M., Kahn, D., Gibson, W. S. J., Round, J. L., Scholz, R. L., Chaudhuri, A. A., Kahn, M. E., Rao, D. S. and Baltimore, D. (2010) MicroRNA-155 promotes autoimmune inflammation by enhancing inflammatory T cell development. *Immunity* **33**, 607–619
- 56 Anand, S., Majeti, B. K., Acevedo, L. M., Murphy, E. A., Mukthavaram, R., Scheppeke, L., Huang, M., Shields, D. J., Lindquist, J. N., Lapinski, P. E. et al. (2010) MicroRNA-132-mediated loss of p120RasGAP activates the endothelium to facilitate pathological angiogenesis. *Nat. Med.* **16**, 909–914
- 57 Feng, B., Chen, S., McArthur, K., Wu, Y., Sen, S., Ding, Q., Feldman, R. D. and Chakrabarti, S. (2011) *miR-146a*-mediated extracellular matrix protein production in chronic diabetes complications. *Diabetes* **60**, 2975–2984
- 58 McArthur, K., Feng, B., Wu, Y., Chen, S. and Chakrabarti, S. (2011) MicroRNA-200b regulates vascular endothelial growth factor-mediated alterations in diabetic retinopathy. *Diabetes* **60**, 1314–1323
- 59 Nyengaard, J. R., Ido, Y., Kilo, C. and Williamson, J. R. (2004) Interactions between hyperglycemia and hypoxia: implications for diabetic retinopathy. *Diabetes* **53**, 2931–2938
- 60 Kovacs, B., Lumayag, S., Cowan, C. and Xu, S. (2011) microRNAs in early diabetic retinopathy in streptozotocin-induced diabetic rats. *Invest. Ophthalmol. Visual Sci.* **21**, 4402–4409
- 61 Bai, Y., Bai, X., Wang, Z., Zhang, X., Ruan, C. and Miao, J. (2011) MicroRNA-126 inhibits ischemia-induced retinal neovascularization via regulating angiogenic growth factors. *Exp. Mol. Pathol.* **91**, 471–477
- 62 Boulton, A. J. M., Vinik, A. I., Arezzo, J. C., Bril, V., Feldman, E. L., Freeman, R., Malik, R. A., Maser, R. E., Soslenko, J. M. and Ziegler, D. (2005) Diabetic neuropathies: a statement by the American Diabetes Association. *Diabetes Care* **28**, 956–962
- 63 Bansal, V., Kalita, J. and Misra, U. K. (2006) Diabetic neuropathy. *Postgrad. Med. J.* **82**, 95–100

- 64 Wright, D. E. and Wilson, N. M. (2011) Inflammatory mediators in diabetic neuropathy. *J. Diabetes Metab.* **55**, 004, doi:10.4172/2155-6156.S5-004
- 65 Denby, L., Ramdas, V., McBride, M. W., Wang, J., Robinson, H., McClure, J., Crawford, W., Lu, R., Hillyard, D. Z. and Khanin, R. (2011) *miR-21* and *miR-214* are consistently modulated during renal injury in rodent models. *Am. J. Pathol.* **179**, 661–672
- 66 Ropper, A. H., Gorson, K. C., Gooch, C. L., Weinberg, D. H., Pieczek, A., Ware, J. H., Kershen, J., Rogers, A., Simovic, D., Schratzberger, P et al. (2009) Vascular endothelial growth factor gene transfer for diabetic polyneuropathy: a randomized, double-blinded trial. *Ann. Neurol.* **65**, 386–393
- 67 Anjaneyulu, M., Berent-Spillon, A., Inoue, T., Choi, J., Cherian, K. and Russell, J. W. (2008) Transforming growth factor- $\beta$  induces cellular injury in experimental diabetic neuropathy. *Exp. Neurol.* **211**, 469–479
- 68 Tesch, G. H. (2010) Macrophages and diabetic nephropathy. *Semin. Nephrol.* **30**, 290–301
- 69 Lim, A. K. H. and Tesch, G. H. (2012) Inflammation in diabetic nephropathy. *Mediators Inflamm.* **2012**, 146154
- 70 Schena, F. P. and Gesualdo, L. (2005) Pathogenetic mechanisms of diabetic nephropathy. *J. Am. Soc. Nephrol.* **16**, S30–S33
- 71 Qian, Y., Feldman, E., Pennathur, S., Kretzler, M. and Brosius, F. C. (2008) From fibrosis to sclerosis. *Diabetes* **57**, 1439–1445
- 72 Aclouque, H., Adams, M. S., Fishwick, K., Bronner-Fraser, M. and Nieto, M. A. (2009) Epithelial-mesenchymal transitions: the importance of changing cell state in development and disease. *J. Clin. Invest.* **119**, 1438–1449
- 73 Gregory, P. A., Bert, A. G., Paterson, E. L., Barry, S. C., Tsykin, A., Farshid, G., Vadas, M. A., Khew-Goodall, Y. and Goodall, G. J. (2008) The *miR-200* family and *miR-205* regulate epithelial to mesenchymal transition by targeting ZEB1 and SIP1. *Nat. Cell Biol.* **10**, 593–601
- 74 Wang, B., Koh, P., Winbanks, C., Coughlan, M. T., McClelland, A., Watson, A., Jandeleit-Dahm, K., Burns, W. C., Thomas, M. C., Cooper, M. E. and Kantharidis, P. (2011) *miR-200a* prevents renal fibrogenesis through repression of TGF- $\beta$ 2 expression. *Diabetes* **60**, 280–287
- 75 Fujimoto, M., Maezawa, Y., Yokote, K., Joh, K., Kobayashi, K., Kawamura, H., Nishimura, M., Roberts, A. B., Saito, Y. and Mori, S. (2003) Mice lacking Smad3 are protected against streptozotocin-induced diabetic glomerulopathy. *Biochem. Biophys. Res. Commun.* **305**, 1002–1007
- 76 Wang, B., Komers, R., Carew, R., Winbanks, C. E., Xu, B., Herman-Edelstein, M., Koh, P., Thomas, M., Jandeleit-Dahm, K., Gregorevic, P et al. (2011) Suppression of microRNA-29 expression by TGF- $\beta$ 1 promotes collagen expression and renal fibrosis. *J. Am. Soc. Nephrol.* **23**, 252–265
- 77 Wang, B., Herman-Edelstein, M., Koh, P., Burns, W., Jandeleit-Dahm, K., Watson, A., Saleem, M., Goodall, G. J., Twigg, S. M., Cooper, M. E. and Kantharidis, P. (2010) E-cadherin expression is regulated by miR-192/215 by a mechanism that is independent of the profibrotic effects of transforming growth factor- $\beta$ . *Diabetes* **59**, 1794–1802
- 78 Kato, M., Zhang, J., Wang, M., Lanting, L., Yuan, H., Rossi, J. J. and Natarajan, R. (2007) MicroRNA-192 in diabetic kidney glomeruli and its function in TGF- $\beta$ -induced collagen expression via inhibition of E-box repressors. *Proc. Natl. Acad. Sci. U.S.A.* **104**, 3432
- 79 Chung, A. C. K., Huang, X. R., Meng, X. and Lan, H. Y. (2010) *miR-192* mediates TGF- $\beta$ /Smad3-driven renal fibrosis. *J. Am. Soc. Nephrol.* **21**, 1317–1325
- 80 Krupa, A., Jenkins, R., Luo, D. D., Lewis, A., Phillips, A. and Fraser, D. (2010) Loss of microRNA-192 promotes fibrogenesis in diabetic nephropathy. *J. Am. Soc. Nephrol.* **21**, 438–447
- 81 Kato, M., Putta, S., Wang, M., Yuan, H., Lanting, L., Nair, I., Gunn, A., Nakagawa, Y., Shimano, H., Todorov, I. et al. (2009) TGF- $\beta$  activates Akt kinase through a microRNA-dependent amplifying circuit targeting PTEN. *Nat. Cell Biol.* **11**, 881–889
- 82 Zhang, Z., Peng, H., Chen, J., Chen, X., Han, F., Xu, X., He, X. and Yan, N. (2009) MicroRNA-21 protects from mesangial cell proliferation induced by diabetic nephropathy in db/db mice. *FEBS Lett.* **583**, 209–2014
- 83 Chung, A. C. K., Dong, Y., Yang, W., Zhong, X., Li, R. and Lan, H. Y. (2013) Smad7 suppresses renal fibrosis via altering expression of TGF- $\beta$ /Smad3-regulated microRNAs. *Mol. Ther.* **21**, 388–398
- 84 Zhong, X., Chung, A. C. K., Chen, H. Y., Meng, X. M. and Lan, H. Y. (2011) Smad3-mediated upregulation of *miR-21* promotes renal fibrosis. *J. Am. Soc. Nephrol.* **22**, 1668–1681
- 85 Godwin, J. G., Ge, X., Stephan, K., Jurisch, A., Tullius, S. G. and Iacomini, J. (2010) Identification of a microRNA signature of renal ischemia reperfusion injury. *Proc. Natl. Acad. Sci. U.S.A.* **107**, 14339–14344
- 86 Saal, S. and Harvey, S. J. (2009) MicroRNAs and the kidney: coming of age. *Curr. Opin. Nephrol. Hypertens.* **18**, 317–323
- 87 Wang, Q., Wang, Y., Minto, A. W., Wang, J., Shi, Q., Li, X. and Quigg, R. J. (2008) MicroRNA-377 is up-regulated and can lead to increased fibronectin production in diabetic nephropathy. *FASEB J.* **22**, 4126–4135
- 88 Ross, R. (1999) Atherosclerosis: an inflammatory disease. *N. Engl. J. Med.* **340**, 115–126
- 89 Chen, L.-J., Lim, S., Yeh, Y.-T., Lien, S.-C. and Chiu, J.-J. (2012) Roles of microRNAs in atherosclerosis and restenosis. *J. Biomed. Sci.* **19**, 79
- 90 Raitoharju, E., Lyytikäinen, L. P., Levula, M., Oksala, N., Mennander, A., Tarkka, M., Klopp, N., Illig, T., Kähönen, M. and Karhunen, P. J. (2011) *miR-21*, *miR-210*, *miR-34a* and *miR-146a/b* are up-regulated in human atherosclerotic plaques in the Tampere Vascular Study. *Atherosclerosis* **219**, 211–217
- 91 Yamakuchi, M. and Lowenstein, C. J. (2009) *MIR-34*, *SIRT1* and *p53*: the feedback loop. *Cell Cycle* **8**, 712–715
- 92 Zhu, N., Zhang, D., Chen, S., Liu, X., Lin, L., Huang, X., Guo, Z., Liu, J., Wang, Y. and Yuan, W. (2011) Endothelial enriched microRNAs regulate angiotensin II-induced endothelial inflammation and migration. *Atherosclerosis* **215**, 286–293
- 93 Fichtlscherer, S., De Rosa, S., Fox, H., Schwietz, T., Fischer, A., Liebetrau, C., Weber, M., Hamm, C. W., Röxe, T., Müller-Ardogan, M. et al. (2010) Circulating microRNAs in patients with coronary artery disease. *Circ. Res.* **107**, 677–684
- 94 Tang, B., Xiao, B., Liu, Z., Li, N., Zhu, E. D., Li, B. S., Xie, Q. H., Zhuang, Y., Zou, Q. M. and Mao, X. H. (2010) Identification of *MyD88* as a novel target of *miR-155*, involved in negative regulation of *Helicobacter pylori*-induced inflammation. *FEBS Lett.* **584**, 1481–1486
- 95 Huang, R., Hu, G., Lin, B., Lin, Z. and Sun, C. (2010) MicroRNA-155 silencing enhances inflammatory response and lipid uptake in oxidized low-density lipoprotein-stimulated human THP-1 macrophages. *J. Investig. Med.* **58**, 961–967
- 96 Li, D., Yang, P., Xiong, Q., Song, X., Yang, X., Liu, L., Yuan, W. and Rui, Y.-C. (2010) MicroRNA-125a/b-5p inhibits endothelin-1 expression in vascular endothelial cells. *J. Hypertens.* **28**, 1646–1654
- 97 Chen, T., Huang, Z., Wang, L., Wang, Y., Wu, F., Meng, S. and Wang, C. (2009) MicroRNA-125a-5p partly regulates the inflammatory response, lipid uptake and ORP9 expression in oxLDL-stimulated monocyte/macrophages. *Cardiovasc. Res.* **83**, 131–139
- 98 Villeneuve, L. M., Kato, M., Reddy, M. A., Wang, M., Lanting, L. and Natarajan, R. (2010) Enhanced levels of microRNA-125b in vascular smooth muscle cells of diabetic db/db mice lead to increased inflammatory gene expression by targeting the histone methyltransferase *Suv39h1*. *Diabetes* **59**, 2904–2915

- 99 Sabatel, C., Malvaux, L., Bovy, N., Deroanne, C., Lambert, V., Gonzalez, M. L. A., Colige, A., Rakic, J. M., Noël, A. and Martial, J. A. (2011) MicroRNA-21 exhibits antiangiogenic function by targeting RhoB expression in endothelial cells. *PLoS ONE* **6**, e16979
- 100 Chen, W. J., Yin, K., Zhao, G. J., Fu, Y. C. and Tang, C. K. (2012) The magic and mystery of microRNA-27 in atherosclerosis. *Atherosclerosis* **222**, 314–323
- 101 Miki, T., Yuda, S., Kouzu, H. and Miura, T. (2012) Diabetic cardiomyopathy: pathophysiology and clinical features. *Heart Failure Rev.* **18**, 149–166
- 102 Schilling, J. D., Machkovech, H. M., Kim, A. H. J., Schwedwener, R. and Schaffer, J. E. (2012) Macrophages modulate cardiac function in lipotoxic cardiomyopathy. *Am. J. Physiol. Heart Circ. Physiol.* **303**, H1366–H1373
- 103 Cheng, Y. and Zhang, C. (2010) MicroRNA-21 in cardiovascular disease. *J. Cardiovasc. Transl. Res.* **3**, 251–255
- 104 Van Rooij, E., Sutherland, L. B., Thatcher, J. E., DiMaio, J. M., Naseem, R. H., Marshall, W. S., Hill, J. A. and Olson, E. N. (2008) Dysregulation of microRNAs after myocardial infarction reveals a role of *miR-29* in cardiac fibrosis. *Proc. Natl. Acad. Sci. U.S.A.* **105**, 13027–13032
- 105 Duisters, R. F., Tijssen, A. J., Schroen, B., Leenders, J. J., Lentink, V., van der Made, I., Herias, V., van Leeuwen, R. E., Schellings, M. W., Barenbrug, P. et al. (2009) *miR-133* and *miR-30* regulate connective tissue growth factor: implications for a role of microRNAs in myocardial matrix remodeling. *Circ. Res.* **104**, 170–178
- 106 Shantikumar, S., Caporali, A. and Emanuelli, C. (2012) Role of microRNAs in diabetes and its cardiovascular complications. *Cardiovasc. Res.* **93**, 583–593
- 107 Latronico, M. V. G. and Condorelli, G. (2011) microRNAs in hypertrophy and heart failure. *Exp. Biol. Med.* **236**, 125–131
- 108 Maslov, L. N. and Sazonova, S. I. (2006) Using cytokines to stimulate neoangiogenesis and cardiac regeneration. *Eksp. Klin. Farmakol.* **69**, 70–76
- 109 Chen, X., Ba, Y., Ma, L., Cai, X., Yin, Y., Wang, K., Guo, J., Zhang, Y., Chen, J., Guo, X. et al. (2008) Characterization of microRNAs in serum: a novel class of biomarkers for diagnosis of cancer and other diseases. *Cell Res.* **18**, 997–1006
- 110 Vickers, K. C., Palmisano, B. T., Shoucri, B. M., Shamburek, R. D. and Remaley, A. T. (2011) MicroRNAs are transported in plasma and delivered to recipient cells by high-density lipoproteins. *Nat. Cell Biol.* **13**, 423–433
- 111 Zampetaki, A., Kiechl, S., Drozdov, I., Willeit, P., Mayr, U., Prokopi, M., Mayr, A., Wegger, S., Oberhollenzer, F., Bonora, E. et al. (2010) Plasma microRNA profiling reveals loss of endothelial *miR-126* and other microRNAs in type 2 diabetes. *Circ. Res.* **107**, 810–817
- 112 Kong, L., Zhu, J., Han, W., Jiang, X., Xu, M., Zhao, Y., Dong, Q., Pang, Z., Guan, Q., Gao, L. et al. (2011) Significance of serum microRNAs in pre-diabetes and newly diagnosed type 2 diabetes: a clinical study. *Acta Diabetol.* **48**, 61–69
- 113 Thum, T., Gross, C., Fiedler, J., Fischer, T., Kissler, S., Bussen, M., Galuppo, P., Just, S., Rottbauer, W. and Frantz, S. (2008) MicroRNA-21 contributes to myocardial disease by stimulating MAP kinase signalling in fibroblasts. *Nature* **456**, 980–984
- 114 Rottiers, V. and Näär, A. M. (2012) MicroRNAs in metabolism and metabolic disorders. *Nat. Rev. Mol. Cell Biol.* **13**, 239–250
- 115 Neal, C. S., Michael, M. Z., Pimlott, L. K., Yong, T. Y., Li, J. Y. Z. and Gleadle, J. M. (2011) Circulating microRNA expression is reduced in chronic kidney disease. *Nephrol. Dial. Transplant.* **26**, 3794–3802
- 116 Wang, G., Kwan, B. C., Lai, F. M., Chow, K. M., Li, P. K. and Szeto, C. C. (2011) Elevated levels of *miR-146a* and *miR-155* in kidney biopsy and urine from patients with IgA nephropathy. *Dis. Markers* **30**, 171–179
- 117 Argyropoulos, C., Wang, K., McClarty, S., Huang, D., Bernardo, J., Ellis, D., Orchard, T., Galas, D. and Johnson, J. (2013) Urinary microRNA profiling in the nephropathy of Type 1 diabetes. *PLoS ONE* **8**, e54662
- 118 Tijssen, A. J., Pinto, Y. M. and Creemers, E. E. (2012) Circulating microRNAs as diagnostic biomarkers for cardiovascular diseases. *Am. J. Physiol. Heart Circ. Physiol.* **303**, H1085–H1095
- 119 Olivieri, F., Antonicelli, R., Lorenzi, M., D'Alessandra, Y., Lazzarini, R., Santini, G., Spazzafumo, L., Lisa, R., La Sala, L., Galeazzi, R. et al. (2012) Diagnostic potential of circulating *miR-499-5p* in elderly patients with acute non ST-elevation myocardial infarction. *Int. J. Cardiol.* **167**, 531–536
- 120 Li, T., Cao, H., Zhuang, J., Wan, J., Guan, M., Yu, B., Li, X. and Zhang, W. (2011) Identification of *miR-130a*, *miR-27b* and *miR-210* as serum biomarkers for atherosclerosis obliterans. *Clin. Chim. Acta* **412**, 66–70
- 121 Meder, B., Keller, A., Vogel, B., Haas, J., Sedaghat-Hamedani, F., Kayvanpour, E., Just, S., Borries, A., Rudloff, J., Leidinger, P. et al. (2011) MicroRNA signatures in total peripheral blood as novel biomarkers for acute myocardial infarction. *Basic Res. Cardiol.* **106**, 13–23
- 122 Diehl, P., Fricke, A., Sander, L., Stamm, J., Bassler, N., Htun, N., Ziemann, M., Helbing, T., El-Osta, A., Jowett, J. B. M. and Peter, K. (2012) Microparticles: major transport vehicles for distinct microRNAs in circulation. *Cardiovasc. Res.* **93**, 633–644
- 123 Thomson, D. W., Bracken, C. P. and Goodall, G. J. (2011) Experimental strategies for microRNA target identification. *Nucleic Acids Res.* **39**, 6845–6853
- 124 Lennox, K. A. and Behlke, M. A. (2010) A direct comparison of anti-microRNA oligonucleotide potency. *Pharm. Res.* **27**, 1788–1799
- 125 Kato, M., Arce, L., Wang, M., Putta, S., Lanting, L. and Natarajan, R. (2011) A microRNA circuit mediates transforming growth factor- $\beta$ 1 autoregulation in renal glomerular mesangial cells. *Kidney Int.* **80**, 358–368
- 126 Putta, S., Lanting, L., Sun, G., Lawson, G., Kato, M. and Natarajan, R. (2012) Inhibiting microRNA-192 ameliorates renal fibrosis in diabetic nephropathy. *J. Am. Soc. Nephrol.* **23**, 458
- 127 Zhou, Q., Gallagher, R., Ufret-Vincenty, R., Li, X., Olson, E. N. and Wang, S. (2011) Regulation of angiogenesis and choroidal neovascularization by members of microRNA-23~27~24 clusters. *Proc. Natl. Acad. Sci. U.S.A.* **108**, 8287–8292
- 128 Grueter, C. E., van Rooij, E., Johnson, B. A., DeLeon, S. M., Sutherland, L. B., Qi, X., Gautron, L., Elmquist, J. K., Bassel-Duby, R. and Olson, E. N. (2012) A cardiac microRNA governs systemic energy homeostasis by regulation of *MED13*. *Cell* **149**, 671–683
- 129 Montgomery, R. L., Hullinger, T. G., Semus, H. M., Dickinson, B. A., Seto, A. G., Lynch, J. M., Stack, C., Latimer, P. A., Olson, E. N. and van Rooij, E. (2011) Therapeutic inhibition of *miR-208a* improves cardiac function and survival during heart failure. *Circulation* **124**, 1537–1547
- 130 Hermeking, H. (2009) The *miR-34* family in cancer and apoptosis. *Cell Death Differ.* **17**, 193–199
- 131 Thorsen, S. B., Obad, S., Jensen, N. F., Stenvang, J. and Kauppinen, S. (2012) The therapeutic potential of microRNAs in cancer. *Cancer J.* **18**, 275–284
- 132 Mitchell, P. S., Parkin, R. K., Kroh, E. M., Fritz, B. R., Wyman, S. K., Pogosova-Agadjanyan, E. L., Peterson, A., Noteboom, J., O'Brian, K. C. and Allen, A. (2008) Circulating microRNAs as stable blood-based markers for cancer detection. *Proc. Natl. Acad. Sci. U.S.A.* **105**, 10513–10518
- 133 Zicarelli, C., Soltys, S., Rengo, G. and Rabinowitz, J. E. (2008) Analysis of AAV serotypes 1–9 mediated gene expression and tropism in mice after systemic injection. *Mol. Ther.* **16**, 1073–1080

- 134 Kota, J., Chivukula, R. R., O'Donnell, K. A., Wentzel, E. A., Montgomery, C. L., Hwang, H. W., Chang, T. C., Vivekanandan, P., Torbenson, M. and Clark, K. R. (2009) Therapeutic delivery of miR-26a inhibits cancer cell proliferation and induces tumor-specific apoptosis. *Cell* **137**, 1005
- 135 Uchino, K., Takeshita, F., Takahashi, R.-u., Kosaka, N., Fujiwara, K., Naruoka, H., Sonoke, S., Yano, J., Sasaki, H., Nozawa, S. et al. (2013) Therapeutic effects of microRNA-582-5p and -3p on the inhibition of bladder cancer progression. *Mol. Ther.* **21**, 610–619
- 136 Broderick, J. A. and Zamore, P. D. (2011) MicroRNA therapeutics. *Gene Ther.* **18**, 1104–1110
- 137 Ebert, M. S. and Sharp, P. A. (2010) MicroRNA sponges: progress and possibilities. *RNA* **16**, 2043–2050
- 138 Du, C., Liu, C., Kang, J., Zhao, G., Ye, Z., Huang, S., Li, Z., Wu, Z. and Pei, G. (2009) MicroRNA miR-326 regulates TH-17 differentiation and is associated with the pathogenesis of multiple sclerosis. *Nat. Immunol.* **10**, 1252–1259

Received 14 February 2013/14 May 2013; accepted 21 June 2013

Published on the Internet 13 September 2013, doi: 10.1042/CS20130079

### **1.5.1.2. Conclusion**

There has been considerable progress in identifying and exploring the role of various miRNA in the development and progression of diabetic complications. However, tissue and cell specific miRNA regulatory profiles somewhat complicate the development of any therapeutics. Regardless, a number of miRNA-based therapeutics are currently in, or preparing for, clinical trials. Furthermore, utilisation of miRNA as highly stable, non-invasive biomarkers is gaining traction with a number of profiles currently appearing in the literature.

## **1.5.2. Where are we in diabetic nephropathy: microRNAs and biomarkers**

### **1.5.2.1. Introduction**

Of all micro- and macrovascular complications of DM, diabetic nephropathy is one of the most complex and is the culmination of coordinated actions of several cell types in response to a plethora of environmental factors beginning directly with chronic hyperglycaemia. Part of this response involves dysregulation of miRNA which are increasingly recognised as important players in the propagation and progression of DN. The following review outlines what is presently known about miRNA in DN with special consideration to their relationship with important fibrotic growth factors.



# Where are we in diabetic nephropathy: microRNAs and biomarkers?

Aaron McClelland, Shinji Hagiwara, and Phillip Kantharidis

## Purpose of review

Several factors are now known to contribute to the development and progression of nephropathy, particularly in diabetes. In recent times, there has been surge of interest in the role of small noncoding RNA, with several reports focusing on the effects of microRNAs on their target genes that are of relevance to nephropathy. This review focuses on recent progress in this field.

## Recent findings

The list of microRNAs that have been identified to play a role in nephropathy continues to grow. Of particular interest is the fact that most microRNAs that are implicated in nephropathy are regulated by the profibrotic factor, transforming growth factor- $\beta$ . Additionally, some recent studies have used the presence of microRNAs in biofluids as a source of potential biomarkers for many diseases, particularly in diabetic nephropathy.

## Summary

MicroRNAs hold much promise given their novelty, promiscuity and involvement in many biological and pathological processes. There are promising early signs of their potential as biomarkers as well as therapeutic targets.

## Keywords

biomarkers, fibrosis, microRNA, TGF- $\beta$

## INTRODUCTION

Despite many advances in our understanding of the development and progression of renal disorders, the currently available treatments have not been very effective at preventing the development of this disease. Several factors are known to play a role in progressive renal diseases. Among the most important is transforming growth factor- $\beta$  (TGF- $\beta$ ), which directly stimulates extracellular matrix (ECM) production in the kidney, and transforms cells to a profibrotic phenotype. Many fibrogenic mechanisms converge on TGF- $\beta$  and its receptors and signal via the SMAD (mothers against decapentaplegic homolog), mitogen-activated protein kinase (MAPK) and other pathways [1–4] to drive renal fibrosis. However, the direct targeting of TGF- $\beta$  as an antifibrotic treatment presents a problem because of the critical role that this factor plays in immune surveillance [5]. The challenge is to identify other therapeutic targets downstream of TGF- $\beta$ .

In identifying new targets, a novel family of small, noncoding RNA, called microRNA (miRNA), has received prominent attention in both physiology and disease. Exciting data demonstrating the

potential to attenuate renal disease in experimental diabetes by modulating the expression of certain miRNAs provide impetus for further studies in this area. That multiple miRNAs can target a single RNA, whereas each miRNA can target multiple RNAs continues to challenge our notion of linear signaling and the concept of cause and effect. The ability of certain miRNAs to positively regulate their own expression as exemplified in the case of miR-200b and zinc finger E-box binding homeobox 2 (ZEB2) [6], to target epigenetic regulators [7,8] and to interact with promoter sequences [9,10], and the potential of a single dysregulated miRNA

Diabetes Division, JDRF Danielle Alberti Memorial Centre for Diabetes Complications, Baker IDI Heart and Diabetes Institute, Melbourne, Australia

Correspondence to Phillip Kantharidis, JDRF Danielle Alberti Memorial Centre for Diabetes Complications, Diabetes Division, Baker IDI Heart and Diabetes Institute, 75 Commercial Road, Melbourne 3004, Australia.

**Curr Opin Nephrol Hypertens** 2014, 23:80–86

DOI:10.1097/01.mnh.0000437612.50040.ae

**KEY POINTS**

- Several factors drive the development and progression of renal fibrosis, including a clear role for microRNAs.
- The most potent driver of renal fibrosis is TGF-β and its downstream signaling pathways.
- The expression of many microRNAs deregulated in diabetic nephropathy is regulated by TGF-β.
- The recent identification of a microRNA signature that predicted the development of diabetes in otherwise healthy patients has generated much interest in identifying potential microRNA biomarkers for renal disease by using easily accessible biofluids.

to influence an entire signaling network present a clear challenge to our understanding of how miRNAs regulate and are regulated by factors that contribute to kidney and related disease.

**MICRORNA AND RENAL DISEASE**

A number of miRNAs have emerged as key players in diabetic nephropathy, in particular miR-29 and miR-200 families along with miR-192 and miR-21. A common theme between these miRNAs is that all are regulated by TGF-β in renal cells and that normalization of their expression reverses fibrogenesis in in-vitro and in-vivo models of diabetic

and nondiabetic renal disease. Thus, there is speculation that improved treatment of diabetic nephropathy downstream of TGF-β may be afforded by targeting these miRNAs. Indeed, most miRNAs implicated in renal disease are regulated by TGF-β (Fig. 1 and Fig. 2).

Although epithelial to mesenchymal transition (EMT)-mediated production of renal fibroblasts remains contentious, it is clear that fibrogenesis in many cell types overlaps with part of the EMT program [11–13]. The miR-200 family plays an important role in EMT in part by targeting ZEB1/2, the transcriptional repressors of E-cadherin (E-cad) [6,14,15]. Overexpression of miR-200b in human proximal tubule cells (PTCs) increased E-cad expression, even in the presence of TGF-β [16<sup>¶</sup>]. Fibronectin (FN1) was also repressed, whereas plasminogen activator inhibitor 1 (PAI1) was increased [16<sup>¶</sup>], with the latter suggesting that SMAD3 signaling was unlikely to be contributing to the antifibrotic properties of miR-200b. Decreased miR-200a/141 was observed in a unilateral ureteral obstruction (UUO) model of renal fibrosis along with increased FN1 and alpha-smooth muscle actin (α-SMA) [17<sup>¶</sup>]. These findings were replicated in PTCs in which TGF-β reduced the expression of the miR-200 family, whereas exogenous SMAD7 restored miRNA expression thereby providing a mechanistic insight into the induction of the fibrotic program. Interestingly, in another

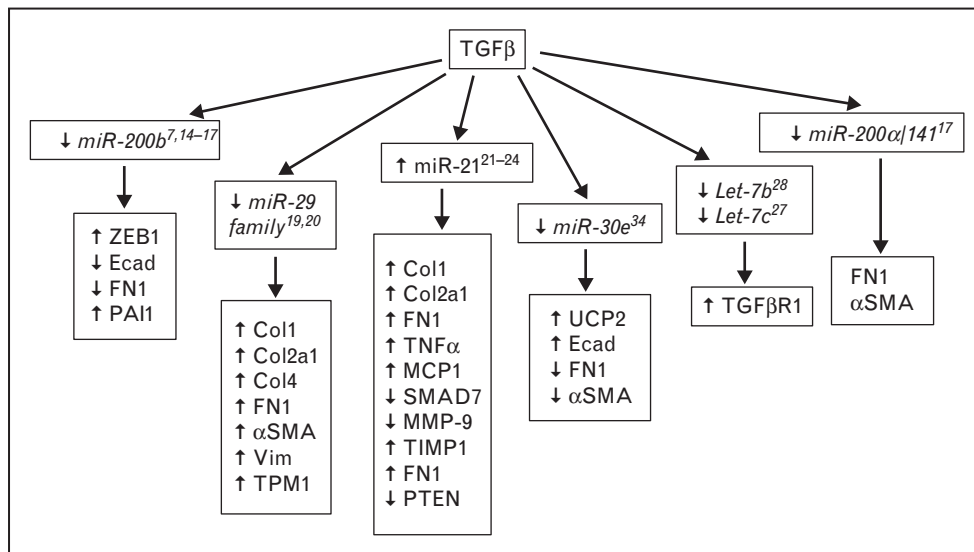


**FIGURE 1.** TGF-β1 regulated microRNAs recently reported in the literature, along with a number of their target genes that are relevant to diabetic nephropathy. α-SMA, alpha-smooth muscle actin; col2α1, collagen 2α1; E-cad, E-cadherin; FN1, fibronectin; MCP-1, monocyte chemoattractant protein 1; MMP-9, matrix metalloproteinase 9; PAI1, plasminogen activator inhibitor 1; PTEN, phosphatase and tensin homolog; SMAD, mothers against decapentaplegic homolog; TGF-β, transforming growth factor-β; TIMP, tissue inhibitor of metalloproteinase; TPM, tropomyosin; UCP2, uncoupling protein 2; VIM, vimentin; ZEB1, zinc finger E-box binding homeobox 1.

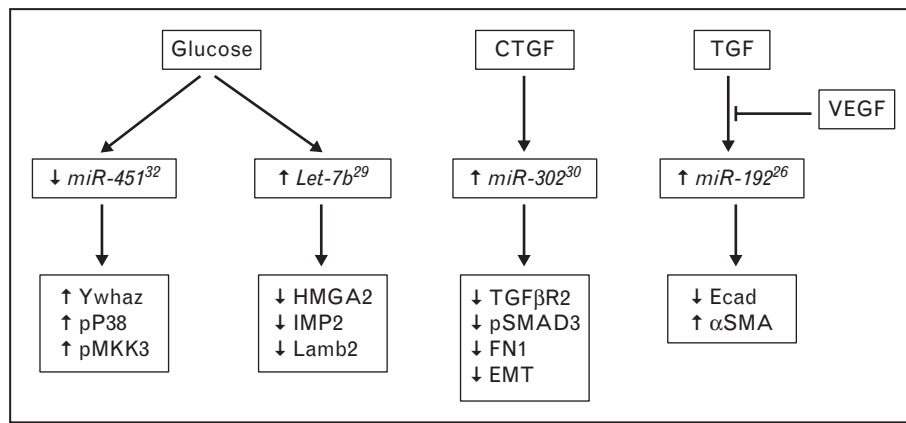


**FIGURE 2.** Glucose, CTGF and VEGF-regulated miRNA recently reported in the literature, and their target genes that are of relevance to diabetic nephropathy. α-SMA, alpha-smooth muscle actin; CTGF, connective tissue growth factor; E-cad, E-cadherin; EMT, epithelial to mesenchymal transition; FN1, fibronectin; TGF-β, transforming growth factor-β; VEGF, vascular endothelial growth factor.

study, no changes in miR-200a/c/141 were observed with TGF-β treatment in biopsy-derived tubular cells; however, 70% of those cells were from distal tubules, potentially masking any changes in PTCs [18].

TGF-β-mediated fibrosis also involves down-regulation of the miR-29 family in renal cells concurrent with increased expression of various collagens [19]. Ectopic expression of these miRNAs was sufficient to partially restore expression of FN1, αSMA, collagens and vimentin in TGF-β treated human podocytes. Several collagens were found to be direct targets of the miR-29 family providing a direct mechanism for collagen upregulation by TGF-β. Importantly, correlative data were presented demonstrating decreased expression of miR-29 family members in conjunction with diabetic nephropathy. For example, treatment of uninephrectomized rats with streptozotocin (STZ)-induced diabetes with either fasudil or losartan prevented diabetes induced renal damage and restored miR-29a and miR-29c expression supporting the therapeutic potential of these miRNA. miR-29c was also recently shown to directly target tropomyosin 1α and collagen 2α1 [20]. Validation of these target genes with other miR-29 family members would be of interest as all members share the same target sequence and are similarly deregulated in diabetic nephropathy.

TGF-β also induces expression of miR-21. Increased miR-21 levels were recently demonstrated in renal cortex in db/db mice, a model of type 2 diabetes [21]. Knockdown of miR-21 decreased mesangial expansion via decreased collagen I/IV and FN1 expression and also reduced macrophage infiltration and tumor necrosis factor-α (TNF-α) and monocyte chemoattractant protein 1 (MCP-1) expression. These gene expression changes were

replicated *in vitro* in both PTC and mesangial cells, with miR-21 overexpression enhancing fibrogenesis via a mechanism which in part involved the direct targeting of SMAD7. Recently, miR-21 was also shown to target matrix metalloproteinase 9 (MMP-9) thus contributing to the fibrotic scarring observed in diabetic kk-ay mice, a model of type 2 diabetes [22]. Inhibition of miR-21 resulted in decreased tissue inhibitor of metalloproteinase 1 (TIMP1), FN1 and collagen expression as well as reduced glomerulosclerosis index. Expression of miR-21 is also inversely correlated with phosphatase and tensin homolog (PTEN) expression in mesangial cells [23] via interaction with a noncanonical target site [24]. miR-21 inhibition correlated with decreased TGF-β-mediated phosphorylation of Akt, a serine/threonine-specific protein kinase, and deactivation of mammalian target of rapamycin signaling. Accordingly, global protein synthesis was decreased leading to reduced TGF-β-induced FN1 and collagen 1α2 expression, providing further mechanistic links with miR-21 expression and mesangial expansion.

miR-192 is the most controversial of the ‘classic’ nephropathic miRNAs exhibiting both up and downregulation depending on the cell type and model utilized. The evidence supporting either observation has recently been reviewed [25]. Adding to the arguments that miR-192 is profibrotic, Hong *et al.* [26] recently reported that TGF-β-mediated upregulation of miR-192 and SMAD3 phosphorylation were reduced in a human kidney cell line stably overexpressing vascular endothelial growth factor (VEGF), another important growth factor. Furthermore, this effect was also observed in regard to TGF-β-induced E-cad downregulation.

One of the most ubiquitous and evolutionarily conserved miRNA families is the Let-7 family, and

there is a role emerging for this family in diabetic nephropathy. Indeed, Let-7c was shown to be central to the antifibrotic effects of lipoxin A4 in PTCs [27<sup>■</sup>]. Lipoxin A4 decreased TGF- $\beta$ -induced expression of a number of fibrotic genes via derepression of Let-7c, which acts to directly repress TGF- $\beta$  receptor 1 (TGF- $\beta$ RI). Furthermore, in fibrotic renal biopsies, Let-7c was downregulated with a number of Let-7c targets also being derepressed. Collectively, these data highlight the therapeutic potential for lipoxins against the progression of diabetic nephropathy.

In another study, Let-7b was shown to regulate the expression of TGF- $\beta$ RI in PTCs, leading to reduced TGF- $\beta$ 1 signaling and fibrogenesis in these cells as well as in diabetic and nondiabetic models of renal fibrosis [28<sup>■</sup>]. In podocytes, Let-7b is greatly upregulated under high-glucose conditions leading to downregulation of the high mobility group protein HMGA2, a transcription factor required for expression of the insulin-like growth factor 2 mRNA-binding protein 2 (IGF2BP2). IGF2BP2 binds laminin $\beta$ 2 mRNA and is required for efficient translation of this transcript thus providing the link between Let-7b dysregulation, laminin $\beta$ 2 and diabetes-mediated glomerular dysfunction [29<sup>■</sup>].

Other recently reported miRNAs that are of relevance to the kidney include miR-302, which is upregulated by connective tissue growth factor (CTGF) and which targets TGF- $\beta$ RI in mesangial cells, leading to decreased TGF- $\beta$ -induced SMAD3 activation, decreased FN1 expression and reduced mesangial expansion [30<sup>■</sup>]. Decreased TGF $\beta$ RI levels are observed in human renal disease and UUO rat kidney. This miRNA reduced the effects of TGF- $\beta$  in terms of EMT and fibrogenesis by targeting TGF $\beta$ RI.

Diabetic renal damage is also induced by miR-215, which positively regulates  $\beta$ -catenin signaling by targeting beta-catenin-interacting protein 1 protein (CTNBP1) [31<sup>■</sup>]. This miRNA, which is also induced by both high glucose and TGF- $\beta$ , induces FN1 and  $\alpha$ SMA expression in mesangial cells *in vitro*. In db/db mice, overexpression of this miRNA leads to expansion, whereas inhibition leads to decreases, in mesangial area with the accompanied respective decreases and increases in CTNBP1.

MiR-451 regulates expression of 14-3-3 protein zeta/delta (Ywhaz) leading to a reduced p38 MAPK phosphorylation and decreased MAPK kinase 3 (MKK3) activation in mesangial cells [32<sup>■</sup>]. In db/db mice, delivery of this miRNA produced similar results leading to decreased glomerular diameter. As Ywhaz binds to insulin receptor substrate 2, a key post insulin receptor signaling molecule, it is tempting to speculate that the miR-451/Ywhaz axis may play an important role in insulin signaling in metabolic tissues [33].

Finally, miR-30e has been implicated in direct regulation of uncoupling protein 2 (UCP2) in rats with UUO [34<sup>■</sup>]. Exogenous miR-30e decreased UCP2 in UUO and in TGF- $\beta$ -treated PTCs, reducing fibrogenesis. Furthermore, delivery of UCP2 *in vitro* was sufficient to overcome the protective effects of miR-30e suggesting that the miR-30e/UCP2 interaction is a major player in the TGF- $\beta$ -mediated fibrogenesis in PTCs.

## MICRORNA, THE RENIN-ANGIOTENSIN SYSTEM AND KIDNEY DISEASE

The kidney has long been linked to the cause of essential hypertension with chronic kidney disease (CKD), an established cardiovascular risk factor [35]. Few studies have focused on a link between hypertension, microRNAs and kidney disease [36].

Chen *et al.* [37<sup>■</sup>] have reported decreased miR-145 and miR-155 levels in blood from 90 patients with CKD with progressive loss of eGFR. Expression was also decreased in the thoracic aorta in CKD rats compared with normal, with concordant changes in target genes. Overexpression of miR-155 in vascular smooth muscle cells (VSMCs) from CKD rats inhibited angiotensin II receptor, type 1 (AT1R) expression and decreased cellular proliferation, thus confirming a protective role in VSMCs. Whether downregulation of these miRNAs are the cause or are the result of the widespread vascular phenotype abnormalities in patients with CKD remains to be determined.

In primary cardiac fibroblasts and in HEK293N cells, miR-29b, miR-129-3p, miR-132, miR-132\* and miR-212 are regulated by angiotensin II (AngII) via activation of Erk1/2 by G $\alpha$ q/11-dependent and independent pathways [38]. More recently, Jin *et al.* [39<sup>■</sup>] also demonstrated upregulation of miR-132/212 by AngII via AT1R in rat VSMCs leading to the induction of MCP1 through the repression of PTEN by miR-132. Moreover, it was demonstrated that miR-132 increased phosphorylation of the cAMP response element-binding protein (CREB) via RAS P21 protein activator 1 downregulation and that miR-132 upregulation by AngII required CREB activation, demonstrating a positive feedback loop. Eskildsen *et al.* [40<sup>■</sup>] used profiling experiments to identify significantly increased miR-132 and miR-212 in heart, aorta and kidney of hypertensive rats following chronic AngII infusion. Significant decreases in miR-132 and miR-212 were observed in arteries of angiotensin receptor blocker (ARB)-treated patients, but treatment with  $\beta$ -blockers had no effect. It thus appears that AngII-induced hypertension increases miR-132 and miR-212 in organs associated with blood pressure control,

including the kidney, via the  $G\alpha_q$ -dependent pathway.

## BIOMARKERS IN RENAL DISEASE

The availability and access to new technologies has led to the identification of several novel genetic factors potentially contributing to diabetic nephropathy [41,42]. Several recent studies have explored the use of noncoding RNA, including miRNA, as potential biomarkers in diabetic and nondiabetic renal disease. Indeed, the pioneering study by Zampetaki *et al.* [43] has generated considerable excitement as differential expression of a certain miRNA signature enabled the identification of 70% of patients that progressed to overt disease, prior to any symptoms. Whether any of these miRNAs might be related to renal disease remains to be determined.

Biomarker studies have generally focused on miRNA analysis in easily accessible biofluids (plasma, urine) isolated from cell sediments or in microparticles and exosomes. It is now thought that up to 90% of circulating miRNAs are in fact extravesicular, complexed with proteins, particularly with Ago2, high-density lipoprotein and other proteins [44]. Whether released by active secretion [45] or as a result of tissue damage, in-vitro studies demonstrate efficient uptake of these miRNAs, suggesting that this form of miRNA transport has a biological role at distal sites and can be potentially used to deliver miRNAs for therapeutic purposes.

In the Pittsburgh Epidemiology of Diabetes study [46], urinary miRNA profiles were assessed in four groups of 10 patients ranging from no renal disease to overt diabetic nephropathy with intermittent or persistent microalbuminuria. Differential expression of 27 miRNAs was identified between these groups with unique expression patterns associated with each group. Although significant, these results will need to be replicated in larger cohorts.

Urinary levels of miR-10a and miR-30d may represent specific and sensitive biomarkers of renal injury in diabetic and nondiabetic animal models [47]. Expression levels of these miRNAs in renal cortex and serum from experimental animals correlated with the degree of renal injury. Finally, these miRNAs were also elevated in urine from patients with focal segmental glomerulosclerosis when compared with healthy patients, and may therefore turn out to be general markers of renal disease.

In another study, urinary sediments and kidney biopsies from 56 patients were used to identify potential miRNA biomarkers for CKD [48]. Diabetic nephropathy was associated with decreased urinary miR-15 levels, whereas elevated miR-17 was observed

in patients with IgA nephropathy. Among other observations, urinary miR-21 and miR-216a levels correlated with the rate of decline of renal function and with the risk of progression to renal failure.

Wang *et al.* [49] demonstrated that urinary miR-21, miR-29 and miR-93 are biomarkers of renal fibrosis in patients with IgA nephropathy. More specifically, miR-29b/c correlated with proteinuria and renal function, whereas miR-93 correlated with glomerular scarring. Another study demonstrated increased circulating miR-21 in 42 renal transplant patients with fibrotic kidney disease [50], the level of expression correlating with increasing interstitial fibrosis.

Emerging trends point to a significant involvement of miRNAs previously associated with a role in diabetic nephropathy, but new miRNAs have also been identified. Larger trials need to be conducted in order to establish the utility of miRNAs as biomarkers of renal disease. What is evident so far is that there is much we do not yet understand about miRNAs in biofluids and their role in disease. For example, the observation that some miRNA expression changes in diseased renal tissue are sometimes reversed in biofluids, whereas others are conserved [51–56].

## CIRCULATING MICRORNA

Given circulating miRNAs probably act on distal tissues, how this form of inter-tissue communication is regulated in normal physiological versus pathological states is not clear, but prompts the question: are the complications of diabetes such as diabetic nephropathy the cause or the result of deregulated circulating miRNAs? A confounding factor in the equation is the observation that certain miRNAs may be elevated in one tissue and decreased in another under the same disease condition. For example, miR-29 family members are strongly implicated in tissue fibrogenesis, yet are decreased in serum of diabetes patients [57–59]. However, these miRNAs are upregulated in the pancreas and metabolic tissues leading to decreased insulin secretion [60] and decreased insulin sensitivity [61]. One can speculate whether the decreased levels in nonmetabolic tissues may reflect an attempt to normalize systemic glucose via maintenance of insulin sensitivity at the expense of tissue architecture.

The presence of miRNAs in the circulation adds weight to the thought that these molecules act as a novel class of autocrine or paracrine mediators and begs the question of specificity in the targeting of their activity. As the majority of circulating miRNA appears to be chaperoned, uncharacterized exosome and high density lipoproteins are likely candidates

for targeting miRNA to specific cells or tissues. Investigation of circulating miRNA specificity is likely to prove fruitful in the years to come.

Another challenge for biomarker identification in diabetic nephropathy is that none of the miRNAs identified to date are truly kidney specific. Furthermore, analysis of miRNAs differentially expressed in urine of diabetic versus nondiabetic patients shows a general lack of correlation with the levels in blood or plasma [62]. This appears to hold true for the miRNAs generally observed to be increased in body fluids in diabetic patients (miR-144, miR-192, miR-216/217, miR-377) as well as those that are decreased (miR-21, miR-375).

## CONCLUSION

Much progress has been made in our understanding of miRNA biology in normal and pathological conditions. Several miRNAs have been identified as playing an important role in diabetic nephropathy, contributing to different aspects of this disease. The fact that many of these miRNAs in diabetic nephropathy are regulated by TGF- $\beta$ 1 suggests that a common treatment may be able to reverse these changes and improve the clinical outcome for patients with diabetic nephropathy. In contrast, there is still a large gap in our understanding of the role and importance of circulating miRNAs in normal physiology and pathology. There is considerable interest in determining how circulating miRNAs are packaged, released, trafficked and delivered to the distal tissues. Easy access to biofluids that contain circulating miRNAs holds promise for the identification of potential biomarkers not only for the diagnosis of but also for the prediction of the development of diabetic nephropathy.

## Acknowledgements

*This work was supported by the Diabetes Australia Research Trust, the National Health and Medical Research Council, and a Vera Dalgleish Phillips Fellowship.*

## Conflicts of interest

*There are no conflicts of interest.*

## REFERENCES AND RECOMMENDED READING

Papers of particular interest, published within the annual period of review, have been highlighted as:

- of special interest
- of outstanding interest

1. Li JH, Huang XR, Zhu HJ, *et al.* Advanced glycation end products activate Smad signaling via TGF- $\beta$ -dependent and independent mechanisms: implications for diabetic renal and vascular disease. *FASEB J* 2004; 18:176–178.
2. Li JH, Wang W, Huang XR, *et al.* Advanced glycation end products induce tubular epithelial-myofibroblast transition through the RAGE-ERK1/2 MAP kinase signaling pathway. *Am J Pathol* 2004; 164:1389–1397.
3. Meng XM, Huang XR, Chung AC, *et al.* Smad2 protects against TGF- $\beta$ /Smad3-mediated renal fibrosis. *J Am Soc Nephrol* 2010; 21:1477–1487.
4. Lee JM, Dedhar S, Kalluri R, Thompson EW. The epithelial-mesenchymal transition: new insights in signaling, development, and disease. *J Cell Biol* 2006; 172:973–981.
5. Wahl SM, Wen J, Moutsopoulos N. TGF- $\beta$ : a mobile purveyor of immune privilege. *Immunol Rev* 2006; 213:213–227.
6. Gregory PA, Bert AG, Paterson EL, *et al.* The miR-200 family and miR-205 regulate epithelial to mesenchymal transition by targeting ZEB1 and SIP1. *Nat Cell Biol* 2008; 10:593–601.
7. Winbanks CE, Wang B, Beyer C, *et al.* TGF- $\beta$  regulates miR-206 and miR-29 to control myogenic differentiation through regulation of HDAC4. *J Biol Chem* 2011; 286:13805–13814.
8. Duursma AM, Kedde M, Schrier M, *et al.* miR-148 targets human DNMT3b protein coding region. *RNA* 2008; 14:872–877.
9. Kim DH, Saetrom P, Snove O Jr, Rossi JJ. MicroRNA-directed transcriptional gene silencing in mammalian cells. *Proc Natl Acad Sci U S A* 2008; 105:16230–16235.
10. Younger ST, Corey DR. Transcriptional gene silencing in mammalian cells by miRNA mimics that target gene promoters. *Nucleic Acids Res* 2011; 39:5682–5691.
11. Zeisberg M, Duffield JS. Resolved: EMT produces fibroblasts in the kidney. *J Am Soc Nephrol* 2010; 21:1247–1253.
12. Carew RM, Wang B, Kantharidis P. The role of EMT in renal fibrosis. *Cell Tissue Res* 2012; 347:103–116.
13. Kalluri R, Weinberg RA. The basics of epithelial-mesenchymal transition. *J Clin Invest* 2009; 119:1420–1428.
14. Park SM, Gaur AB, Lengyel E, Peter ME. The miR-200 family determines the epithelial phenotype of cancer cells by targeting the E-cadherin repressors ZEB1 and ZEB2. *Genes Dev* 2008; 22:894–907.
15. Korpala M, Lee ES, Hu G, Kang Y. The miR-200 family inhibits epithelial-mesenchymal transition and cancer cell migration by direct targeting of E-cadherin transcriptional repressors ZEB1 and ZEB2. *J Biol Chem* 2008; 283:14910–14914.
16. Tang O, Chen XM, Shen S, *et al.* MiRNA-200b represses transforming growth factor- $\beta$ 1-induced EMT and fibronectin expression in kidney proximal tubular cells. *Am J Physiol Renal Physiol* 2013; 304:F1266–F1273.
- Repression of fibronectin by miR-200b in PTCs is probably not via effects on SMAD3 signaling.
17. Xiong M, Jiang L, Zhou Y, *et al.* The miR-200 family regulates TGF- $\beta$ 1-induced renal tubular epithelial to mesenchymal transition through Smad pathway by targeting ZEB1 and ZEB2 expression. *Am J Physiol Renal Physiol* 2012; 302:F369–F379.
- This article confirmed that the miR-200 family regulates TGF- $\beta$ -induced EMT in PTCs.
18. Keller C, Kroening S, Zuehlke J, *et al.* Distinct mesenchymal alterations in N-cadherin and E-cadherin positive primary renal epithelial cells. *PLoS One* 2012; 7:e43584.
- Although TGF- $\beta$  regulates levels of the miR-200 family in PTCs, this does not appear to happen in distal tubular epithelial cells.
19. Wang B, Komers R, Carew R, *et al.* Suppression of microRNA-29 expression by TGF- $\beta$ 1 promotes collagen expression and renal fibrosis. *J Am Soc Nephrol* 2012; 23:252–265.
- This article demonstrates the antifibrotic properties of the miR-29 family in PTCs, mesangial cells and podocytes. It was also demonstrated that the miR-29 family is decreased in diabetic and nondiabetic models of renal fibrosis.
20. Fang Y, Yu X, Liu Y, *et al.* miR-29c is downregulated in renal interstitial fibrosis in humans and rats and restored by HIF- $\alpha$  activation. *Am J Physiol Renal Physiol* 2013; 304:F1274–F1282.
- miR-29c directly targets tropomyosin 1 $\alpha$  and collagen 2 $\alpha$ 1.
21. Zhong X, Chung AC, Chen HY, *et al.* miR-21 is a key therapeutic target for renal injury in a mouse model of type 2 diabetes. *Diabetologia* 2013; 56:663–674.
- Knockdown of miR-21 *in vivo* attenuates renal fibrosis in the diabetic db/db mouse.
22. Wang J, Gao Y, Ma M, *et al.* Effect of miR-21 on renal fibrosis by regulating MMP-9 and TIMP1 in kk-ay diabetic nephropathy mice. *Cell Biochem Biophys* 2013; 67:537–546.
- This study demonstrated that miR-21 contributes in part to renal fibrosis by targeting MMP-9 and TIMP1 in experimental diabetic nephropathy.
23. Dey N, Ghosh-Choudhury N, Kasinath BS, Choudhury GG. TGF- $\beta$ -stimulated microRNA-21 utilizes PTEN to orchestrate AKT/mTORC1 signaling for mesangial cell hypertrophy and matrix expansion. *PLoS One* 2012; 7:e42316.
- This study demonstrated that miR-21 regulates PTEN and therefore AKT signaling and fibrosis in renal cells.

24. Liu ZL, Wang H, Liu J, Wang ZX. MicroRNA-21 (miR-21) expression promotes growth, metastasis, and chemo- or radioresistance in nonsmall cell lung cancer cells by targeting PTEN. *Mol Cell Biochem* 2013; 372: 35–45.
- This study confirmed that miR-21 targets PTEN and hence AKT signaling.
25. Jenkins RH, Martin J, Phillips AO, *et al.* Pleiotropy of microRNA-192 in the kidney. *Biochem Soc Trans* 2012; 40:762–767.
- This is a nice review about the controversial role of miR-192 in renal disease.
26. Hong J-P, Li X-M, Li M-X, Zheng F-L. VEGF suppresses epithelial-mesenchymal transition by inhibiting the expression of Smad3 and miR-192, a Smad3-dependent microRNA. *Int J Mol Med* 2013; 31:1436–1442.
- This study demonstrated that SMAD3 signaling and miR-192 are attenuated by VEGF.
27. Brennan EP, Nolan KA, Borgeson E, *et al.* Lipoxins attenuate renal fibrosis by inducing let-7c and suppressing TGFβ1. *J Am Soc Nephrol* 2013; 24:627–637.
- This study demonstrates restoration of a microRNA by a 'natural' product can attenuate renal fibrosis.
28. Wang B, Jha JC, Hagiwara S, *et al.* Transforming growth factor-β1-mediated renal fibrosis is dependent on the regulation of transforming growth factor receptor 1 expression by let-7b. *Kidney Int* 2013. doi:10.1038/ki.2013.372. [Epub ahead of print]
- This study demonstrates that Let-7b also targets TGF-β1 and that reduced levels of Let-7b result in increased fibrotic signaling and renal fibrogenesis.
29. Schaeffer V, Hansen KM, Morris DR, *et al.* RNA-binding protein IGF2BP2/IMP2 is required for laminin-β2 mRNA translation and is modulated by glucose concentration. *Am J Physiol Renal Physiol* 2012; 303:F75–F82.
- This study demonstrated that elevated glucose reduces laminin-β2 expression by a complex mechanism that involves RNA-binding proteins and Let-7b.
30. Faherty N, Curran SP, O'Donovan H, *et al.* CCN2/CTGF increases expression of miR-302 microRNAs, which target the TGFβ type II receptor with implications for nephropathic cell phenotypes. *J Cell Sci* 2012; 125 (Pt 23):5621–5629.
- This study demonstrated that CTGF induces miR-302, which targets TGF-β2 in mesangial cells.
31. Mu J, Pang Q, Guo YH, *et al.* Functional implications of microRNA-215 in TGF-β1-induced phenotypic transition of mesangial cells by targeting CTNBP1. *PLoS One* 2013; 8:e58622.
- This study demonstrated that miR-215 which is upregulated by TGF-β causes a change in mesangial cells phenotype by a mechanism that involves the targeting of CTNBP1.
32. Zhang Z, Luo X, Ding S, *et al.* MicroRNA-451 regulates p38 MAPK signaling by targeting of Ywhaz and suppresses the mesangial hypertrophy in early diabetic nephropathy. *FEBS Lett* 2012; 586:20–26.
- This is the first study to describe a potential role for miR-451 in early diabetic nephropathy.
33. Ogihara T. 14-3-3 Protein binds to insulin receptor substrate-1, one of the binding sites of which is in the phosphotyrosine binding domain. *J Biol Chem* 1997; 272:25267–25274.
34. Jiang L, Qiu W, Zhou Y, *et al.* A microRNA-30e/mitochondrial uncoupling protein 2 axis mediates TGF-β1-induced tubular epithelial cell extracellular matrix production and kidney fibrosis. *Kidney Int* 2013; 84:285–296.
- This study demonstrated the induction of UCP2 after TGF-β-mediated down-regulation of miR-30e.
35. Go AS, Chertow GM, Fan D, *et al.* Chronic kidney disease and the risks of death, cardiovascular events, and hospitalization. *N Engl J Med* 2004; 351:1296–1305.
36. Hagiwara S, Kantharidis P, Cooper ME. microRNA as biomarkers and regulator of cardiovascular development and disease. *Curr Pharm Des* 2013. [Epub ahead of print]
37. Chen NX, Kiattisunthorn K, O'Neill KD, *et al.* Decreased microRNA is involved in the vascular remodeling abnormalities in chronic kidney disease (CKD). *PLoS One* 2013; 8:e64558.
- This study identified elevated miR-145 and miR-155 levels in blood in patients with CKD.
38. Jeppesen PL, Christensen GL, Schneider M, *et al.* Angiotensin II type 1 receptor signalling regulates microRNA differentially in cardiac fibroblasts and myocytes. *Br J Pharmacol* 2011; 164:394–404.
39. Jin W, Reddy MA, Chen Z, *et al.* Small RNA sequencing reveals microRNAs that modulate angiotensin II effects in vascular smooth muscle cells. *J Biol Chem* 2012; 287:15672–15683.
- This is the study showing that miR-132 and miR-212 are induced by AngII in VSMCs.
40. Eskildsen TV, Jeppesen PL, Schneider M, *et al.* Angiotensin II regulates microRNA-132/212 in hypertensive rats and humans. *Int J Mol Sci* 2013; 14:11190–11207.
- This study shows that miR-132 and miR-212 are significantly increased in tissues associated with blood pressure control such as kidney and heart by AngII, and reduced in ARB-treated patients.
41. DiStefano JK. Identification of novel genetic markers and improved treatment options for diabetic kidney disease. *Biomarkers Med* 2010; 4:739–741.
42. Thomas MC, Groop PH, Tryggvason K. Towards understanding the inherited susceptibility for nephropathy in diabetes. *Curr Opin Nephrol Hypertens* 2012; 21:195–202.
43. Zampetaki A, Kiechl S, Drozdov I, *et al.* Plasma microRNA profiling reveals loss of endothelial miR-126 and other microRNAs in type 2 diabetes. *Circ Res* 2010; 107:810–817.
44. Shantikumar S, Caporali A, Emanuelli C. Role of microRNAs in diabetes and its cardiovascular complications. *Cardiovas Res* 2012; 93:583–593.
45. Aggio RB, Ruggiero K, Villas-Boas SG. Pathway activity profiling (PAPi): from the metabolite profile to the metabolic pathway activity. *Bioinformatics* 2010; 26:2969–2976.
46. Argyropoulos C, Wang K, McClarty S, *et al.* Urinary microRNA profiling in the nephropathy of type 1 diabetes. *PLoS One* 2013; 8:e54662.
47. Wang N, Zhou Y, Jiang L, *et al.* Urinary microRNA-10a and microRNA-30d serve as novel, sensitive and specific biomarkers for kidney injury. *PLoS One* 2012; 7:e51140.
48. Szeto CC, Ching-Ha KB, Ka-Bik L, *et al.* Micro-RNA expression in the urinary sediment of patients with chronic kidney diseases. *Dis Markers* 2012; 33:137–144.
49. Wang G, Kwan BC, Lai FM, *et al.* Urinary miR-21, miR-29, and miR-93: novel biomarkers of fibrosis. *Am J Nephrol* 2012; 36:412–428.
50. Glowacki F, Savary G, Gnemmi V, *et al.* Increased circulating miR-21 levels are associated with kidney fibrosis. *PLoS One* 2013; 8:e58014.
51. Natarajan R, Putta S, Kato M. MicroRNAs and diabetic complications. *J Cardiovasc Translat Res* 2012; 5:413–422.
52. Denby L, Ramdas V, McBride MW, *et al.* miR-21 and miR-214 are consistently modulated during renal injury in rodent models. *Am J Pathol* 2011; 179:661–672.
53. Zhong X, Chung AC, Chen HY, *et al.* Smad3-mediated upregulation of miR-21 promotes renal fibrosis. *J Am Soc Nephrol* 2011; 22:1668–1681.
54. Sabatel C, Malvaux L, Bovy N, *et al.* MicroRNA-21 exhibits antiangiogenic function by targeting RhoB expression in endothelial cells. *PLoS One* 2011; 6:e16979.
55. Thum T, Gross C, Fiedler J, *et al.* MicroRNA-21 contributes to myocardial disease by stimulating MAP kinase signalling in fibroblasts. *Nature* 2008; 456:980–984.
56. Raitoharju E, Lyytikäinen LP, Levula M, *et al.* miR-21, miR-210, miR-34a, and miR-146a/b are up-regulated in human atherosclerotic plaques in the Tampere Vascular Study. *Atherosclerosis* 2011; 219:211–217.
57. Kantharidis P, Wang B, Carew RM, Lan HY. Diabetes complications: the microRNA perspective. *Diabetes* 2011; 60:1832–1837.
58. Kovacs B, Lumayag S, Cowan C, Xu S. MicroRNAs in early diabetic retinopathy in streptozotocin-induced diabetic rats. *Invest Ophthalmol Visual Sci* 2011; 52:4402–4409.
59. van Rooij E, Sutherland LB, Thatcher JE, *et al.* Dysregulation of microRNAs after myocardial infarction reveals a role of miR-29 in cardiac fibrosis. *Proc Natl Acad Sci U S A* 2008; 105:13027–13032.
60. Pullen TJ, da Silva Xavier G, Kelsey G, Rutter GA. miR-29a and miR-29b contribute to pancreatic beta-cell-specific silencing of monocarboxylate transporter 1 (Mct1). *Mol Cell Biol* 2011; 31:3182–3194.
61. Rottiers V, Naar AM. MicroRNAs in metabolism and metabolic disorders. *Nat Rev Mol Cell Biol* 2012; 13:239–250.
62. Yang Y, Xiao L, Li J, *et al.* Urine miRNAs: potential biomarkers for monitoring progression of early stages of diabetic nephropathy. *Med Hypotheses* 2013; 81:274–278.

### **1.5.2.2. Conclusion**

Considerable progress has been made in recent years in regards to understanding the role of miRNA in diabetic nephropathy and the ways in which they regulate or contribute to the effects of a number of classic growth factors and effectors. Many miRNA are seen to reside in and expand already large regulatory networks such as that formed by TGF $\beta$  and its many downstream effector pathways. Furthermore, miRNA profiles from biofluids appear to be both disease state and tissue specific thereby adding promise to the notion of utilising miRNA biomarkers in clinical diagnosis and prognosis in diabetes and more specifically, DN.

## **1.6. Mitochondria in diabetic nephropathy**

Mitochondria are the powerhouses of cellular metabolism in aerobic organisms. Through a series of thermodynamically efficient reactions, glucose and other carbohydrates along with fatty acids (FA) are converted into cellular energy. However, inefficiencies in these systems can lead to production of toxic by-products which have been implicated in the development of various diseases including DM (46, 104).

### **1.6.1. Mitochondrial role in cellular metabolism**

Glucose reabsorption in the PCT is insulin independent and is mediated by SGLT2 and SGLT1 Na<sup>+</sup>-glucose co-transporters which utilise an electrochemical gradient established by active Na<sup>+</sup>-K<sup>+</sup> antiporters on the basolateral side of PTC (86, 105, 106). Intracellular glucose is rapidly metabolised via glycolysis to reduced nicotinamide adenine dinucleotide (NADH), pyruvate (which is later converted into acetyl-CoA) and adenosine triphosphate (ATP), a process which is allosterically regulated by cellular energy demands (Figure 1-8) (107). The PCT is also the primary site for protein reabsorption and as such is also susceptible to increased uptake and subsequent metabolism of FA as these are transported bound to albumin and are leaked from the glomerulus in increased quantities during diabetes (108, 109). Unlike glucose, FA are metabolised entirely within the mitochondria through  $\beta$ -oxidation, however,  $\beta$ -oxidation generates NADH with additional reduced flavin adenine dinucleotide (FADH<sub>2</sub>) and acetyl-CoA, all in much larger quantities than glycolysis.

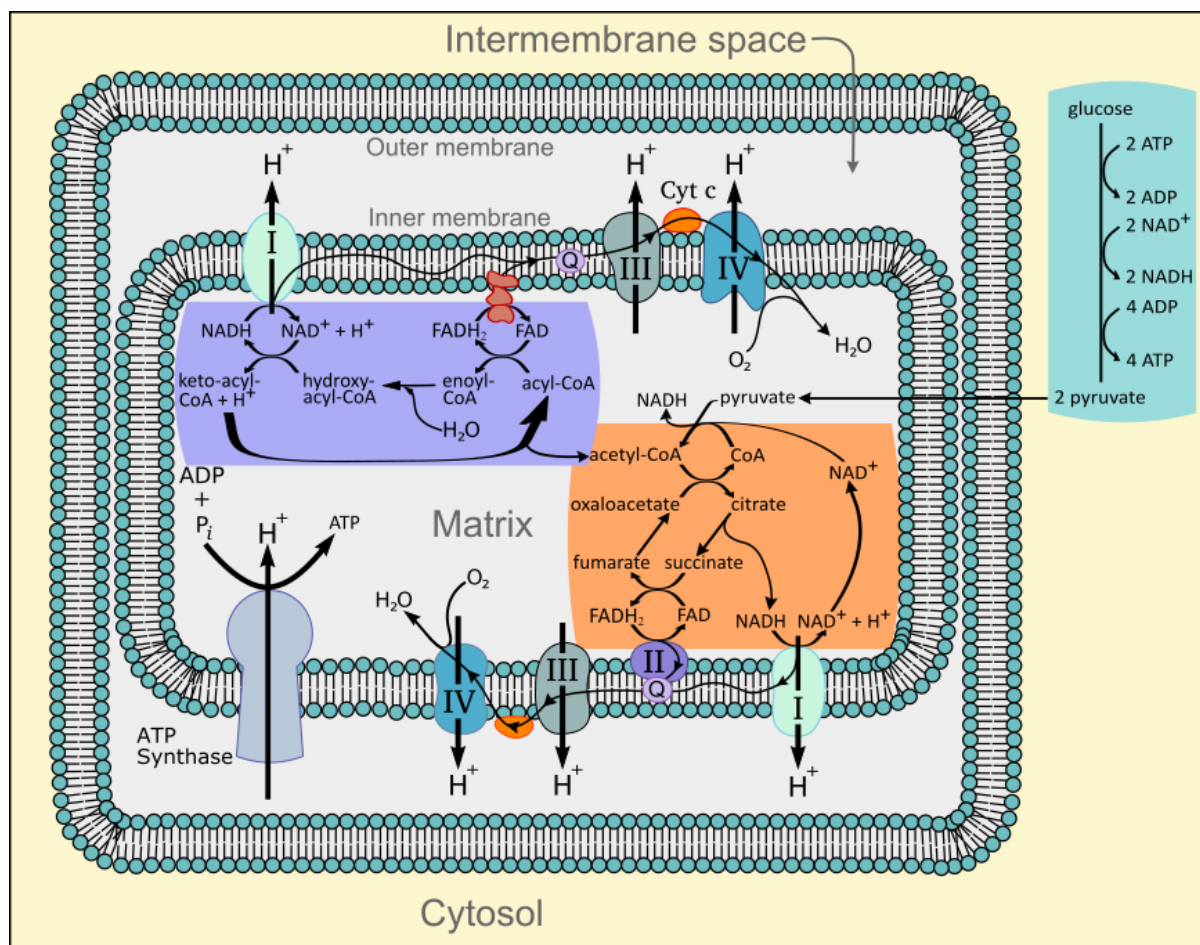


**Figure 1-8 Inter-relationship between glycolysis, beta-oxidation and ATP production.**

Glycolysis (blue box) produces ATP, pyruvate and electron donors. Pyruvate is reduced to acetyl-CoA which enters the TCA cycle (orange box) which produces NADH (there is additional NADH producing reactions in the TCA cycle which are not shown) and FADH<sub>2</sub> through reduction of succinate to fumarate.  $\beta$ -oxidation (purple box) produces FADH<sub>2</sub> which is utilised by ETF:QOR to inject electrons into the ETC by passing them to ubiquinone (Q), NADH and acetyl-CoA. The beta-oxidation loop continues until the final reaction produces two acetyl-CoA molecules at which point the FA chain has been fully broken down. Protons are pumped into the intermembrane space by electron flow at complex I, III and IV. The resultant membrane potential generates proton motive force which is utilised by ATP synthase to generate ATP thereby dissipating membrane potential. Superoxide (not shown) can be produced at most points where electron transfer occurs including complex I, complex II, complex III, ubiquinone and ETF:QOR (electron transfer flavoprotein:ubiquinone oxidoreductase). Adapted from Fvasconcellos, Wikimedia Commons (2007).

In the mitochondria, acetyl-CoA from  $\beta$ -oxidation and pyruvate metabolised by pyruvate dehydrogenase complex (PDC), enter the tricarboxylic acid (TCA) cycle with the acetyl group being bound to oxaloacetate to form citrate and NADH (110). A series of TCA cycle substrate oxidation reactions reduce oxidised electron donors resulting in the production of NADH, FADH<sub>2</sub>, CO<sub>2</sub> and guanosine triphosphate (GTP) and ending with the regeneration of oxaloacetate ready to accept another acetyl group (111). As with glycolysis, the TCA cycle is essentially substrate driven and will continue to restore electron donors so long as they are being consumed and acetyl-CoA is being produced. The electron donors NADH and FADH<sub>2</sub> will continue to be spent in the electron transport chain (ETC) so long as ATP is consumed and a membrane potential exists.

The ETC is comprised of four multimeric complexes which act to generate a proton gradient across the inner mitochondrial membrane via oxidation of NADH and FADH<sub>2</sub> (112). Electrons are stripped from NADH by complex I and passed to coenzyme Q which then passes them to cytochrome C via complex III and then to complex IV where they are utilised to reduce molecular oxygen to water (113). FADH<sub>2</sub> is also reduced at complex II with the electrons also being passed to coenzyme Q following the same route as those from oxidation of NADH (114). Protons are pumped at complex I, III and IV providing electrons can be passed to the next complex or in the case of complex IV, used to reduce oxygen.

However, imbalances in this process lead to electron leakage and partial reduction of oxygen thereby generating superoxide (O<sub>2</sub><sup>-</sup>) which may then form other reactive oxygen species including hydrogen peroxide (H<sub>2</sub>O<sub>2</sub>) or hydroxyl radicals ( $\cdot$ OH) (115, 116). Despite 1-2% of transferred electrons being leaked from the ETC, these are dealt with by both mitochondrial and cellular antioxidant enzymes and compounds. However, increased traffic or defects within the ETC or ROS handling machinery can disrupt this balance (117, 118). Regardless, in healthy mitochondria, the transfer of electrons between complexes is utilised to pump protons into the mitochondrial intermembrane space for ATP synthesis by ATP synthase (119). Providing this large mechanical protein is assembled correctly and a proton gradient exists across the inner mitochondrial membrane, ATP synthase will continue to generate ATP from adenosine diphosphate (ADP) and inorganic phosphate, dissipating the proton gradient in the process (120). If the proton gradient becomes excessive due to a lack of ATP synthase substrates or dysfunctional subunits, the membrane potential may be dissipated by uncoupling proteins (121).

## 1.6.2. Mitochondrial dysfunction in proximal tubule epithelial cells

### 1.6.2.1. *Hyperglycaemia and energy homeostasis in PTC*

The PCT is the primary site of reabsorption in the kidney and is responsible for bulk reclamation of glucose, electrolytes, protein and bicarbonate, amongst others (11). Much of this reabsorption occurs against concentration gradients or as the result of an enforced concentration gradient as is the case with glucose,  $\text{Na}^+$  and bicarbonate. Reabsorption of a number of products occurs through electrochemical gradients established via the activity of ATP-dependent  $\text{Na}^+/\text{K}^+$  and  $\text{Na}^+/\text{H}^+$  pumps on either the apical or basolateral surfaces of PTC (122, 123). As such, PTC are highly dependent upon ATP generation and therefore efficient and controlled mitochondrial function. A growing body of evidence indicates that PTC suffer from mitochondrial dysfunction but it is not known whether this dysfunction is primary or secondary to DN (124, 125). Regardless, given the role that the PCT plays in renal function in general, maintenance of healthy mitochondria is paramount to renal tissue homeostasis.

Hyperglycaemia itself is considered to be the primary cause of tubular dysfunction and is an initiating factor in mitochondrial dysfunction in PTC due to the increased energy demands generated from elevated plasma filtrate glucose. SGLT2 and SGLT1 are glucose cotransporters which are dependent upon intracellular  $\text{Na}^+$  concentrations (Figure 1-9) (35, 126). PTC actively maintain low intracellular  $\text{Na}^+$  by way of  $\text{Na}^+/\text{K}^+$  ATPase pumps located on their basolateral surface. Glucose reabsorption dissipates the  $\text{Na}^+$  gradient forcing increased activity of the active  $\text{Na}^+/\text{K}^+$  antiporters which inevitably increases energy demands on the cell and therefore ETC activity. In healthy mitochondria, 1-2% of electrons will be leaked from the ETC and result in partial reduction of oxygen and formation of ROS (118). Therefore, increasing energy demands placed upon PTC by elevated urinary glucose will lead to increased ROS production which may overwhelm the resident antioxidant proteins and metabolites such as superoxide dismutase 2 (SOD2) and glutathione respectively.

### 1.6.2.2. *Mitochondrial reactive oxygen species and PTC*

Despite the toxicity of ROS, mitochondria actively and constitutively produce ROS in the form of  $\text{H}_2\text{O}_2$  and to a lesser extent,  $\text{O}_2^-$ , from NADPH oxidase 4 (NOX4) indicating a physiological role for ROS (127). Indeed, ROS, in particular  $\text{H}_2\text{O}_2$ , is known to be involved in apoptosis via  $\text{TNF}\alpha$  stimulation, cellular migration through facilitation of basement membrane degradation and proliferation through activation of MAPK signalling (128-130). However, these wide reaching physiological roles of ROS highlight the importance of proper

maintenance of ROS levels. Importantly, NOX4 levels and activity can be stimulated by other factors known to be elevated in PTC or which PTC are exposed to at increasing levels under hyperglycaemic conditions such as VEGF, TGF $\beta$  and PDGF (131-133).

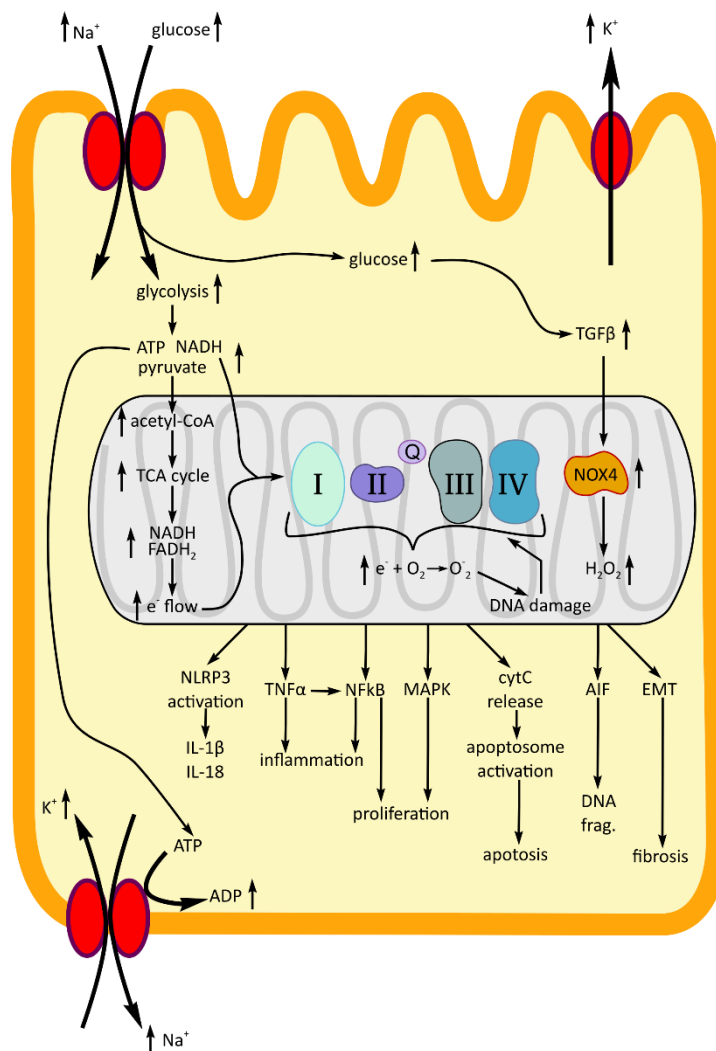


**Figure 1-9 Role of hyperglycaemia in ROS generation and its effects in proximal tubule epithelial cells.**

Elevated luminal glucose concentrations increase insulin independent glucose uptake via the SGLT1/2 Na<sup>+</sup>-glucose symporters. Uptake is facilitated through utilisation of a Na<sup>+</sup> gradient actively established by Na<sup>+</sup>/K<sup>+</sup> antiporters on the basolateral surface. Increased ATP consumption here aids in pushing metabolic reactions which are to a large extent allosterically regulated. The reactions are also driven by increased substrate availability initiated by intracellular hyperglycaemia. Increased electron flow inevitably increases O<sub>2</sub><sup>-</sup> production. Intracellular hyperglycaemia also increases TGF $\beta$  production which drives increases in NOX4 thereby increasing H<sub>2</sub>O<sub>2</sub> production. Collectively, increased ROS lead to changes in a number of important pathways and signalling intermediates which are involved in various aspects of PTC pathobiology in DN.

Regardless of the enzymatic source, mitochondrial ROS can also impact on the regulation of inflammatory signals from PTC and subsequent recruitment of inflammatory cells into the tubulointerstitial space which is an important aspect of DN. The NLRP3 inflammasome may be activated by ROS leading to increased IL-1 $\beta$  and IL-18 production with subsequent increases in macrophage and neutrophil recruitment respectively (134, 135). Apoptosis is also pro-inflammatory and PTC ROS production has been linked with production of pro-apoptotic caspase-3 (136, 137). Furthermore, mitochondrial dysfunction may lead directly to apoptosis through cytochrome C (cytC) and apoptosis inducing factor (AIF) release leading to apoptosome assembly and DNA fragmentation respectively (138).

### **1.6.2.3. *Reactive oxygen species, energy homeostasis and EMT***

Mitochondrial DNA is also susceptible to ROS mediated damage leading to decreased ETC efficiency due to impairment of production of various ETC components. Decreases in electron transport efficiency or complete blockade of transport efficiency results in elevated electron leakage from the ETC and consequentially increased ROS production (117). Furthermore, inefficient transport can lead to decreased ATP production. Not only does this impact on metabolic homeostasis in PTC but it may also impact on structural homeostasis as actin polymerization is ATP-dependent (139). Cytoskeletal remodelling is important in EMT and decreased ATP content may be one way in which mitochondrial dysfunction contributes to the EMT-like events observed in DN and the subsequent fibrotic signalling (140).

Aldosterone is increased in diabetic plasma and decreases mitochondrial membrane potential and ATP production while increasing mitochondrial ROS O<sub>2</sub><sup>-</sup> content (141, 142). The aldosterone induced mitochondrial phenotype was found to occur concurrently with induction of an EMT-like phenotype in PTC. Peroxisome proliferator-activated receptor gamma coactivator 1 alpha (PGC-1 $\alpha$ ) regulates mitochondrial biogenesis and metabolism and increased by aldosterone. This was associated with restoration of both mitochondrial function and an epithelial phenotype in PTC. Despite these clear links between mitochondrial dysfunction and PTC biology in DN, the role of miRNA in this setting is less clear with the among TGF $\beta$ , microRNA and mitochondrial dysfunction in DN having received little attention from the research community.

### **1.6.3. Interactions among mitochondria, TGF $\beta$ and miRNA**

A growing body of evidence links TGF $\beta$  and miRNA to mitochondrial biology either through direct regulation of mitochondrial genes and gene products or through factors that mediate

mitochondrial biogenesis and activity. Despite this, there is little evidence of TGF $\beta$  regulated miRNA exerting any effect over mitochondria.

#### **1.6.3.1. TGF $\beta$ and mitochondria**

Mitochondrial dysfunction, as a result of TGF $\beta$ , predominantly manifests as oxidative stress with some studies linking TGF $\beta$ -mediated ROS formation to inflammation, apoptosis, altered cellular metabolism and EMT-like phenotypes. Indeed, a PTC specific, tetracyclin inducible, constitutively active TGF $\beta$ RI transgenic mouse model displayed significant infiltration of a number of leukocytes such as F4/80<sup>+</sup> macrophages, CD11<sup>+</sup> dendritic cells and T cells into the tubulointerstitium (97). Leukocyte infiltration was associated with acute kidney injury marked by PTC apoptosis, EMT-like phenotypes, PTC proliferation, ROS production and reduced renal function. Importantly, inhibition of mitochondrial ROS by administration of the SOD mimetic mitoTEMPO attenuated T cell and dendritic cell infiltration but this was not associated with decreased tubular cell apoptosis. Conversely, TGF $\beta$  has been shown to induce SMAD4 translocation to the mitochondria resulting in SMAD4-cytochrome C oxidase complex II (COXII) complex formation and induction of apoptosis in Hep3b cells (143). However, this mechanism has not been explored in the kidney nor PTC.

In podocytes, TGF $\beta$  was found to increase oxygen consumption with an associated increase in ATP concentration,  $\beta$ -oxidation, glycolysis, mitochondrial membrane potential and enhanced ROS production (144). Inhibition of TGF $\beta$ -mediated activation of the mTOR pathway via rapamycin treatment largely attenuated these changes. Interestingly, in TGF $\beta$  treated lung fibroblasts, antioxidant treatment with MitoVit E or TPP decreased transcription of  $\alpha$ SMA, CTGF and NOX4 without altering SMAD3 phosphorylation (145). Furthermore, prevention of complex II ROS production, but not complex III electron transport activity, through rieske iron-sulphur protein (RISP) inhibition, resulted in decreased TGF $\beta$ -induced gene expression providing strong evidence of a role for ROS induced fibrotic signalling. Conversely, TGF $\beta$  plays a protective role in mitochondria through induction of PTEN-induced putative kinase 1 (PINK1) which maintains mitochondrial homeostasis through mitophagy. These findings emphasise that the role of TGF $\beta$  in mitochondrial biology is as complex as its role is in immunoregulation (146).

#### **1.6.3.2. microRNA and mitochondria**

miRNA research in mitochondrial biology has revealed regulation of a number of mitochondrially associated, and in some cases expressed, genes which contribute to mitochondrial and cellular dysfunction. The prototypical mitochondrial miRNA, or mito-

miR, is miR-181c which was detected in the mitochondrial matrix (147). Here, miR-181c represses COXI translation leading to complex IV remodelling, ETC dysfunction and ultimately increased ROS production in cardiomyocytes. This has not been explored in the kidney although miR-181c is also expressed in PTC. In human fibroblasts, miR-210 was shown to target COX10, a cytochrome C oxidase assembly factor indicating this miRNA may also contribute to complex IV dysfunction (148). ATP production is decreased by miR-141 which reduces inorganic phosphate transport into the mitochondrial intermembrane space by targeting solute carrier family 25 member Slc25a3 (149). Furthermore, a number of miRNA have been implicated in lipid metabolism including miR-143 and -24 which target apolipoprotein 1-6 (APOL6), miR-204 which is involved in FA oxidation through targeting acetyl-CoA carboxylase B (ACACB) and miR-149 which is involved in high fat diet induced increases in poly ADP-ribose polymerase 2 (PARP2) and an associated decrease in mitochondrial biogenesis (150-152).

Despite the breadth of studies regarding the role of miRNA in mitochondrial metabolism, there has been little development in this area with regard to renal physiology. However, one such study, which utilised streptozotocin induced diabetic Sprague-Dawley rats, demonstrated increased NOX4 expression in renal cortices in association with decreased miR-25 expression (153). The authors verified high glucose mediated upregulation of NOX4 in rat MC as well as showing that and that high glucose also downregulated miR-25. Furthermore, direct targeting of NOX4 by miR-25 was verified by way of 3' untranslated region (UTR) assay. Although there was no functional analysis of that interaction in this study, elevated NOX4 levels are known to contribute to increased ROS levels in the diabetic kidney thereby leading to induction of a fibrotic phenotype in both MC and PTC (97, 154).

### ***1.6.3.3. The interface between TGF $\beta$ , microRNA and mitochondria***

Finally, TGF $\beta$ -mediated miRNA dysregulation has been proposed to play a role in uncoupling protein 2 knockout (UCP2<sup>-/-</sup>) C57BL/6J mice in the unilateral ureteral obstruction (UUO) model of renal fibrosis (155). Development of the fibrotic phenotype observed in obstructive nephropathy was found to be dependent upon tubule specific TGF $\beta$ -induced expression of UCP2 with UCP2 deletion protecting the mice from UUO induced fibrosis, a finding which was validated *in vitro* in PTC. miRNA microarray identified miR-30e as being downregulated in renal cortices of UUO mice with this downregulation localised to the tubular region of the cortex as assessed by *in situ* hybridisation. The mitochondrially localised UCP2 was identified as a target of miR-30e, both *in silico* and *in vitro*, with data

presented demonstrating a direct link between TGF $\beta$ -mediated downregulation of miR-30e, derepression of UCP2 and induction of fibrotic gene expression.

This study clearly illustrates that the regulatory effects of miRNA and TGF $\beta$  do indeed interweave with mitochondrial biology, especially in models of renal fibrosis. Furthermore, given the wide reaching effects of TGF $\beta$  in regard to miRNA regulation, and the promiscuity of miRNA-gene interactions, it stands to reason that this is only one of many of the TGF $\beta$ -miRNA-mitochondrial networks that exist. Exploration of these networks will provide valuable information for development of future therapeutic interventions in DN and expand our knowledge about microRNA signalling networks in general.

### **1.7. Conclusion**

Diabetic nephropathy is a complex disease resulting in pathological changes in various cell types and ultimately culminating in ESRD. Although initially propagated by chronic hyperglycaemia associated with DM, these changes are elicited via activation and modulation of a wide range of pathways and their products. PTC are particularly important in DN where they act as indicators of future renal health and are the primary instigators of tubulointerstitial fibrosis and possibly also play a role, albeit indirect, in glomerulosclerosis. TGF $\beta$  plays a central role in the pathophysiology of PTC and also deregulates a large number of miRNA known to be involved in DN. Mitochondrial dysfunction is increasingly recognised in PTC biology in DN, as is the role of TGF $\beta$  and miRNA in mitochondrial biology. However, the interplay between mitochondria, TGF $\beta$  and miRNA has not been extensively explored in DN.

### **1.8. Hypothesis and specific aims**

This thesis is focused on the exploration and delineation of the role of miRNA in TGF $\beta$ -mediated fibrotic signalling in PTC under hyperglycaemic conditions. The bulk of the work has been performed using *in vitro* models with some utilisation of *ex vivo* human and animal tissues.

The first results chapter (chapter 3) explores the association of a known fibrotic miRNA, miR-21, with clinical and histopathological markers in human renal biopsy material from DN subjects. The nature of miR-21 in mediating fibrotic signalling in PTC, specifically its contribution to TGF $\beta$  signalling is explored *in vitro*. Furthermore, the coordination and

interplay of regulation of multiple targets by miR-21 and its role in TGF $\beta$  signalling in PTC is also explored *in vitro*.

The second results chapter (chapter 4) utilises massively parallel high-throughput mRNA sequencing data acquired from PTC treated with TGF $\beta$ . These data were explored in order to gain a global perspective on the role of TGF $\beta$  in PTC pathophysiology, a perspective that is not readily available in the current literature.

The third results chapter (chapter 5) integrates data gathered in the previous chapter with massively parallel high-throughput short-RNA sequencing data in identical *in vitro* conditions. Integration of these datasets is performed using a naïve (all miRNA data was used) and a biased (only ‘classic’ DN miRNA data were used) approach to gain a better understanding of the global contribution of miRNA to TGF $\beta$ -induced PTC pathology.

The fourth and final results chapter (chapter 6) utilises the datasets generated in the previous chapters to identify novel targets of miR-21 which may impact upon mitochondrial biology and function. A number of targets are identified and explored with regards to aspects of mitochondrial biology including ATP production, mitochondrial membrane potential and O<sub>2</sub><sup>-</sup> production. The role of these targets in classic fibrotic gene expression are also explored.

The central hypothesis of this work is that miR-21 contributes to PTC pathology in DN through targeting of multiple targets downstream of TGF $\beta$ . This thesis aims to expand our understanding of the scope of both miRNA- and TGF $\beta$ -mediated gene dysregulation in PTC and the ways in which these effects intersect. Given the already accepted notion that both miRNA and TGF $\beta$  are important in DN, this work provides valuable information for future investigation and development of potential and current therapeutic interventions against the development and progression of DN.

## 2. Methods and Materials

### 2.1. Cell culture

#### 2.1.1. Cell lines (maintenance and passaging)

##### 2.1.1.1. *Proximal tubule epithelial cells (NRK-52E)*

The well-characterised, normal rat kidney tubular epithelial cell line (NRK-52E) was obtained from the American Tissue Culture Collection (Rockville, MD). Cells were maintained in high glucose DMEM media containing 4.5 g/L glucose (Gibco; 11960), with 10% foetal bovine serum (FBS; In Vitro Technologies; IVT3008403), 1% penicillin/streptomycin (50000 units penicillin, 50000 µg streptomycin and 100 µg amphotericin B/ml; Gibco; 15240) and 1% L-glutamine (Gibco; 25030). Cells were cultured at 37°C in 5% atmospheric CO<sub>2</sub> in a humidified incubator.

NRK-52E were maintained at no more than 80% confluency. Upon reaching ~80% confluency, adherent cells were washed twice with phosphate buffered saline without added Ca<sup>2+</sup>/Mg<sup>2+</sup> and incubated with 2ml 0.25% trypsin without EDTA (Gibco; 15050) at 37°C until cells detached from the flask surface. Trypsin was neutralised with 5x volume media as defined above. The resulting cell suspension was then split 1/25 to fresh 175cm<sup>2</sup> cell culture flasks with the remaining cells being committed to cryopreservation as described below (2.12)

##### 2.1.1.2. *Mesangial cells (MC)*

MC were supplied by Dr. Josephine Forbes and Sally A. Penfold and were originally isolated from renal cortices of ApoE<sup>-/-</sup> C57BL/6 mice (156). Cryopreserved cells were thawed in a 37°C water bath and resuspended in 1ml maintenance media containing 20% foetal bovine serum, 1% penicillin/streptomycin (50000 units penicillin, 50000 µg streptomycin and 100 µg amphotericin B/ml) and 1% L-glutamine (Table 2-1). Resuspended cells were added to 20ml maintenance media in a 175cm<sup>2</sup> culture flask before being incubated at 37°C in 5% atmospheric CO<sub>2</sub>.

MC were maintained at no more than 80% confluency. Upon reaching ~80% confluency, adherent cells were washed twice with phosphate buffered saline without added Ca<sup>2+</sup>/Mg<sup>2+</sup> and incubated with 2ml 0.25% trypsin with EDTA (Gibco; 25200) at 37°C until cells

detached from the flask surface. Trypsin was neutralised with 5x volume media as defined above. The resulting cell suspension was then split 1/10 to fresh 175cm<sup>2</sup> cell culture flasks with the remaining cells being committed to cryopreservation as described below (2.12)

### **2.1.2. Cryopreservation of cells**

Cells remaining after passaging (as described) above were cryopreserved for future experiments as follows.

The cell suspension was centrifuged at 500rcf for 5 minutes in order to pellet the cells. The supernatant was removed and the pellet resuspended in ice-cold FBS containing 10% dimethyl sulfoxide (Amresco; 0231). The resulting cell suspension was aliquoted in 800µl volumes to 2ml pre-chilled cryopreservation tubes. Aliquots were chilled on ice for 10 minutes before being transferred to -80°C. Frozen cell stocks were transferred to liquid nitrogen the following day.

### **2.1.3. Cell quantitation**

Cells were counted before seeding for experimentation. Cells were removed from growth flasks as described above (2.1.1.1, 2.1.1.2). 100µl of cell suspension was incubated with 1µl of Tali Dead Cell Red reagent (ThermoFisher; A10786) for 5 minutes. 25µl of the stained cell suspension was loaded onto a Tali Cellular Analysis slide and cells counted utilising an image based cytometer (Invitrogen; Tali image based cytometer).

## **2.2. Cell seeding density**

### **2.2.1. 6-well plates**

6-well tissue culture plates were utilised in reporter construct experiments, fluorescence activated cell sorting (FACS) experiments, ATP assays and for generating protein samples for western blot analysis.

16hrs prior to commencement of the experiment, cells were counted as previously described (2.1.3) and seeded at a density of 60,000 cells per well in 2ml of media appropriate for the cell type used (defined in sections 2.1.1.1, 2.1.1.2).

### **2.2.2. 12-well plates**

12-well tissue culture plates were utilised for preparation of RNA samples and also growing cells on coverslips for confocal microscopy.

For RNA experiments, 16 hours prior to commencement of the experiment, cells were counted as previously described (2.1.3) and seeded at a density of 20,000 cells per well in 1ml of media appropriate for the cell type used (defined in sections 2.1.1.1, 2.1.1.2).

For confocal microscopy, sterile coverslips were adhered to the surface of 12-well plate wells with 5 $\mu$ l FBS at 37°C until dry. 16hrs prior to the experiment, cells were counted as previously described (2.1.3) and seeded at a density of 3,500 cells per well in 1ml of media appropriate for the cell type used (defined in sections 2.1.1.1, 2.1.1.2).

### **2.2.3. Seahorse XF24 plates**

XF24 culture plates are a proprietary design and are used in conjunction with the Seahorse Bioanalyser platform by Seahorse Biosciences.

16hrs prior to the commencement of the experiment, cells were counted as previously described (2.1.3) and seeded at a density of 4,000 cells per well in 200 $\mu$ l of media appropriate for the cell type used (defined in sections 2.1.1.1, 2.1.1.2).

## **2.3. Treatments**

All treatments were performed in the indicated media supplemented with 2% FBS to allow cell-cycle synchronisation.

### **2.3.1. TGF $\beta$ treatment**

Both MC and NRK-52E were treated with TGF $\beta$  at 10ng/ml for a period of 72 hours where indicated.

### **2.3.2. LY294002 treatment**

NRK-52E were treated with LY294002 at 50nM for a period of 72 hours where indicated.

## 2.4. Transfection

### 2.4.1. Transfection concentration of oligonucleotides and vectors

The following oligonucleotides were transfected into cells where indicated. Concentrations are calculated based on well volume at the time of transfection.

**Table 2-1 List of miRNA, siRNA and expression vectors utilised.**

Final in-well concentrations utilised are also listed.

Reagent	Concentration	Supplier; Part number
siRNA control # 2	10/20/25nM*	Sigma-Aldrich; SIC002
anti-SMAD3 siRNA	25nM	Sigma-Aldrich; SASI_Rn02_00260862
anti-ACAT1 siRNA	20nM	Sigma-Aldrich; SASI_Rn01_00083600
anti-AK2 siRNA	20nM	Sigma-Aldrich; SASI_Rn02_00203842
anti-MPV17L siRNA	10nM	Sigma-Aldrich; SASI_Rn02_00209111
<i>mirVana</i> negative control #1	10/20nM*	Ambion; 4464059
hsa-miR-21 <i>mirVana</i> mimic	10nM	Ambion; MC10206
hsa-miR-21-3p <i>mirVana</i> mimic	10nM	Ambion; MC12979
hsa-miR-200a-3p <i>mirVana</i> mimic	20nM	Ambion; MC10991
hsa-miR-200b-3p <i>mirVana</i> mimic	20nM	Ambion; MC11073
hsa-miR-30a <i>mirVana</i> mimic	20nM	Ambion; MC11062
hsa-miR-let-7b <i>mirVana</i> mimic	20nM	Ambion; MC11050
hsa-miR-29b <i>mirVana</i> mimic	20nM	Ambion; MC10103
LNA negative control	25nM	Exiqon; 199004
anti-hsa-miR-21 LNA	25nM	Exiqon; 410135
anti-hsa-miR-21-3p LNA	25nM	Exiqon; 410136
$\beta$ -galactosidase expression vector	0.8 $\mu$ g	Promega; E1081
ACAT1 3'UTR luciferase expression vector (wild type)	1.2 $\mu$ g	GenScript; custom order
ACAT1 3'UTR luciferase expression vector (mutant)	1.2 $\mu$ g	GenScript; custom order
AK2 3'UTR luciferase expression vector (wild type)	1.2 $\mu$ g	GenScript; custom order
AK2 3'UTR luciferase expression vector (mutant)	1.2 $\mu$ g	GenScript; custom order

\*Concentration used depends on which mimic/target miRNA/siRNA is utilised.

## **2.4.2. 6-well transfection complexes**

### **2.4.2.1. *Oligonucleotides***

The day after seeding cells as previously described (2.2.1), growth media was aspirated and cells were washed with 1x volume Opti-MEM reduced serum media (Gibco; 31985), supplemented to 25mM glucose and without antibiotic/antimycotics and FBS. 900µl of high glucose Opti-MEM was added to the wells and the cells returned to 37°C for 30 minutes to allow equilibration to the new media.

Lipofectamine RNAiMAX (ThermoFisher; 13778075) transfection complexes were prepared according to the manufacturers protocol. Briefly, for each well, 1.3µl of RNAiMAX was equilibrated in 50µl Opti-MEM for 5 minutes before incubating with oligonucleotides at the appropriate concentration (Table 2-1) in a total volume of 100µl per well. Transfection complexes were allowed to form for 10 minutes before being added drop-wise to the appropriate wells. After addition to the wells, complexes were mixed by gentle rocking.

### **2.4.2.2. *Reporter vectors***

The day after seeding cells as previously described (2.2.1), growth media was aspirated and cells were washed with 1x volume Opti-MEM reduced serum media (Gibco; 31985), supplemented to 25mM glucose and without antibiotic/antimycotics and FBS. 900µl of high glucose Opti-MEM was added to the wells and the cells returned to 37°C for 30 minutes to allow equilibration to the new media.

Lipofectamine 2000 (ThermoFisher; 11668) transfection complexes were prepared according to the manufacturers protocol. Briefly, for each well, 3µl of Lipofectamine 2000 was equilibrated in 50µl Opti-MEM for 5 minutes before incubating with expression vectors at appropriate concentration (Table 2-1) in a total volume of 100µl per well. Transfection complexes were allowed to form for 10 minutes before being added drop-wise to the appropriate wells. After addition to the wells, complexes were mixed by gentle rocking.

## **2.4.3. 12-well transfection complexes**

The day after seeding cells as previously described (2.2.1), growth media was aspirated and cells were washed with 1x volume Opti-MEM reduced serum media (Gibco; 31985), supplemented to 25mM glucose and without antibiotic/antimycotics and FBS. 400µl of high glucose Opti-MEM was added to the wells and the cells returned to 37°C for 30 minutes to allow equilibration to the new media.

Lipofectamine RNAiMAX (ThermoFisher; 13778075) transfection complexes were prepared according to the manufacturers protocol. Briefly, for each well, 0.6 $\mu$ l of RNAiMAX was equilibrated in 50 $\mu$ l Opti-MEM for 5 minutes before incubating with oligonucleotides at the appropriate concentration (Table 2-1) in a total volume of 100 $\mu$ l per well. Transfection complexes were allowed to form for 10 minutes before being added drop-wise to the appropriate wells. After addition to the wells, complexes were mixed by gentle rocking. Transfection of cells grown on coverslips was identical to that described above with the exception of 0.3 $\mu$ l of RNAiMAX being utilised per well.

#### **2.4.4. XF24 plate transfection complexes**

The day after seeding cells as previously described (2.2.1), growth media was aspirated and cells were washed with 1x volume Opti-MEM reduced serum media (Gibco; 31985), supplemented to 25mM glucose and without antibiotic/antimycotics and FBS. 150 $\mu$ l of high glucose Opti-MEM was added to the wells and the cells returned to 37°C for 30 minutes to allow equilibration to the new media.

Lipofectamine RNAiMAX (ThermoFisher; 13778075) transfection complexes were prepared according to the manufacturers protocol. Briefly, for each well, 0.3 $\mu$ l of RNAiMAX was equilibrated in 25 $\mu$ l Opti-MEM for 5 minutes before incubating with oligonucleotides at the appropriate concentration (Table 2-1) in a total volume of 50 $\mu$ l per well. Transfection complexes were allowed to form for 10 minutes before being added drop-wise to the appropriate wells. After addition to the wells, complexes were mixed by gentle rocking.

#### **2.4.5. Post transfection**

5 hours after the addition of transfection complexes, transfection media was supplemented with 2% vol/vol final concentration of FBS in a final volume of 1.5ml for 6-well plates, 1ml for 12-well plates and 250 $\mu$ l for XF24 plates. At this time, where required, cells were also treated with TGF $\beta$  and/or LY294002 as specified in 2.3.

## **2.5. RNA preparation**

### **2.5.1. Harvesting cells and RNA extraction**

At the time of cell harvesting, cells were washed twice with equal volume ice-cold PBS without added  $\text{Ca}^{2+}/\text{Mg}^{2+}$ . Cells were scraped in 800 $\mu\text{l}$  ice-cold TRIzol (Invitrogen; 15596) and transferred to fresh 1.5ml microcentrifuge tubes. In order to shear genomic DNA, the lysate was passed through a 21-gauge needle five times. DNA, protein and lipids were removed by the addition of 1/5 volume chloroform:isoamyl alcohol (49:1) followed by vortexing and centrifugation at 16000rcf/4°C for 7 minutes. The aqueous phase was removed to a fresh 1.5ml microcentrifuge tube and 1/2 volume ice-cold isopropanol added. RNA was precipitated overnight at -20°C.

The following day, samples were centrifuged at 20000rcf/4°C for 30 minutes to pellet the precipitated RNA. The supernatant was removed and the pellet washed with 1x volume ice-cold 75% ethanol, briefly vortexed and centrifuged at 16000rcf for 7 minutes. The wash procedure was repeated then samples were allowed to air dry for 5 minutes to evaporate any remaining ethanol. The resulting RNA pellet was resuspended in 16 $\mu\text{l}$  nuclease free water.

### **2.5.2. RNA quantitation/quality control**

Total RNA was quantified and its purity determined utilising the NanoDrop 2000 spectrophotometer (ThermoFisher). After blanking with 1 $\mu\text{l}$  nuclease free water, the absorbance of 1 $\mu\text{l}$  of sample at 230, 260 and 280nm is recorded and sample concentration ( $\mu\text{g}/\mu\text{l}$ ) is returned. Samples with a 260nm/280nm ratio less than 1.5 were reprecipitated to remove excess protein. Samples with a 260nm/230nm ratio less than 1.8 were reprecipitated to remove excess phenol and/or guanidine thiocyanate carried over from TRIzol extraction.

RNA was repurified by the addition of 5M ammonium acetate to a final concentration of 2.5M with 2.5x volume ice-cold ethanol. The samples were briefly vortexed and incubated at -20°C for a minimum of 4 hours to precipitate the RNA. After the precipitation incubation, the RNA was recovered and quantified as detailed above (2.5.1, 2.5.2).

### **2.5.3. DNase treatment**

In order to remove contaminating genomic DNA from the samples, 6 $\mu\text{g}$  of total RNA was incubated with 0.35U DNase (Ambion; AM2222) in a total volume of 12 $\mu\text{l}$  at 37°C for 30 minutes. The reaction was stopped by incubating the samples with 2 $\mu\text{l}$  of DNase inactivation

reagent (Ambion; 8174G) for 3 minutes at room temperature. The samples were centrifuged at 16000rcf for 2 minutes and the supernatant transferred to new microcentrifuge tubes without disturbing the inactivation bead pellet. Samples were stored at -80°C.

## **2.6. cDNA synthesis**

### **2.6.1. Total cDNA**

Total cDNA was synthesised in a reaction volume of 20µl containing 1µg DNase treated total RNA. RNA was combined with 100ng random primers in a volume of 10µl and incubated at 70°C for 5 minutes to allow denaturation of secondary structure in RNA strands and therefore allow primer annealing. After cooling on ice, the reaction was incubated for 10 minutes at room temperature with 2µl 10mM dNTP mix (Invitrogen; 18247), 2µl 0.1M DTT (Invitrogen; Y00147); 4µl First-Strand buffer (Invitrogen; Y02321), 0.1µl 20U/µl RNase inhibitor (TaKaNa; 2313A) and 1µl 200U/µl M-MLV reverse transcriptase (Invitrogen; 28025) in a total volume of 20µl. The reaction was then incubated at 37°C for 1.5hrs. The reaction was terminated at 70°C for 5 minutes, chilled on ice and diluted four-fold with nuclease-free water before being stored at -20°C.

### **2.6.2. miRNA specific cDNA**

miRNA specific cDNA was synthesis from 7.5ng total RNA utilising the Taqman microRNA reverse transcription kit from Applied Biosystems (4366597). Briefly, RNA was combined with 1.2µl reverse transcription buffer (Applied Biosystems; 4319981), 0.8µl 50U/µl Multiscribe reverse transcriptase (Applied Biosystems; 4319983), 0.12µl 100mM dNTP mix (Applied Biosystems; 4367381), 0.15µl 20U/µl RNase inhibitor (Applied Biosystems; 1103120) and 2.4µl of miRNA specific primer (Table 2-2) in a total volume of 20µl. Synthesis was performed utilising a thermocycler with the following conditions: 16°C/30 minutes, 42°C/60 minutes, 85°C/5 minutes, 4°C/∞. Samples were stored at -20°C.

**Table 2-2 miRNA-specific reverse transcription primer mixes as supplied by Applied Biosciences.**

Sequences are proprietary.

Reagent	Part number
miRNA-29b	RT000413
miRNA-200a	RT000502
miRNA-200b	RT001800
miRNA-let7b	RT002619
miRNA-21	RT000397
U6	RT1973
RNU6B	RT001093
U87	RT1712

## 2.7. qRT-PCR

### 2.7.1. mRNA qRT-PCR

mRNA qRT-PCR was performed on either the 96-well 7500 Fast qRT-PCR platform, using 96-well qRT-PCR plates (Applied Biosystems; 4346906) or the 384-well QuantStudio 7 Flex qRT-PCR platform, using 384-well qRT-PCR plates (Applied Biosystems; 4483320) utilising either FAM-labelled TaqMan sequence specific probes or, if no probe was available, SybrGreen detection dyes. Signals from target specific amplification were normalised to signals from 18s ribosomal-RNA amplification utilising the ddCT method (Dheda *et al.*, 2004). Reactions were run for 40-cycles on the respective platforms.

Table 2-3 lists all primers and probes utilised throughout the study.

**Table 2-3 Sequences of qRT-PCR primer/probe sets.**

Those listed without probes were used with SybrGreen detection dye.

Gene	Element	Sequence (5' - 3')
rat Col I	Probe	6- FAM CCTTCCTGCGCCTGA
	F primer	TGCCGATGTCGCTATCCA
	R primer	TCTTGCAGTGATAGGTGATGTTCTG
rat Col IV	Probe	6- FAM ATTTGCGTAACTAACACACC
	F primer	CACTATGAAAACCGTAAAGTGCCTTA
	R primer	GCAAACAGAGGCCAACGAA
rat FN1	Probe	6- FAM CCCCGTCAGGCTTA

	F primer	CATGGCTTTAGGCGAACCA
	R primer	CATCTACATTCGGCAGGTATGG
rat ECAD	Probe	6- FAM TGCCCCAGTATCGTC
	F primer	TGGCTCCCACCCTCATGA
	R primer	TCGATGAAGTTCCCGATTCA
rat PAI1	Probe	6- FAM CACTGGTGACTCACTTC
	F primer	TGTGTGACCTAACAGGACAGAACTTT
	R primer	CAGCCGGAAATGACACATTG
rat $\alpha$ SMA	Probe	6- FAM TGCCAGATCTTTTCC
	F primer	GACCCTGAAGTATCCGATAGAACA
	R primer	CACGCGAAGCTCGTTATAGAAG
rat TGF $\beta$	Probe	6- FAM CATGACATGAACCGACC
	F primer	GAGGTGACCTGGGCACCAT
	R primer	GGCCATGAGGAGCAGGAA
rat CTGF	Probe	6- FAM ACTGCCTGGTCCAGAC
	F primer	TGGCCCTGACCCAACTATGA
	R primer	CTTAGAACAGGCGCTCCACTCT
rat VEGF	Probe	6- FAM CTGTACCTCCACCATGC
	F primer	GCACTGGACCCTGGCTTTACT
	R primer	TGCAGCCTGGGACCACTT
rat PINK1	Probe	Syber
	F primer	GCCTTGGGTTCAGCAAACA
	R primer	AGTGACTGTCTACCGCCTGAACT
rat UCP2	Probe	Syber
	F primer	GGACAGCAGCCTGTATTGCA
	R primer	CGGACTTTGGCGGTGTCTAG
rat PARK2	Probe	Syber
	F primer	ATCGCGTGCACGGATGT
	R primer	CACGTGGCGGTGGTTACA
rat ACAT1	Probe	Syber
	F primer	TGTCTGGAGCTCGGATTGTTG
	R primer	AGACCGAATTCTCCTTGCTTCA
rat AK2	Probe	Syber
	F primer	TTGCCTGCTCTGGTGACAGA
	R primer	TGAAGGCAAGGCTGTAAGACTCT
mouse ACAT1	Probe	Syber
	F primer	TGGCACGAATTGCAGCAT
	R primer	GCAGGCGCAAGTGGAAAAT
mouse AK2	Probe	Syber
	F primer	CAGACCCCTGACATCGTGTT
	R primer	TCCCTCCACCTTCTAACCA
rat SLC25a25	Probe	Syber
	F primer	AAGGATTTGGTTCAGAAGGACAAG
	R primer	CCCAGGCTCTCTGAAAGTG
rat	Probe	Syber

TXNRD1	F primer	GCATCAGCAGTGACGATCTTTT
	R primer	CGCCAACCACTAGGGTCTTC
rat MPV17L	Probe	6-FAM CTGGCCTGCTGTGCA
	F primer	CGCCCTCATCACCAACTACTATC
	R primer	GGGACCAGGTAGAAGTTGGCTAA
mouse MPV17L	Probe	6-FAM CTGGCCTGCTGTGCA
	F primer	TGAAGCGGGACTACCCTGAT
	R primer	GGGACCAGGTAGAAGTTGGCTAA
rat DNM1L	Probe	Syber
	F primer	TGGGCGCCGACATCA
	R primer	CTGCTCTGAGTTCCCACTACGA
rat MFN2	Probe	Syber
	F primer	GGCACATGAAGGTGGCTTTT
	R primer	CCAAAGCATGGCATTGATCA
rat MFF	Probe	Syber
	F primer	TGCATCGTCTGCCGTTTTT
	R primer	TTCCCTGCATTCTGCAAGAA
rat OMA1	Probe	Syber
	F primer	AAGACTCCGAGAAAGAGGACCTAAA
	R primer	CATGAGAAGGGTGTGTAGATAACCA
rat OPA1	Probe	Syber
	F primer	TGGGCTGCAGAGGATGGT
	R primer	TGCCTGATGTCACAGTGTTGATAA
rat MFN1	Probe	Syber
	F primer	TGGCATCCCTCACGTCTAGAA
	R primer	AAATCACGCCCCCAACAA

### 2.7.1.1. 96-well format

Reactions were performed in 12µl volumes for both TaqMan and SybrGreen based reactions. TaqMan reactions were composed of 2µl cDNA, 0.6µl TaqMan probe, 0.6µl forward primer, 0.6µl reverse primer and 6µl TaqMan Universal Master Mix (Applied Biosystems; 4304437). Each reaction also contained 0.336µl 18s ribosomal-RNA primer/probe mix (Applied Biosystems; 4319413E) for normalisation of signals gathered from sequence specific amplification.

SybrGreen reactions were composed of 2µl cDNA, 0.6µl forward primer, 0.6µl reverse primer and 6µl Fast SYBR Green Master Mix (Applied Biosystems; 4385612). 18s housekeeping signals were generated in 12µl reactions for each sample composed of 2µl cDNA, 0.336µl 18s primer/probe mix and 6µl TaqMan Universal Master Mix.

### 2.7.1.2. 384-well format

Reactions were performed in 7µl volumes for both TaqMan and SybrGreen based reactions. TaqMan reactions were composed of 1µl cDNA, 0.35µl TaqMan probe, 0.35µl forward primer, 0.35µl reverse primer and 3.5µl TaqMan Universal Master. Each reaction also contained 0.196µl 18s ribosomal-RNA primer/probe mix for normalisation of signals gathered from sequence specific amplification.

SybrGreen reactions were composed of 1µl cDNA, 0.35µl forward primer, 0.35µl reverse primer and 3.5µl Fast SYBR Green Master Mix. 18s housekeeping signals were generated in 7µl reactions for each sample composed of 1µl cDNA, 0.196µl 18s primer/probe mix and 3.5µl TaqMan Universal Master Mix.

### 2.7.2. miRNA qRT-PCR

miRNA qRT-PCR was performed on either the 96-well 7500 Fast qRT-PCR platform or 384-well QuantStudio 7 Flex qRT-PCR platform utilising FAM-labelled TaqMan miRNA specific probes. Signals from target specific amplification were normalised to signals from U87 nuclear small RNA (for rat and mouse) or RNU6B/U6 nuclear small RNA (for human) utilising the ddCT method (157). Reactions were run for 40-cycles on the respective platforms.

Table 2-4 lists TaqMan miRNA probes utilised throughout the study.

**Table 2-4 TaqMan miRNA probes utilised.**

Sequences are proprietary.

Reagent	Part number
<b>miRNA-29b</b>	TM000413
<b>miRNA-200a</b>	TM000502
<b>miRNA-200b</b>	TM001800
<b>miRNA-let7b</b>	TM002619
<b>miRNA-21</b>	TM000397
<b>U6</b>	RT1973
<b>RNU6B</b>	RT001093
<b>U87</b>	TM1712

### **2.7.2.1. 96-well format**

Reactions were performed in 12 $\mu$ l volumes composed of 2 $\mu$ l miRNA-specific cDNA, 0.6 $\mu$ l TaqMan miRNA assay and 6 $\mu$ l TaqMan Universal Master Mix. Nuclear RNA housekeeping signals were generated in 12 $\mu$ l reactions for each sample composed of 2 $\mu$ l nuclear RNA-specific cDNA, 0.6 $\mu$ l TaqMan nuclear RNA assay and 6 $\mu$ l TaqMan Universal Master Mix.

### **2.7.2.2. 384-well format**

Reactions were performed in 7 $\mu$ l volumes for both TaqMan composed of 1 $\mu$ l miRNA-specific cDNA, 0.35 $\mu$ l TaqMan miRNA assay and 3.5 $\mu$ l TaqMan Universal Master Mix. Nuclear RNA housekeeping signals were generated in 7 $\mu$ l reactions for each sample composed of 1 $\mu$ l cDNA, 0.6 $\mu$ l TaqMan nuclear RNA assay and 3.5 $\mu$ l TaqMan Universal Master Mix.

## **2.8. Amplification of reporter constructs**

### **2.8.1. Bacterial transformation**

Heat competent DH5- $\alpha$  *Escherichia coli* were thawed on ice and 1ng of reporter construct was added to the bacterial aliquot. The bacteria were incubated on ice for 20 minutes before heat shocked at 42°C for 90 seconds, at which time the cell were placed immediately back on ice. 500 $\mu$ l of non-selective Lauria-Bertani (LB) liquid broth was added to the cells and the cell suspension places on an orbital shaker (New Brunswick Scientific; Innova 45) at 220rpm/37°C for 45 minutes. 100 $\mu$ l of transformed bacterial cells were spread on LB agar plates containing 100 $\mu$ g/ml ampicillin and incubated at 37°C overnight.

### **2.8.2. Mini prep**

Single colonies were transferred from overnight cultures on selective agar plates to 50ml conical bottom tubes containing 5ml LB media containing 100 $\mu$ g/ml ampicillin. The inoculated broth was incubated on orbital shakers for 8 hours at 220rpm/37°C. 100 $\mu$ l of the resulting bacterial culture was added to 100 $\mu$ l LB containing 50% glycerol (25% glycerol final) and stored at -80°C.

The remaining culture was pelleted and the construct recovered for validation using a plasmid purification kit according to the manufacturers' protocol (Promega; Wizard Plus SV

Miniprep Kit; A1460). The recovered plasmid was quantitated and qualitated as described above (2.5.2).

### **2.8.3. 3'UTR luciferase vector quality control**

For 3'UTR luciferase vectors, a portion of the purified vector was digested with *XhoI* in a reaction containing 3µl NEB Buffer 2 (New England Biolabs; B7002S), 0.3µl BSA (New England Biolabs; B9000S), 0.3µl *XhoI* (New England Biolabs; R0146S) and 15µl 3' UTR vector for 1 hour at 37°C. The resulting digestion product was then electrophoresed through a 0.1% Lo-melt agarose (Amresco; 0815) containing 5ng/ml ethidium bromide at 80 volts until the dye front was approximately 2cm from the end of the gel. 5µl of 1Kb Plus DNA ladder (Invitrogen; 10488085) was run in adjacent lanes to allow determination of the vector size. The resulting DNA bands were visualised at 312nm and imaged with a GelDoc system (Bio-Rad; Universal Hood II).

### **2.8.4. Maxi prep**

Miniprep clones (from Table 2-1) were thawed and a starter culture generated as previously described (2.8.2). The resulting culture was diluted 1/500 in 200 ml LB media containing 100 µg/ml ampicillin and incubated overnight on an orbital shaker at 220rpm/37°C (New Brunswick Scientific; Innova 44). Plasmids were recovered using a plasmid purification kit (Qiagen; Plasmid MaxiKit; 12163) following the manufacturers protocol. Plasmids were resuspended in 1ml nuclease-free water and quantified using the 'Nanodrop' (Thermo Scientific; Nanodrop 2000) as detailed above (2.5.2). Quantified constructs were subsequently stored at -20 °C.

## **2.9. Reporter assays**

ACAT1 and AK2 3'UTR luciferase reporter construct activity were determined as detailed below. Signals from luciferase assays were normalised against those from β-galactosidase constructs

### **2.9.1. β-galactosidase assay**

Cells were washed twice with ice-cold PBS and 120 µl 1x reporter lysis buffer (Promega; E397A) added to each well. Cells were scraped into 1.5 ml microcentrifuge tubes and frozen

at  $-80^{\circ}\text{C}$  to lyse the cells. Lysates were centrifuged at 10000 rcf/ $4^{\circ}\text{C}$  for 5 minutes to pellet cellular debris. 40  $\mu\text{l}$  of the resulting supernatant was incubated with 40  $\mu\text{l}$  2x assay buffer (Promega; E203A) at  $37^{\circ}\text{C}$  for 45 minutes with the remaining lysate being reserved for luciferase assays. The colorimetric reaction was terminated with the addition of 120  $\mu\text{l}$  1 M sodium carbonate (Promega; E202A). 140  $\mu\text{l}$  of each reaction was loaded into 96-well translucent microtest plates (Sarstedt; 82.1581) and optical density read at 420 nm on a microplate reader (PerkinElmer; Enspire).

### **2.9.2. Luciferase assay**

Remaining cell lysate obtained in section 2.9.1 was utilised for determination of luciferase reporter construct activity. 40  $\mu\text{l}$  of lysate was loaded into 96-well, white opaque microtest plates (BD; 353296) before loading into a microplate luminometer equipped with reagent injection systems (BMG LabTech; FluoStar Omega). The luminometer was set to inject 100  $\mu\text{l}$  of luciferase assay substrate and measure luminescence for 10 seconds after allowing the reaction to develop for 2 seconds.

## **2.10. Protein expression analysis**

### **2.10.1. Cell harvest for protein**

At the time of harvest, cells were washed twice with ice-cold PBS without  $\text{Ca}^{2+}/\text{Mg}^{2+}$  and 50 $\mu\text{l}$  RIPA buffer containing 10mM Tris-HCl (Amresco; 0234), 150mM NaCl (Amresco; X190), 1% w/v sodium deoxycholate (Sigma-Aldrich; D6750), 1% v/v NP-40 (Sigma-Aldrich; NP40S) and 0.1% w/v SDS (Sigma-Aldrich; L3371) added to each well. RIPA buffer was supplemented with 1/100 volume phosphatase inhibitor cocktail (Sigma-Aldrich; P5726), 1mM PMSF (ThermoFisher; 36978) and 2mM sodium orthovanadate (Sigma-Aldrich; S6508) immediately before use. Cells were scraped into 1.5ml microcentrifuge tubes, pooling two wells into a single tube. Cells were frozen at  $-80^{\circ}\text{C}$  to facilitate lysis then thawed on ice before sonication with a hand-held sonicator for 10 seconds at 70% amplitude (Hielscher; UP50H). Samples were briefly centrifuged at 10,000rcf to pellet any large debris and sonicated for a further 5 seconds. Cellular debris was removed by centrifugation at 10,000rcf/ $4^{\circ}\text{C}$  for 5 minutes with the resulting supernatant being transferred to fresh microcentrifuge tubes. Samples were stored at  $-20^{\circ}\text{C}$ .

### 2.10.2. BCA assay

Cell lysates protein concentrations were determined with the use of a BCA protein assay kit following the manufacturer's protocol (Pierce; 23225). A standard curve was generated using BSA of known concentration in the range of 1000 $\mu$ g/ml to 0 $\mu$ g/ml. Both the standards and cell lysate samples (diluted 1/13) were loaded in duplicate in clear 96-well microtest plates (Sarsedt; 82.1581). 200 $\mu$ l of BCA assay buffer was loaded into each well, the plate was covered with parafilm and was incubated at 37°C for 20 minutes or until sufficient colour development had occurred. Absorbance was measured at 562nm. Sample concentration was determined from the line-of-best-fit equation generated from the standard curve.

### 2.10.3. SDS-PAGE

SDS-PAGE was performed using Any kD™ Mini-PROTEAN TGX pre-cast gels (Bio-Rad; 4569034). Gels were assembled in Mini-PROTEAN Tetra Cell electrophoresis cells (Bio-Rad; 1658004) with 1x Tris/Glycine/SDS running buffer (Bio-Rad; 1610732). Wells of pre-cast gels were flushed with running buffer before loading.

30 $\mu$ g of cell lysate was prepared in a total volume of no more than 35 $\mu$ l containing 10% volume  $\beta$ -mercaptoethanol (Sigma-Aldrich; M3148) and 20% volume 5x loading buffer comprised of 0.5M Tris-Cl (Mallinckrodt; H590), 10% volume glycerol (Sigma-Aldrich; G7893), 10% w/v SDS (Sigma-Aldrich; L5750) and 0.5% volume bromophenol blue (Sigma-Aldrich; B0126). Samples were boiled for 5 minutes at 95°C and loaded into individual wells of the prepared gels. Gels were run at 200 volts until the dye front reached the end of the gel.

### 2.10.4. Western blotting

Electrophoresed proteins were transferred to PVDF membrane using Trans-Blot Turbo semi-dry transfer system (Bio-Rad; 1704155) and Trans-Blot Turbo Mini PVDF transfer packs (Bio-Rad; 1704156). Transfer was performed for 3 minutes at 25 volts.

Following transfer, membranes were blocked by being placed in 50ml conical tubes containing 10ml 5% w/v BSA (Jackson ImmunoResearch; 001-000-173) in PBS and placed a roller-mixer for 1 hour at room-temperature. Primary antibodies were applied under the conditions listed in Table 2-5 in 1% BSA in PBS. Membranes were washed three times with 10ml PBS containing 0.05% v/v Tween (Sigma-Aldrich; P1379) for 15 minutes each wash. Secondary antibodies were applied at 1/2000 or 1/5000 in 5% w/v BSA in PBS containing 0.05% v/v Tween or 1% w/v BSA in PBS containing 0.1% v/v Tween as indicated (Table 2-

6, Table 2-7). Membranes were washed as described above and rinsed with PBS following the final wash to remove excess Tween. Membranes probed with infra-red secondary antibodies were visualised using Odyssey Infra-Red imaging platform (LI-COR Biosciences; Odyssey). Those probed with HRP-conjugated secondary antibodies were developed with enhanced chemiluminescent reagent (Sigma-Aldrich; CPS3500-1KT) and visualised with GelDoc system (Bio-Rad; Universal Hood II).

Protein bands were quantified using ImageStudio and normalised against  $\beta$ -actin bands.

**Table 2-5 Primary antibodies used in western blot immunodetection during the course of this study.**

All antibodies were applied in 1% BSA w/v in PBS.

<b>Target protein</b>	<b>Supplier/ Part number</b>	<b>Raised species</b>	<b>Dilution</b>	<b>Application time</b>	<b>Application temperature</b>
<b>SMAD7</b>	Imgenex; IMG-531A	Rabbit	1/500	Overnight	4°C
<b>SMAD3</b>	Origene; TA312265	Rabbit	1/500	Overnight	4°C
<b>p-SMAD3</b>	Invitrogen; MA5-14936	Rabbit	1/500	Overnight	4°C
<b>PTEN</b>	Cell Signalling Technology; 13866	Rabbit	1/1000	Overnight	4°C
<b>AKT</b>	Cell Signalling Technology; 9272S	Rabbit	1/1000	Overnight	4°C
<b>p-AKT</b>	Cell Signalling Technology; 9271S	Rabbit	1/1000	Overnight	4°C
<b>ACAT1</b>	Abcam; ab168342	Rabbit	1/1000	Overnight	4°C
<b>AK2</b>	Abcam; ab166901	Rabbit	1/1000	Overnight	4°C
<b>MFN2</b>	Cell Signalling Technology; 94825	Rabbit	1/1000	Overnight	4°C
<b>OPA1</b>	BD Transduction Laboratories; 612606	Mouse	1/1000	Overnight	4°C

<b>DNML1/DRP1</b>	Abcam; ab56788	Mouse	1/1000	Overnight	4°C
<b>β-actin</b>	Abcam; ab6276	Mouse	1/1000	1 hour	Room temperature

**Table 2-6 HRP-conjugated secondary antibodies used in western blot.**

All HRP-secondary antibodies were applied in 5% BSA w/v in PBS with 0.05% v/v Tween.

<b>Target species</b>	<b>Supplier/ Part number</b>	<b>Raised species</b>	<b>Dilution</b>	<b>Application time</b>	<b>Application temperature</b>
<b>Rabbit</b>	Dako; P0448	Goat	1/2000	1 hour	Room temperature
<b>Rabbit</b>	Dako; P0448	Goat	1/2000	1 hour	Room temperature
<b>Mouse</b>	Dako; P0260	Rabbit	1/2000	1 hour	Room temperature

**Table 2-7 Infra-red secondary antibodies used in western blot immunodetection.**

All infra-red secondary antibodies were applied in 1% BSA w/v in PBS with 0.1% v/v Tween.

<b>Target species</b>	<b>Supplier/ Part number</b>	<b>Raised species</b>	<b>Dilution</b>	<b>Application time</b>	<b>Application temperature</b>
<b>Rabbit</b>	Li-Cor; 926-3221	Goat	1/5000	1 hour	Room temperature
<b>Rabbit</b>	Li-Cor; 926-3213	Donkey	1/5000	1 hour	Room temperature
<b>Mouse</b>	Li-Cor; 926-3210	Goat	1/5000	1 hour	Room temperature

### 2.10.5. Membrane stripping/reprobing

Where required, membranes were stripped of any bound antibodies and reprobed for further protein detection as follows.

10ml 0.2M NaOH was added to membranes and placed on a roller mixer at room temperature for 20 minutes. Membranes were then rinsed several times with PBS followed by a 15 minute wash with PBS containing 0.05% v/v Tween. Membranes were then re-blocked for 1 hour at room temperature with 5% w/v BSA in PBS and reprobed as previously described (2.10.4).

## 2.11. FACS assays

### 2.11.1. Staining procedures

#### 2.11.1.1. *Mitochondrial superoxide assay*

Cells were washed twice with PBS without add  $\text{Ca}^{2+}/\text{Mg}^{2+}$  add detached from the surface of 6-well plates with 200 $\mu\text{l}$  trypsin without EDTA. Trypsin was inactivation with addition of 5x volume PBS containing 10% v/v FBS. Cells were removed to 10ml conical tubes combining two wells per tubes. Cells were pelleted by centrifugation at 800rcf for 5 minutes. The supernatant was aspirated and cells washed with PBS containing 1% v/v FBS. Following aspiration of the wash buffer, cells were resuspended in 600 $\mu\text{l}$  PBS with 1% v/v FBS and 200 $\mu\text{l}$  were aliquoted to three 5ml round bottom polycarbonate tubes (Falcon; 352008).

1ml PBS with 1% v/v FBS was added to each tube with one tube receiving 50nM MitoSOX mitochondrial superoxide detection reagent (Life Technologies; M36008). Cells were subsequently incubated at 37°C for 10 minutes. Cells were washed with the addition of 2ml PBS with 1% v/v FBS and centrifuged at 800rcf for 5 minutes. The wash buffer was aspirated from all samples leaving approximately 100 $\mu\text{l}$  in each tube. One tube representing each sample received propidium iodide at a final concentration of 1 $\mu\text{g}/\text{ml}$  to allow gating of dead cells (Sigma-Aldrich; P4170).

#### 2.11.1.2. *Mitochondrial membrane potential assay*

Cells were washed twice with PBS without add  $\text{Ca}^{2+}/\text{Mg}^{2+}$  add detached from the surface of 6-well plates with 200 $\mu\text{l}$  trypsin without EDTA. Trypsin was inactivation with addition of 5x volume PBS containing 10% v/v FBS. Cells were removed to 10ml conical tubes combining two wells per tubes. Cells were pelleted by centrifugation at 800rcf for 5 minutes. The supernatant was aspirated and cells washed with PBS containing 1% v/v FBS. Following aspiration of the wash buffer, cells were resuspended in 800 $\mu\text{l}$  PBS with 1% v/v FBS and 200 $\mu\text{l}$  were aliquoted to four 5ml round bottom polycarbonate tubes (Falcon; 352008).

1ml PBS with 1% v/v FBS was added to each tube with two tubes receiving 150nM TMRM mitochondrial membrane potential detection reagent (Life Technologies; T-668). Cells were subsequently incubated at 37°C for 15 minutes. To obtain baseline fluorescence for TMRM stained samples, mitochondria were depolarised by the addition of 1 $\mu\text{M}$  FCCP for 5minutes to one tube for each sample group.

Cells were washed with the addition of 2ml PBS with 1% v/v FBS and centrifuged at 800rcf for 5 minutes. The wash procedure was repeated and the wash buffer was aspirated from all samples leaving approximately 100µl in each tube. One tube representing each sample received propidium iodide at a final concentration of 1µg/ml to allow gating of dead cells (Sigma-Aldrich; P4170).

### **2.11.1.3. Mitochondrial content**

Cells were washed twice with PBS without  $\text{Ca}^{2+}/\text{Mg}^{2+}$  and detached from the surface of 6-well plates with 200µl trypsin without EDTA. Trypsin was inactivated with the addition of 5x volume PBS containing 10% v/v FBS. Cells were transferred to 10ml conical tubes combining two wells per tube. Cells were pelleted by centrifugation at 800rcf for 5 minutes. The supernatant was aspirated and cells washed with PBS containing 1% v/v FBS. Following aspiration of the wash buffer, cells were resuspended in 700µl PBS with 1% v/v FBS and cell density ascertained as previously described (2.1.3). For all samples, an equal number of cells were aliquoted to three 5ml round bottom polycarbonate tubes (Falcon; 352008). Normalisation of cell density is required as MitoTracker Green FM (Life Technologies; M-7514) is a completely passive dye and therefore differences in cell numbers relative to stain concentration will result in artificial differences in fluorescence signals.

1ml PBS with 1% v/v FBS was added to each tube with one tube receiving 200nM MitoTracker Green mitochondrial stain. Cells were subsequently incubated at 37°C for 30 minutes. Cells were washed with the addition of 2ml PBS with 1% v/v FBS and centrifuged at 800rcf for 5 minutes. The wash procedure was repeated and the wash buffer was aspirated from all samples leaving approximately 100µl in each tube. One tube representing each sample received propidium iodide at a final concentration of 1µg/ml to allow gating of dead cells (Sigma-Aldrich; P4170).

### **2.11.2. Gating and acquisition procedures**

Cells were counted and fluorescence intensity obtained on the BD FACScalibur platform (Beckton Dickinson) using CellQuest Pro operating software. Forward scatter voltage was set to E00 and amp gain was adjusted, in conjunction with side scatter voltage, to attain an even distribution of cells on a side scatter vs forward scatter plot.

FL1, FL2 and FL3 voltages were adjusted using unstained samples to ensure signal detection did not exceed  $10^1$  units. MitoTracker Green was detected using FL1, MitoSOX red and

TMRM were detected using FL2 and propidium iodide was detected using FL3. For all experiments, 20,000 gated events were recorded.

Analysis of FACS data were performed using BD FACSDiva software (version 8.0). Dead cells were gated using FL3 scatter plot of propidium iodide stained cells and sub-gates for FL1 and FL2 were set using FL1/FL2 height histograms on unstained samples. Once gates had been set, batch analysis was carried out returning mean fluorescence intensity of FL1, FL2 and FL3. Further analysis was performed in Microsoft Excel, 2007.

### **2.11.3. ATP assay**

ATP assays were performed on cell lysates prepared and quantitated as previously described (2.10.1, 2.10.2).

Determination of ATP concentration in cell lysates was performed using a chemiluminescent ATP determination kit (Life Technologies; A22066) according to the manufacturers' protocol. To accommodate for potentially low concentrations, reactions were scaled up to utilise 225µl of assay buffer in place of the recommended 100µl. A standard curve was generated using ATP solution of known concentration in the range of 1µM to 1nM.

225µl of assay buffer was loaded into individual wells of a white 96-well microtest plate and background chemiluminescence measured (BMG labtech; FluoStar Omega). 25µl of standards were loaded in duplicate alongside duplicate wells 20µg cell protein in a total volume of 25µl. The reaction dark incubated for 3 minutes before the resultant chemiluminescent signal was measured. ATP concentration of the samples was determined from the line-of-best-fit equation generated from the standard curve and subsequently normalised to the protein concentration of the cell lysates.

## **2.12. Confocal microscopy**

For confocal microscopy imaging, cells were grown and transfected as previously described (2.4.2, 2.4.3).

Media was aspirated and cells stained with 100nM MitoTracker Deep Red in Opti-MEM media containing 2% v/v FBS for 45 minutes at 37°C in 5% atmospheric CO<sub>2</sub>. Staining media was aspirated and the cells were washed with PBS with added Ca<sup>2+</sup>/Mg<sup>2+</sup>. Cells were then fixed with Opti-MEM media containing 3.7% v/v formaldehyde for 15 minutes and subsequently washed twice with PBS with added Ca<sup>2+</sup>/Mg<sup>2+</sup>.

Nuclei were counterstained with 300nM DAPI (Sigma-Aldrich; D9542) in distilled water for 10 minutes. Cells were washed twice with PBS and mounted on microscopy slide with aqueous mounting media (Calbiochem; 345789) and allowed to dry overnight at room temperature. Prepared slides were stored at 4°C.

Stained cells were imaged using Nikon A1R-Si confocal microscope using an oil immersion 60x objective lens. Images were prepared using ImageJ/FIJI image processing and analysis software.

## **2.13. Next-Generation sequencing**

### **2.13.1. Sample Isolation**

RNA samples used for next-generation sequencing were extracted and prepared as previously described (2.5). RNA was analysed on a microchip electrophoresis system (MultiNA Bioanalyzer; Shimadzu) for sample integrity and concentration.

### **2.13.2. Library Preparation**

mRNA was enriched from 1µg total RNA utilising NEBNext Poly(A) mRNA Magnetic Isolation Module (NEB; E7490L) according to the manufacturers protocol. Barcoded libraries were prepared using NEBNext Ultra Directional RNA Library Prep Kit (NEB; E7420L) following the manufacturers protocol. Libraries were validated utilising the MultiNA Bioanalyzer and pooled in equimolar ratios for sequencing.

Short RNA libraries were prepared using NEBNext Multiplex Small RNA Library Prep Set for Illumina (NEB; E7580L) according to the manufacturers protocol and were subsequently size selected via gel electrophoresis on a 6% polyacrylamide gel. Libraries were validated utilising the MultiNA Bioanalyzer and pooled in equimolar ratios for sequencing.

### **2.13.3. Sequencing**

The pooled libraries were sequenced at the Australian Genome Research Facility (Melbourne, Australia) on a ultra-high throughput sequencing platform (HiSeq2500; Illumina) using a version 4 single read flow cell for 60 cycles.

#### 2.13.4. Read data pre-processing

Quality trimming was performed on mRNA-seq data to remove low quality bases from the 3' end of reads using *FASTX-Toolkit* (ver 0.0.14; [http://hannonlab.cshl.edu/fastx\\_toolkit/](http://hannonlab.cshl.edu/fastx_toolkit/)) using a Phred threshold of 20 and a minimum 20 nucleotide read length.

Adapter clipping was performed on microRNA-seq data using *FASTX-Toolkit* with reads of less than 18 nucleotides being discarded.

#### 2.13.5. Read assembly and processing

Reads were aligned to the respective reference genome using *STAR* (ver 3.2.0.1) (158). Mouse (*Mus\_muliscus.GRCm38.dna.toplevel.fa*) and rat (*Rattus\_norvegicus.Rnor\_5.0.dna.toplevel.fa*) genomes were obtained from Ensembl (<http://www.ensembl.org/info/data/ftp/>) and used for sequence alignments. Gene annotations were made against Ensembl version 77 species specific annotation libraries (*Mus\_muliscus.GRCm38.77.gtf* and *Rattus\_norvegicus.Rnor\_5.0.77.gtf*).

Exon-mapped reads were counted using *featureCounts* (ver 1.4.2) [PMID: 24227677] with a mapQ threshold of 10 (159). Genes with fewer than 10 reads per sample on average were excluded from downstream analysis.

#### 2.13.6. Differential gene expression analysis

Differential gene expression analysis was performed using the R package, *edgeR*, version 2.4.0. (160). log<sub>2</sub> fold-change with false discovery rate (FDR) adjusted *p*-values  $\leq 0.05$  were considered significant.

### 2.14. In silico analysis

Various *in silico* analyses were performed throughout the study. Specific methods, scripts and workflows utilised (as listed below) are available in the supplementary digital media files.

#### 2.14.1. Online databases utilised

Predicted miRNA target lists were acquired from *microRNA.org*.

Mitochondrially expressed and associated gene lists were obtained from Mouse MitoCarta 2.0 at Broad institute at <http://www.broadinstitute.org/scientific->

*community/science/programs/metabolic-disease-program/publications/mitocarta/mitocarta-in-0.*

Gene names conversion tables used to update gene symbols and to convert mouse/rat ENSEMBL identifiers to human ENSEMBL identifiers were obtained from ENSEMBL Biomart at <http://asia.ensembl.org/biomart/martview/2406c0e9df6fc43bbcd399e13803c825>. Kyoto Encyclopedia of Genes and Genomes (KEGG) was also indirectly accessed through the R packages *gage* and *pathview*.

### 2.14.2. R Packages utilised

This project has made extensive use of the statistical programming language *R* (161)

A number of R extension packages were utilised, each of which afforded either low level functions for data manipulation or high-level data analysis. There are a large number of packages which are loaded as dependences of some packages. As these packages are neither explicitly installed nor loaded, they are not listed here. Depending on the source of the package, information on package dependencies can be found at either the Comprehensive R Archive Network (<https://cran.r-project.org/>) or Bioconductor (<https://www.bioconductor.org/>)

*dplyr* (ver 0.4-2): provides various function for dataframe manipulation (162).

*edgeR* (ver 2.4.0): facilitates normalisation of raw read counts and generation of differential gene expression data (160).

*gage* (ver 2.18.0): facilitates KEGG gene set analysis of RNA-seq data (163).

*gageData* (ver 2.6.0): auxillary data for *gage* the package(164).

*mirIntegrator* (ver 1.1.0): facilitates augmentation of KEGG pathways with miRNA and their predicted targets (165).

*org.Mm.eg.db* (ver 3.1.2): provides gene identifier mapping functions for mouse (166).

*org.Rn.eg.db* (ver 3.1.2): provides gene identifier mapping functions for rat (167).

*pathview* (ver 1.8.0): facilitates mapping of RNA-seq data onto KEGG pathway maps (168).

*plyr* (1.8.3): provides operations similar to *dplyr* (169)

*ROntoTools* (ver 1.10.0): provides a number of functions from *Onto-Tools* such as performing impact factor analysis on custom pathways (170).

*stringi* (ver 0.5-5): provides various functions for string manipulation (171).

### 2.14.3. List of custom functions, scripts and workflow files

*Data\_preparation\_workglow.R*: workflow for conversion of rat/mouse ENSEMBL IDs to human ENSEMBL IDs to allow direct comparison between the datasets

*DF\_intersect.R*: custom function to find and report similarities between two sets of differential gene expression data.

*DF\_outhersect.R*: custom function to find and differences between two sets of differential gene expression data.

*extractUniqueSets.R*: custom function to find similarities and differences between two *gage* objects.

*gagePaths\_X.R*: workflow for performing GAGE analysis on mRNA datasets against KEGG pathways gene sets. Workflow outputs both rendered KEGG pathways and also tests significantly enriched pathways for essential genes. There are separate workflows for both rat and mouse data.

*generate\_paths.R*: workflow renders networks generated from *Impact\_factor\_X* to pdf.

*geneOntology\_workflow.R*: workflow performs GAGE analysis on mRNA datasets against GO ontology terms. Both *molecular function* and *biological process* terms are tested against both rat and mouse datasets.

*Impact\_factor\_X.R*: workflow to perform integration of miRNA-target interactions into KEGG pathways, integration of miRNA and mRNA expression data into modified KEGG networks and carry out IFA on the resultant networks. There are separate workflows for both rat and mouse data.

*Mining\_mitos.R*: workflow for mining of mitochondrially associated miR-21 targets against the PTC RNA-seq dataset. Workflow outputs a dataframe representing each data intersection performed.

## 2.15. Statistical analysis

Statistical analyses were performed using GraphPad Prism 6. Experimental data comprised of only two groups was tested for statistical significance with the use of unpaired Students T-test utilising Welch's Correction. This accounts for possible inequalities in sample variances between the test groups where appropriate. The significance threshold was set at 0.05 and comparisons exceeding this were deemed non-significant. Significance is reported as  $p <$

0.05,  $p < 0.01$  and  $p < 0.001$  and is defined in each data set. All data are presented as mean  $\pm$  SEM.

Experimental data comprised of greater than two groups were tested for statistical significance with the use of one-way ANOVA utilising Tukey multiple comparisons test. This test adjusts  $p$ -values for multiple comparisons. The significance threshold was set at 0.05 and comparisons exceeding this were deemed non-significant. Significance is reported as  $p < 0.05$ ,  $p < 0.01$  and  $p < 0.001$  and is defined in each data set. All data are presented as mean  $\pm$  SEM.

## Declaration for Thesis Chapter

Monash University

### Declaration for Thesis Chapter 3: miR-21 promotes renal fibrosis in diabetic nephropathy by targeting SMAD7 and PTEN

#### Declaration by candidate

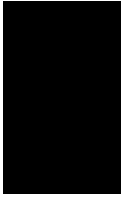
In the case of Chapter 3, the nature and extent of my contribution to the work was the following:

Nature of contribution	Extent of contribution (%)
Design of project, execution of <i>in vitro</i> studies, RNA analysis of animal tissues in addition to researching, writing and editing the manuscript.	90

The following co-authors contributed to the work. If co-authors are students at Monash University, the extent of their contribution in percentage terms must be stated:

Name	Nature of contribution	Extent of contribution (%) for student co-authors only
<b>Michal Herman-Edelstein</b>	Histological and clinical analysis/data of human renal biopsies, editing manuscript.	
<b>Radko Komers</b>	Histological analysis of rat renal cortex, editing manuscript.	
<b>Jay C. Jha</b>	Histological analysis of mouse renal cortex, editing manuscript.	
<b>Catherine E. Winbanks</b>	Technical assistance with SMAD western blots, editing manuscript.	
<b>Paul Gregorevic</b>	Technical assistance with SMAD western blots, editing manuscript	
<b>Phillip Kantharidis</b>	Editing Manuscript	
<b>Mark E. Cooper</b>	Editing Manuscript	

The undersigned hereby certify that the above declaration correctly reflects the nature and extent of the candidate's and co-authors' contributions to this work\*.

<b>Candidate's Signature</b>		<b>Date</b> <b>04/04/2016</b>
<b>Main Supervisor's Signature</b>		<b>Date</b> <b>04/04/2016</b>

\*Note: Where the responsible author is not the candidate's main supervisor, the main supervisor should consult with the responsible author to agree on the respective contributions of the authors.

### **3. Results I – miR-21 promotes renal fibrosis in diabetic nephropathy by targeting PTEN and SMAD7**

#### **3.1. Introduction**

Tubulointerstitial fibrosis is a hallmark feature of diabetic nephropathy which is propagated by increased ECM production with concomitant decreases in ECM turnover (172). While the pathophysiology of interstitial fibrosis is well characterised current pharmaceutical treatments do little to prevent the development and progression of DN with up to 40% of diabetic patients developing this condition. In the search for novel therapeutic targets, current research has turned to the exploration of post-transcriptional regulation in the form of microRNAs which have proven to be important in a wide variety of tissues and pathologies. Amongst these, miR-21 has emerged as an important regulator of fibrotic signalling and epithelial-mesenchymal transition, both of which are core pathological processes mediating tubulointerstitial fibrosis (173-175).

While there have been numerous miR-21 targets studied in tissue culture and in experimental models, little has been published on miR-21 in human DN nor has there been in-depth exploration of the networks which are formed by miRNA interacting with multiple targets (173, 176-178). The present study sought to elucidate the nature of miR-21 dysregulation in human DN and to explore the relationships that exist between miR-21 and two of its targets, PTEN and SMAD7. Furthermore, the network that is formed by miR-21 co-regulating two different TGF $\beta$ -mediated pathways was also explored.

# *miR-21* promotes renal fibrosis in diabetic nephropathy by targeting PTEN and SMAD7

Aaron D. McClelland\*†<sup>1</sup>, Michal Herman-Edelstein†<sup>1</sup>, Radko Komers§, Jay C. Jha†, Catherine E. Winbanks||, Shinji Hagiwara†, Paul Gregorevic||, Phillip Kantharidis\*<sup>2</sup> and Mark E. Cooper\*<sup>2</sup>

\*JDRF Danielle Alberti Memorial Centre for Diabetes Complications, Diabetes Domain, Baker IDI Heart and Diabetes Institute, 75 Commercial Road, Melbourne, VIC 3004, Australia

†Department of Medicine, Central Clinical School, Monash University, 75 Commercial Road, Melbourne, VIC 3004, Australia

‡Department of Nephrology & Hypertension, Rabin Medical Center, Petah Tikva, 4941492, Israel; Felsenstein Medical Research Institute, Rabin Medical Center, Petah Tikva, 49100, Israel; Sackler School of Medicine, Tel Aviv University, Ramat Aviv 69978, Israel

§Division of Nephrology & Hypertension, Oregon Health & Science University, Portland, OR 97239, U.S.A.

||Division of Cell Signalling and Metabolism, Baker IDI Heart and Diabetes Institute, 75 Commercial Road, Melbourne, VIC 3004, Australia

## Abstract

The cytokine transforming growth factor (TGF)- $\beta$ 1 plays a central role in diabetic nephropathy (DN) with data implicating the miRNA (miR) *miR-21* as a key modulator of its pro-sclerotic actions. In the present study, we demonstrate data indicating that *miR-21* up-regulation positively correlates with the severity of fibrosis and rate of decline in renal function in human DN. Furthermore, concomitant analyses of various models of fibrotic renal disease and experimental DN, confirm tubular *miR-21* up-regulation. The fibrotic changes associated with increased *miR-21* levels are proposed to include the regulation of TGF- $\beta$ 1-mediated mothers against decapentaplegic homolog 3 (SMAD3)- and phosphoinositide 3-kinase (PI3K)-dependent signalling pathways via co-ordinated repression of mothers against decapentaplegic homolog 7 (SMAD7) and phosphatase and tensin homologue (PTEN) respectively. This represents a previously uncharacterized interaction axis between *miR-21* and PTEN–SMAD7. Targeting of these proteins by *miR-21* resulted in de-repression of the respective pathways as reflected by increases in SMAD3 and V-Akt murine thymoma viral oncogene homolog 1 (AKT) phosphorylation. Many of the changes typically induced by TGF- $\beta$ 1, including phosphorylation of signalling mediators, were further enhanced by *miR-21*. Collectively, these data present a unified model for a key role for *miR-21* in the regulation of renal tubular extracellular matrix (ECM) synthesis and accumulation and provide important insights into the molecular pathways implicated in the progression of DN.

**Key words:** biopsy, diabetic nephropathy, fibrosis, micro ribonucleic acid (RNA), signalling, transforming growth factor (TGF)- $\beta$ 1.

## INTRODUCTION

Progression of diabetic nephropathy (DN) is characterized by the gradual scarring of the renal glomerulus and fibrosis of the tubulointerstitial region. The degree of fibrosis of the diabetic kidney strongly associates with progression to end-stage renal disease (ESRD). Although mesangial expansion and podocyte effacement and loss are the primary drivers of glomerulosclerosis, tubulointerstitial fibrosis (TIF) is primarily mediated by renal fibroblasts and tubular epithelial cells [1,2]. Transforming growth factor (TGF)- $\beta$ 1 plays a central role in the onset and progression of the structural changes seen in the fibrotic diabetic kidney [3].

The fibrotic effects of TGF- $\beta$ 1 are primarily mediated by the well characterized mothers against decapentaplegic homolog 3 (SMAD3)-dependent pathway with other pathways such as those mediated by V-Akt murine thymoma viral oncogene homolog 1 (AKT) also participating [4]. Intracellularly, these pathways are negatively regulated by mothers against decapentaplegic homolog 7 (SMAD7) and phosphatase and tensin homologue (PTEN) respectively [5,6].

TGF- $\beta$ 1 also mediates its effects via small non-coding RNAs, aptly named miRNA (miR), which have rapidly emerged as important regulatory molecules [7–10]. The role of a number of miRs is well established in DN, including the *miR-29* family,

**Abbreviations:** ACE, angiotensin-converting enzyme; ARB, angiotensin receptor blockers; BTBS-t, 5% BSA in Tris-buffered saline containing 0.05% Tween; DMEM, Dulbecco's modified Eagle's medium; DN, diabetic nephropathy; ECM, extracellular matrix; FFPE, formalin-fixed paraffin-embedded; GFR, glomerular filtration rate; GSI, glomerular sclerosis index; ISH, *in situ* hybridization; LCM, laser capture microdissection; LNA, locked nucleic acid; miR, miRNA; PI3K, phosphoinositide 3-kinase; pre-miR, precursor-miRNA; PTC, proximal tubule epithelial cells; PTEN, phosphatase and tensin homologue; STZ, streptozotocin; T2DM, type 2 diabetes mellitus; TGF, transforming growth factor; TIF, tubulointerstitial fibrosis.

**Correspondence:** Phillip Kantharidis

<sup>1</sup> These authors contributed equally to the paper.

<sup>2</sup> These authors share senior authorship of the paper.

the *miR-200* family and *miR-192* [8]. These miRs are known to interact with and modulate various components of the TGF- $\beta$ 1-induced fibrotic programme.

Among these, *miR-21* has been extensively studied because many of its targets are relevant to DN and especially related to the modulation of TGF- $\beta$ 1 and AKT activation [11,12]. *miR-21* has been associated with fibrosis in experimental models of lung, heart and kidney sclerosis [9–14]. Expression of *miR-21* was recently studied in kidney biopsies of American–Indian patients with early stage of DN [glomerular filtration rate (GFR) above 90 cc/min] where it was up-regulated only in the glomerular fraction and correlated with the level of proteinuria [15].

In the present study, we aimed to study *miR-21* expression in kidney biopsies from diabetic patients with advanced fibrotic stages of DN and to explore the potential pathogenic role of differentially expressed *miR-21* in human kidney. We hypothesized that *miR-21* is associated with the development of DN and that co-ordinated targeting of SMAD7–PTEN is essential to the role of *miR-21* in TGF $\beta$ -mediated fibrotic signalling. The interactions of these particular signalling cascades with *miR-21* or the extent to which these interactions individually contribute to the fibrotic milieu have not been previously delineated [13,14,16,17].

## RESEARCH DESIGN AND METHODS

### Kidney biopsy and histological assessment

Formalin-fixed paraffin-embedded (FFPE) kidney specimens ( $n=43$ ) including diagnostic kidney biopsies of patients with DN ( $n=35$ ) and normal living kidney donors ( $n=8$ ) were obtained from the pathological archives of the Department of Pathology at Rabin Medical Centre. The study was approved by the hospital Institutional Ethics Committee [18].

Renal biopsy was performed according to clinical indications and in order to exclude the co-existence of other types of kidney disease, the presence of atypical features including short duration between the diagnosis of diabetes and the onset of nephropathy or the absence of concomitant diabetic retinopathy. Cases were defined by the presence of histological changes consistent with DN and the absence of other potential causes of renal disease [18,19].

### In situ hybridization

*In situ* hybridization (ISH) of *miR-21* was performed on eight kidney biopsies with mild fibrosis, eight with severe fibrosis and eight normal kidneys. A *miR-21* probe was used for ISH as per the manufacturer's recommendations (Exiqon). A scrambled probe was used for negative control and U6 was used as a positive control probe (Exiqon) [20].

### Laser capture microdissection

Laser capture microdissection (LCM) was performed using the PALM MicroBeam instrument (PALM). FFPE blocks used in immunohistochemistry (IHC)/ISH and for miR analysis were cut into sections (5- $\mu$ m thick) on to PALM membrane slides (PALM), baked and deparaffinized with xylene, lightly stained with haematoxylin and eosin and air-dried. All the glomeruli or

the tissue surrounding the captured glomeruli were microdissected and captured on PALM adhesive caps tubes followed by total RNA extraction using the RNeasy FFPE Kit (Qiagen).

### Experimental kidney disease models

*miR-21* expression was assessed in renal cortices from three rodent models of renal fibrosis as previously described [20] (Supplementary Methods). These comprised two models of DN, the streptozotocin (STZ)-induced diabetic ApoE<sup>-/-</sup> mouse and the STZ-induced diabetic uni-nephrectomized (UNx) Sprague–Dawley rat. A third model of non-diabetic renal disease was utilized, specifically adenine-induced renal fibrosis.

### Detection of tubulointerstitial fibrosis and immunohistochemistry

Immunohistochemistry was performed on serial, 4- $\mu$ m sections of FFPE kidneys or renal biopsies, as previously described [21]. Sections were processed in parallel with the appropriate control tissues. IHC staining intensity was ascertained via standard procedures [22]. TIF was detected by Masson's Trichrome staining [23].

### Cell culture, treatments and transfections

Rat proximal tubule epithelial cells (PTC; A.T.C.C.) were maintained and passaged in DMEM (Dulbecco's modified Eagle's medium; Life Technologies) supplemented to 25 mM glucose with 10% FBS. For treatments, media contained only 2% FBS and treatments were for 72 h. TGF- $\beta$ 1 (R&D systems) was used at 10 ng/ml. The phosphoinositide 3-kinase (PI3K) inhibitor LY294002 (LY, Cell Signalling Technology) was used at 50 nM. TGF- $\beta$ 1 and LY were added simultaneously where indicated. For transfection, PTCs were seeded in 12-well plates and were transfected with 100 nM of precursor-miR (pre-miR; Life Technologies) or 50 nM locked nucleic acids (LNA, Exiqon) in Opti-MEM (Life Technologies) using Oligofectamine (Life Technologies). Negative control pre-miR and LNA were used at 50 nM. Cells were transfected with 25 nM anti-SMAD3 siRNA (si-SMAD3, Sigma–Aldrich) or scrambled control siRNA (si-Ctrl, Sigma–Aldrich) for 48 h. Following transfection, media were changed to 2% FBS DMEM without antibiotics after 5 h at which time appropriate treatments were added. Cells were harvested for RNA or protein 3 days later.

### RNA extraction and qRT-PCR

RNA was extracted from PTCs and renal cortical tissue samples using TRIzol (Ambion). RNA from human renal biopsies was extracted using RNeasy mini columns (Qiagen). DNase treatment and cDNA synthesis were performed as previously described [24]. Gene expression was determined utilizing TaqMan reagents (Life Technologies) with fluorescence signals being normalized to 18s rRNA utilizing the ddCT method [25].

### miRNA assay

miR expression was measured using TaqMan miRNA assays (Life Technologies). Fluorescence was normalized to U87 small-RNA for PTC. Pre-amplification was performed for human tissue samples using TaqMan PreAmp Master Mix with Megaplex PreAmp Primers, Human Pool A and B (Life Technologies).

### Western blotting and densitometry

Denatured cell lysates (40  $\mu$ g) were run on 4%–12% pre-cast gels and transferred to PVDF membranes. Membranes were blocked with 5% BSA in Tris-buffered saline containing 0.05% Tween (BTBS-t) and primary antibodies applied overnight with 0.5% BTBS-t. After washing, horseradish peroxidase (HRP)-conjugated secondary antibodies were incubated with membranes for 1 h with BTBS-t. Secondary antibodies were detected with chemiluminescent peroxidase substrate and imaged with the Gel-Doc XRS (BioRad).

### Statistical analysis

All statistical analyses were performed utilizing GraphPad Prism software. Correlative analyses were evaluated using Pearson's correlation test. Comparisons of both mRNA and protein expression datasets were evaluated using Tukey one-way ANOVA. Experiments with only one treatment were assessed by Student's *t*-test. A *P*-value < 0.05 was considered statistically significant. Significance between groups is indicated for each figure. Data are presented as mean  $\pm$  S.E.M.

## RESULTS

### miR-21 levels correlate with tubulointerstitial fibrosis and estimated glomerular filtration rate (eGFR) in human DN biopsies

Renal biopsies were collected from a total of 35 patients with varying degrees of type 2 diabetes mellitus (T2DM) associated renal damage and eight control subjects (Supplementary Table S1; Supplementary Figure S1a). Renal biopsies revealed significantly greater *miR-21* expression in patients displaying fast progression (median time to dialysis 18 months) in the rate of renal function decline compared with control or with those diabetic subjects with slow progression (time to dialysis 60 months) of declining renal function (Figure 1A). Patients were further divided into normal, mildly fibrotic and moderate to severely fibrotic groups based on histological analysis of the renal architecture and pathology assessment of the degree of tubulointerstitial sclerosis (Figures 1B, 2A and 2B). Again, *miR-21* levels were increased with increasing renal fibrosis. Patients with moderate to severe fibrosis displayed the highest levels of *miR-21* (Figure 1B). Approximately 80% of T2DM subjects in each group were being administered angiotensin-converting enzyme (ACE) inhibitors or angiotensin receptor blockers (ARB) at the time of study. Although *miR-21* levels were reduced in these patients, *miR-21* expression was still significantly higher than that seen in control subjects (Figure 1C).

eGFR was found to be negatively correlated with increasing *miR-21* levels (Figure 1D). *miR-21* levels were also positively correlated with proteinuria in DN subjects only, whereas glomerulosclerotic injury was positively correlated with *miR-21* expression in all subjects (Figures 1E and 1F).

### Cellular localization of miR-21 in human DN biopsies

Localization of *miR-21* expression in biopsy sections was determined via ISH and compared with the degree of fibrosis as determined by Masson's Trichrome staining,  $\alpha$ -smooth muscle

actin ( $\alpha$ SMA) and SMAD7 mRNA (Figures 2A–2C). Increased *miR-21* probe binding (Figure 2A) in biopsies from both mild and moderate to severe fibrosis was observed predominantly in tubulointerstitial regions of the biopsies and correlated with degree of TIF and glomerular sclerosis index (GSI; Supplementary Table S1). Providing further support for this observation, *miR-21* levels were studied in 12 selected biopsies with a high degree of fibrosis by LCM. *miR-21* was significantly up-regulated in the tubulointerstitial fraction in DN patients compared with controls (Figure 2D). *miR-21* levels were significantly lower in the glomerular fraction and did not change between biopsies from control and DN groups.

### miR-21 is consistently up-regulated in experimental models of renal fibrosis

Renal cortical tissue from a number of experimental models of kidney fibrosis revealed elevated *miR-21* expression compared with control. In the STZ-induced diabetic ApoE<sup>-/-</sup> mice, a model representing early DN, *miR-21* was increased  $\sim$ 2-fold in the renal cortex when compared with control mice (Figure 3A). In a model of more advanced DN, UNx STZ-induced diabetic Sprague–Dawley rats, a  $\sim$ 3.5-fold increase in renal *miR-21* levels was observed compared with non-diabetic UNx controls (Figure 3B). In both models, increased *miR-21* was associated with increased expression of collagen and FN1 (Fibronectin 1) (Figures 3C and 3D).

GSI and TIF were also increased in diabetic UNx rats when compared with control UNx rats (Figure 3E). Finally, in a model representing severe, non-diabetic fibrotic renal disease, C57Bl/6 mice administered adenine by gavage [20,26], *miR-21* expression was increased  $\sim$ 3-fold in whole cortex from these animals when compared with controls and was associated with increased collagen deposition as indicated by Masson's Trichrome staining (Figures 3F and 3G). These data, in addition to those from human renal biopsies, support a role for *miR-21* in fibrotic renal disease of both a diabetic and a non-diabetic nature, thus highlighting a potential role for *miR-21* in the pathogenesis of fibrosis in DN.

### miR-21 is induced by TGF $\beta$ 1 and alters TGF- $\beta$ 1 induced Col1 (Collagen 1), ColIV and FN1 expression in PTCs

PTCs maintained in high glucose (25 mM) were subjected to 72 h treatment with TGF- $\beta$ 1, resulting in up-regulation of Coll, ColIV, FN1 and *miR-21* (Figures 4A and 4B). These data, together with the human renal biopsy data, confirm that *miR-21* is up-regulated in tubular epithelial cells (Figure 2C). To delineate the role of *miR-21* in PTCs, cells were transfected with *miR-21* precursor mimics (pre-miR) or miR LNA inhibitors under high glucose conditions. Ectopic expression of *miR-21* increased expression of ColIV and TGF- $\beta$ 1 (Figures 4C and 4D). Consistent with a role in TGF- $\beta$ 1 signalling, *miR-21* enhanced the effect of TGF- $\beta$ 1 on a number of extracellular matrix (ECM) genes and pro-fibrotic growth factors (Figures 4C and 4D).

As observed with *miR-21* up-regulation, LNA repression of *miR-21* levels did not affect basal gene expression (Figures 4E

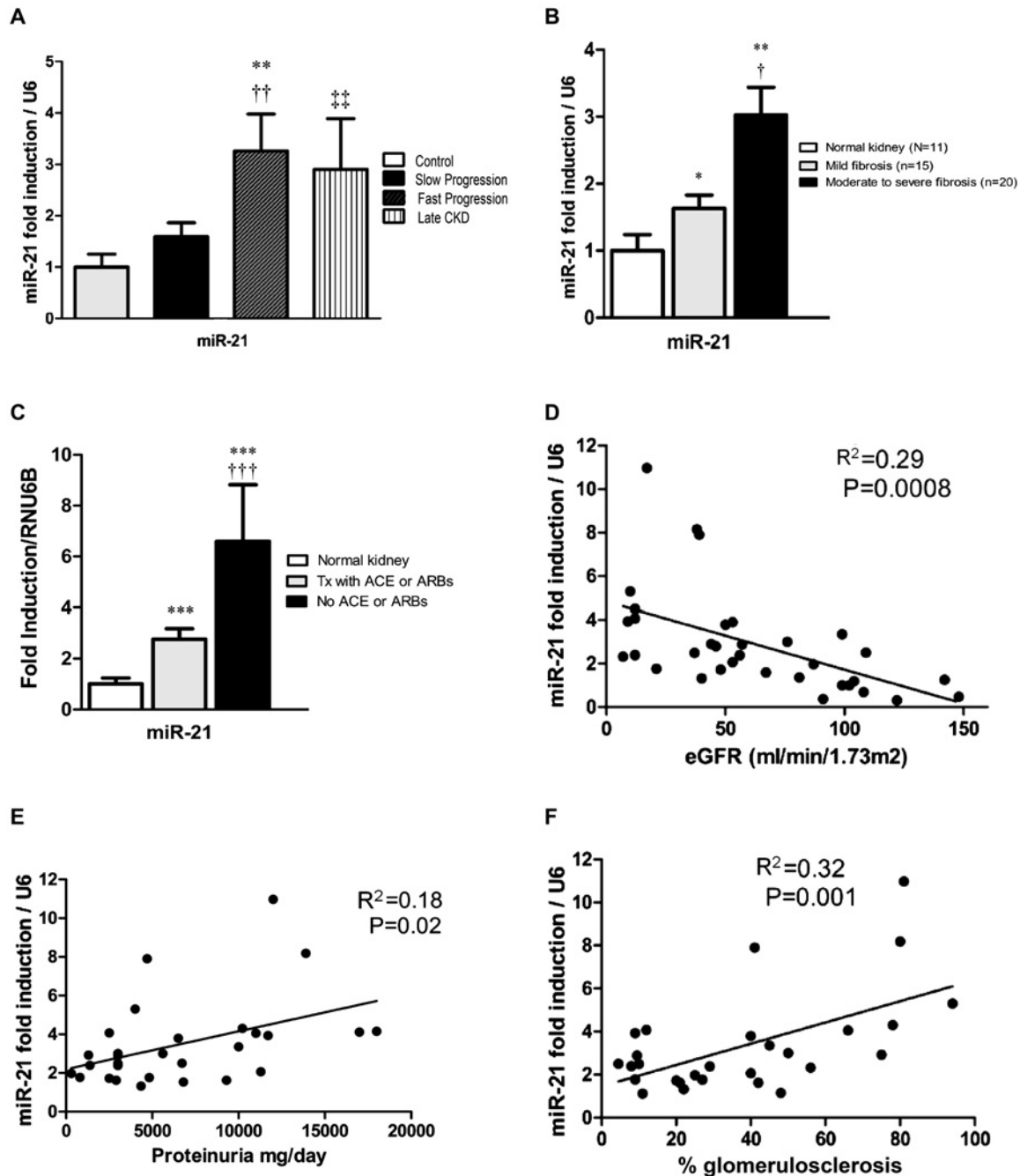


**Figure 1** *miR-21* is positively associated with the rate of progression of DN and degree of tubulointerstitial pathology (A) *miR-21* expression in normal and in T2DM subjects with slow or fast decline in eGFR and those with late presenting CKD (chronic kidney disease). \*\* $P < 0.01$ , slow compared with fast; †† $P < 0.01$ , normal compared with late; ††† $P < 0.005$ , normal compared with fast. (B) *miR-21* expression in normal and DN with mild and moderate to severe TIF. \* $P < 0.05$ , moderate to severe compared with mild; † $P < 0.05$ , normal compared with mild; \*\* $P < 0.005$ , normal compared with moderate to severe. (C) *miR-21* expression in control and DN subjects receiving and not receiving ACE/ARB treatment. \*\*\* $P < 0.001$ , normal compared with ACE/ARB, normal compared with no ACE/ARB; ††† $P < 0.005$ , ACE/ARB compared with no ACE/ARB. (D) Pearson correlation ( $R^2 = 0.29$ ,  $P = 0.0008$ ) between *miR-21* expression and eGFR. (E) Pearson's correlation ( $R^2 = 0.18$ ,  $P = 0.02$ ) between *miR-21* and proteinuria for subjects with DN (mg/day). (F) Pearson correlation ( $R^2 = 0.32$ ,  $P = 0.001$ ) between *miR-21* and percentage global glomerulosclerosis.

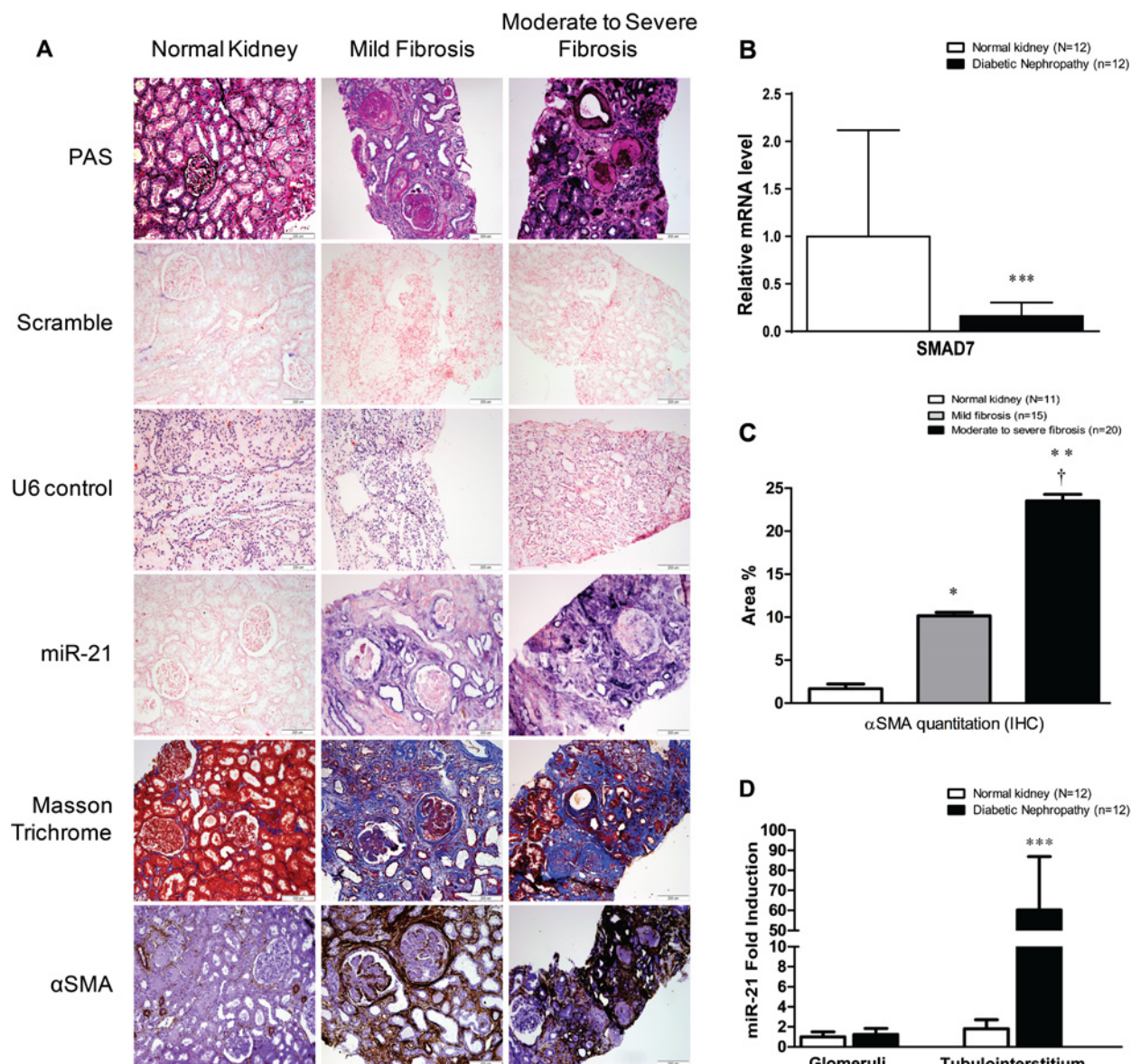


**Figure 2** *miR-21* is associated with increased renal pathology and up-regulated in microdissected tubules (A) HC, IHC and *in-situ* analysis of human renal biopsies from control and DN subjects with mild or moderate to severe TIF. Scramble is a non-specific RNA probe and U6 is a positive control *in situ* probe. (B) SMAD7 mRNA expression in normal and in DN subjects. \*\*\* $P < 0.0005$ , normal compared with DN. (C) Quantification of  $\alpha$ -SMA IHC in control and DN subjects with mild or moderate to severe fibrosis. \* $P < 0.05$ , normal compared with mild; \*\* $P < 0.005$ , normal compared with moderate to severe; † $P < 0.05$ , mild compared with moderate to severe. (D) *miR-21* expression in laser-capture micro-dissected tubulointerstitial fraction and glomeruli from control and DN subjects. \*\*\* $P < 0.001$ , control tubuli compared with DN tubuli.

and 4F). However, the TGF- $\beta$ 1 mediated up-regulation of the genes was attenuated with *miR-21* inhibition (Figures 4E and 4F). These data suggest that *miR-21* mediates the effects of TGF- $\beta$ 1 in PTCs in hyperglycaemic conditions in a manner that could be conducive to the development and progression of renal fibrosis.

#### *miR-21* targets known fibrotic signalling proteins

SMAD7 and PTEN, the repressors of SMAD3-dependent and PI3K-dependent TGF- $\beta$ 1-signalling respectively, are known tar-

gets of *miR-21* [12,14,27–29]. Ectopic expression of *miR-21* in PTCs reduced SMAD7 protein under basal conditions but also prevented the TGF- $\beta$ 1-induced increase in SMAD7 protein (Figure 5A). Consistent with these observations, SMAD3 phosphorylation was increased by *miR-21* and TGF- $\beta$ 1-induced SMAD3 phosphorylation was further enhanced (Figure 5B).

PTEN protein was decreased by *miR-21* (Figure 5C). Additionally, this miR further enhanced the TGF- $\beta$ 1-induced down-

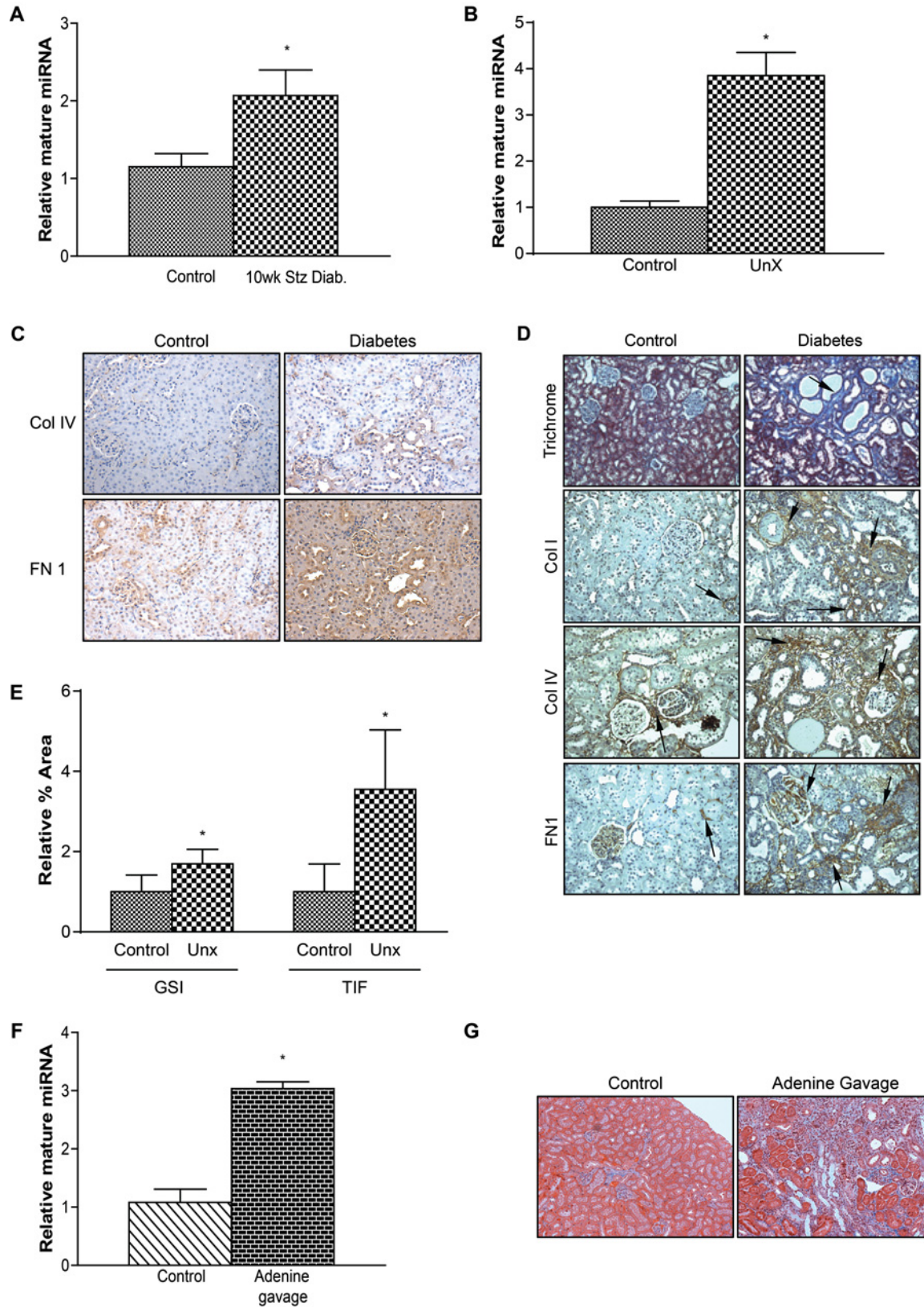


**Figure 3** *miR-21* expression is positively associated with tissue pathology in experimental renal disease

regulation of PTEN (Figure 5C). AKT phosphorylation was increased by exogenous *miR-21* (Figure 5D) and elicited greater TGF- $\beta$ 1-induced phospho-AKT levels than TGF- $\beta$ 1 alone. These data, combined with those assessing SMAD7 regulation (Figure 5A), demonstrate that *miR-21* plays an important role in the regulation of these distinct regulatory proteins and therefore TGF- $\beta$ 1-mediated fibrotic signalling pathways in PTCs [2].

### Fibrotic consequences of the SMAD7–*miR-21* and PTEN–*miR-21* axes

In order to delineate the role of *miR-21*-mediated repression of SMAD7 and PTEN in TGF- $\beta$ 1-mediated signalling, the effect of *miR-21* on SMAD7 and PTEN was abrogated by either inhibition of PI3K with LY294002 (LY) [5] or siRNA for SMAD3. The rationale for this approach is depicted in Figure 7(A).

LY treatment reduced ColI expression even in the presence of TGF- $\beta$ 1, a known inducer of ColI expression, indicating that the expression of ColI is mainly dependent on PI3K signalling (Figure 6A) rather than SMAD3 and therefore dependent on the effect of *miR-21* on PTEN rather than SMAD7. In contrast, TGF- $\beta$ 1-induced PAI1 (plasminogen activator inhibitor 1) expression was further up-regulated by LY treatment (Figure 6B) and even further enhanced by *miR-21* overexpression, indicating the importance of both SMAD7 and PTEN in the regulation of PAI1 expression and therefore ECM accumulation. Finally, PI3K inhibition did not attenuate FN1 induction by TGF- $\beta$ 1 or the combination treatment of TGF- $\beta$ 1 and *miR-21* (Figures 6C and 6H). Interrogation and specific targeting of the PTEN–*miR-21* axis reveals this interaction is required for *miR-21* augmentation of TGF- $\beta$ 1-induced ColI expression and is also an important negative regulator of TGF- $\beta$ 1-induced PAI1 expression.

SMAD3 siRNA reduced ColI expression in control and TGF- $\beta$  treated cells (Figure 6D). *miR-21* significantly enhanced ColI expression in both the presence and the absence of TGF- $\beta$ , even in the presence of SMAD3 siRNA. Taken together with the findings above, these data provide evidence that the PTEN–*miR-21* axis is a significant contributor to TGF- $\beta$ 1-mediated ColI up-regulation.

SMAD3 siRNA also reduced the expression of PAI1 under control conditions and significantly attenuated TGF- $\beta$ 1-mediated induction of PAI1 (Figure 6E). This is in contrast with PI3K inhibition which greatly enhanced PAI1 expression (Figure 6B). These data indicate that despite the negative effect of PI3K on PAI1 expression, SMAD3 is still required for the expression of PAI1. Finally, SMAD3 inhibition had minimal impact on FN1 expression and only partially attenuated the effect of *miR-21* on TGF- $\beta$ 1-mediated induction of FN1 (Figure 6F). Examination of the SMAD7–*miR-21* axis demonstrates this interaction

is required for both baseline expression and *miR-21*–TGF- $\beta$ 1-induced expression of ColI and PAI1.

### The PTEN–SMAD7–*miR-21* axis is required for TGF- $\beta$ 1-induced fibrotic response

To determine if the ability of *miR-21* to enhance TGF- $\beta$ 1-mediated fibrotic response in PTCs is indeed mediated by repression of PTEN and SMAD7, both pathways were simultaneously inhibited (Figure 7A). Co-repression of these signalling intermediates resulted in reduced baseline expression of ColI indicating a dependence on the *miR-21*–TGF $\beta$  axis for increased ColI expression (Figure 6G).

Conversely, PAI1 expression was increased 3.5-fold above baseline when both pathways were inhibited in the presence of the combination of *miR-21* and TGF- $\beta$ 1 (Figure 6H). This is significantly greater than the expression induced by *miR-21* alone confirming the importance of the inhibitory role of PI3K signalling on PAI1 and thus PAI1-mediated ECM accumulation [30]. Additionally, simultaneous repression of both of these pathways resulted in restoration of FN1 expression to baseline levels (Figure 6I). Simultaneous repression of both *miR-21*–PTEN and *miR-21*–SMAD7 interactions reveals that these pathways are essential to *miR-21*-augmentation of TGF- $\beta$ 1-induced ColI and FN1 expression.

## DISCUSSION

There is increasing interest in the role of miRs in various chronic diseases including diabetic complications. miRs mediate post transcriptional regulation of genes via repressing translation of target mRNA [31,32]. In the present study, we studied the expression of *miR-21* in human DN kidney biopsies with advanced renal fibrosis and also the role of *miR-21* in TGF- $\beta$ 1-mediated expression of fibrotic genes induced under hyperglycaemic conditions [33,34].

Increased *miR-21* was detected in the tubular regions of human kidney biopsies. Furthermore, in laser-capture microdissected tubuli, increased *miR-21* expression correlated with TIF, glomerulosclerosis and declining renal function. Consistent with the findings in human DN, increased *miR-21* was also consistently observed in experimental models of diabetic and non-diabetic fibrotic renal disease. The data presented in the present study not only confirm a pro-fibrotic role in the kidney for *miR-21*, but importantly defined the mechanism of action of this miR which appears to involve targeting the negative regulators of TGF- $\beta$ 1-induced prosclerotic SMAD3- and AKT-mediated signalling pathways in tubular epithelial cells, namely SMAD7 and

### Figure 3 Continued.

(A) *miR-21* expression in renal cortices from control and STZ-induced diabetic ApoE<sup>-/-</sup> mice. (B) *miR-21* expression in renal cortices from control and STZ-induced diabetic uni-nephrectomized Sprague–Dawley rats (UNx). (C) IHC detection of ColIV and FN1 kidney sections from control and STZ-induced diabetic ApoE<sup>-/-</sup> mice. (D) HC and IHC analysis of kidney sections from control and UNx rats for the indicated proteins/stains. Arrows indicate areas of interest. (E) Percentage total area scores for glomerulosclerosis and TIF in renal sections from control and UNx rats. (F) *miR-21* expression from renal cortices from control and adenine gavaged C57B/16 mice. (G) Masson Trichrome staining in control and adenine gavage C57bl6.

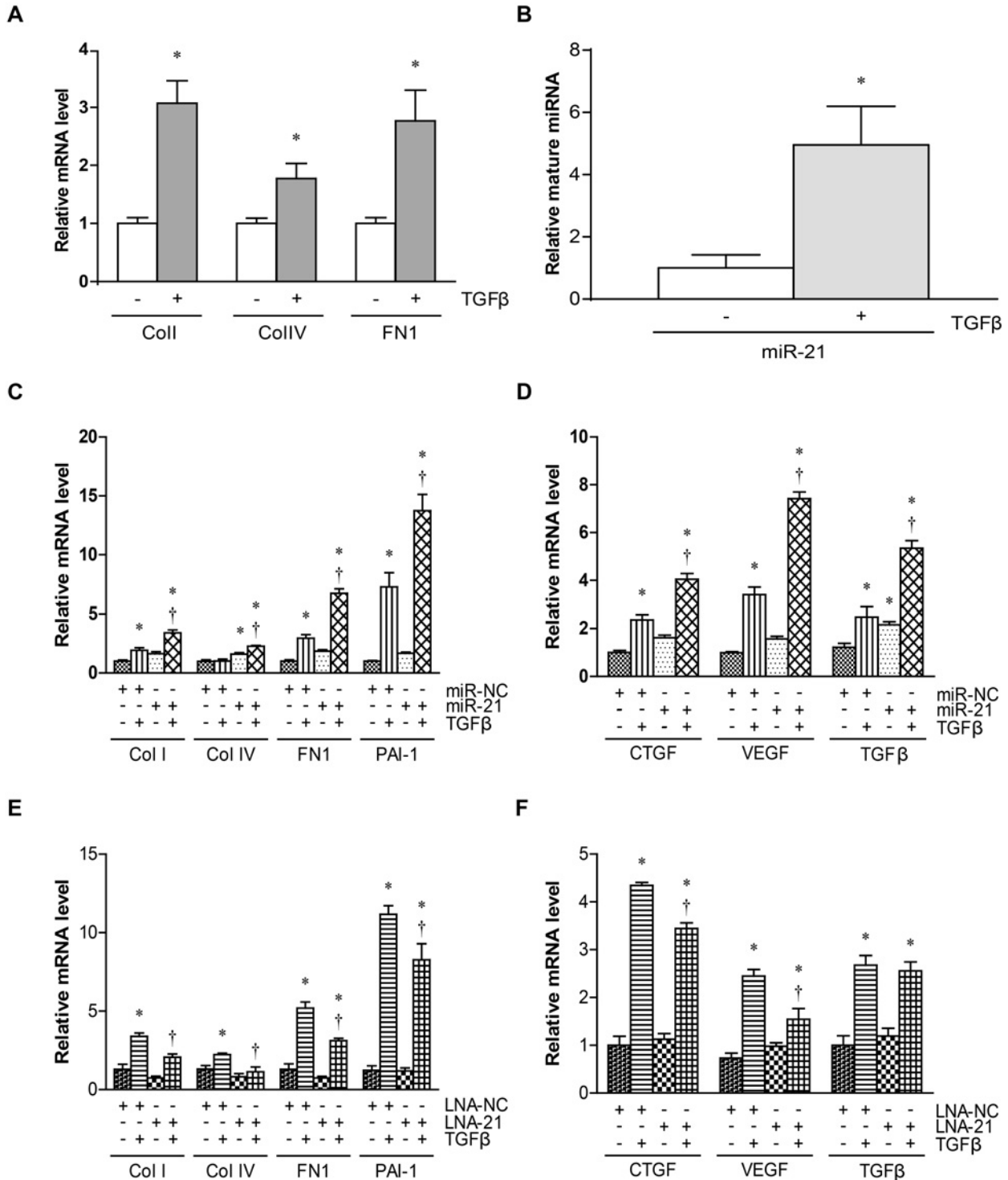


**Figure 4** *miR-21* is up-regulated by and enhances TGF-β-mediated fibrotic gene expression (A) mRNA expression for the indicated genes from control and TGF-β treated NRK-52E proximal tubular cells. (B) *miR-21* expression from control and TGF-β treated NRK-52E cells. RNA expression for ECM genes (C) and pro-fibrotic growth factors (D) from control, TGF-β treated, *miR-21* mimic transfected and *miR-21* transfected/TGF-β treated NRK-52E cells. \**P* < 0.05, control compared with all groups; †*P* < 0.05, TGF-β compared with *miR-21* + TGF-β. mRNA expression for ECM genes (E) and pro-fibrotic growth factors (F) from control, TGF-β treated, *miR-21* inhibitor transfected *miR-21* inhibited/TGF-β treated NRK-52E cells. \**P* < 0.05, control compared with all groups; †*P* < 0.05, TGF-β compared with *miR-21* inhibitor + TGF-β.

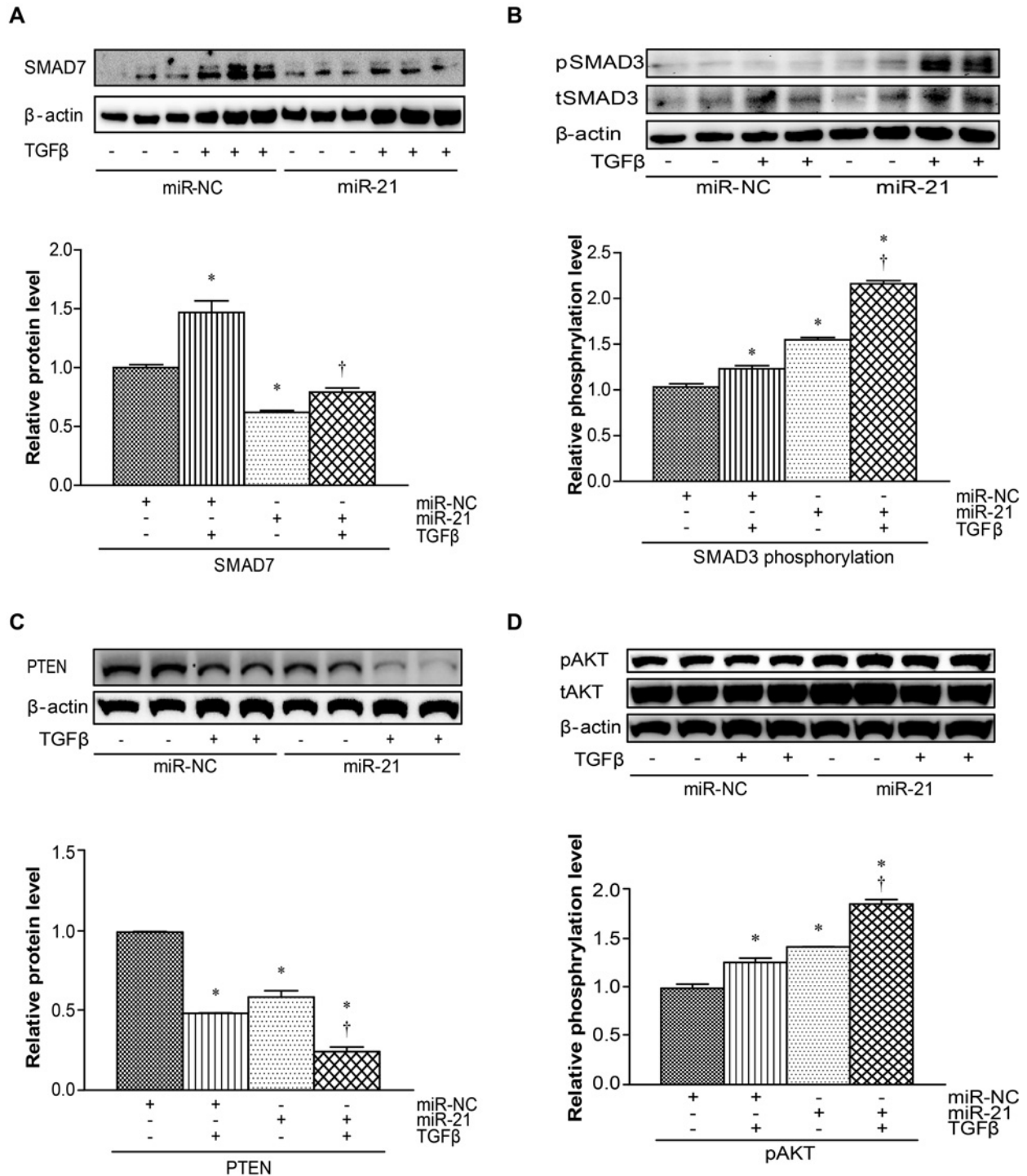


**Figure 5 SMAD7 and PTEN protein translation is modulated by miR-21 levels**

Immunoblot detection of SMAD7 (A), pSMAD3 (B), PTEN (C) and pAKT (D) from whole cell lysates of NRK-52E treated as indicated. Densitometric analysis of SMAD7/PTEN levels relative to β-actin and pSMAD3/pAKT relative to total SMAD3-AKT respectively for control, TGF-β treated, miR-21 transfected and miR-21 transfected/TGF-β treated are shown below each blot. \*P < 0.05, control compared with all; †P < 0.05, TGF-β compared with TGF-β-miR-21.

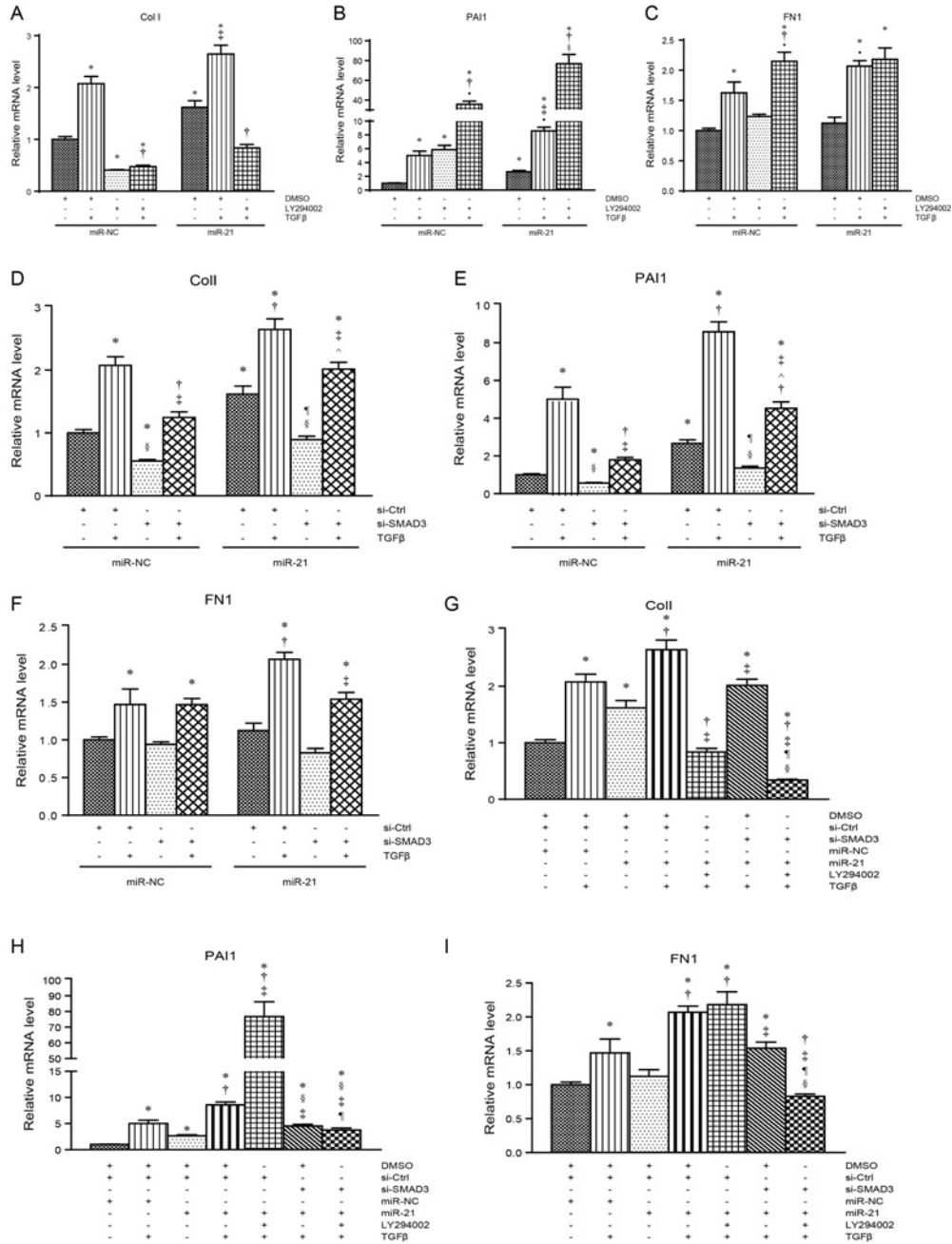


**Figure 6** *miR-21* mediates its effects via SMAD3-dependent and PI3K-dependent signalling mRNA expression of Coll (A), PAI1 (B) and FN1 (C) from control, TGF- $\beta$  treated, LY294002 and LY294002/TGF- $\beta$  treated NRK-52E cells. Cells were transfected with control or *miR-21* mimic oligonucleotides as indicated. \* $P < 0.05$ , control compared with all; † $P < 0.05$ , LY294002 compared with LY294002 + TGF- $\beta$ ; ‡ $P < 0.05$ , miR-NC + TGF- $\beta$  compared with miR-NC + TGF- $\beta$  + LY294002; § $P < 0.05$ , miR-NC + TGF- $\beta$  compared with miR-NC + TGF- $\beta$  + LY294002. RNA expression of Coll (D), PAI1 (E) and FN1 (F) from control, TGF- $\beta$  treated, SMAD3 siRNA transfected and SMAD3 transfected/TGF cells- $\beta$  treated NRK-52E. \* $P < 0.05$ , control compared with all; † $P < 0.05$ , miR-NC + TGF- $\beta$  compared with all + TGF- $\beta$ ; ‡ $P < 0.05$ , miR + siSMAD3 + TGF- $\beta$ ; § $P < 0.05$ , miR compared with miR + siSMAD3; ¶ $P < 0.05$ , siSMAD3 compared with miR-21 + siSMAD3; ¶¶ $P < 0.05$ , siSMAD3 + TGF- $\beta$  compared with miR-21 + siSMAD3 + TGF- $\beta$ . RNA expression of Coll (G), PAI1 (H) and FN1 (I) from control cells, TGF- $\beta$  treated, *miR-21* transfected, *miR-21* transfected/TGF- $\beta$  treated, *miR-21* transfected/LY294002/TGF- $\beta$  treated, *miR-21*-SMAD3 siRNA transfected/TGF- $\beta$  treated and *miR-21*-SMAD3 siRNA transfected/LY294002/TGF- $\beta$  treated. Data were analysed via Tukey one-way ANOVA. \* $P < 0.05$ , control compared with all; † $P < 0.05$ , miR-NC + TGF- $\beta$  compared with all + TGF- $\beta$ ; ‡ $P < 0.05$ , *miR-21* + TGF- $\beta$  compared with all + *miR-21* + TGF- $\beta$ ; § $P < 0.05$ , *miR-21* + LY294002 + TGF- $\beta$  compared with *miR-21* + siSMAD3 + LY294002 + TGF- $\beta$ ; ¶ $P < 0.05$ , *miR-21* + siSMAD3 + TGF- $\beta$  compared with *miR-21* + siSMAD3 + LY294002 + TGF- $\beta$ .

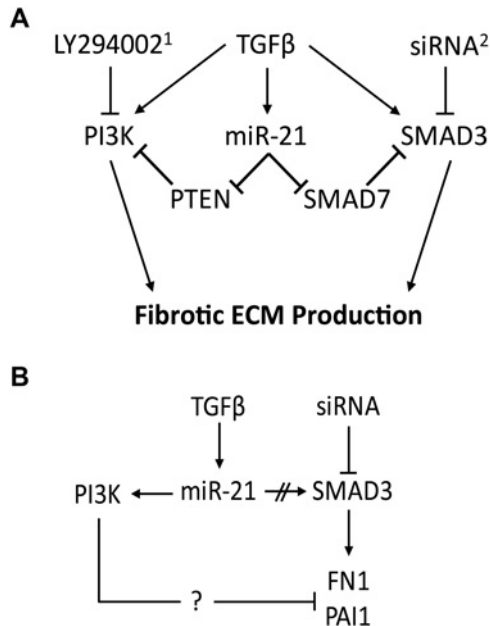


**Figure 7 Rationale for dual inhibition experiments**

(A) <sup>1</sup>Addition of LY294002 inhibits PI3K and effectively bypasses the effect of *miR-21* on PTEN and its downstream signalling intermediates. <sup>2</sup>Conversely, anti-SMAD3 siRNA blocks the effect of *miR-21* on SMAD7 and the up-regulating role it has on SMAD3-dependent signalling. These treatments therefore isolate and highlight the effect of the reciprocal pathways targeted by *miR-21*. (B) Data from isolation of these pathways indicates that when the effect of *miR-21* on SMAD3 is blocked by SMAD3 siRNA, PI3K mediates repression of both FN1 and PAI1 through a third, unknown pathway.

PTEN. These targets contribute individually and cooperatively to induce many of the fibrogenic changes typical of DN and which are regulated by *miR-21*.

The present work adds to a number of studies demonstrating involvement of *miR-21* in human renal pathology [12,35,36] although the present study has particularly focused on DN. *miR-21* is reported to be up-regulated in allograft nephropathy with serum levels being increased independently of disease progression and also more recently in Alport syndrome [37]. It is therefore likely that *miR-21* dysregulation is a common feature of renal disease where there is concomitant fibrosis. This is supported by our observations of increased *miR-21* levels not only in a number of experimental models of diabetic renal disease but also in a model of non-diabetic renal disease. Despite a number of recent publications demonstrating increased *miR-21* in mesangial cells and podocytes [12,13,35,36,38], our human *in vivo* data have demonstrated elevation of *miR-21* primarily in the tubular compartment in DN. Thus, the present study has focused on the role of *miR-21* in proximal tubule cells in the context of elevated glucose levels.

In PTCs, TGF- $\beta$ 1 increases *miR-21* expression in conjunction with the expression of pro-fibrotic and ECM genes. Exogenous *miR-21* augments these changes and repression of *miR-21* dampens the effects of TGF- $\beta$ 1. These data indicate that *miR-21* plays a pivotal role in the regulation of processes down-

stream of TGF- $\beta$ 1. The SMAD- and AKT-dependent signalling pathways are both well-characterized and directly mediate TGF- $\beta$ 1-induced signalling thus contributing to the pathogenesis of DN [2]. Importantly, the negative regulators of these pathways, SMAD7 and PTEN respectively, are targeted and repressed by *miR-21*. The co-ordination of flux through these pathways with respect to *miR-21* has not been investigated previously. Interrogation of the *miR-21*–SMAD7 axis via SMAD3 knockdown and the *miR-21*–PTEN axis via the use of the PI3K inhibitor LY294002 revealed that both of these pathways contribute to the regulation of classic effects of TGF- $\beta$ 1 including modulation of Col1, PAI1 and FN1 expression in PTCs.

Indeed, when both SMAD3 and AKT pathways were inhibited, both Col1 and FN1 expression were not elevated by either *miR-21* or TGF- $\beta$ 1 alone or in combination. Conversely, PAI1 expression was still elevated by combination treatment with *miR-21* and TGF- $\beta$ 1 when both SMAD3 and AKT pathways were inhibited. Given that PAI1 possesses multiple SMAD3 promoter elements and that SMAD3 translation may not be fully inhibited by siRNA [39], this outcome is not unreasonable especially considering the changes in PAI1 expression seen under PI3K inhibition. PI3K–PTEN signalling acts as a negative regulator of FN1 and this pathway is also absolutely required for Col1 expression. In all cases, *miR-21* is seen to amplify the effect of TGF- $\beta$ 1 and its role in signalling through either pathway. The observation that TGF- $\beta$ 1 has some pro-fibrotic effects independent of SMAD3 and AKT, may indicate that yet another *miR-21* targeted pathway mediates some of the pro-fibrotic effects of TGF- $\beta$ 1.

From our experiments, it is clear that *miR-21* is an important player in the TGF- $\beta$ 1 signalling environment. Indeed, *miR-21* levels were elevated concordantly with increasing disease pathology in human renal biopsies and experimental models of early/late DN and non-DN. It was shown that *miR-21* is consistently up-regulated in the tubular compartment in models of diabetic and non-diabetic renal fibrosis. The observation of increased *miR-21* in association with renal fibrosis could reflect a functional interaction between *miR-21* and regulators of important signalling pathways in tubular cells. These interactions form part of a previously uncharacterized signalling system involving *miR-21*, PTEN and SMAD7. This system acts to co-ordinately regulate the TGF- $\beta$ 1-mediated fibrotic response of PTCs by concomitant de-repression of both SMAD3- and AKT-dependent signalling. In summary, this comprehensive approach to the study of the function of *miR-21* in renal fibrosis provides important insight into the onset and progression of DN and could assist in defining alternative renoprotective strategies in diabetes.

## CLINICAL PERSPECTIVE

- The present study analysed expression and correlation of *miR-21* to fibrosis and renal function in biopsy material from DN subjects. Delineation of the role of *miR-21* targets in PTCs was also performed.
- The results have highlighted the complexity of *miR-21* action in TGF- $\beta$ 1-mediated fibrotic signalling in DN and also added

a level of understanding to the interplay of *miR-21* and *TGF- $\beta$ 1* which had been previously unrecognized.

- These findings are important in developing targeted therapeutics against the development and progression of DN.

#### AUTHOR CONTRIBUTION

Michal Herman-Edelstein, Radko Komers, Jay Jha, Shinji Hagiwara and Phillip Kantharidis researched data. Catherine Winbanks, Paul Gregorevic, Phillip Kantharidis and Mark Cooper reviewed/edited manuscript. Aaron McClelland researched data and wrote manuscript.

#### FUNDING

This work was supported by the Heart Foundation [grant number G11M 6134]; the Diabetes Australia Research Trust; the Skip Martin Award; the Vera Dalgleish Phillips Fellowship (to PK.); the National Health and Research Council of Australia [grant number 106448 (to M.E.C.)]; and the Victorian Government's Operational Infrastructure Support (OIS) Program.

#### REFERENCES

- 1 Wolf, G. and Ziyadeh, F.N. (2007) Cellular and molecular mechanisms of proteinuria in diabetic nephropathy. *Nephron Physiol.* **106**, 26–31 [CrossRef PubMed](#)
- 2 Khoury, C.C., Buller, C.L. and Chen, S. (2010) Abnormalities in signaling pathways in diabetic nephropathy. *Expert Rev. Endocrinol. Metab.* **5**, 51–64 [CrossRef PubMed](#)
- 3 Schena, F.P. and Gesualdo, L. (2005) Pathogenetic mechanisms of diabetic nephropathy. *J. Am. Soc. Nephrol.* **16** 3 suppl 1, S30–S33 [CrossRef PubMed](#)
- 4 Derynck, R. and Zhang, Y.E. (2003) Smad-dependent and smad-independent pathways in TGF family signalling. *Nature* **425**, 577–584 [CrossRef PubMed](#)
- 5 Song, M.S., Salmena, L. and Pandolfi, P.P. (2012) The functions and regulation of the PTEN tumour suppressor. *Nat. Rev. Mol. Cell. Biol.* **13**, 283–296 [PubMed](#)
- 6 Yan, X., Liu, Z. and Chen, Y. (2009) Regulation of TGF- $\beta$  signaling by Smad7. *Acta Biochim. Biophys. Sin.* **41**, 263–272 [CrossRef](#)
- 7 Butz, H., Rácz, K., Hunyady, L. and Patócs, A. (2012) Crosstalk between TGF- $\beta$  signaling and the microRNA machinery. *Trends Pharmacol. Sci.* **33**, 382–393 [CrossRef PubMed](#)
- 8 Kantharidis, P., Wang, B., Carew, R.M. and Lan, H.Y. (2011) Diabetes complications: the microRNA perspective. *Diabetes* **60**, 1832–1837 [CrossRef PubMed](#)
- 9 Van Rooij, E. and Olson, E.N. (2009) Searching for miR-acles in cardiac fibrosis. *Circ. Res.* **104**, 138–140 [CrossRef PubMed](#)
- 10 Patel, V. and Noureddine, L. (2012) MicroRNAs and fibrosis. *Curr. Opin. Nephrol. Hypertens.* **21**, 410–416 [CrossRef PubMed](#)
- 11 Godwin, J.G., Ge, X., Stephan, K., Jurisch, A., Tullius, S.G. and Iacomini, J. (2010) Identification of a microRNA signature of renal ischemia reperfusion injury. *Proc. Natl. Acad. Sci. U.S.A.* **107**, 14339–14344 [CrossRef PubMed](#)
- 12 Zhong, X., Chung, A.C.K., Chen, H.Y., Meng, X.M. and Lan, H.Y. (2011) Smad3-mediated upregulation of miR-21 promotes renal fibrosis. *J. Am. Soc. Nephrol.* **22**, 1668–1681 [CrossRef PubMed](#)
- 13 Zhong, X., Chung, A.C.K., Chen, H.Y., Dong, Y., Meng, X.M., Li, R., Yang, W., Hou, F.F. and Lan, H.Y. (2013) miR-21 is a key therapeutic target for renal injury in a mouse model of type 2 diabetes. *Diabetologia* **56**, 663–674 [CrossRef PubMed](#)
- 14 Liu, G., Friggeri, A., Yang, Y., Milosevic, J., Ding, Q., Thannickal, V.J., Kaminski, N. and Abraham, E. (2010) miR-21 mediates fibrogenic activation of pulmonary fibroblasts and lung fibrosis. *J. Exp. Med.* **207**, 1589–1597 [CrossRef PubMed](#)
- 15 Lai, J.Y., Luo, J., O'Connor, C., Jing, X., Nair, V., Ju, W., Randolph, A., Ben-Dov, I.Z., Matar, R.N., Briskin, D. et al. (2014) MicroRNA-21 in glomerular injury. *J. Am. Soc. Nephrol.* **26**, 805–816 [CrossRef PubMed](#)
- 16 Dey, N., Ghosh-Choudhury, N., Kasinath, B.S. and Choudhury, G.G. (2012) TGF- $\beta$ -stimulated microRNA-21 utilizes PTEN to orchestrate AKT/mTORC1 signaling for mesangial cell hypertrophy and matrix expansion. *PLoS One* **7**, e42316 [CrossRef PubMed](#)
- 17 Kato, M., Putta, S., Wang, M., Yuan, H., Lanting, L., Nair, I., Gunn, A., Nakagawa, Y., Shimano, H. and Todorov, I. (2009) TGF- $\beta$  activates Akt kinase through a microRNA-dependent amplifying circuit targeting PTEN. *Nat. Cell Biol.* **11**, 881–889 [CrossRef PubMed](#)
- 18 Herman-Edelstein, M., Scherzer, P., Tobar, A., Levi, M. and Gafter, U. (2014) Altered renal lipid metabolism and renal lipid accumulation in human diabetic nephropathy. *J. Lipid. Res.* **55**, 561–572 [CrossRef PubMed](#)
- 19 Tervaert, T.W., Mooyaart, A.L., Amann, K., Cohen, A.H., Cook, H.T., Drachenberg, C.B., Ferrario, F., Fogo, A.B., Haas, M., de Heer, E. et al. (2010) Pathologic classification of diabetic nephropathy. *J. Am. Soc. Nephrol.* **21**, 556–563 [CrossRef PubMed](#)
- 20 Wang, B., Komers, R., Carew, R., Winbanks, C.E., Xu, B., Herman-Edelstein, M., Koh, P., Thomas, M., Jandeleit-Dahm, K., Gregorevic, P. et al. (2012) Suppression of microRNA-29 expression by TGF- $\beta$ 1 promotes collagen expression and renal fibrosis. *J. Am. Soc. Nephrol.* **23**, 252–265 [CrossRef PubMed](#)
- 21 Komers, R., Schutzer, W.E., Reed, J.F., Lindsley, J.N., Oyama, T.T., Buck, D.C., Mader, S.L. and Anderson, S. (2006) Altered endothelial nitric oxide synthase targeting and conformation and caveolin-1 expression in the diabetic kidney. *Diabetes* **55**, 1651–1659 [CrossRef PubMed](#)
- 22 Soro-Paavonen, A., Watson, A.M.D., Li, J., Paavonen, K., Koitka, A., Calkin, A.C., Barit, D., Coughlan, M.T., Drew, B.G., Lancaster, G.I. et al. (2008) Receptor for advanced glycation end products (RAGE) deficiency attenuates the development of atherosclerosis in diabetes. *Diabetes* **57**, 2461–2469 [CrossRef PubMed](#)
- 23 Tu, Y., Wu, T., Dai, A., Pham, Y., Chew, P., de Haan, J.B., Wang, Y., Toh, B.H., Zhu, H., Cao, Z. et al. (2011) Cell division autoantigen 1 enhances signaling and the profibrotic effects of transforming growth factor- $\beta$  in diabetic nephropathy. *Kidney Int.* **79**, 199–209 [CrossRef PubMed](#)
- 24 Oldfield, M.D., Bach, L.A., Forbes, J.M., Nikolic-Paterson, D., McRobert, A., Thallas, V., Atkins, R.C., Osicka, T., Jerums, G. and Cooper, M.E. (2001) Advanced glycation end products cause epithelial-myofibroblast transdifferentiation via the receptor for advanced glycation end products (RAGE). *J. Clin. Invest.* **108**, 1853–1863 [CrossRef PubMed](#)
- 25 Cikos, S. and Koppel, J. (2009) Transformation of real-time PCR fluorescence data to target gene quantity. *Anal. Biochem.* **384**, 1–10 [CrossRef PubMed](#)
- 26 Wang, B., Koh, P., Winbanks, C., Coughlan, M.T., McClelland, A., Watson, A., Jandeleit-Dahm, K., Burns, W.C., Thomas, M.C., Cooper, M.E. et al. (2011) miR-200a prevents renal fibrogenesis through repression of TGF- $\beta$ 2 expression. *Diabetes* **60**, 280–287 [CrossRef PubMed](#)
- 27 Zhu, H., Luo, H., Li, Y., Zhou, Y., Jiang, Y., Chai, J., Xiao, X., You, Y. and Zuo, X. (2013) MicroRNA-21 in scleroderma fibrosis and its function in TGF- $\beta$ -regulated fibrosis-related genes expression. *J. Clin. Immunol.* **33**, 1100–1109 [CrossRef PubMed](#)
- 28 Li, Q., Zhang, D., Wang, Y., Sun, P., Hou, X., Larner, J., Xiong, W. and Mi, J. (2013) MiR-21/Smad 7 signaling determines TGF- $\beta$ 1-induced CAF formation. *Sci. Rep.* **3**, 2038 [PubMed](#)

- 29 Dey, N., Das, F., Mariappan, M.M., Mandal, C.C., Ghosh-Choudhury, N., Kasinath, B.S. and Choudhury, G.G. (2011) MicroRNA-21 orchestrates high glucose-induced signals to TOR complex 1, resulting in renal cell pathology in diabetes. *J. Biol. Chem.* **286**, 25586–25603 [CrossRef PubMed](#)
- 30 Ghosh, A.K. and Vaughan, D.E. (2012) PAI-1 in tissue fibrosis. *J. Cell Physiol.* **227**, 493–507 [CrossRef PubMed](#)
- 31 Fabian, M.R., Sonenberg, N. and Filipowicz, W. (2010) Regulation of mRNA translation and stability by microRNAs. *Ann. Rev. Biochem.* **79**, 351–379 [CrossRef](#)
- 32 Jiang, X., Tsitsiou, E., Herrick, S.E. and Lindsay, M.A. (2010) MicroRNAs and the regulation of fibrosis. *FEBS J.* **277**, 2015–2021 [CrossRef PubMed](#)
- 33 Bartram, M., Höhne, M., Dafinger, C., Völker, L., Albersmeyer, M., Heiss, J., Göbel, H., Brönneke, H., Burst, V., Liebau, M. et al. (2013) Conditional loss of kidney microRNAs results in congenital anomalies of the kidney and urinary tract (CAKUT). *J. Mol. Med.* **91**, 739–748 [CrossRef PubMed](#)
- 34 Sequeira-Lopez, M.L.S., Weatherford, E.T., Borges, G.R., Monteagudo, M.C., Pentz, E.S., Harfe, B.D., Carretero, O., Sigmund, C.D. and Gomez, R.A. (2010) The microRNA-processing enzyme dicer maintains juxtaglomerular cells. *J. Am. Soc. Nephrol.* **21**, 460–467 [CrossRef PubMed](#)
- 35 Glowacki, F., Savary, G., Gnemmi, V., Buob, D., Van der Hauwaert, C., Lo-Guidice, J.M., Bouye, S., Hazzan, M., Pottier, N., Perrais, M. et al. (2013) Increased circulating miR-21 levels are associated with kidney fibrosis. *PLoS One* **8**, e58014 [CrossRef PubMed](#)
- 36 Chau, B.N., Xin, C., Hartner, J., Ren, S., Castano, A.P., Linn, G., Li, J., Tran, P.T., Kaimal, V., Huang, X. et al. (2012) MicroRNA-21 promotes fibrosis of the kidney by silencing metabolic pathways. *Sci. Transl. Med.* **4**, 121ra18 [CrossRef PubMed](#)
- 37 Gomez, I.G., MacKenna, D.A., Johnson, B.G., Kaimal, V., Roach, A.M., Ren, S., Nakagawa, N., Xin, C., Newitt, R., Pandya, S. et al. (2015) Anti-microRNA-21 oligonucleotides prevent Alport nephropathy progression by stimulating metabolic pathways. *J. Clin. Invest.* **125**, 141–156 [CrossRef PubMed](#)
- 38 Chung, A.C.K., Dong, Y., Yang, W., Zhong, X., Li, R. and Lan, H.Y. (2013) Smad7 suppresses renal fibrosis via altering expression of TGF- $\beta$ /Smad3-regulated microRNAs. *Mol. Ther.* **21**, 388–398 [CrossRef PubMed](#)
- 39 Dennler, S., Itoh, S., Vivien, D., Dijke, P., Huet, S. and Gauthier, J.M. (1998) Direct binding of Smad3 and Smad4 to critical TGF- $\beta$ -inducible elements in the promoter of human plasminogen activator inhibitor-type 1 gene. *EMBO J.* **17**, 3091–4100 [CrossRef PubMed](#)

Received 15 June 2015/17 September 2015; accepted 25 September 2015

Accepted Manuscript online 25 September 2015, doi: 10.1042/CS20150427

### 3.2. Conclusion

The present study has shown a clear association between miR-21 expression levels and the degree of fibrosis in human diabetic nephropathy biopsy samples. Increased miR-21 levels were also correlated the severity of renal disease as reflected by increasing proteinuria and decreasing estimated glomerular filtration rate. Increasing miR-21 levels were also correlated with increasing glomerulosclerosis.

*In situ* hybridization of miR-21 in human DN biopsy sections indicates that miR-21 expression is primarily increased in the tubular regions. This was supported through qRT-PCR analysis of laser-capture micro-dissected tubuli and glomeruli which demonstrated strong upregulation of miR-21 in tubules from DN biopsies when compared to controls.

*In vitro*, miR-21 was shown to augment TGF $\beta$ -mediated expression of a number of important fibrotic growth factors and fibrotic genes, while inhibition of miR-21 dampened the effect of TGF $\beta$  on these genes. These effects were shown to be mediated through direct targeting of SMAD7 and PTEN which are negative regulators of SMAD3-mediated and PI3K-mediated signalling pathways respectively. Further investigation of these interactions revealed that miR-21 mediates a complex regulatory network downstream of TGF $\beta$ .

The findings of this study have added important information about the nature of miR-21 dysregulation in DN. Furthermore, the findings of the pathway interrogation experiments have provided important insight into the molecular mechanisms whereby miR-21 mediates fibrotic signalling in the kidney. This work may be translatable to other tissues where fibrotic pathologies are known to occur. Finally, the present study provides valuable information towards the understanding of miR-21 biology and developing future therapeutic interventions to combat DN.

## 4. Results II - Genome wide effects of TGF $\beta$ on proximal tubule epithelial cells and mesangial cells

### 4.1. Introduction

DN is marked by a progressive loss of renal function and eventual failure due to two main processes, namely, glomerulosclerosis and tubulointerstitial fibrosis (12). These processes result in glomerular expansion and scarring as well as increased deposition of ECM. Both processes ultimately result in irreversible scarring of the kidney and are primarily mediated by glomerular mesangial cells and proximal tubule epithelial cells respectively.

These cells respond to a number of factors in the diabetic milieu such as growth factors, inflammatory cytokines and glucose itself (172). However, TGF $\beta$  is well regarded as one of the most potent pathological factors in DN due to its ability to induce fibrotic signalling pathways and also to induce pathogenic cellular phenotypes and transformations (59). The profound effects of TGF $\beta$  make it an attractive therapeutic target however efforts to reduce its expression or activities *in vivo* have not been successful for a variety of reasons (179).

It is therefore imperative to gain a better understanding of TGF $\beta$  biology in DN in order to develop future interventions targeted downstream of TGF $\beta$  itself. This deeper understanding can best be gained from genome-wide analysis of TGF $\beta$ -mediated mRNA gene dysregulation of cells important to the pathophysiology of DN. Direct comparison of the effects TGF $\beta$  in different cell types may reveal novel targets or pathways for future investigation in a given cell type. Furthermore, by taking a genome-wide approach, the transcriptional topology induced by TGF $\beta$  in a specific cell type may become clearer and reveal the nature of pathophysiology of certain cell populations in DN. Therefore, it is hoped through genome-wide analysis of high-throughput sequencing datasets that a better understanding of the role of TGF $\beta$  in cellular pathology in DN can be gained.

## 4.2. TGF $\beta$ induces gross disturbances to cellular function and signalling through genome wide mRNA dysregulation

In order to investigate the genome wide effects of TGF $\beta$ , high-throughput massively parallel sequencing was performed on mRNA from mouse MC and rat PTC. Cells were maintained in high glucose conditions and treated with 10ng/ml TGF $\beta$  for 72 hours.

### 4.2.1. Suitability of normalisation methods and treatment effectiveness

High throughput sequencing data from PTC were aligned to rat genomic build rn4 while data from mesangial cells were aligned to mouse genomic build mm9. Genes having, on average, fewer than 10 reads per million were considered to be background noise and removed from the datasets. The resultant per sample read count libraries are listed in Table 4-1 and indicate that sufficient sequencing depth was achieved for each sample. A total of 12402 genes were detected in PTC samples and 15332 were detected in MC samples. Of those detected in PTC, 887 were aligned to novel or predicted protein coding regions of the rat genome while there only 2 such contiguous sequences (contigs) detected in the MC samples. This reflects the greater annotation depth present in the mouse genome compared to that of the rat.

**Table 4-1 Summary data for mRNA-seq in PTC and MC.**

Listed are total genes identified and the number of contigs which were aligned to novel or predicted protein coding regions of the respective genomes.

		Cell type	
		PTC	MC
Reads	Samples		
	Control_1	1.58E+07	8.35E+06
	Control_2	1.41E+07	8.47E+06
	Control_3	1.58E+07	8.36E+06
	TGF $\beta$ _1	1.25E+07	9.75E+06
	TGF $\beta$ _2	1.27E+07	9.04E+06
TGF $\beta$ _3	1.33E+07	9.52E+06	
Genes	Total Genes	12402	15332
	Predicted Genes	887	2

Read counts were normalised and estimated utilising the *R* package, *edgeR* (160). Normalisation estimates relative abundance of a given mRNA to all others in a given sample through assignment of sample-specific normalisation factors taking into account the samples library size. By correcting for sequence abundance at both the sample and experimental level, read count bias due to sequence length and composition is essentially negated. Determination of variance in sequence detection levels against gene abundance is essential to accurately assess differential gene expression (180). Initially, negative binomial parameters are estimated including the common dispersion across all genes according to conditional maximum likelihood method and tag-wise dispersion utilising an empirical Bayes method based on weighted conditional maximum likelihood (160).

These are utilised to generate trended dispersion values predicting gene-wise dispersion based on sequence abundance. Dispersion values are plotted against the biological coefficient of variance (BCV) which is defined as the square root of the dispersion parameter under the negative binomial model. Read counts in PTC were seen to be more dispersed than those in MC, although this dispersion occurred over a much smaller range (Figure 4-1a, 4-1b). The greatest variation in both cell types is seen in genes with low read counts with those having high read counts possessing the lowest variation. Importantly, the trend in biological coefficient of variance was seen to converge upon the common dispersion value indicating that there are no outstanding effects of outliers in terms of sample-sample variation of any given gene/s (180).

Accuracy of the negative binomial generalised linear models utilised for read count normalisation is assessed via normally-distributed z-scores acquired from deviance statistics for the goodness of fit testing of the dispersion data (180). Z-scores are plotted against theoretical quantiles with the resultant quantile-quantile (QQ) plots indicating model accuracy (Figure 4-1c, 4-1d). Data from both MC and PTC follow an approximately normal distribution with variance of high count genes being over-estimated. This indicates variance in the sample is greater than that predicted by the utilised model and is preferable over under-estimation of variance.

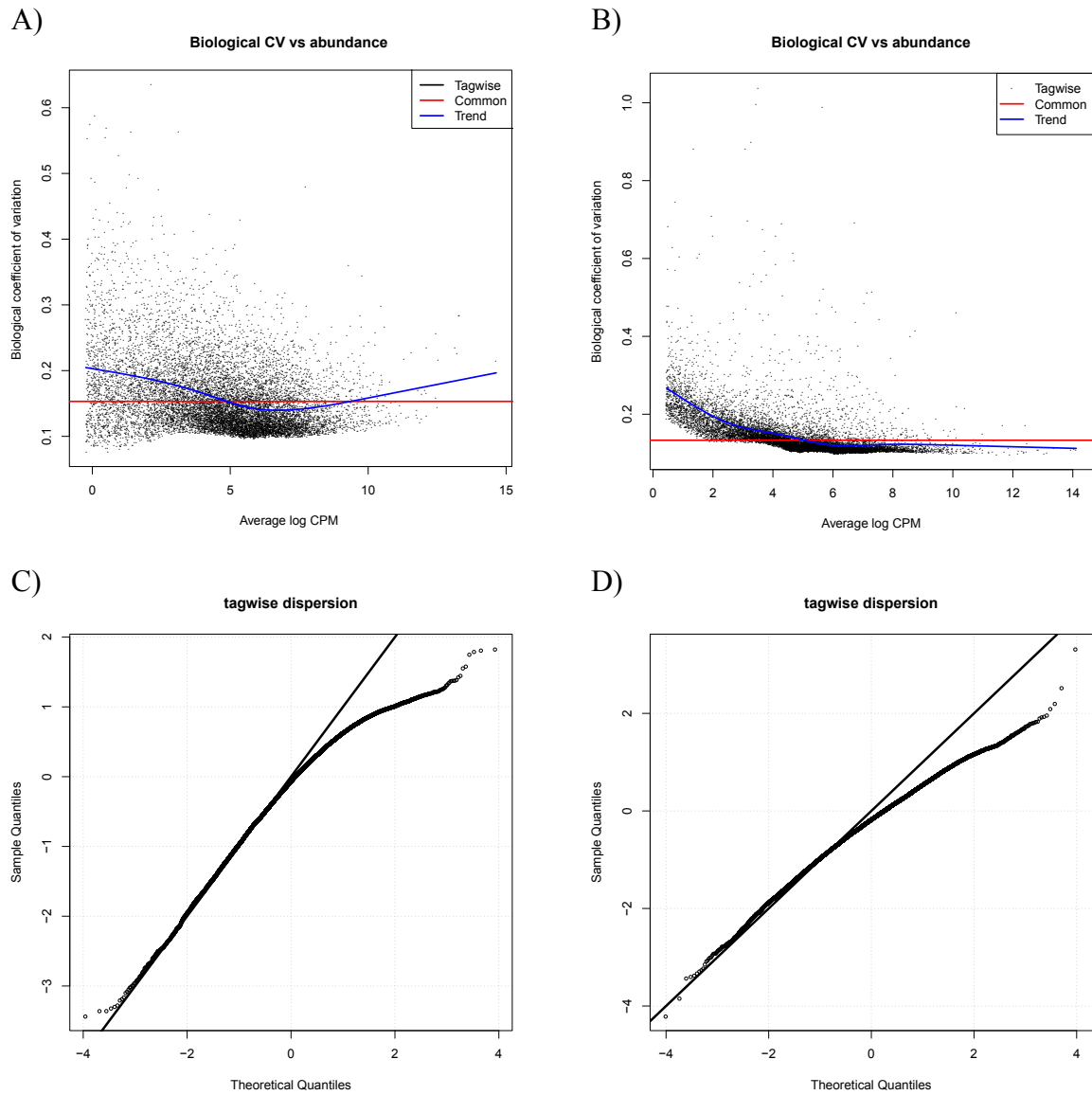


**Figure 4-1 Negative binomial models effectively estimated normalised read counts in mRNA-seq data from proximal tubule epithelial cells and mesangial cells.**

Trended biological coefficient of variance is seen to converge on the common dispersion as read log counts per million increases in both PTC (A) and MC (B) mRNA sequencing (mRNA-seq) data. Tag-wise dispersion is accurately estimated by the negative binomial model used in both PTC (C) and MC (D). Tag-wise dispersions were transformed to normality and plotted against theoretical quantiles.

log<sub>2</sub> transformation of the difference of log read counts per million (CPM) for each gene provides a measure of sample-sample vs. group-group similarity and can be represented in 2-dimensional space as a multi-dimensional scaling (MDS) plot (180). In both PTC (Figure 4-2a) and MC (Figure 4-2b), TGF $\beta$  induces a distinct phenotype as indicated by group separation on the x-axis. Control samples are similar to one another but slight variation in sample-wise *in vitro* micro-environments results in marginally different treatment samples. However, these differences are appropriately controlled for during normalisation as indicated by Figures 1b-d. Interestingly, response to TGF $\beta$  appears to be more severe in MC indicated by greater separation between TGF $\beta$ -treated and control samples in MC (Figure 4-2b) than in PTC (Figure 4-2a).

Following testing with the negative binomial generalised linear models, gene dysregulation is assessed by means of normalisation of gene-wise *p*-values generated from the above models. As with assessment of tag-wise dispersion, normalised *p*-value are plotted with a QQ plot (Figure 4-2c, 4-2d). Although the *p*-values can be transformed to approximate normality, it can be seen that they are grossly underestimated by the models. This is partly due to the large number of samples with near zero *p*-values, as indicated by the slope of the line-of-best-fit, but also because there are large, statistically significant changes occurring as a result of TGF $\beta$  treatment and also low read tags. This pattern is observed in both PTC and MC.

Finally, in order to assess the scale of experiment wide gene dysregulation, log<sub>2</sub> fold-change is plotted against read counts per million reads (Figure 4-2e, 4-2f). The resulting smear plots indicate that there is considerable dysregulation in both directions as indicated by spread around  $y = 0$ , but also considerable spread in gene detection levels as indicated by spread on the x axis. Genes being significantly dysregulated (false discovery rate (FDR) = 0.05) are coloured red and are seen to be dispersed across the range of tag abundances. There is considerable increase in the spread of log<sub>2</sub> fold-change (logFC) values at lower CPM values which is to be expected as a function of low level gene expression and/or detection which therefore amplifies statistical variation in detection.

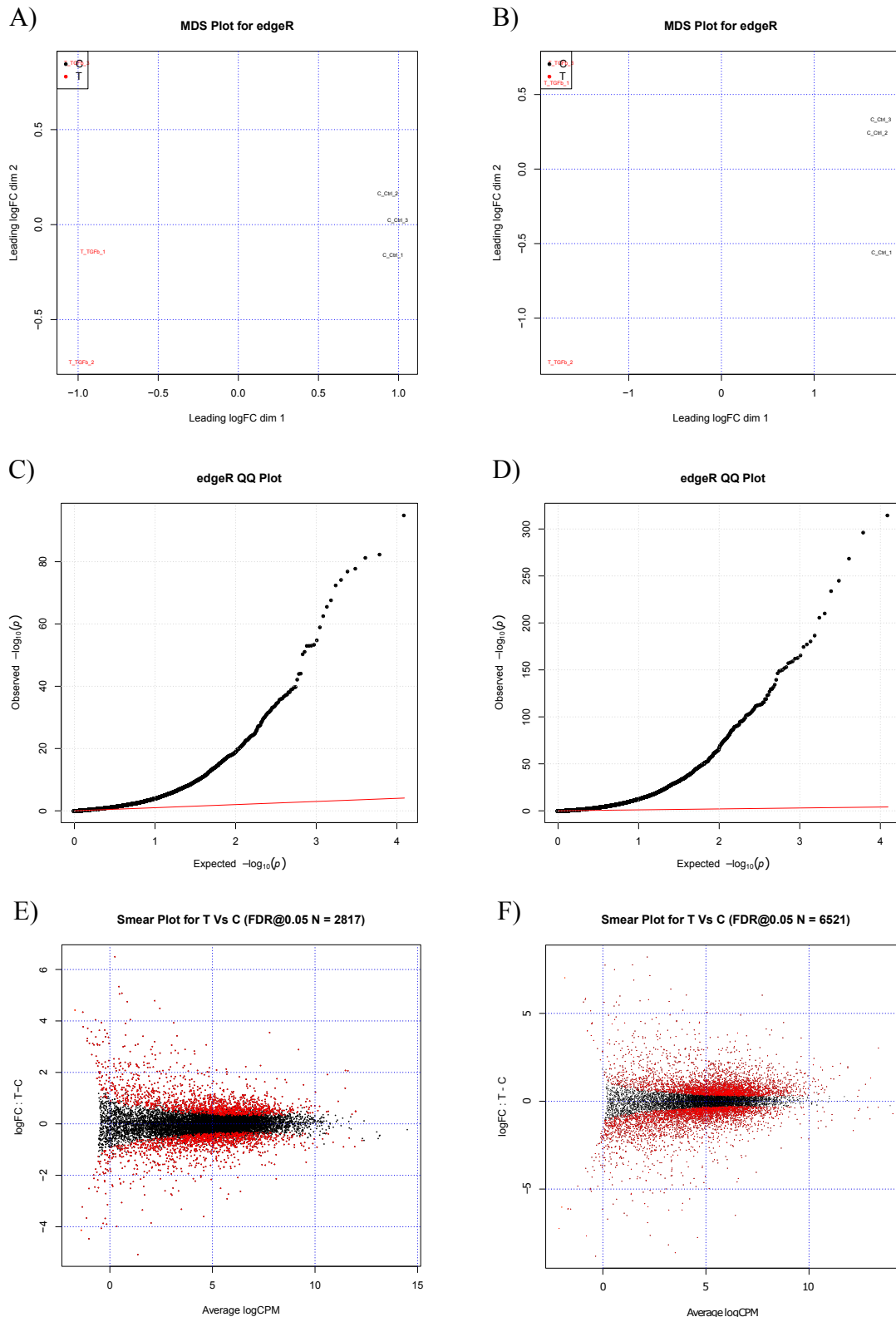


**Figure 5-2 TGF $\beta$  treatment induces significant short RNA dysregulation in both proximal tubule epithelial cells and mesangial cells.**

Multidimensional scaling (MDS) plots demonstrate TGF $\beta$  treatment induces a distinct phenotype in both PTC (A) and MC (B). p-values, although normally distributed against theoretical quantiles, were grossly under-estimated in PTC (C) and MC (D) due to a large number of near zero p-values. Smear plots highlight the distribution of significantly dysregulated genes in both PTC (E) and MC (F).

#### 4.2.2. Overview of common and cell-specific TGF $\beta$ -induced mRNA gene dysregulation in PTC and MC

The scale of TGF $\beta$ -induced gene dysregulation is illustrated in Figure 2. This dysregulation appears to be remarkably balanced in both PTC and MC in regard to directionality of dysregulation (Figure 4-3a, 4-3c). Furthermore, directionality of significantly dysregulated genes (adjusted  $p$ -value  $\leq 0.05$ ) are similarly balanced in both PTC and MC (Figure 4-3b, 4-3d). As indicated by Figure 2, the response of MC to TGF $\beta$  is greater than that of PTC with over 50% of all genes being dysregulated in MC compared to only 23% in PTC (Figure 4-3e, 4-3f).

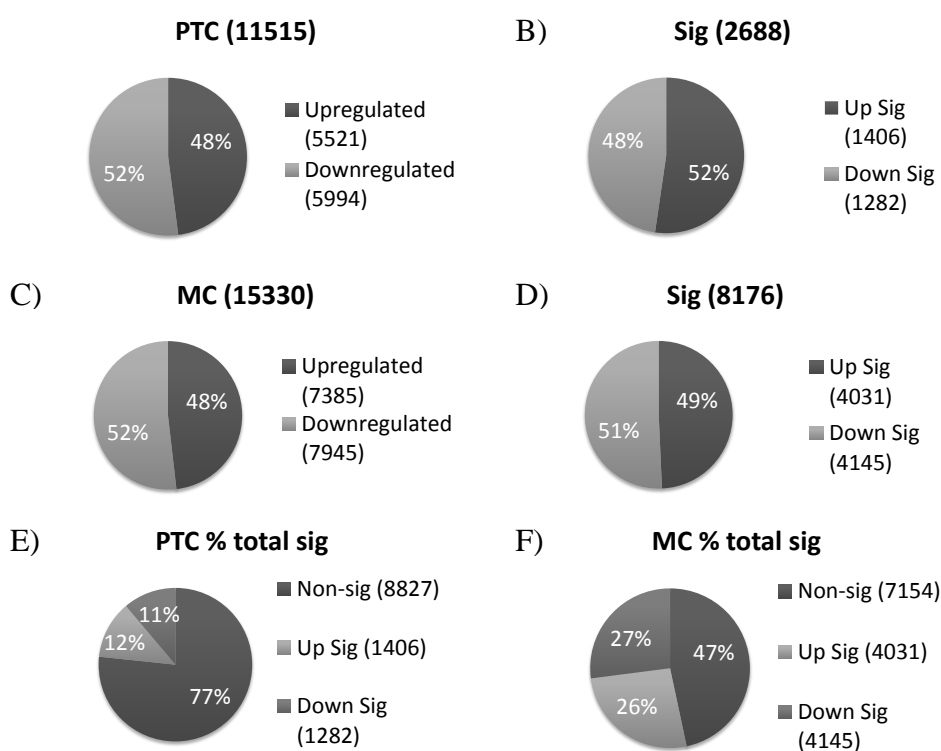


**Figure 4-3 Summary of TGF $\beta$ -induced gene dysregulation in proximal tubule epithelial cells and mesangial cells**

Proportion of total number of genes dysregulated in PTC (B) and MC (B) by TGF $\beta$ . Breakdown of significantly up and down regulated genes in PTC (C) and MC (D) tubule epithelial cells. Percentage of total detected genes which are significantly dysregulated by TGF $\beta$  in PTC (E) and MC (F).

~//Results2\_supp//Figure3\_supp

Considering the top 100 significantly dysregulated genes, balanced dysregulation is relatively preserved in MC (Figure 4-4). However, in PTC, there is a clear bias towards gene overexpression with 68% of the top 100 significantly dysregulated genes being unregulated by TGF $\beta$  treatment (Figure 4-5). Despite the wide reaching effects of TGF $\beta$  and its inherent role in fibrotic signalling, only two genes in the top 100 were found to be commonly upregulated in the two cell types while there were no genes commonly downregulated within this list (Figure 4-4, Figure 4-5). Both genes were detected at similar levels in both cell types with fibulin 2 (FBLN2) being dysregulated ~3.5 fold (log<sub>2</sub>) in both cell types whilst Serpine1/PAI1 was upregulated 2-fold (log<sub>2</sub>) higher than in PTC. Expanding comparative analysis to the genome-wide level, the scale of the core role of TGF $\beta$  in cellular physiology begins to become more apparent.

The mRNA-seq datasets were filtered against each other to allow direct comparison and to remove species and cell-type specific gene detection. Filtering resulted in new datasets containing 9704 genes, a number which would likely increase following reassembly of the PTC data to updated rat genome annotations. Of the commonly detected genes, ~40% were nonsignificantly up or downregulated with ~10% being significantly up or downregulated with these significantly dysregulated genes likely representing a core TGF $\beta$  target gene set (Figure 4-6a). Of the genes which were unique to either cell type, ~15% were significantly up or downregulated in PTC (Figure 4-6b). In MC, 30% of uniquely detected genes were significantly downregulated while 19% were significantly upregulated, a clear deviation from the balanced dysregulation seen at the genome wide level (Figure 4-6c). Finally, almost half of the 9702 genes commonly detected in both cell types were found to be inversely regulated between MC and PTC (Figure 4-6d). Although only 344 of these 4062 inversely regulated genes were significantly altered, this subset of genes highlights considerable cell specificity in the actions of TGF $\beta$ .

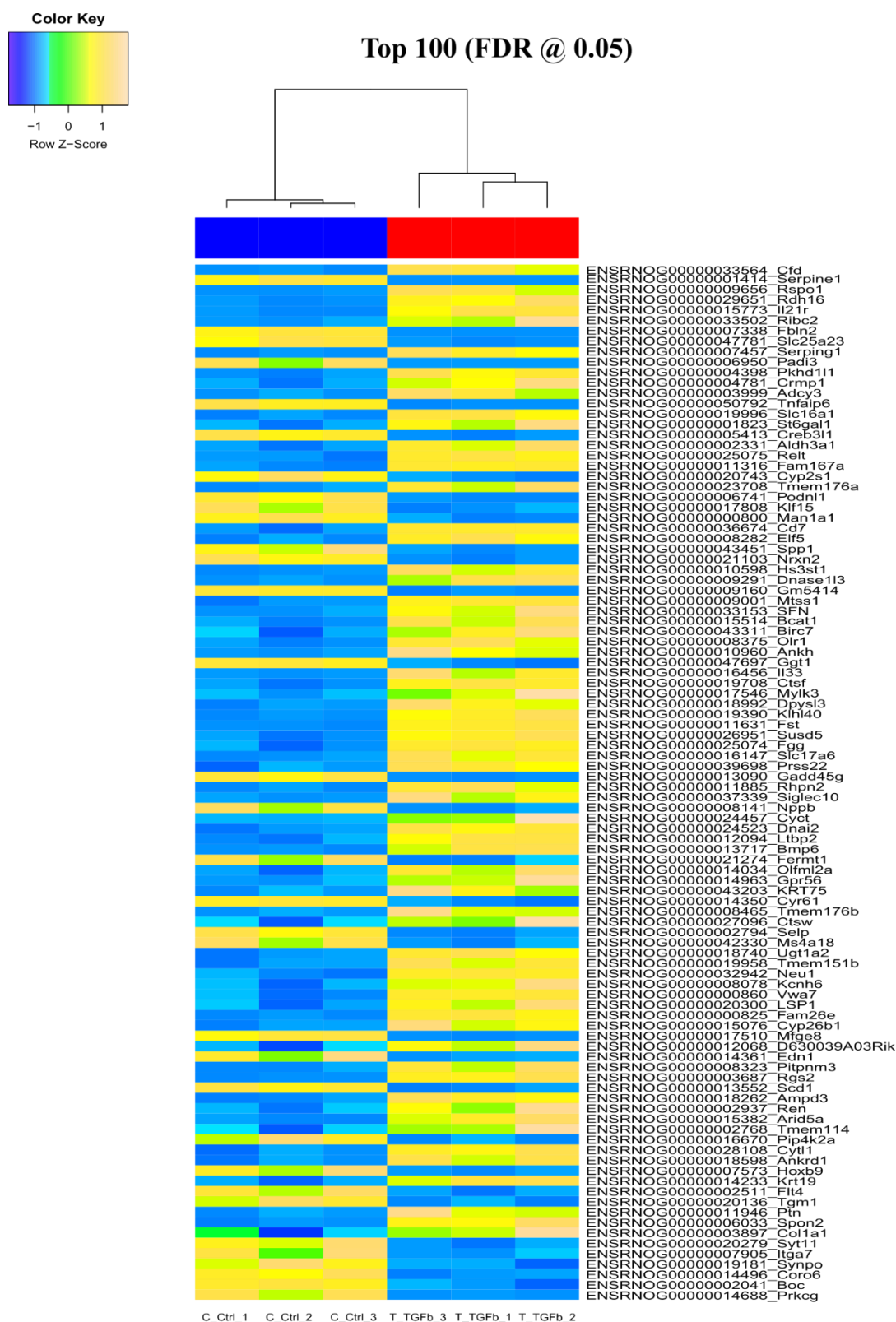


**Figure 4-4 Top 100 significantly dysregulated genes in proximal tubule epithelial cells.**

Blues indicate greater than 2-fold downregulation, dark yellows indicate greater than 2-fold upregulation, greens indicate  $\pm$  50% dysregulation. Genes are labelled with both Ensembl gene identifiers and official gene symbols.

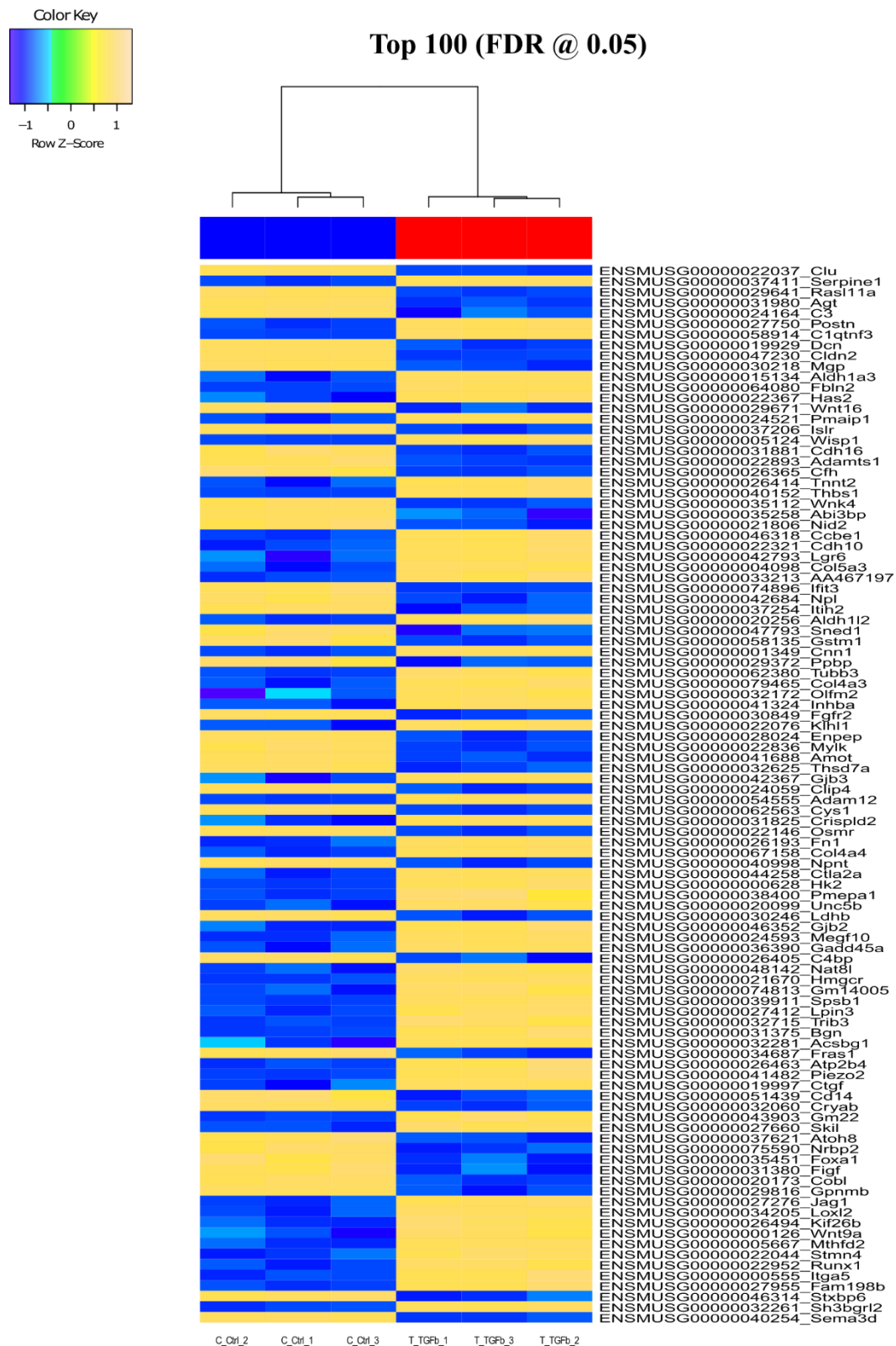


**Figure 4-5 Top 100 significantly dysregulated genes in mesangial cells.**

Dark blues indicate greater than 2-fold downregulation, dark yellows indicate greater than 2-fold upregulation, greens indicate  $\pm 50\%$  dysregulation. Genes are labelled with both Ensembl gene identifiers and official gene symbols.

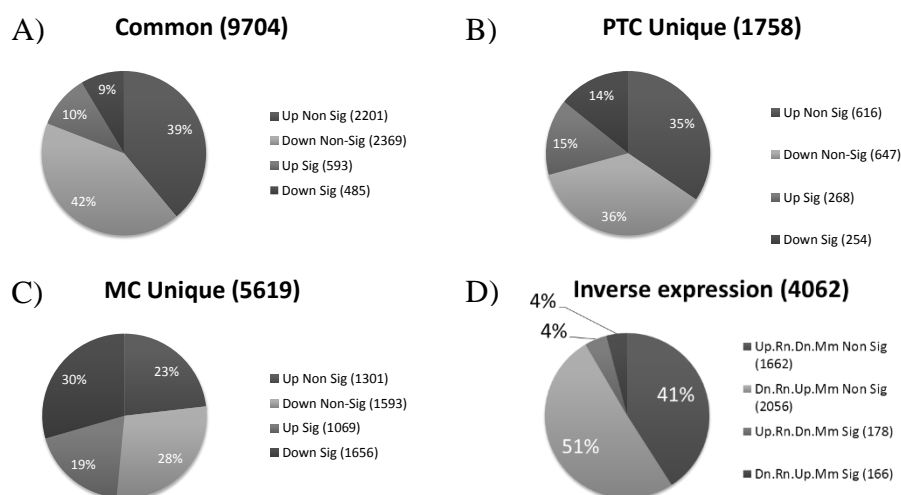


**Figure 4-6: Comparative summary of TGF $\beta$ -induced gene dysregulation in proximal tubule epithelial cells and mesangial cells**

A) Proportions of genes which were commonly dysregulated in PTC and MC. B) Breakdown of genes which were detected in PTC and not MC. C) Breakdown of genes which were detected in MC and PTC. D) Genes which were commonly detected between cell types and were inversely expressed between PTC (Rn) and MC (Mm). [~//Results2\\_supp//Figure6\\_supp](#)

### 4.3. Potential functional consequences of TGF $\beta$ induced gene dysregulation

#### 4.3.1. An ontological perspective of common and cell specific effects of TGF $\beta$

Ontology analysis was performed using the *R* package *gage*, in addition to a number of extension packages and datasets (163, 164, 166, 167, 171). Commonly detected genes were enriched for upregulation of a number of molecular function gene ontology (MF) terms including growth factor receptor binding and growth factor activity along with a number of terms associated with nucleoside and nucleoside derivative binding (Table 4-2). This data subset was also enriched for downregulation of various MF terms including protein complex formation and phosphatase activity (Table 4-2). Of particular interest, the commonly dysregulated genes were associated with a number of ontology groups which were enriched for both upregulated and downregulated genes concerned with various binding processes including extracellular matrix binding, receptor binding and activity and growth factor binding (Table 4-2).

**Table 4-2 Genes commonly dysregulated in PTC and MC were enriched for a number of molecular function ontology terms.**

~/Results2\_supp/Table2\_supp

Molecular Function gene ontology term	p.val	q.val	set.size	enrichment
GO:0070851 growth factor receptor binding	5.18E-02	7.72E-01	14	up
GO:0001883 purine nucleoside binding	8.77E-02	7.72E-01	119	up
GO:0008092 cytoskeletal protein binding	8.79E-02	7.72E-01	53	up
GO:0001882 nucleoside binding	9.39E-02	7.72E-01	120	up
GO:0032549 ribonucleoside binding	9.58E-02	7.72E-01	118	up
GO:0032550 purine ribonucleoside binding	9.58E-02	7.72E-01	118	up
GO:0035639 purine ribonucleoside triphosphate binding	9.58E-02	7.72E-01	118	up
GO:0008083 growth factor activity	9.84E-02	7.72E-01	13	up
GO:0008270 zinc ion binding	3.11E-02	9.18E-01	96	down
GO:0003676 nucleic acid binding	4.41E-02	9.18E-01	153	down
GO:0004721 phosphoprotein phosphatase activity	6.17E-02	9.18E-01	13	down
GO:0046914 transition metal ion binding	6.62E-02	9.18E-01	111	down
GO:0016791 phosphatase activity	6.78E-02	9.18E-01	19	down
GO:0003677 DNA binding	6.81E-02	9.18E-01	110	down
GO:0042578 phosphoric ester hydrolase activity	7.30E-02	9.18E-01	23	down
GO:0033218 amide binding	7.40E-02	9.18E-01	17	down
GO:0042277 peptide binding	7.40E-02	9.18E-01	17	down
GO:0003723 RNA binding	8.92E-02	9.18E-01	40	down
GO:0046983 protein dimerization activity	8.94E-02	9.18E-01	84	down
GO:0046982 protein heterodimerization activity	9.69E-02	9.18E-01	38	down
GO:0005539 glycosaminoglycan binding	2.42E-04	4.09E-02	25	bidir
GO:0097367 carbohydrate derivative binding	6.70E-04	4.26E-02	28	bidir
GO:0008201 heparin binding	9.23E-04	4.26E-02	21	bidir
GO:1901681 sulfur compound binding	1.01E-03	4.26E-02	27	bidir
GO:0019838 growth factor binding	1.09E-02	3.68E-01	18	bidir
GO:0050840 extracellular matrix binding	2.16E-02	5.80E-01	10	bidir
GO:0005509 calcium ion binding	2.40E-02	5.80E-01	44	bidir
GO:0008237 metalloproteinase activity	2.76E-02	5.84E-01	12	bidir
GO:0008083 growth factor activity	4.75E-02	8.51E-01	13	bidir
GO:0070011 peptidase activity, acting on L-amino acid peptides	5.03E-02	8.51E-01	25	bidir
GO:0005515 protein binding	5.72E-02	8.79E-01	486	bidir
GO:0004872 receptor activity	7.38E-02	9.68E-01	53	bidir
GO:0005102 receptor binding	9.07E-02	9.68E-01	110	bidir

Over 110 biological process gene ontology (BP) terms related to cell growth/cycle, ion transport and biosynthetic processes were enriched for upregulated genes (Table 4-3). Conversely, BP terms enriched for downregulated genes were primarily associated with protein transport and secretion in addition to chromatin and chromosomal organisation. However, a considerable number of catabolic functions were also identified (Table 4-3). Over 220 BP terms were bidirectionally enriched with the most significant terms being associated with adhesion and developmental processes (Table 4-3). Collectively, enriched MF and BP terms demonstrate that the role TGF $\beta$  plays in diabetic nephropathy extends well beyond classical fibrotic signalling and instead impacts on a vast array of core cellular processes in PTC and MC.

**Table 4-3 Genes commonly dysregulated in PTC and MC were enriched for a number of biological process ontology terms.**

~//Results2\_supp//Table3\_supp

Biological Process gene ontology term	p.val	q.val	set.size	enrichment
GO:0044283 small molecule biosynthetic process	6.89E-03	7.19E-01	42	up
GO:0008610 lipid biosynthetic process	6.91E-03	7.19E-01	38	up
GO:0044711 single-organism biosynthetic process	1.13E-02	7.19E-01	43	up
GO:0043542 endothelial cell migration	1.25E-02	7.19E-01	13	up
GO:0006816 calcium ion transport	1.25E-02	7.19E-01	23	up
GO:0006812 cation transport	1.31E-02	7.19E-01	52	up
GO:0051726 regulation of cell cycle	1.34E-02	7.19E-01	59	up
GO:0070838 divalent metal ion transport	1.49E-02	7.19E-01	25	up
GO:0072511 divalent inorganic cation transport	1.49E-02	7.19E-01	25	up
GO:0031401 positive regulation of protein modification process	1.67E-02	7.19E-01	55	up
GO:0000075 cell cycle checkpoint	1.84E-02	7.19E-01	14	up
GO:0015833 peptide transport	2.18E-02	9.90E-01	15	down
GO:0042886 amide transport	2.18E-02	9.90E-01	15	down
GO:0002790 peptide secretion	2.72E-02	9.90E-01	14	down
GO:0030072 peptide hormone secretion	2.72E-02	9.90E-01	14	down
GO:0016311 dephosphorylation	2.92E-02	9.90E-01	26	down
GO:0051276 chromosome organization	3.44E-02	9.90E-01	34	down
GO:0060271 cilium morphogenesis	3.56E-02	9.90E-01	10	down
GO:0006325 chromatin organization	4.18E-02	9.90E-01	29	down
GO:0016568 chromatin modification	4.18E-02	9.90E-01	29	down
GO:0050778 positive regulation of immune response	4.19E-02	9.90E-01	20	down
GO:0002791 regulation of peptide secretion	4.83E-02	9.90E-01	11	down
GO:0007155 cell adhesion	1.19E-03	3.04E-01	86	bidir
GO:0022610 biological adhesion	1.19E-03	3.04E-01	86	bidir
GO:0031214 biomineral tissue development	1.71E-03	3.04E-01	13	bidir
GO:0001568 blood vessel development	1.98E-03	3.04E-01	59	bidir
GO:0009888 tissue development	2.30E-03	3.04E-01	118	bidir
GO:0051216 cartilage development	2.60E-03	3.04E-01	24	bidir
GO:0001503 ossification	2.62E-03	3.04E-01	37	bidir
GO:0044707 single-multicellular organism process	2.62E-03	3.04E-01	341	bidir
GO:0001944 vasculature development	2.84E-03	3.04E-01	61	bidir
GO:0030282 bone mineralization	2.95E-03	3.04E-01	12	bidir
GO:0032501 multicellular organismal process	3.54E-03	3.04E-01	345	bidir
GO:0072358 cardiovascular system development	3.57E-03	3.04E-01	82	bidir

A number of MF terms were uniquely enriched for upregulated genes in MC which were concerned with binding of cyclic compounds and adenyly nucleotides and their derivatives (Table 4-4). Over 50% of MF terms uniquely enriched for downregulated genes in MC were concerned with peptide activity and regulation (Table 4-4). The most significant bidirectionally enriched MF terms unique to MC were primarily related to signal transduction highlighting the impact of TGF $\beta$  as a major player in cell signalling. Interestingly, no MF terms were found to be uniquely enriched in PTC despite the specialised role that these cells play in renal physiology. This may be a consequence of genomic annotation rather than a lack of unique molecular functional effects of TGF $\beta$  or merely a lack of MF terms which capture the unique biology of PTC.

**Table 4-4 Genes uniquely dysregulated in MC were uniquely enriched for a number of molecular function ontology terms.**

~//Results2\_supp//Table4\_supp

MolecularFunction gene ontology terms	p.val	q.val	se	tsize	unique to	enrichment
GO:0008234 cysteine-type peptidase activity	1.87E-02	6.10E-01	11	MC	up	
GO:1901363 heterocyclic compound binding	2.63E-02	6.10E-01	360	MC	up	
GO:0019901 protein kinase binding	2.75E-02	6.10E-01	35	MC	up	
GO:0097159 organic cyclic compound binding	2.85E-02	6.10E-01	368	MC	up	
GO:0003676 nucleic acid binding	4.60E-02	6.10E-01	184	MC	up	
GO:0019900 kinase binding	5.78E-02	6.10E-01	37	MC	up	
GO:0003677 DNA binding	6.76E-02	6.10E-01	144	MC	up	
GO:0016790 thiolester hydrolase activity	6.92E-02	6.10E-01	10	MC	up	
GO:0016874 ligase activity	6.95E-02	6.10E-01	29	MC	up	
GO:0030554 adenylyl nucleotide binding	8.73E-02	6.10E-01	121	MC	up	
GO:0032559 adenylyl ribonucleotide binding	8.73E-02	6.10E-01	121	MC	up	
GO:0005524 ATP binding	8.84E-02	6.10E-01	119	MC	up	
GO:0061135 endopeptidase regulator activity	3.10E-02	9.62E-01	18	MC	down	
GO:0004866 endopeptidase inhibitor activity	5.66E-02	9.62E-01	17	MC	down	
GO:0030414 peptidase inhibitor activity	5.66E-02	9.62E-01	17	MC	down	
GO:0004857 enzyme inhibitor activity	6.59E-02	9.62E-01	25	MC	down	
GO:0030165 PDZ domain binding	7.58E-02	9.62E-01	18	MC	down	
GO:0061134 peptidase regulator activity	7.86E-02	9.62E-01	21	MC	down	
GO:0005088 Ras guanyl-nucleotide exchange factor activity	9.00E-02	9.62E-01	10	MC	down	
GO:0004867 serine-type endopeptidase inhibitor activity	9.12E-02	9.62E-01	11	MC	down	
GO:0004879 ligand-activated sequence-specific DNA binding RNA polymerase II transcription factor activity	9.72E-02	9.62E-01	11	MC	down	
GO:0061135 endopeptidase regulator activity	5.04E-04	3.77E-02	18	MC	bidir	
GO:0061134 peptidase regulator activity	5.69E-04	3.77E-02	21	MC	bidir	
GO:0004888 transmembrane signaling receptor activity	1.31E-03	3.82E-02	93	MC	bidir	
GO:0038023 signaling receptor activity	1.59E-03	4.05E-02	106	MC	bidir	
GO:0004857 enzyme inhibitor activity	4.87E-03	1.10E-01	25	MC	bidir	
GO:0004871 signal transducer activity	1.19E-02	1.76E-01	132	MC	bidir	
GO:0060089 molecular transducer activity	1.19E-02	1.76E-01	132	MC	bidir	
GO:0004867 serine-type endopeptidase inhibitor activity	1.23E-02	1.76E-01	11	MC	bidir	
GO:0005261 cation channel activity	1.33E-02	1.76E-01	27	MC	bidir	
GO:0015267 channel activity	1.38E-02	1.76E-01	40	MC	bidir	

Conversely, a wide array of BP terms were uniquely enriched in both cell types, some of which are indicative of unique cellular physiology (Table 4-5). In PTC, terms related to epithelium development and epithelial cell differentiation were enriched for upregulated genes while MC, which possess a smooth muscle cell-like phenotype, returned a number of muscle specific BP terms (20). BP terms uniquely enriched for downregulated genes including stress-activated MAPK cascade in MC and immune response in PTC, may indicate an attempt to preserve normal cellular biology in response to TGF $\beta$ . Also, BP terms enriched for both up and downregulated genes, at least in the case of PTC, appear to also be relevant to specific cell-type biology with terms related to the biosynthesis and processing of organic nitrogen compounds being detected (181).

**Table 4-5 Genes uniquely dysregulated in either PTC or MC were uniquely enriched for a number of *biological process* ontology terms.**

~/Results2\_supp/Table5\_supp

Biological Process gene ontology term	p.val	q.val	set.size	unique to	enrichment
GO:0008285 negative regulation of cell proliferation	3.02E-02	7.68E-01	11	PTC	up
GO:0030855 epithelial cell differentiation	6.21E-02	7.68E-01	11	PTC	up
GO:1901361 organic cyclic compound catabolic process	6.56E-02	7.68E-01	16	PTC	up
GO:0046700 heterocycle catabolic process	7.59E-02	7.68E-01	15	PTC	up
GO:0060429 epithelium development	9.83E-02	7.68E-01	17	PTC	up
GO:0007517 muscle organ development	1.56E-04	1.84E-01	35	MC	up
GO:0061061 muscle structure development	1.81E-03	4.65E-01	45	MC	up
GO:0014706 striated muscle tissue development	2.57E-03	4.65E-01	36	MC	up
GO:0060537 muscle tissue development	2.90E-03	4.65E-01	37	MC	up
GO:0044087 regulation of cellular component biogenesis	4.69E-03	4.65E-01	39	MC	up
GO:0003012 muscle system process	3.96E-02	8.89E-01	10	PTC	down
GO:0032940 secretion by cell	5.50E-02	8.89E-01	16	PTC	down
GO:0006955 immune response	6.53E-02	8.89E-01	20	PTC	down
GO:0055114 oxidation-reduction process	6.77E-02	8.89E-01	12	PTC	down
GO:0046903 secretion	7.02E-02	8.89E-01	17	PTC	down
GO:0050878 regulation of body fluid levels	3.53E-02	9.98E-01	19	MC	down
GO:0051403 stress-activated MAPK cascade	3.99E-02	9.98E-01	15	MC	down
GO:0031098 stress-activated protein kinase signaling cascade	4.89E-02	9.98E-01	16	MC	down
GO:0001101 response to acid	5.92E-02	9.98E-01	11	MC	down
GO:0009755 hormone-mediated signaling pathway	6.65E-02	9.98E-01	12	MC	down
GO:1901566 organonitrogen compound biosynthetic process	3.77E-02	7.24E-01	14	PTC	bidir
GO:1901564 organonitrogen compound metabolic process	4.98E-02	7.24E-01	38	PTC	bidir
GO:1901137 carbohydrate derivative biosynthetic process	7.39E-02	7.24E-01	11	PTC	bidir
GO:0009987 cellular process	7.49E-02	7.24E-01	230	PTC	bidir
GO:0044763 single-organism cellular process	8.15E-02	7.24E-01	187	PTC	bidir
GO:0044765 single-organism transport	8.34E-04	1.23E-01	222	MC	bidir
GO:0051049 regulation of transport	8.64E-04	1.23E-01	111	MC	bidir
GO:0065008 regulation of biological quality	1.72E-03	1.23E-01	220	MC	bidir
GO:0007186 G-protein coupled receptor signaling pathway	2.35E-03	1.38E-01	80	MC	bidir
GO:0006955 immune response	2.61E-03	1.39E-01	78	MC	bidir

The inversely dysregulated gene subset yielded no MF terms enriched in downregulated genes (Table 4-6). Furthermore, few terms were either bidirectionally enriched or enriched for upregulated genes, with those that were returned having been previously identified in common and cell specific gene sets. Conversely, BP ontology analysis returned considerably more terms across all enrichment types with many related to cell-type pathology in DN (Table 4-7). Terms including cell morphogenesis, cytoskeletal rearrangement, cell motility and cell localization, all of which are involved in the EMT-like phenotype were detected in PTC (49). In MC, terms associated with cell differentiation, evasion of programmed cell death and apoptosis and downregulation of phosphorylation machinery were detected and are related to the process of mesangial expansion and MC proliferation leading to glomerulosclerosis (182).

**Table 4-6 Genes inversely expressed between PTC and MC were uniquely enriched for a number of molecular function ontology terms.**

~//Results2\_supp//Table6\_supp

Molecular Function gene ontology term	p.val	q.val	set.size	unique to	enrichment
GO:0004872 receptor activity	2.88E-02	7.86E-01	16	PTC	up
GO:0038023 signaling receptor activity	8.85E-02	7.86E-01	12	PTC	up
GO:0042803 protein homodimerization activity	7.66E-02	8.06E-01	12	MC	up
GO:0005083 small GTPase regulator activity	8.04E-02	8.06E-01	12	MC	up
GO:0022891 substrate-specific transmembrane transporter activity	9.95E-02	9.35E-01	11	PTC	bidir

**Table 4-7 Genes inversely expressed between PTC and MC were uniquely enriched for a number of biological process ontology terms.**

~//Results2\_supp//Table7\_supp

Biological Process gene ontology term	p.val	q.val	set.size	unique to	enrichment
GO:0044702 single organism reproductive process	2.88E-02	7.86E-01	16	PTC	up
GO:0000003 reproduction	8.85E-02	7.86E-01	12	PTC	up
GO:0022414 reproductive process	7.66E-02	8.06E-01	12	PTC	up
GO:0000904 cell morphogenesis involved in differentiation	8.04E-02	8.06E-01	12	PTC	up
GO:0051239 regulation of multicellular organismal process	9.95E-02	9.35E-01	11	PTC	up
GO:0046578 regulation of Ras protein signal transduction	2.59E-02	8.55E-01	11	MC	up
GO:0001933 negative regulation of protein phosphorylation	3.11E-02	8.55E-01	11	MC	up
GO:0010563 negative regulation of phosphorus metabolic process	3.11E-02	8.55E-01	11	MC	up
GO:0031400 negative regulation of protein modification process	3.11E-02	8.55E-01	11	MC	up
GO:0042326 negative regulation of phosphorylation	3.11E-02	8.55E-01	11	MC	up
GO:0030029 actin filament-based process	5.89E-02	9.55E-01	12	PTC	down
GO:0030036 actin cytoskeleton organization	5.89E-02	9.55E-01	12	PTC	down
GO:1901135 carbohydrate derivative metabolic process	8.29E-02	9.55E-01	27	PTC	down
GO:0045597 positive regulation of cell differentiation	6.72E-02	9.09E-01	15	MC	down
GO:0000904 cell morphogenesis involved in differentiation	8.40E-02	9.09E-01	16	MC	down
GO:0043066 negative regulation of apoptotic process	8.61E-02	9.09E-01	19	MC	down
GO:0043069 negative regulation of programmed cell death	8.61E-02	9.09E-01	19	MC	down
GO:0010817 regulation of hormone levels	9.35E-02	9.09E-01	11	MC	down
GO:0006952 defense response	1.07E-02	8.33E-01	16	PTC	bidir
GO:0006928 cellular component movement	2.91E-02	8.33E-01	27	PTC	bidir
GO:0048870 cell motility	2.91E-02	8.33E-01	27	PTC	bidir
GO:0051674 localization of cell	2.91E-02	8.33E-01	27	PTC	bidir
GO:0032879 regulation of localization	2.96E-02	8.33E-01	26	PTC	bidir
GO:0045597 positive regulation of cell differentiation	2.25E-02	7.42E-01	15	MC	bidir
GO:0007155 cell adhesion	3.06E-02	7.42E-01	29	MC	bidir
GO:0022610 biological adhesion	3.06E-02	7.42E-01	29	MC	bidir
GO:0043066 negative regulation of apoptotic process	4.27E-02	7.42E-01	19	MC	bidir
GO:0043069 negative regulation of programmed cell death	4.27E-02	7.42E-01	19	MC	bidir

TGF $\beta$  is considered to primarily mediate fibrosis through canonical signalling pathways leading to overexpression and accumulation of ECM products and decreased production of ECM turnover machinery (183). However, it is apparent from these datasets that there are few cellular processes which are unaffected by TGF $\beta$ . Furthermore, although TGF $\beta$  induces gross genome gene expression changes, it also exhibits a considerable degree of cell specificity in its actions against cellular processes and molecular functions. It stands to reason that these changes would be observable from a pathway perspective, just as they have been observable from the broad stroke gene ontology perspective above.

#### **4.3.2. A pathway orientated perspective of common and cell-specific effects of TGF $\beta$**

Conceptually, pathways and their processes encapsulate gene functions and by extension may contain various gene ontology groups within a single pathway. Whole genome, pathway orientated analysis of TGF $\beta$ -induced differential gene expression was performed on mRNA-seq data from PTC and MC. Pathway analysis was performed using *gage* and, as was seen with gene ontology analysis, there are a number of common and cell-specific pathways which are altered by TGF $\beta$  (Figure 4-7, Figure 4-8). Furthermore, in contrast to the directionally balanced dysregulation seen at the gene level in both cell types, there is a clear and inverse bias in the directionality of pathway specific enrichment. In PTC, significantly enriched pathways are dominated by downregulated genes (Figure 4-7) and MC significantly enriched pathways are dominated by upregulated genes (Figure 4-8). Despite this, there are a core set of pathways which are commonly enriched by TGF $\beta$ -mediated gene dysregulation (Table 4-8).

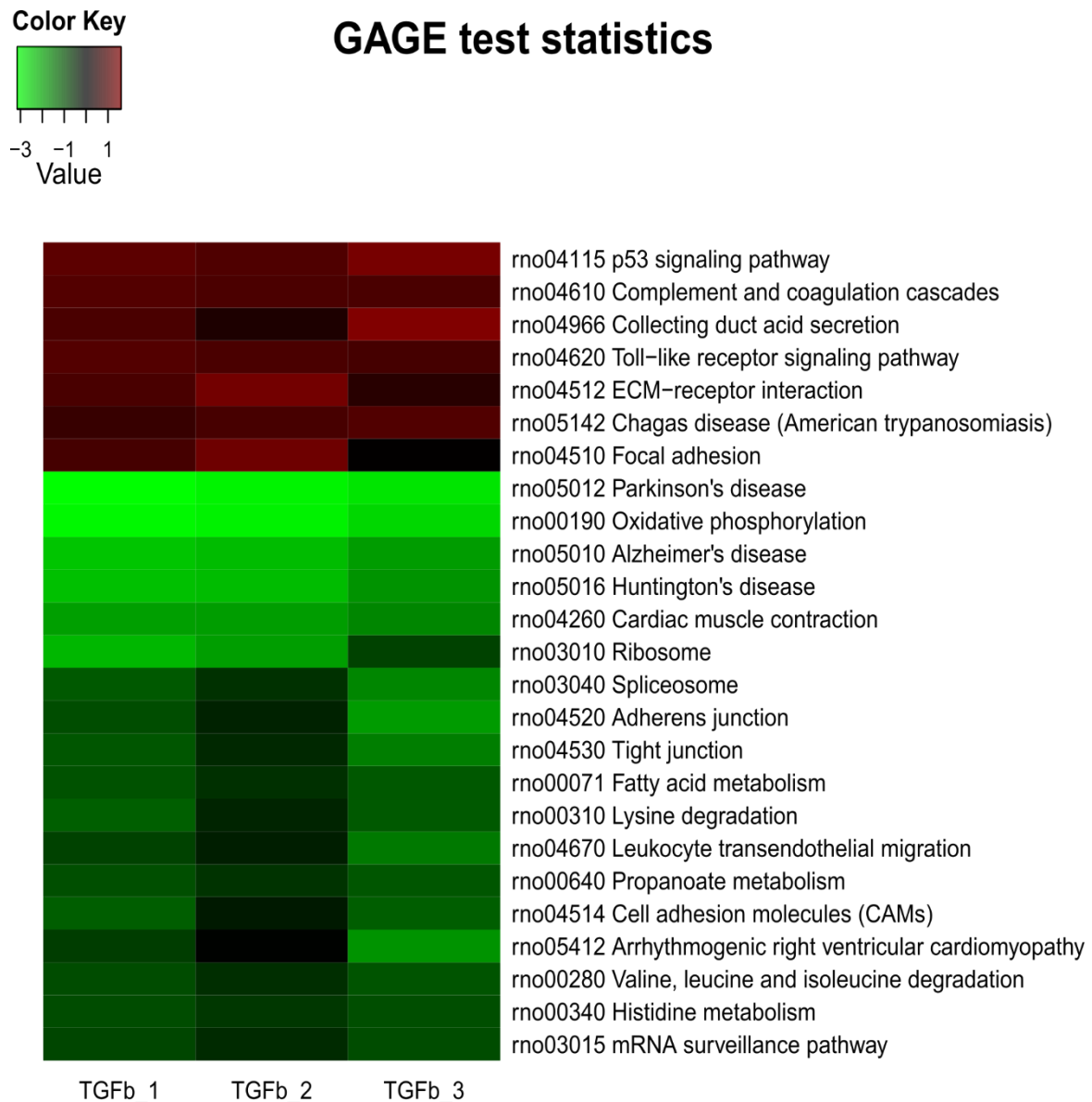


**Figure 4-7 TGF $\beta$  preferentially downregulates pathways in proximal tubule epithelial cells.**

Heat map representation of positively (red) and negatively (green) enriched pathways as detected by Gage analysis of mRNA-seq data from proximal tubule epithelial cells.

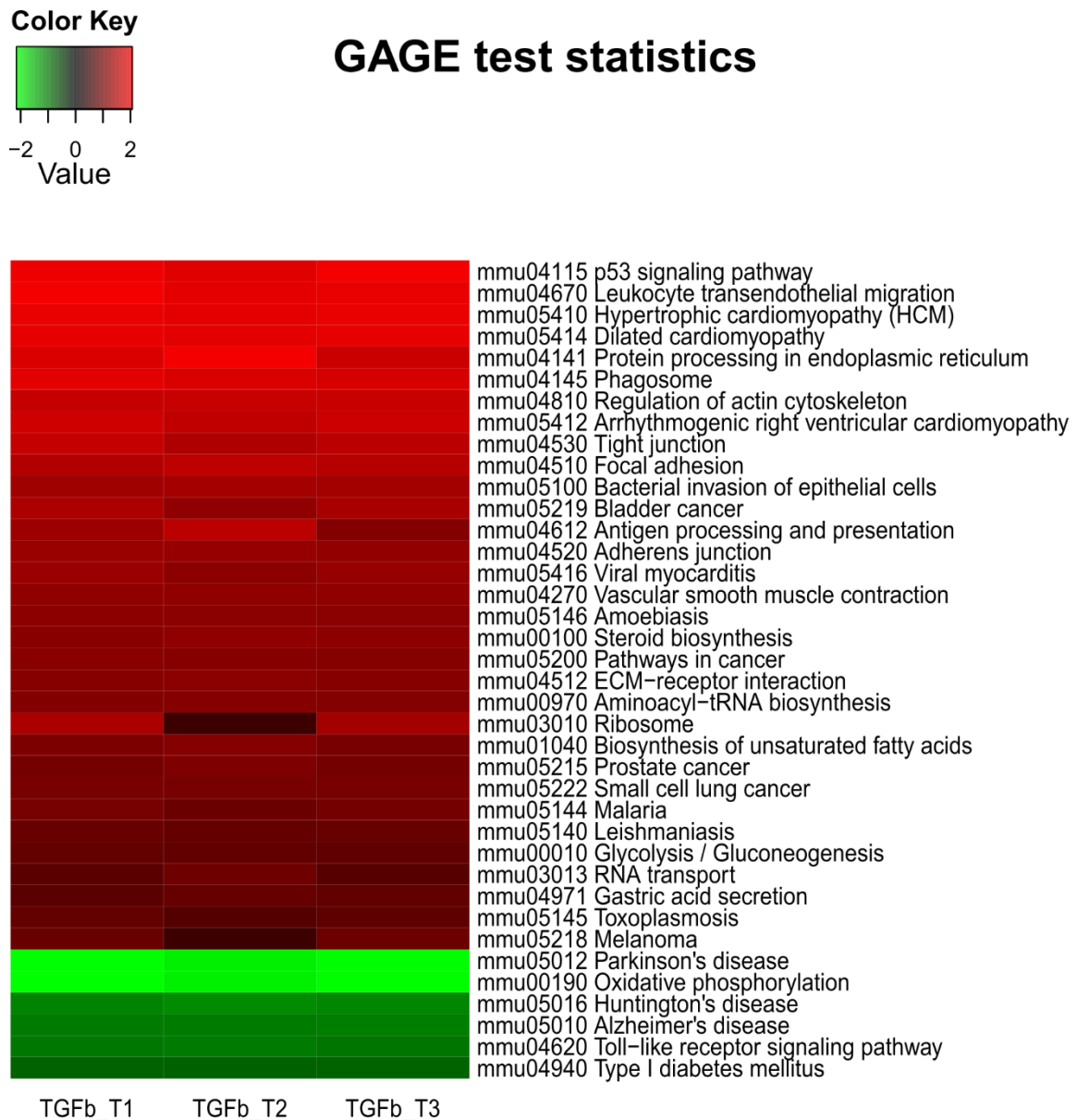


**Figure 4-8 TGF $\beta$  preferentially upregulates pathways in mesangial cells.**

Heat map representation of positively (red) and negatively (green) enriched pathways as detected by gage analysis of mRNA-seq data from mesangial cells.

**Table 4-8 Results of KEGG pathway analysis on proximal tubule epithelial cells and mesangial cells.**

The listed pathways were detected in both PTC and MC and also dysregulated in the same direction and are sourced from Kyoto encyclopaedia of genes and genomes (KEGG).  
 ~//Results2\_supp//Table8\_supp

path ID	Name	p.val (MC)	q.val (MC)	set.size (MC)	p.val (PTC)	q.val (PTC)	set.size (PTC)	enrichment
4115	p53 signaling pathway	3.43E-04	2.55E-02	62	1.97E-02	8.66E-01	48	up
4510	Focal adhesion	4.05E-03	7.94E-02	169	9.86E-02	8.66E-01	120	up
4512	ECM-receptor interaction	2.48E-02	2.43E-01	70	5.44E-02	8.66E-01	39	up
190	Oxidative phosphorylation	1.69E-04	1.66E-02	106	4.64E-07	4.34E-05	103	down
5010	Alzheimer's disease	3.65E-02	9.68E-01	135	7.34E-05	4.57E-03	122	down
5012	Parkinson's disease	1.64E-04	1.66E-02	103	2.17E-07	4.07E-05	101	down
5016	Huntington's disease	2.52E-02	9.68E-01	149	1.09E-04	5.08E-03	131	down
3010	Ribosome	2.85E-02	2.54E-01	65	7.33E-03	1.14E-01	58	bidir
4115	p53 signaling pathway	3.43E-04	2.55E-02	62	4.95E-02	3.94E-01	48	bidir
4141	Protein processing in endoplasmic reticulum	6.64E-04	2.55E-02	154	1.00E-02	1.40E-01	134	bidir
4145	Phagosome	7.81E-04	2.55E-02	99	2.94E-02	2.89E-01	87	bidir
4510	Focal adhesion	4.05E-03	7.94E-02	169	1.16E-04	4.35E-03	120	bidir
4512	ECM-receptor interaction	2.48E-02	2.43E-01	70	1.70E-04	5.29E-03	39	bidir
4514	Cell adhesion molecules (CAMs)	1.05E-01	5.85E-01	57	9.14E-02	5.11E-01	53	bidir
4520	Adherens junction	1.51E-02	2.12E-01	66	4.57E-02	3.89E-01	52	bidir
4530	Tight junction	3.73E-03	7.94E-02	93	2.89E-02	2.89E-01	77	bidir
4612	Antigen processing and presentation	1.18E-02	1.78E-01	36	8.82E-02	5.11E-01	36	bidir
4670	Leukocyte transendothelial migration	3.58E-04	2.55E-02	75	1.82E-02	2.13E-01	58	bidir
4810	Regulation of actin cytoskeleton	2.05E-03	5.04E-02	163	1.13E-02	1.40E-01	127	bidir
4971	Gastric acid secretion	8.09E-02	5.29E-01	47	9.57E-02	5.11E-01	30	bidir
4974	Protein digestion and absorption	1.20E-01	5.86E-01	44	4.34E-03	7.37E-02	37	bidir
5100	Bacterial invasion of epithelial cells	9.90E-03	1.69E-01	60	1.05E-02	1.40E-01	51	bidir
5142	Chagas disease (American trypanosomiasis)	1.04E-01	5.85E-01	74	8.27E-02	5.11E-01	58	bidir
5144	Malaria	5.04E-02	3.80E-01	25	4.33E-03	7.37E-02	16	bidir
5146	Amoebiasis	2.18E-02	2.43E-01	80	1.54E-03	3.60E-02	54	bidir
5200	Pathways in cancer	2.47E-02	2.43E-01	263	5.47E-02	4.09E-01	207	bidir
5222	Small cell lung cancer	4.20E-02	3.29E-01	79	2.86E-02	2.89E-01	59	bidir
5410	Hypertrophic cardiomyopathy (HCM)	4.79E-04	2.55E-02	57	9.44E-02	5.11E-01	41	bidir
5412	Arrhythmogenic right ventricular cardiomyopathy (ARVC)	2.06E-03	5.04E-02	53	5.06E-02	3.94E-01	31	bidir
5414	Dilated cardiomyopathy	5.43E-04	2.55E-02	61	9.39E-02	5.11E-01	43	bidir

Of the positively enriched pathways, focal adhesion and ECM-receptor interaction are of particular importance in DN where they are implicated in PTC-mediated tubulointerstitial fibrosis and MC-mediated glomerular hypertrophy (Figure 4-9, Figure 4-10) (184, 185). However, it is interesting to note that the essential genes, that is those whose dysregulation is above that of experiment wide dysregulation, are different between cell types (Figure 4-11a-4-11d). Notably, FN1 was not essential to focal adhesion scores on PTC, different actin isoforms contribute to focal adhesion enrichment in MC and PTC and collagen 5 alpha 2 (COL5A2) was inversely expressed in the ECM-receptor pathway in PTC and MC.

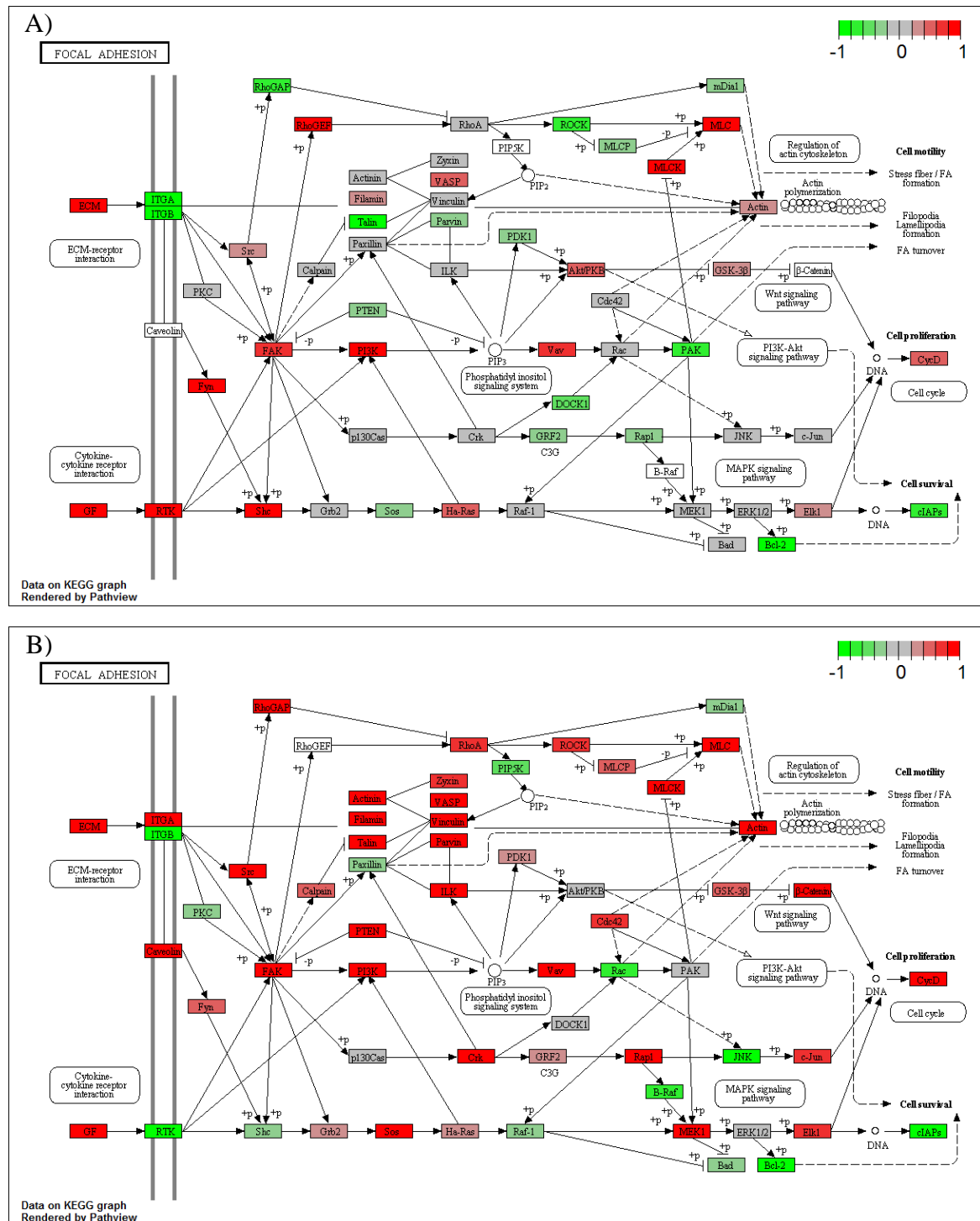


**Figure 4-9 Focal adhesion pathway is positively enriched by TGFβ in both proximal tubule epithelial cells and mesangial cells.**

The KEGG focal adhesion pathway (# 04510) rendered with differential gene expression (DGE) data from PTC (A) and MC (B) illustrating different cell specific pathway landscapes despite both cell types being indicated as positively enriched.

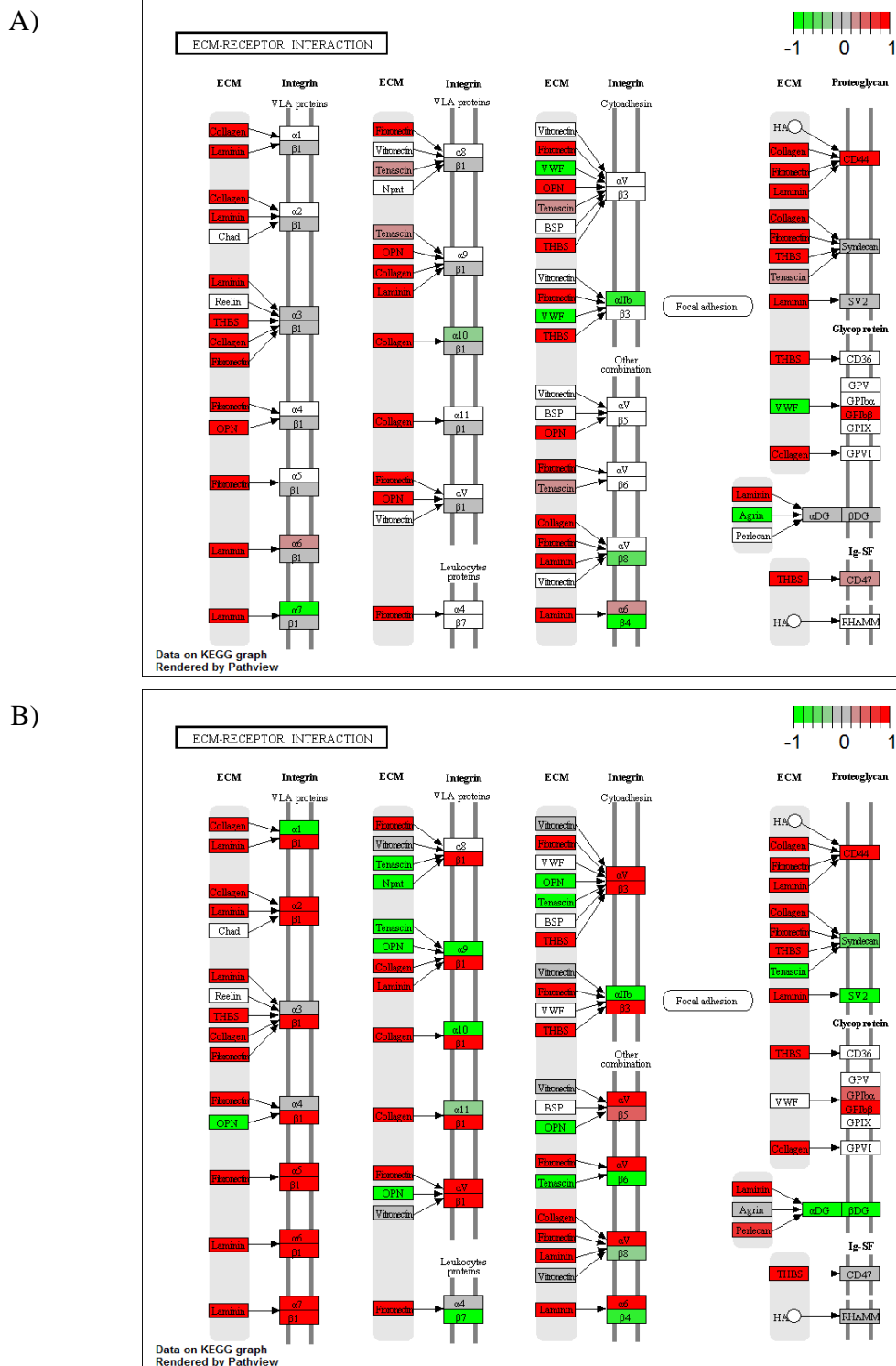


**Figure 4-10** ECM-receptor interaction pathway is positively enriched by TGFβ in proximal tubule epithelial cells and mesangial cells.

The KEGG pathway #04512 is intrinsically linked to focal adhesion with many ECM ligands being strongly upregulated in PTC (A) and MC (B). A considerable number of receptors were not detected in the PTC dataset (white cells).

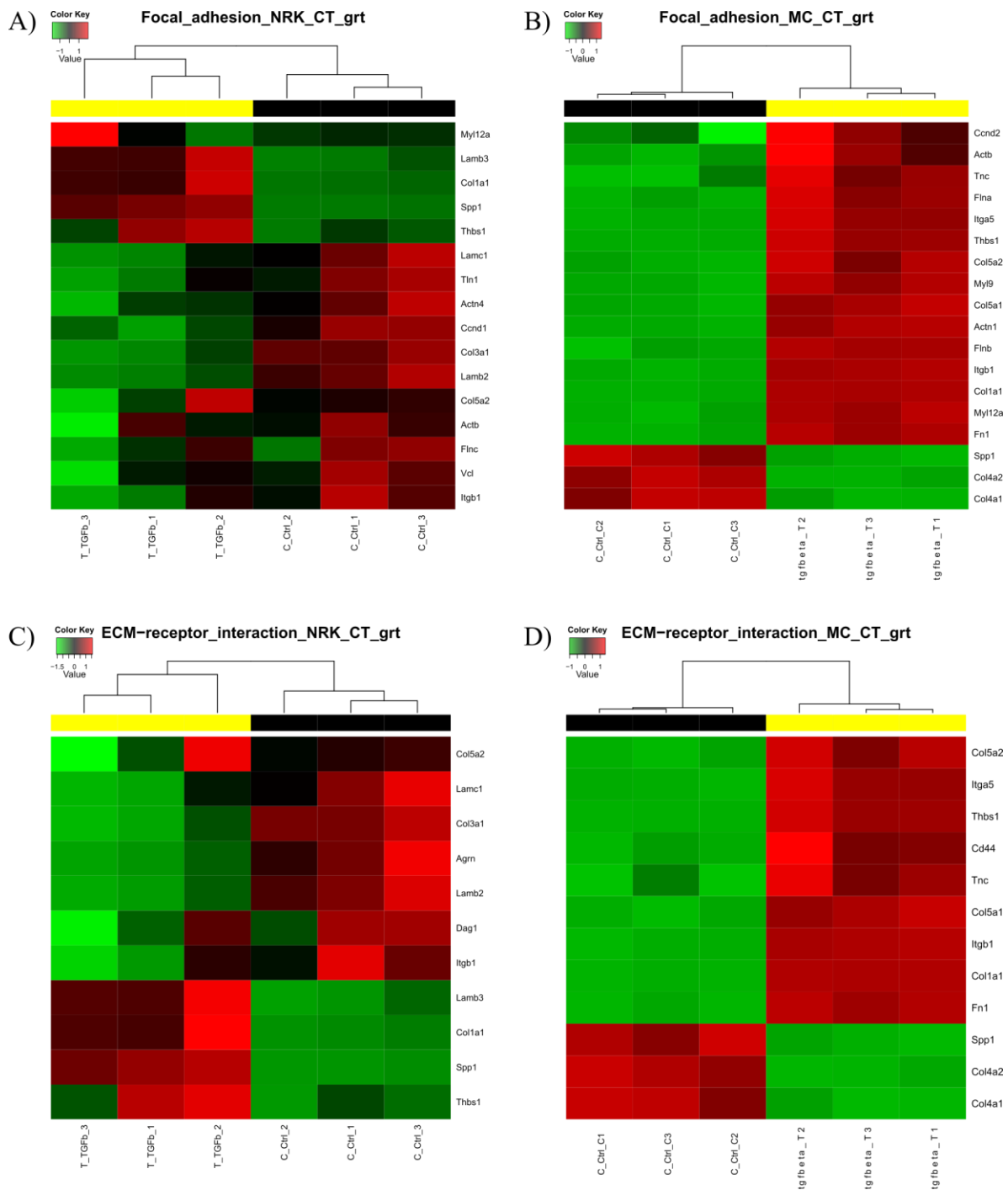


**Figure 4-11 Genes essential to statistical enrichment in pathways between cells types exhibit cell specific responses to TGF $\beta$ .**

Essential genes, those whose dysregulation is above that of background, even within the same pathway gene set, are seen to differ in the focal adhesion pathway between PTC (A) and MC (B). Cell specific changes in essential genes were also seen in the ECM-receptor pathway in PTC (C) and MC (D). Further heatmaps for rat: [~//Gage\\_pathway\\_heatmaps//PTC](#) and mouse: [~//Gage\\_pathway\\_heatmaps//MC](#)

Negatively enriched pathways were predominantly comprised of pathways associated with neurological disorders with which DN and the studied cell types share little in common (Table 4-8). However, oxidative phosphorylation was also negatively enriched by TGF $\beta$ . A large number of gene products at various stages of the electron transport chain are dysregulated by TGF $\beta$  in both MC and PTC (Figure 4-12a, Figure 4-12b). However, when filtering oxidative phosphorylation genes against background dysregulation, few genes were seen to be truly significant in PTC (~//Results2\_supp//Figure12\_supp) with no genes being returned as essential in MC. Underrepresentation of essential genes in this pathway may be the result of the low level of expression detected for the bulk of oxidative phosphorylation pathway genes.

An extensive list of pathways were also returned as being bidirectionally enriched in both PTC and MC (Table 4-8). Among these are those discussed above in addition to the p53 pathway, the cell adhesion and adherens junctions pathways, the actin cytoskeleton pathway and protein processing in the endoplasmic reticulum. The adherens junctions pathway is of particular interest and illustrates the cell specific effects of TGF $\beta$ . Whereas PTC downregulate adherens junction surface markers potentially contributing to tubular breakdown and cellular migration (Figure 4-13a), MC increase cell-cell connections and upregulate actin polymerisation which may facilitate mesangial expansion and glomerular hypertrophy (Figure 4-13b) (186). There are also a number of pathways seemingly unrelated to DN such as Chagas' disease and other parasitic and bacterial diseases. These appear due to cross-over with known TGF $\beta$  targets and highlight the possibility of false hits when using these unbiased omics approaches (Figure 4-14).

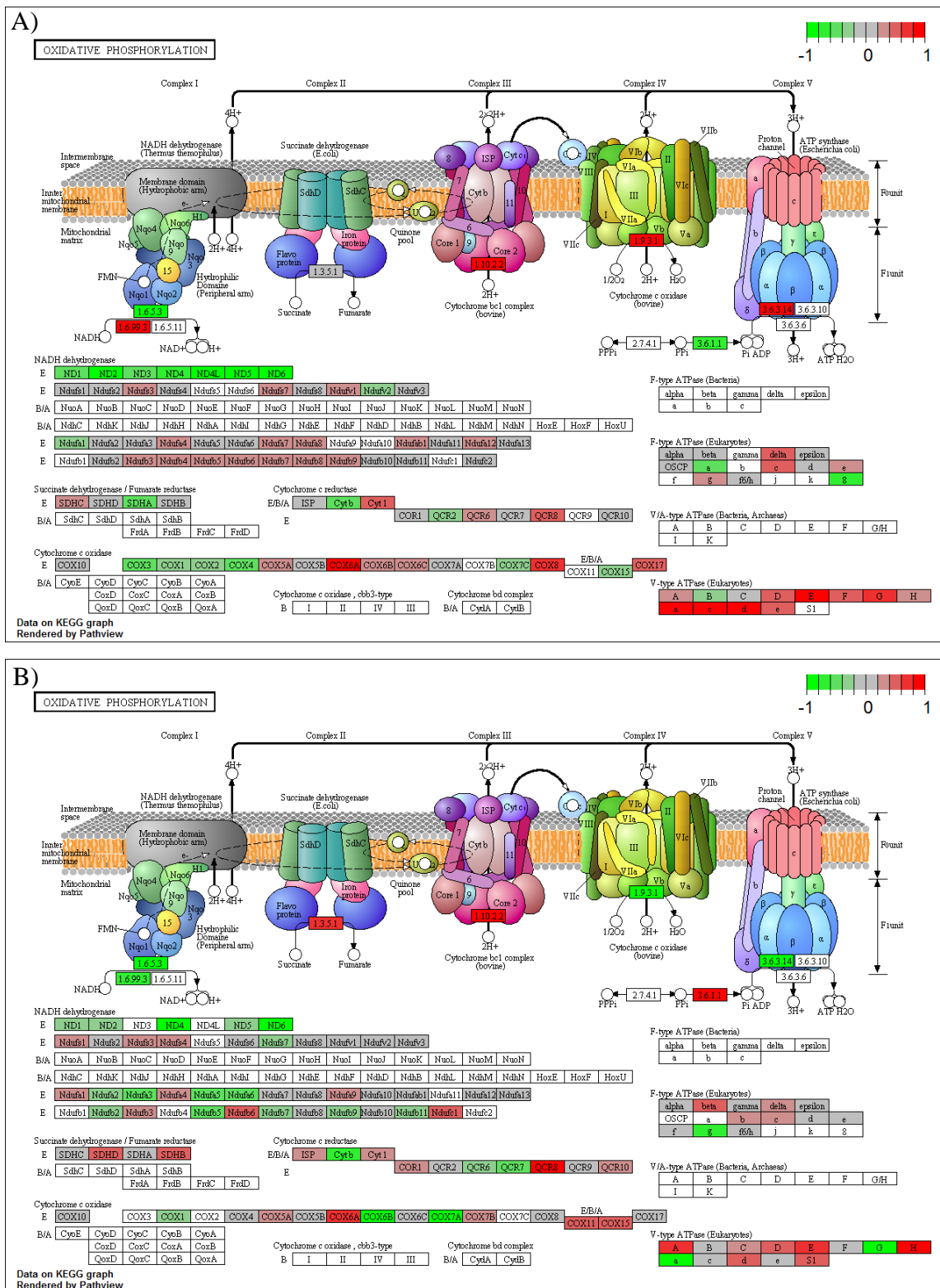


**Figure 4-12 TGF directly dysregulates oxidative phosphorylation by targeting components of the electron transport chain.**

Despite clear dysregulation and negative enrichment in PTC (A), few genes were considered to be dysregulated above background levels whilst in MC (B), no genes were above background due to low detection levels.

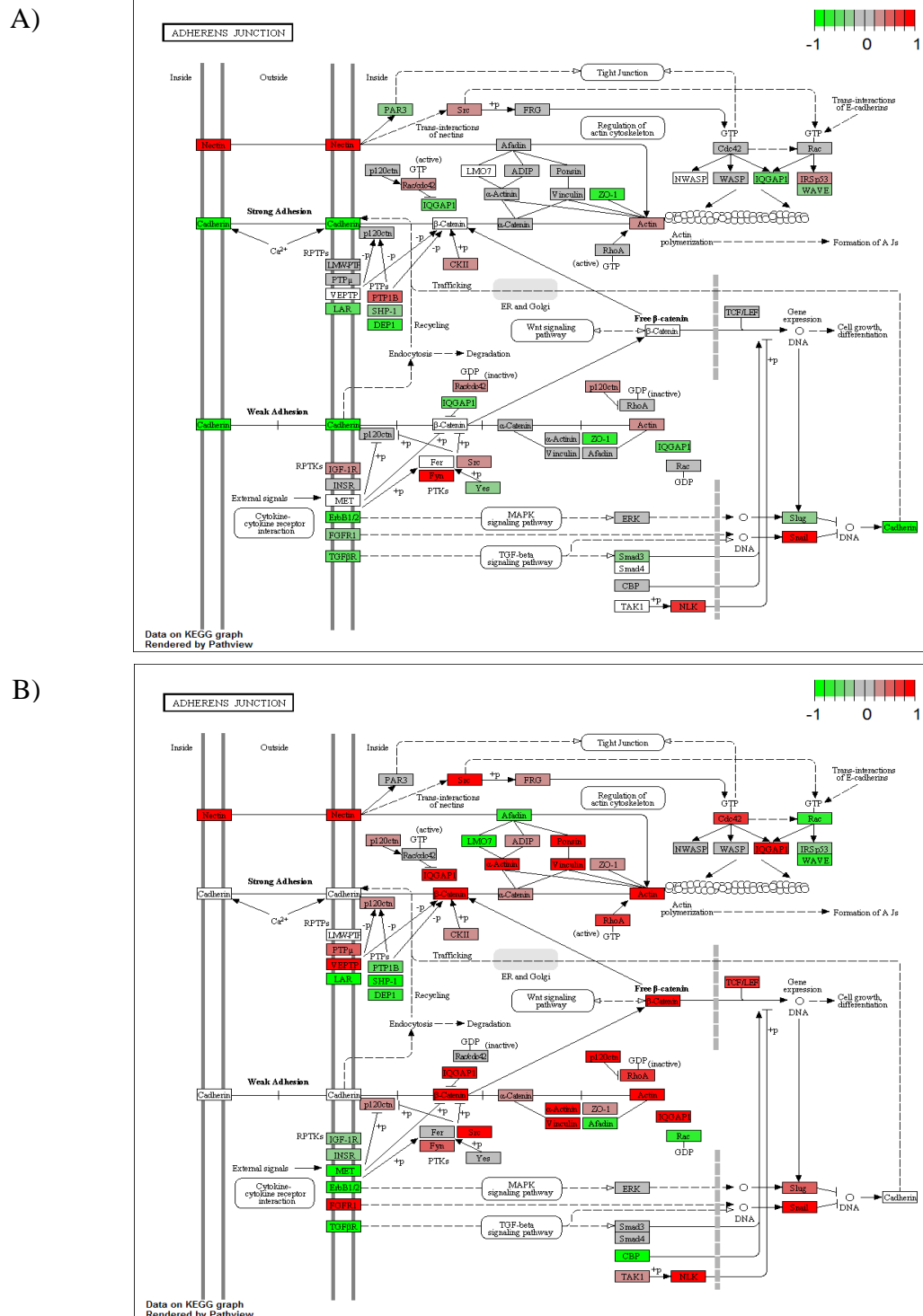


**Figure 4-13 Adherens junctions pathway is bidirectionally enriched by TGFβ in a cell specific manner.**

Both PTC (A) and MC (B) mRNA-seq datasets returned adherens junctions as being bidirectionally enriched. Inspection of the pathway indicates that the net effect in either cell type appears to be one that is specific to the biology of these cells in DN.

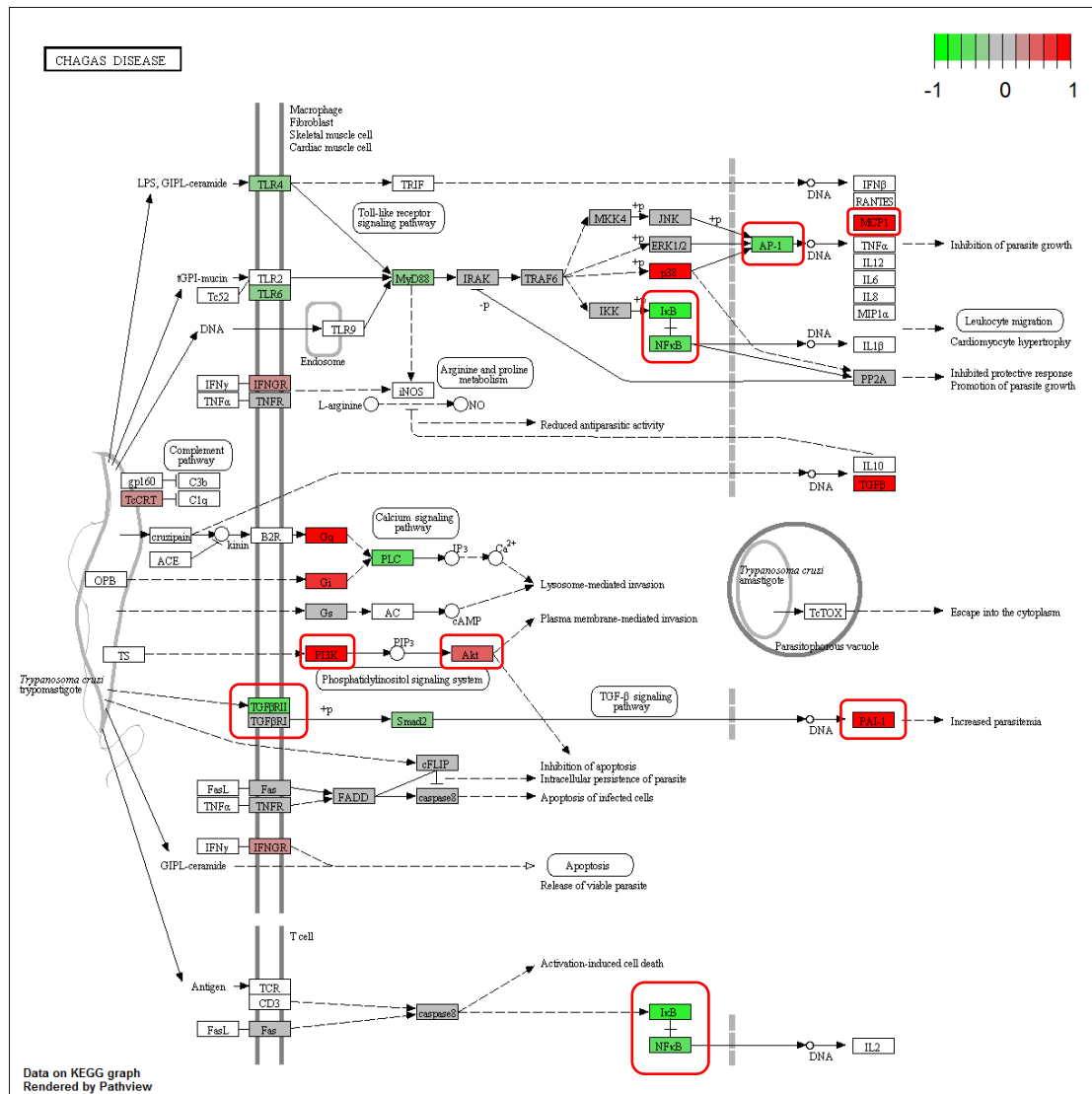


**Figure 4-14** GAGE analysis does not evade false-positives.

Identification of Chagas' disease pathway (mo05142) illustrates the necessity for proper discrimination of data obtained from these types of analyses. Highlighted are a number of genes typically involved in TGFβ induced phenotypes in other pathways and also contribute heavily to the enrichment score.

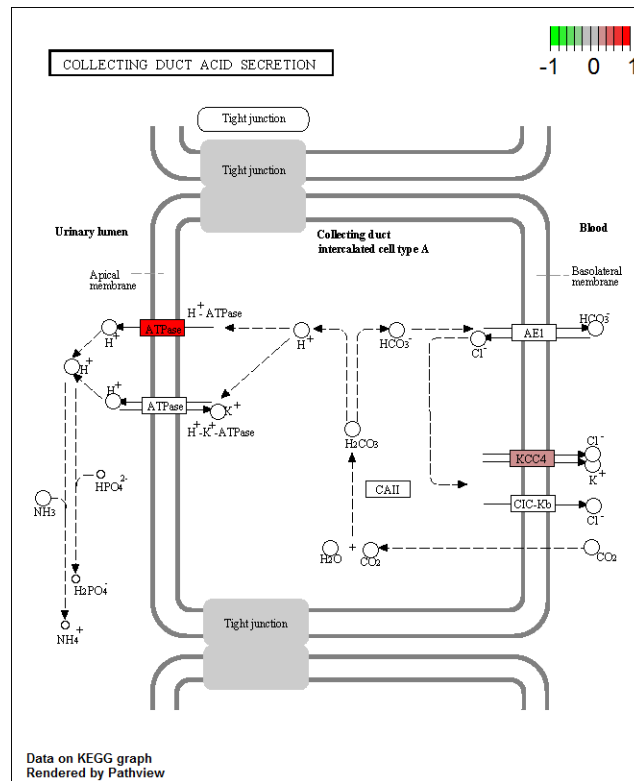
A small number of pathways were also uniquely enriched in either cell type for any given enrichment type (Table 4-9). Although the majority of these appear to be unassociated with DN there are a number of pathways which are enriched and appear to be present as a function of cell specific biology. In particular, collecting duct acid secretion was positively enriched in PTC (Figure 4-15a) and vascular smooth muscle cell contraction was bidirectionally enriched in MC (Figure 4-15b) (187, 188). Although a number of these uniquely detected pathways appear in the list of pathways commonly enriched between cell types, what makes them unique is the type of enrichment they demonstrate. For example, the adherens junctions pathway is significantly enriched for both up and downregulated genes in both PTC and MC while in PTC, this pathway is significantly enriched for downregulated genes alone. Testing for enrichment of either up or downregulated genes are distinct statistical tests and inspection of any given pathway, as in Figure 4-12, reveals distinct cell-type specific pathway topology.

**Table 4-9 Top 5 ranking pathways for different enrichment classes in proximal tubule epithelial cells and mesangial cells.**

Listed are pathways which were uniquely positively, negatively or bidirectionally enriched in PTC and MC following Gage pathway analysis of mRNA-seq datasets. *~/Results2\_supp/Table9\_supp*

path ID	Name	p.val	q.val	set.size	unique to	enrichment
mmu04670	Leukocyte transendothelial migration	0.000358331	0.02550952	75	MC	up
mmu05410	Hypertrophic cardiomyopathy (HCM)	0.000479457	0.02550952	57	MC	up
mmu05414	Dilated cardiomyopathy	0.000543177	0.02550952	61	MC	up
mmu04141	Protein processing in endoplasmic reticulum	0.000664439	0.02550952	154	MC	up
mmu04145	Phagosome	0.000780904	0.02550952	99	MC	up
rno04610	Complement and coagulation cascades	0.05059588	0.8661336	23	PTC	up
rno04966	Collecting duct acid secretion	0.05160884	0.8661336	20	PTC	up
rno04620	Toll-like receptor signaling pathway	0.05338863	0.8661336	56	PTC	up
rno05142	Chagas disease (American trypanosomiasis)	0.07138646	0.8661336	58	PTC	up
mmu04620	Toll-like receptor signaling pathway	0.041919397	0.9681164	69	MC	down
mmu04940	Type I diabetes mellitus	0.080764749	0.9681164	12	MC	down
rno04260	Cardiac muscle contraction	0.000885	0.0331	47	PTC	down
rno03010	Ribosome	0.00211	0.0658	58	PTC	down
rno03040	Spliceosome	0.0273	0.712	101	PTC	down
rno04520	Adherens junction	0.0305	0.712	52	PTC	down
rno04530	Tight junction	0.0368	0.765	77	PTC	down
mmu05219	Bladder cancer	0.010339035	0.16887091	37	MC	bidir
mmu05416	Viral myocarditis	0.01691977	0.22108499	36	MC	bidir
mmu04270	Vascular smooth muscle contraction	0.018048085	0.22108905	76	MC	bidir
mmu00100	Steroid biosynthesis	0.022562028	0.24287945	16	MC	bidir
mmu00970	Aminoacyl-tRNA biosynthesis	0.028326945	0.25424515	42	MC	bidir
rno00190	Oxidative phosphorylation	6.51E-08	8.16E-06	103	PTC	bidir
rno05012	Parkinson's disease	8.73E-08	8.16E-06	101	PTC	bidir
rno05010	Alzheimer's disease	3.35E-05	0.00188	122	PTC	bidir
rno05016	Huntington's disease	4.02E-05	0.00188	131	PTC	bidir
rno04260	Cardiac muscle contraction	0.000467	0.0125	47	PTC	bidir

A)



B)

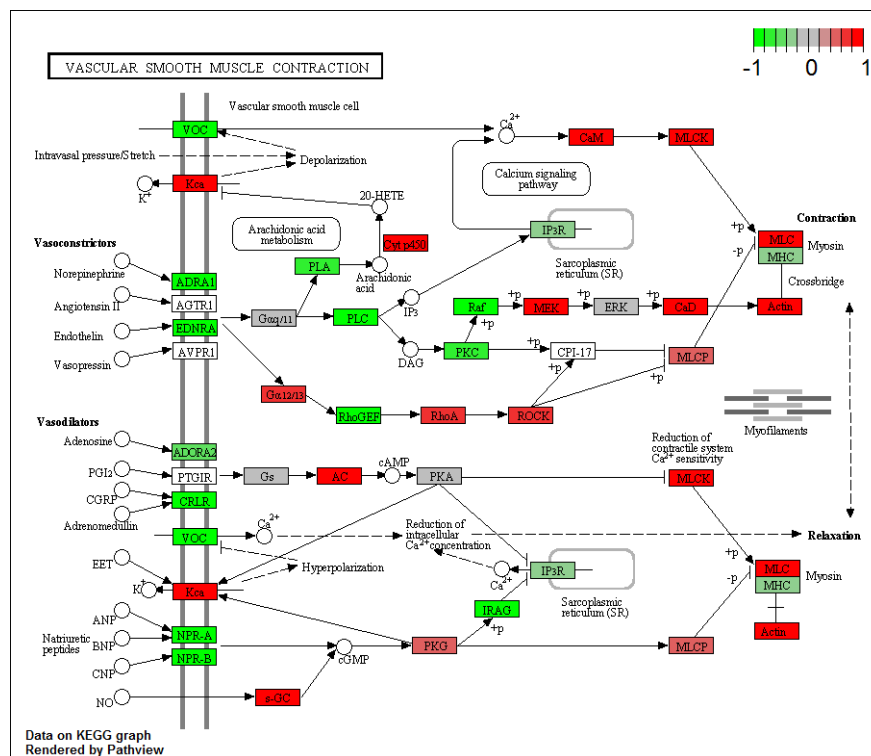


**Figure 4-15 Pathways pertaining to cell specific biology were uniquely enriched in proximal tubule epithelial cells and mesangial cells by TGFβ.**

Pathways loosely connected with cell specific biology such as collecting duct acid secretion (bicarbonate reabsorption) and vascular smooth muscle contraction (intra-glomerular pressure) were uniquely enriched in PTC (A) and MC (B) respectively.

Pathway orientated analysis can provide perspective on what effects any given treatment is having on any particular cell type. As with gene ontology analysis, it is apparent that TGF $\beta$  alters numerous pathways with many of these pathways displaying cell specificity in terms of the enrichment for the directionality of gene expression. Also, it can be seen that the genes which are dysregulated in these pathways vary greatly between cell types potentially resulting in vastly different outcomes in regard to cellular physiology.

#### 4.4. Discussion

This chapter has presented a comparative analysis of both gene ontology and pathway enrichment data garnered from mRNA-seq experiments performed in TGF $\beta$ -treated PTC and MC. Collectively, these data have revealed a number of pathways, biological processes and cellular functions which are targeted by TGF $\beta$  in both a general and a cell specific manner. These effects of TGF $\beta$  are rooted in dysregulation of a core set of mRNA genes in these cells types with further gene expression being uniquely dysregulated in either cell type. These studies provide a solid base from which further exploration of TGF $\beta$  actions in DN may be launched.

The cell types utilised in this study participate in vastly different yet intrinsically linked processes which promote ongoing injury within the diabetic kidney. MC, in conjunction with podocytes, are the main effector cells in glomerulosclerosis, a process which leads to eventual scarring and failure of glomerular function (31). Specifically, MC are responsible for mesangial expansion, the main driver of glomerular expansion (189). This process is driven by MC hypertrophy and replication, increased production of ECM proteins and decreased production of ECM turnover machinery. Conversely, PTC are the primary drivers of interstitial fibrosis which is the result of increased production and deposition of ECM proteins, and, as in MC, decreased production of ECM turnover components (190). Furthermore, both MC and PTC secrete a host of cytokines as a result of biochemical and mechanical stresses in response to the diabetic milieu and these factors can flow downstream from the glomerulus to induce pathological changes in PTC and may also act in a paracrine fashion from PTC to the glomerulus via activation of interstitial fibroblasts (31, 191).

The most potent of these factors responsible for the propagation of these processes in the diabetic kidney, besides chronic hyperglycaemia itself, is TGF $\beta$  (59). This growth factor regulates a wide array of cellular processes and is known to be a major driver of fibrotic

processes in a number of tissues and cell types. This alone suggests TGF $\beta$  is an attractive therapeutic target. However, although efforts to repress this growth factor *in vivo* via neutralising antibodies, pharmacological interventions or genomic manipulation have met with some success, no treatment has successfully completed clinical trials due to various safety concerns (179). It is therefore imperative to gain a better understanding of the general impact of TGF $\beta$  on cellular function in order to identify downstream processes which may be more amenable to therapeutic intervention.

To this end, the present study analysed mRNA differential gene expression (DGE) data via a modified version of gene set analysis termed generally applicable gene set analysis (GAGE). This method differs from typical gene set analysis methods such as gene set enrichment analysis (GSEA) by simultaneously testing a pathway or experimental gene set for both up and downregulated genes and also operates through a parametric gene randomization process similar to parametric analysis of gene set enrichment (PAGE) (163). However, GAGE differs from PAGE in that it assumes that a gene set possesses a different distribution to that of background noise and uses a two-sample t-test to test for gene set and noise variance. Conversely, PAGE assumes that the same distribution is present in the gene set and background and only uses a one-sample t-test which tests variance in background and not the gene set itself (192). Furthermore, GAGE can handle small experimental groups whereas GSEA requires at least 6 samples per group for results to be considered robust (163). Collectively, this makes GAGE more robust than PAGE or GSEA alone and as such was used for both pathway and gene ontology analysis of mRNA-seq data from PTC and MC.

GAGE analysis returned pathways enriched for upregulated genes in both MC and PTC including the p53 pathway and focal adhesion pathways with the p53 pathway, focal adhesion and ECM-receptor interaction. Additionally, cell adhesion molecules, tight junction and regulation of actin cytoskeleton pathways were returned as bidirectionally dysregulated in these cell types. Enrichment of these pathways in both cell types highlights a core set of pathways through which TGF $\beta$  mediates its fibrotic effects and the way in which PTC and MC communicate with their environment. Furthermore, oxidative phosphorylation was detected as being enriched for downregulated genes in both MC and PTC indicating that TGF $\beta$  has a direct effect on cellular metabolism and oxidative stress. Indeed, TGF $\beta$  has been shown to alter activity of complex IV leading to increased reactive oxygen species production and oxidative stress (193).

Despite pathways being commonly identified and even directionally enriched between PTC and MC it is interesting to note that the effect of TGF $\beta$  on these pathways appears to differ between the cell types. Looking at essential genes in any given pathway reveals that TGF $\beta$  dysregulates different subsets of genes which contribute to pathway enrichment in MC and PTC. This is exemplified by essential gene analysis of ECM-receptor interaction pathways where a number of genes are considered to be essential in one cell type and not the other. Furthermore, in this pathway, although considered essential to pathway enrichment, COL5A2 is found to be inversely expressed between MC and PTC. However, inspection of the heatmap for ECM-receptor interaction pathway in PTC reveals detection of this gene is suboptimal in the intra-group samples.

It is tempting to accredit these differences to species specific rather than cell specific effects of TGF $\beta$ . This is potentially exacerbated by the depth to which the mouse genome has been annotated compared to that of rat. However, both the mouse and rat mRNA-seq datasets were normalised against each other so that both datasets were identical with respect to the tags used in downstream analyses. Whilst this does not necessarily remove any bias introduced through species specific biology or indeed genome annotation, it will indeed flatten or reduce any artifacts introduced via these factors.

In PTC, the complement and coagulation cascades pathway and the toll-like receptor signalling pathway were uniquely positively enriched and collectively represent pathways by which TGF $\beta$  mediates inflammatory responses of PTC (194, 195). *In vivo*, these pathways are likely to be triggered as a result of cytokine production and leakage in the glomerulus with concurrent podocyte effacement. Adherens junctions and tight junction pathways were also negatively enriched by TGF $\beta$  and loss of these structures are primary steps in EMT. These findings add weight to the notion that PTC undergo EMT, or EMT-like processes, in the diabetic kidney (196, 197).

Conversely, GAGE analysis detected a number of pathways positively or bidirectionally enriched in MC which are related to either cardiomyopathies or vascular smooth muscle contraction respectively. Although MC lack sarcomeric structures as found in striated and skeletal muscle, they do express many of the proteins found in the contractile units of smooth muscle cells, albeit possibly different isoforms (198). Furthermore, these proteins are assembled in three-dimensional contractile networks as opposed to unidirectional units, as observed in other contractile cells. This allows MC some degree of control over glomerular volume and blood flow (20). Enrichment of these pathways indicates that TGF $\beta$  alters

glomerular pressure which inevitably has flow on effects to pressure sensitive podocytes and microvascular endothelial cells (199, 200).

MF terms returned by this analysis further confirm the wide reaching effects of TGF $\beta$ . An array of terms relating to nucleoside binding were commonly enriched for upregulated genes indicating that the pathway level effects elicited by TGF $\beta$  are potentially rooted in regulation of transcriptional activity in general. Additionally, these terms may be related to cell cycle activity due to the requirement of DNA replication at cell division and may be a contributing factor to the effects of TGF $\beta$  on cellular growth and replication. However, terms including DNA and RNA binding were enriched for downregulated genes as are terms relating to protein complex formation. These terms appear to be in opposition to each other given that gene transcription and DNA replication require assembly of a number of protein complexes which are then needed for strand separation and transcription/replication itself (201, 202).

Furthermore, downregulation of terms relating to multimeric protein complex formation were also detected, which, coupled with those which were upregulated and related to nucleoside binding, may be linked with the negative enrichment of the oxidative phosphorylation pathway as identified in the GAGE pathways analysis. Activity in this pathway is highly dependent upon various nucleoside derivatives as electron donors, carriers and products of the ETC as well as the large protein complexes of the ETC itself. At least in the case of complex I, this requires some degree of directed assembly (203, 204).

BP terms are more closely related to canonical pathway analysis in that they define a process rather than a molecular function which, by its very nature, may be ubiquitously present throughout signalling pathways such as 'peptide binding' or 'phosphatase activity'. Indeed, cell cycle checkpoint and regulation of cell cycle BP terms were positively enriched in both cell types. The presence of these terms is to be expected as a number of pathways identified by GAGE pathway analysis, such as p53, phosphatidylinositol-4,5-bisphosphate 3-kinase (PI3K)- v-akt murine thymoma viral oncogene homolog 1 (AKT) and focal adhesion pathways, converge on cell cycle regulation and cell survival (184, 205, 206). Furthermore, terms negatively enriched in MC and PTC included chromosomal organisation in addition to chromatin organisation and chromatin modification. These terms are intrinsically linked with one another and highlight the most fundamental of processes required for TGF $\beta$  to mediate its effects, activation and repression of gene transcription. Finally, cell and biological adhesion in addition to tissue development were bidirectionally enriched in PTC and MC. Again, the adhesion terms give weight to the pathways returned in the GAGE pathway

analysis. TGF $\beta$  induces developmental phenotypes in various cell types including EMT in PTC and induction of a myofibroblast-like phenotype in MC therefore providing evidence of a role for TGF $\beta$  in tissue development ontology terms (49, 207).

Terms relating to cell specific developmental phenotypes were positively enriched in either cell type by TGF $\beta$  including epithelial cell differentiation and epithelium development in PTC and muscle organ development and muscle tissue development in MC. These terms highlight that although TGF $\beta$  induces developmental phenotypes in these cells it exerts these effects through unique cell specific processes. The presence of negative enrichment in the oxidation-reduction process in PTC is supported by oxidative phosphorylation pathway enrichment detected the GAGE pathway analysis. Furthermore, although PTC are not energy rich in the same way that cardiomyocytes are, they are highly dependent upon the Na<sup>+</sup>/K<sup>+</sup> ATPase pump for reabsorption of organic phosphates, galactose, sulphate and amino acids amongst others (208). As such, disturbances in energy homeostasis in PTC can affect downstream components of the nephron due to abnormally high concentrations of various compounds.

GAGE analysis has identified a number of pathways and processes which are either uniquely enriched in response to TGF $\beta$  in PTC and MC or are enriched in both cell types, thus representing more cell specific *vs.* general effects of TGF $\beta$  respectively. Although there are no known previous high-throughput sequencing experiments in MC, a similar study has been published utilising another PTC model cell line, the HK2 cell (209). The present study finds many parallels with that of Brennan *et al.* (209) in regard to KEGG pathway and gene ontology enrichment despite disparate analysis methods. Whereas the previous study utilised *limma* for read count normalisation this study has used *edger*. Pathway and gene ontology analyses in the Brennan study utilised *Genomatix* and *DAVID* respectively whereas this study has utilised GAGE. Despite these differences, pathways including TGF $\beta$  signalling, focal adhesion pathways and ECM-receptor interaction, adhesion terms and p53 signalling were all identified in the study by Brennan *et al.* study as well as this study. This ratifies the GAGE methodology utilised for analysing PTC and, by extension, in MC also.

Furthermore, the present study utilised comparatively more stringent treatment regimes than that utilised by Brennan *et al.* with the present study utilising 10ng/ml for 72 hours for both PTC and MC compared to 5ng/ml for 48hrs for HK2. It may therefore be argued that a number of the findings in the present study result from secondary or tertiary effects of TGF $\beta$  treatment. This may of course be tested through a series of time course experiments utilising

a dose response curve for each time point. This would undoubtedly provide important and exciting insights into the temporal and stoichiometric properties of TGF $\beta$ -mediated gene dysregulation especially given findings by Thannickal *et al* (210), Dong *et al.* (211) and D'Souza *et al.* (212) which have already identified early *vs.* late TGF $\beta$  response genes. However, studies of this type, although valuable, are beyond the scope of this project.

GAGE-based analysis has demonstrated that TGF $\beta$  exerts a wide array of general and cell specific effects upon PTC and MC. These are intuitively rooted in transcriptional activity. Indeed, as with higher level pathway and ontology analyses, there is widespread TGF $\beta$ -mediated dysregulation of mRNA genes with considerable congruency being detected in which genes are either up or down regulated between the cell types. Conversely, there were a large number of genes which were uniquely dysregulated in either PTC or MC. Direct comparison of these two datasets gives rise to both an intersection and 'outersection' of TGF $\beta$ -induced gene dysregulation give rise to the results garnered in higher level analyses of both mRNA-seq datasets.

This chapter has sought to explore and elucidate the genome wide effects of TGF $\beta$  on two main effector cells in diabetic nephropathy, namely, proximal tubule epithelial cells and glomerular mesangial cells. This has highlighted the need for cell-type specific intervention therapies by exposing the effects of TGF $\beta$  on these disparate cell types. Extensive data have been presented highlighting similarities and differences between the two cell types in regard to their response to TGF $\beta$  with a particular focus on gene ontology and pathway gene set enrichment. These data provide a valuable resource for future development of cell specific therapies both in DN and in non-diabetes related renal pathologies. The following chapter will extend this work by integrating shortRNA-seq data with the present mRNA-seq data to gain an understanding of the effects that TGF $\beta$ -mediated miRNA dysregulation plays in PTC and MC pathophysiology.

## 5. Results III – Contribution of TGF $\beta$ -mediated miRNA dysregulation to transcriptional topography

### 5.1. Introduction

TGF $\beta$  is well regarded as one of the most potent pathological factors in DN due to its ability to induce fibrotic signalling pathways and pathogenic cellular phenotypes (59). An emerging part of this process has been shown to involve a growing network of miRNAs (213). The profound effects of TGF $\beta$  make it an attractive therapeutic target but efforts to reduce its expression or activities *in vivo* have not been successful for a variety of reasons (179). Thus, miRNA, which act as ‘soft’ post-transcriptional regulators have gained considerable attention in an effort to identify therapeutic targets downstream of TGF $\beta$ .

Although considerable progress has been made in the study of miRNA and their targets, little progress has been made in regard to miRNA signalling from a systems biology perspective, especially in context of the kidney (176, 214, 215). Given that current therapies have only modest effects in halting the progression and development of DN it is imperative to gain a better understanding of TGF $\beta$  biology within the kidney in order to develop new interventions targeted downstream of TGF $\beta$  itself. This deeper understanding can best be gained from genome-wide analysis of TGF $\beta$ -mediated mRNA and miRNA genes of cells important to the pathophysiology of DN.

Few tools exist which allow ready integration of mRNA and miRNA high-throughput sequencing. This chapter presents a custom pipeline designed to integrate predicted miRNA-target interactions on a genome wide scale. The interactions are utilised to augment canonical KEGG pathways which are then combined with fold-change and significance data from high-throughput sequencing of both mRNA and miRNA from PTC or MC. The custom networks are then tested for topological perturbation via impact factor analysis which is superior to traditional over-representation analyses in several ways.

Direct comparison of impact factor analysis (IFA) results in different cell types, and from differing miRNA-target interaction sub-lists may reveal novel targets or pathways for future investigation. Furthermore, miRNA play an important role in TGF $\beta$  biology but their very nature makes study via conventional PCR based techniques cumbersome. Therefore, it is hoped that through integration of mRNA and miRNA high-throughput sequencing datasets, a

better understanding of the role of miRNA in TGF $\beta$  mediated cellular pathology in DN can be gained.

## **5.2. TGF $\beta$ induced dysregulation of miRNA coding genes is both general and cell-specific**

In order to investigate the genome wide effects of TGF $\beta$  on miRNA expression, high-throughput massively parallel sequencing was performed on small-RNA from mouse MC and rat PTC. Cells were maintained in high glucose conditions and treated with 10ng/ml TGF $\beta$  for 72 hours.

### **5.2.1. Suitability of normalisation methods and treatment effectiveness**

High throughput sequencing data of short RNA from PTC were aligned to rat genomic build rn4 while data from mesangial cells were aligned to mouse genomic build mm9. Data were cleared of background noise in a similar manner to that performed with the mRNA-seq experiments (see chapter 4). Specifically, this was done by removal of contigs which possessed fewer than 10 reads per million from the per sample read libraries. The resultant per sample read count libraries are listed in Table 5-1 and indicate that sufficient sequencing depth was achieved for each sample. A total of 262 short RNA were detected in PTC samples with 172 being identified as putative miRNA. In MC samples, 10194 short RNA were identified with 448 of these being identified as putative miRNA. Contigs not aligned to miRNA genes were predominantly mapped to mRNA and likely represent natural degradation products or degradation products that may have arisen during sample processing. The difference in the number of identified miRNA species between PTC and MC may have arisen from the differing depth of genome annotation between mouse and rat genomes. However, there is a considerable difference in the number of miRNA identified between the species with miRBase listing 765 mature miRNA for *R.norvegicus* compared to 1915 mature miRNA for *M.musculus*.

**Table 5-1 Summary data for miRNA-seq in PTC and MC.**

Listed are total short RNA identified and the number of contigs which were aligned to putative miRNA.

		Cell type	
		PTC	MC
Reads	Samples		
	Control_1	7442110	8004682
	Control_2	7347429	6723288
	Control_3	6613837	7045240
	TGF $\beta$ _1	7E+06	7008401
	TGF $\beta$ _2	4569902	6480956
TGF $\beta$ _3	6270854	6611176	
Short RNA	Total short RNA	269	10194
	miRNA	172	448

*edgeR* was again utilised for read count normalisation and processing with the same pipeline being utilised in mRNA read count normalisation. Generation of library specific normalisation factors was followed by estimation of dispersion assuming a Poisson distribution. Normalisation estimation and validation of estimation of normalised read counts was performed utilising negative binomial generalised linear models.

High-throughput sequencing of small RNAs, by its very nature, carries much more noise than is present when sequencing long RNAs. This is predominantly due to the presence of biological and technical degradation products. Furthermore, small RNAs are generally expressed at lower levels which reduces the read counts per contig and can affect normalisation estimates. As such, validation of normalisation techniques often needs to be relaxed in order to account for this increased noise. Regardless, BCV for dispersion of aligned contigs in PTC samples are seen to follow the same general distribution as that seen in mRNA BCV dispersion (Figure 5-1a). Contigs with lower reads are seen to be most dispersed with dispersion decreasing with increased read counts. Importantly, the dispersion trend is seen to converge upon the common dispersion factor indicating that there are no outstanding effects from outlier samples. Conversely, in MC short RNA sequencing, the vast majority of contigs are seen to be of low read count and are also dispersed over a range two-fold higher than that seen in PTC samples (Figure 5-1b). Furthermore, the dispersion trend is seen to depart from the common dispersion following convergence. The departure can be attributed to two distinct populations of tags, these being that under the first divergence and those at higher read counts which are seen to decrease sharply in dispersion. This first population is likely to be real. However, the second population may primarily be comprised

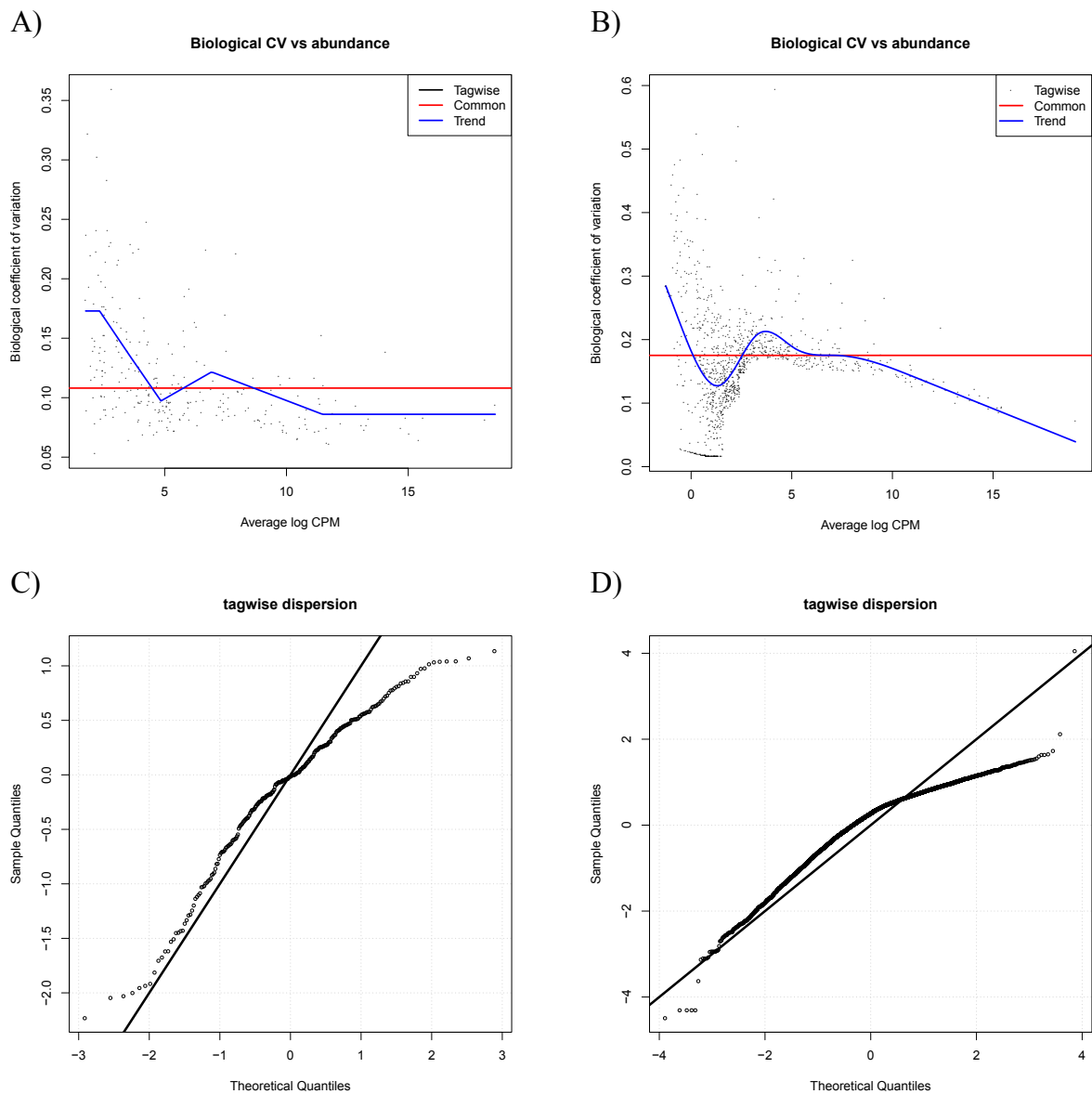


**Figure 5-1 Negative binomial models effectively estimated normalised read counts in miRNA-seq data from proximal tubule epithelial cells and mesangial cells.**

The trended biological coefficient of variance (BCV) is seen to converge on the common dispersion as read log counts per million increases in both PTC (A) and MC (B) miRNA sequencing data. Tag-wise dispersion is accurately estimated by the negative binomial model used in both PTC (C) and MC (D). However, the increased noise inherent in short RNA sequencing is apparent in both the BCV and tag-wise dispersion QQ-plots. Tag-wise dispersions were transformed to normality and plotted against theoretical quantiles.

To assess tag-wise dispersion and the ability of the negative binomial generalised linear model to accurately estimate normalised read counts QQ-plots of normally transformed tag-wise dispersion values were generated. As with QQ-plots of tagwise dispersion from mRNA sequencing experiments, the model over-estimated sample variation at the upper quartile of read counts for both PTC and MC short RNA sequencing (Figure 5-1c, Figure 5-1d). However, in the lower quartiles, the model is seen to under estimate sample variance. This is likely a function of decreased read quantity. Furthermore, these experiments have utilised the Cox-Reid profile adjusted likelihood method of estimating tag-wise dispersion which is considered more robust than the quantile-adjusted conditional maximum likelihood method typically used (160). Therefore, these outcomes represent the best possible normalisation estimates.

As with the mRNA-seq experiments, control samples and those treated with TGF $\beta$  are seen to be well separated in both PTC and MC when visualised via MDS plots (Figure 5-2a, Figure 5-2b). Intra-group sample similarity is however somewhat diminished in comparison to mRNA sequencing samples. Again, this is likely to be a result of the increased noise inherent in short RNA sequencing experiments due to generation of artificial short RNAs during processing. Variation in  $p$ -values was also grossly underestimated by the selected models which, and, as with mRNA sequencing  $p$ -values, are due to a considerable spread in statistical significance of short RNA dysregulation in conjunction with a large number of short RNA possessing near zero  $p$ -values (Figure 5-2c, Figure 5-2d).

Assessment of experiment wide gene dysregulation by way of smear plots reveals similar trends to that seen in mRNA sequencing experiments for both PTC and MC (Figure 5-2e, Figure 5-2f). Genes with the lowest read counts are seen to be the most dysregulated with gene dysregulation generally decreasing as CPM values increase. However, robustness in fold-change detection levels increases to the right as a function of contig detection levels.

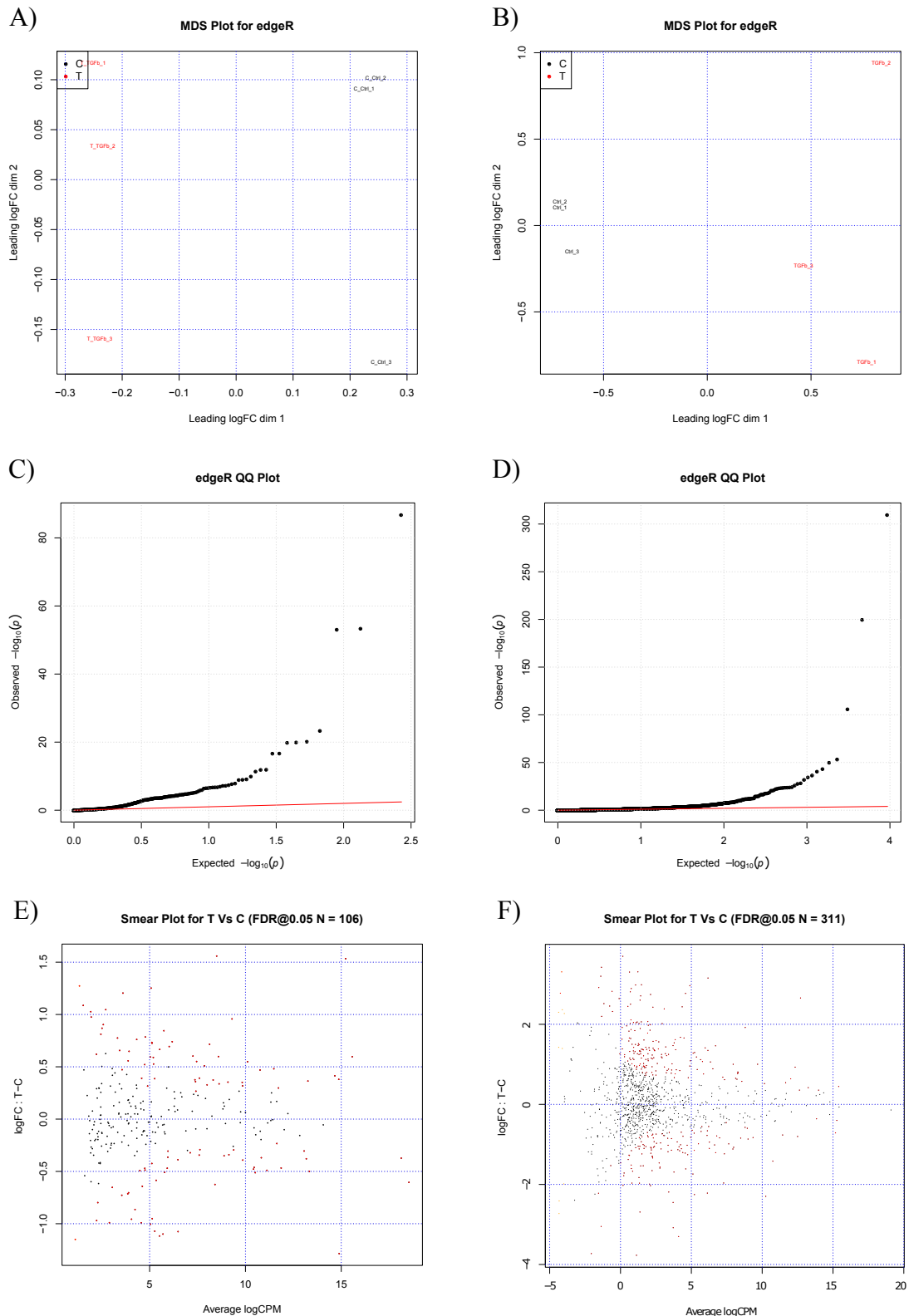


**Figure 5-2 TGF $\beta$  treatment induces significant short RNA dysregulation in both proximal tubule epithelial cells and mesangial cells.**

Multidimensional scaling (MDS) plots demonstrate TGF $\beta$  treatment induces a distinct phenotype in both PTC (A) and MC (B).  $p$ -values, although normally distributed against theoretical quantiles, were grossly under-estimated in PTC (C) and MC (D) due to a large number of near zero  $p$ -values. Smear plots highlight the distribution of significantly dysregulated genes in both PTC (E) and MC (F).

### 5.2.2. Overview of common and cell-specific TGF $\beta$ -induced miRNA gene dysregulation in PTC and MC

Non-miRNA short-RNAs were removed from the miRNA sequencing (miRNA-seq) datasets following read count normalisation to allow comparison of miRNA genes only. Preliminary analysis of the resultant datasets revealed approximately 50% of miRNA were either up or down regulated in PTC with significantly dysregulated miRNA being marginally overrepresented by upregulated contigs (Figure 5-3a, Figure 5-3b). In MC, skewing of the miRNA population towards up regulation is seen at both the global level and in those that are significantly dysregulated (Figure 5-3c, Figure 5-3d). Whereas TGF $\beta$  significantly dysregulated twice the number of mRNA genes in MC compared to PTC, the reverse is true for miRNA. Here, TGF $\beta$  significantly dysregulates 51% of all detected miRNA in PTC compared to only 26% in MC (Figure 5-3e, Figure 5-3f).

Looking at the entire PTC short RNA dataset, a number of the top 100 significantly dysregulated contigs are identified as belonging to predicted or novel protein coding genes with several contigs also identified as known protein coding sequences (Figure 5-4). Of particular importance, miR-21 is the most significantly dysregulated miRNA in TGF $\beta$ -treated PTC. As discussed in the previous chapter, many of the predicted mRNA sequences identified in PTC would likely be identified as putative mRNA sequences as annotation depth increases with successive releases of the *R.norvegicus* genome build. Furthermore, those that are identified as putative mRNA are likely to be the result of biological or technical degradation products. As with the MC mRNA dataset, there are only 2 contigs aligned to novel protein coding genes, however, over half of the top 100 most significantly dysregulated contigs in the short RNA dataset were aligned to protein coding genes (Figure 5-5). This is surprising given that the low level of detection of most miRNA inherently results in higher fold-changes. That is, high fold-change values are mathematically easier to attain for contigs with tens of read counts compared to those with tens of thousands of read counts. Conversely, the high proportion of short-RNA in this list may merely be a function of additional sample noise introduced through sample processing. Regardless, the most significantly dysregulated miRNA in MC, miR-503, is implicated in endometrial cancer progression via cell cycle control and its downregulation by TGF $\beta$  may therefore contribute to MC proliferation in DN (216).

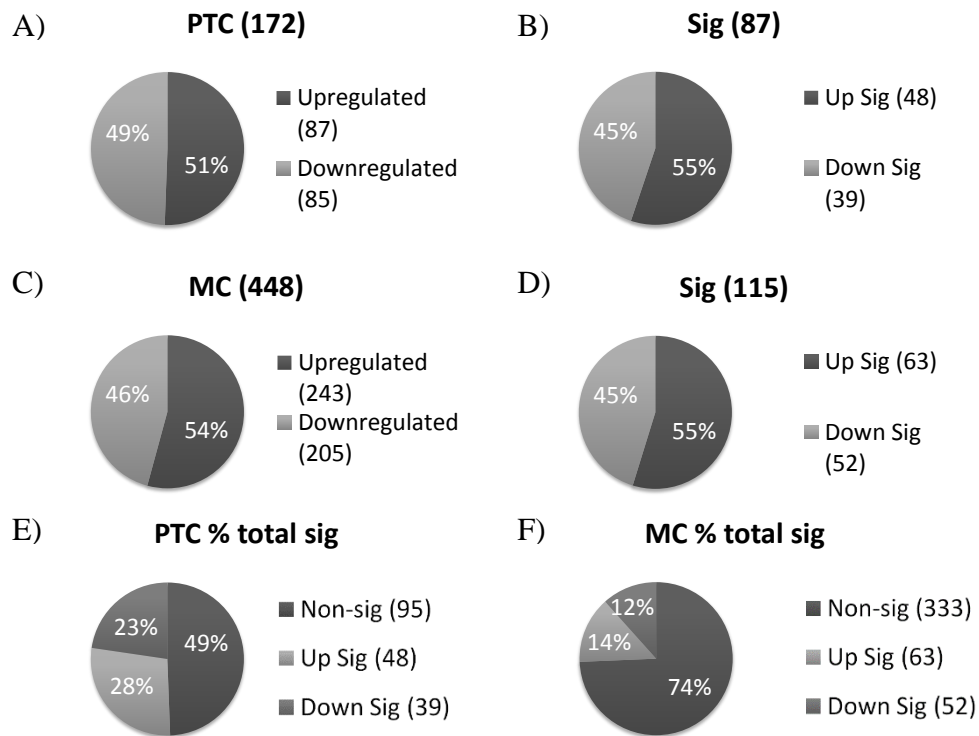


**Figure 5-3 Summary of TGF $\beta$ -induced gene dysregulation in proximal tubule epithelial cells and mesangial cells.**

Proportion of miRNA dysregulated in PTC (B) and MC (B) by TGF $\beta$ . Breakdown of significantly up and down regulated miRNA in PTC (C) and MC (D) tubule epithelial cells. Percentage of total detected miRNA which are significantly dysregulated by TGF $\beta$  in PTC (E) and MC (F).

~//Results3\_supp//Figure3\_supp

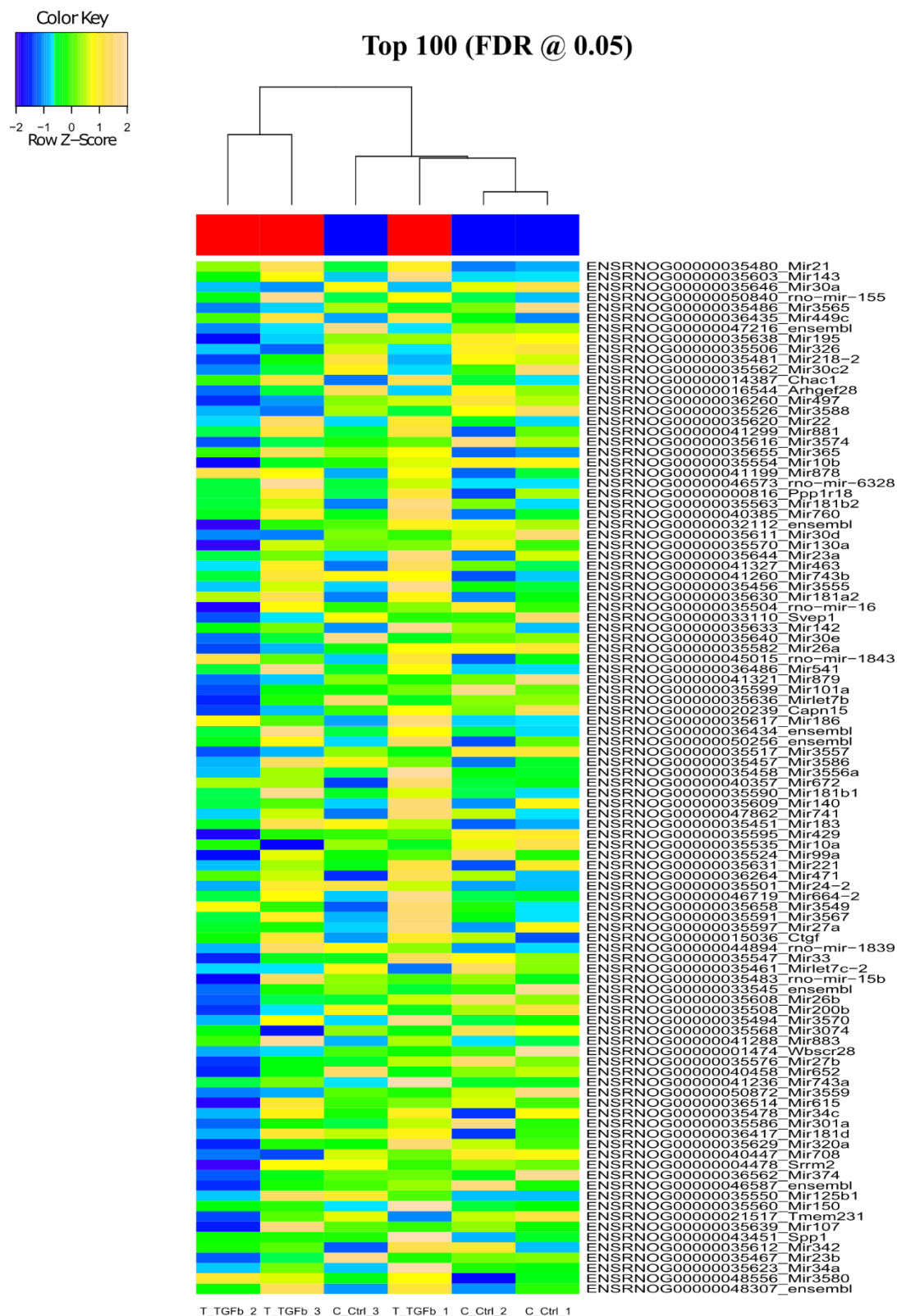


**Figure 5-4** Top 100 significantly dysregulated short RNA in proximal tubule epithelial cells.

Blue indicate greater than 2-fold downregulation, yellow indicate greater than 2-fold upregulation, green indicate  $\pm$  50% dysregulation. Genes are labelled with both Ensembl gene identifiers (ENSRNOG) and official gene symbols.

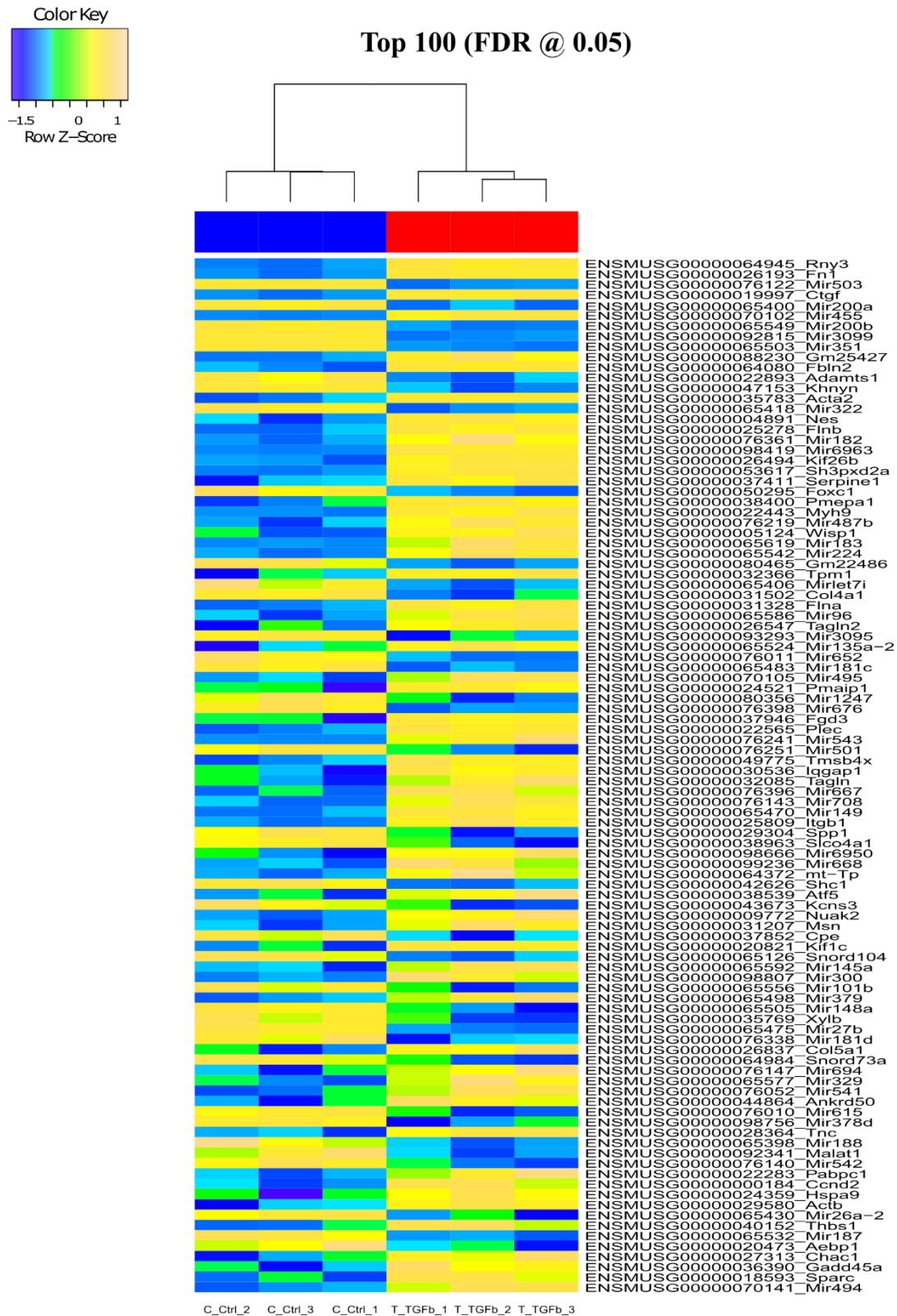


**Figure 5-5 Top 100 significantly dysregulated genes in mesangial cells.**

Blue indicate greater than 2-fold downregulation, yellow indicate greater than 2-fold upregulation, green indicate  $\pm$  50% dysregulation. Genes are labelled with both Ensembl gene identifiers (ENSMUSG) and official gene symbols.

miRNA are classified primarily upon their seed region which allows miRNA to be classified into families based on mRNA targets (217). Many miRNA have undergone genomic duplication and in some places undergone minor sequence mutations giving rise to isoforms that maintain target redundancy (218). Collapsing these duplications and isoforms into core identifiers reveals that there are 95 miRNA which are commonly detected between PTC and MC (Figure 5-6a). Of these, only 5% are seen to be commonly significantly upregulated and 11% are commonly significantly downregulated. These data support the notion that miRNA regulation occurs in a cell specific manner (219).

74 miRNA were also uniquely detected in PTC (Figure 5-6b). Within this population there is a disproportionate percentage of upregulated miRNA with 23% being significantly upregulated and 19% being downregulated. Conversely, there are 344 miRNA uniquely detected in MC (Figure 5-6c). The trend towards upregulation is preserved in MC with 13% of all detected miRNA being significantly upregulated compared to 8% being significantly downregulated. Similar to the mRNA sequencing experiments, there is a subset of miRNA which are inversely expressed between the two cell types (Figure 5-6d). This subset consists of 37 miRNA of which, only 2 are significantly downregulated and 2 are significantly upregulated.

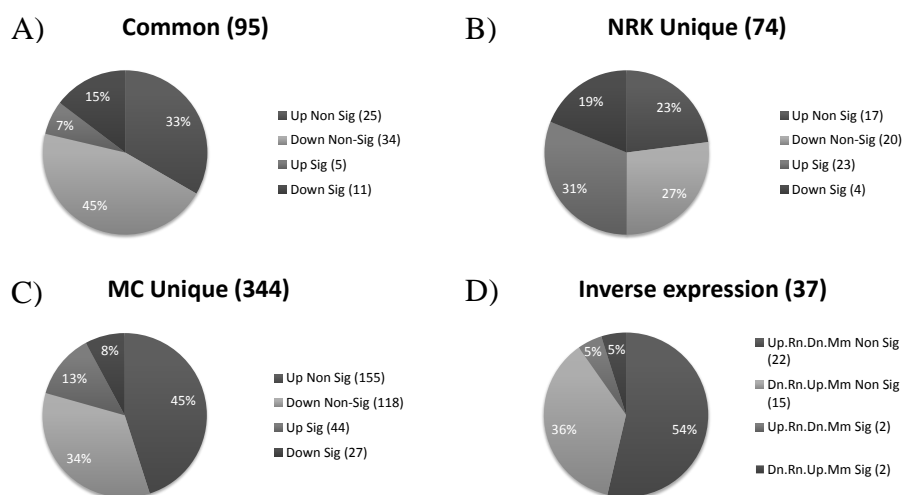


**Figure 5-6 Comparative summary of TGF $\beta$ -induced miRNA dysregulation in proximal tubule epithelial cells and mesangial cells**

A) Proportions of miRNA which were commonly dysregulated in PTC and MC. B) Breakdown of miRNA which were detected in PTC and not MC. C) Breakdown of miRNA which were detected in MC and PTC. D) miRNA which were commonly detected between cell types and were inversely expressed between PTC (Rn) and MC (Mm). *~/Results3\_supp//Figure6\_supp*

TGF $\beta$  is known to dysregulate a number of miRNA which are involved in various aspects of the development and progression of DN (213). A number of these miRNA were detected in the short RNA sequencing datasets. Specifically, miR-let7 and miR-30 family members in addition to miR-200b were all downregulated with miR-29b being upregulated in both PTC and MC (Table 52). Of these, only miR-200b and miR-30c were found to be significantly dysregulated. Furthermore, ‘nephropathic’ miRNA were uniquely dysregulated in PTC with miR-21 being upregulated and miR-30d being downregulated (Table 5-3). There were several DN related miRNA uniquely detected in MC with only miR-200a observed to be significantly downregulated (Table 5-4). It is interesting to note that many of these miRNA which are known to be involved in the cellular pathology of DN display cell specificity in regard to TGF $\beta$ -induced dysregulation.

**Table 5-2 logFC and adjusted *p*-values of miRNA involved in DN.**

miRNA	logFC.MC	adj.Pval.MC	logFC.PTC	adj.Pval.PTC	Direction
miR-192	0.451	2.55E-02	-0.195	1.48E-01	inverse
<i>miR-200b</i>	-2.950	3.56E-41	-0.715	1.66E-03	same
miR-215	0.393	5.97E-01	-0.251	5.05E-01	inverse
miR-29b	1.228	1.51E-03	0.088	8.15E-01	same
miR-30a	-0.256	3.94E-01	-1.285	7.00E-52	same
<i>miR-30c</i>	-0.628	4.02E-02	-1.097	2.79E-11	same
miR-30e	-0.265	3.79E-01	-0.379	7.59E-05	same
miR-let7a	0.872	6.18E-04	-0.575	1.48E-01	inverse
miR-let7b	-0.038	9.49E-01	-0.368	1.48E-04	same
miR-let7c	0.643	1.07E-02	-0.313	3.71E-02	inverse
miR-let7f	0.520	3.95E-02	-0.073	8.84E-01	inverse
miR-let7i	-0.607	3.21E-03	-0.156	2.99E-01	same

**Table 5-3 DN-associated miRNA uniquely detected in PTC.**

miRNA	logFC	adj.Pval
<i>miR-21</i>	1.535	4.20E-85
<i>miR-30d</i>	-0.499	2.48E-06
miR-93	-0.260	9.60E-02
miR-let7d	-0.149	1.90E-01

**Table 5-4 DN-associated miRNA uniquely detected in MC**

miRNA	logFC	adj.Pval
<i>miR-200a</i>	-3.205	4.47E-41
miR-29a	0.406	1.64E-01
miR-30b	-0.421	4.04E-01
miR-200c	0.533	8.92E-01

Both the general and cell specific effects of TGF $\beta$  seen in mRNA sequencing experiments extend to miRNA dysregulation. Although some of the differences observed are likely due to discrepancies between mouse and rat genome annotations in addition to the number of miRNA which have been identified in both species, a portion of these differences are likely to be attributable to cell specific effects of TGF $\beta$ . However, it is encouraging to see detection and dysregulation of a number of miRNA which have previously been implicated in the progression and development of DN including, but not limited to, members of the miR-29 and let-7 families in addition to miR-21 (220-222).

### **5.3. Contribution of TGF $\beta$ -mediated miRNA dysregulation to signalling pathway enrichment**

There are currently few tools available which allow sufficient mining and integration of mRNA and miRNA high-throughput sequencing data. However, it is possible to integrate these two datasets through combined analysis utilising a number of *R* packages. In particular, *mirIntegrator* allows generation of custom miRNA/mRNA networks using KEGG pathways as a base (223). These custom networks can then be tested for gene enrichment utilising *ROntoTools* which is an *R* port for Onto-Tools, an established bioinformatics toolset designed for data mining based on gene ontology (170).

#### **5.3.1. Naïve miRNA-augmentation reveals core TGF $\beta$ -miRNA network pathways and highlights important pathway topology**

In order to perform integration of long and short RNA datasets, predicted miRNA target lists were acquired from *miRNA.org* (<http://www.microrna.org/microrna/getDownloads.do>). To reduce pathway complexity and increase biological relevance, the predicted target lists from *microRNA.org* were filtered against the miRNA datasets so that only miRNA which were both detected and significantly dysregulated were integrated into the KEGG pathways. The remaining miRNA-target interaction lists were then integrated into KEGG pathways using *mirIntegrator* followed by DGE data integration along with pathway enrichment utilising *ROntoTools*.

The top 10 results from IFA on *R.norvegicus* KEGG pathways integrated with miRNA-target interactions are listed in Table 5-5. Extra pathway information resulting from miRNA integration returns a number of pathways important to DN which were previously

unidentified by GAGE pathway analysis in PTC such as PI3K-AKT signalling, Hippo signalling, janus kinase (JAK)-signal transducer and activator of transcription (STAT) signalling, cytokine-cytokine receptor interaction and importantly, TGF $\beta$ -signalling (220, 224-226). Interestingly, only the p53 and focal adhesion pathways were previously identified by GAGE. This indicates that although miRNA may be involved in regulation of these pathways, they may not play any major role in their regulation. Furthermore, IFA is much more conservative than over-representation analysis (ORA) methods such as GSEA thus reducing the likelihood of false-positives (pPert vs. pORA respectively).

**Table 5-5 Top 10 hits from impact factor analysis on augmented rat KEGG signalling pathways.**

~/Results3\_supp/Table5\_supp

pathID	pathNames	pPert	pORA	pComb	pPert.fdr	pORA.fdr	pComb.fdr
path:rno04022	cGMP-PKG signaling pathway	4.98E-03	6.48E-17	1.00E-07	6.74E-02	1.01E-16	1.34E-06
path:rno04060	Cytokine-cytokine receptor interaction	4.98E-03	2.35E-23	1.00E-07	6.74E-02	1.45E-22	1.34E-06
path:rno04115	p53 signaling pathway	4.98E-03	3.54E-25	1.00E-07	6.74E-02	3.81E-24	1.34E-06
path:rno04151	PI3K-Akt signaling pathway	4.98E-03	4.37E-19	1.00E-07	6.74E-02	8.75E-19	1.34E-06
path:rno04350	TGF-beta signaling pathway	4.98E-03	1.86E-16	1.00E-07	6.74E-02	2.71E-16	1.34E-06
path:rno04390	Hippo signaling pathway	4.98E-03	6.55E-14	1.00E-07	6.74E-02	7.83E-14	1.34E-06
path:rno04510	Focal adhesion	4.98E-03	4.48E-20	1.00E-07	6.74E-02	1.19E-19	1.34E-06
path:rno04630	Jak-STAT signaling pathway	4.98E-03	3.02E-19	1.00E-07	6.74E-02	6.25E-19	1.34E-06
path:rno04911	Insulin secretion	4.98E-03	4.43E-19	1.00E-07	6.74E-02	8.75E-19	1.34E-06
path:rno05203	Viral carcinogenesis	4.98E-03	7.05E-10	1.00E-07	6.74E-02	7.44E-10	1.34E-06

IFA on integrated *M.musculus* KEGG pathways highlights a number of pathways also identified by IFA on integrated *R.norvegicus* KEGG pathways. This includes the focal adhesion, PI3K-AKT signalling and cytokine-cytokine receptor interaction pathways (Table 5-6). Identification of these pathways in PTC highlights a potentially core set of pathways which TGF $\beta$  regulates through miRNA-mediated gene dysregulation. Furthermore, IFA reveals a number of pathways not highlighted by GAGE analysis in MC including peroxisome proliferator-activated receptor (PPAR) signalling, Hedgehog signalling, protein processing in endoplasmic reticulum signalling and epidermal growth factor receptor (ErbB) signalling pathways. Not only does this support the cell-specific miRNA-dysregulation presented above but also that the regulation of these pathways, at least in the case of TGF $\beta$ -mediated regulation, is highly dependent upon miRNA expression levels.

**Table 5-6 Top 10 hits from impact factor analysis on augmented mouse KEGG signalling pathways.**

~//Results3\_supp//Table6\_supp

pathID	pathNames	pPert	pORA	pComb	pPert.fdr	pORA.fdr	pComb.fdr
path:mmu03320	PPAR signaling pathway	4.98E-03	3.72E-07	1.00E-07	8.13E-03	2.98E-06	9.18E-07
path:mmu04012	ErbB signaling pathway	4.98E-03	2.11E-07	1.00E-07	8.13E-03	1.97E-06	9.18E-07
path:mmu04015	Rap1 signaling pathway	4.98E-03	6.71E-07	1.00E-07	8.13E-03	4.37E-06	9.18E-07
path:mmu04060	Cytokine-cytokine receptor interaction	4.98E-03	3.73E-09	1.00E-07	8.13E-03	1.09E-07	9.18E-07
path:mmu04141	Protein processing in endoplasmic reticulum	4.98E-03	1.95E-08	1.00E-07	8.13E-03	3.44E-07	9.18E-07
path:mmu04151	PI3K-Akt signaling pathway	4.98E-03	9.16E-10	1.00E-07	8.13E-03	4.03E-08	9.18E-07
path:mmu04310	Wnt signaling pathway	4.98E-03	2.25E-07	1.00E-07	8.13E-03	1.98E-06	9.18E-07
path:mmu04340	Hedgehog signaling pathway	4.98E-03	2.12E-07	1.00E-07	8.13E-03	1.97E-06	9.18E-07
path:mmu04360	Axon guidance	4.98E-03	5.05E-10	1.00E-07	8.13E-03	2.96E-08	9.18E-07
path:mmu04510	Focal adhesion	4.98E-03	1.72E-12	1.00E-07	8.13E-03	1.52E-10	9.18E-07

Although IFA utilises network topology in order to determine pathway perturbation, there is no immediate way to determine which interactions in any given pathway may contribute to a given score. However, visual inspection of pathway topology can be achieved through rendering of KEGG pathways with DGE data for both mRNA and miRNA through utilisation of the *R* packages *graph* and *RgraphViz* (227, 228). There are a number of layout algorithms available within *RgraphViz* but the *fdp* algorithm, which is an implementation of the Fruchterman-Reingold force-directed algorithm, gives the most appropriate layout for immensely complex pathways. The *fdp* algorithm arranges graph nodes based on interconnectivity with those being most connected clustered together and therefore indicates a level of pathway topology not seen in conventional KEGG pathways. For example, inspection of the *fdp* layout of the augmented TGF $\beta$ -signalling pathway reveals that many of the miRNA targeting this pathway are highly connected (Figure 5-7). Pathway elements such as SMAD-family proteins and TGF $\beta$ RI and bone morphogenetic protein (BMP)-receptor 1 being tightly controlled through miRNA action whereas Rho signalling components and BMP-family cytokines are not. Given too much information, as is the case with the MC datasets, these pathways become unsuitable for print. However, since they are scaled vector graphics they are readily browseable digitally (Figure 5-8). As such, it becomes necessary to filter the data beyond mere exclusion of non-significantly differentially expressed miRNA.

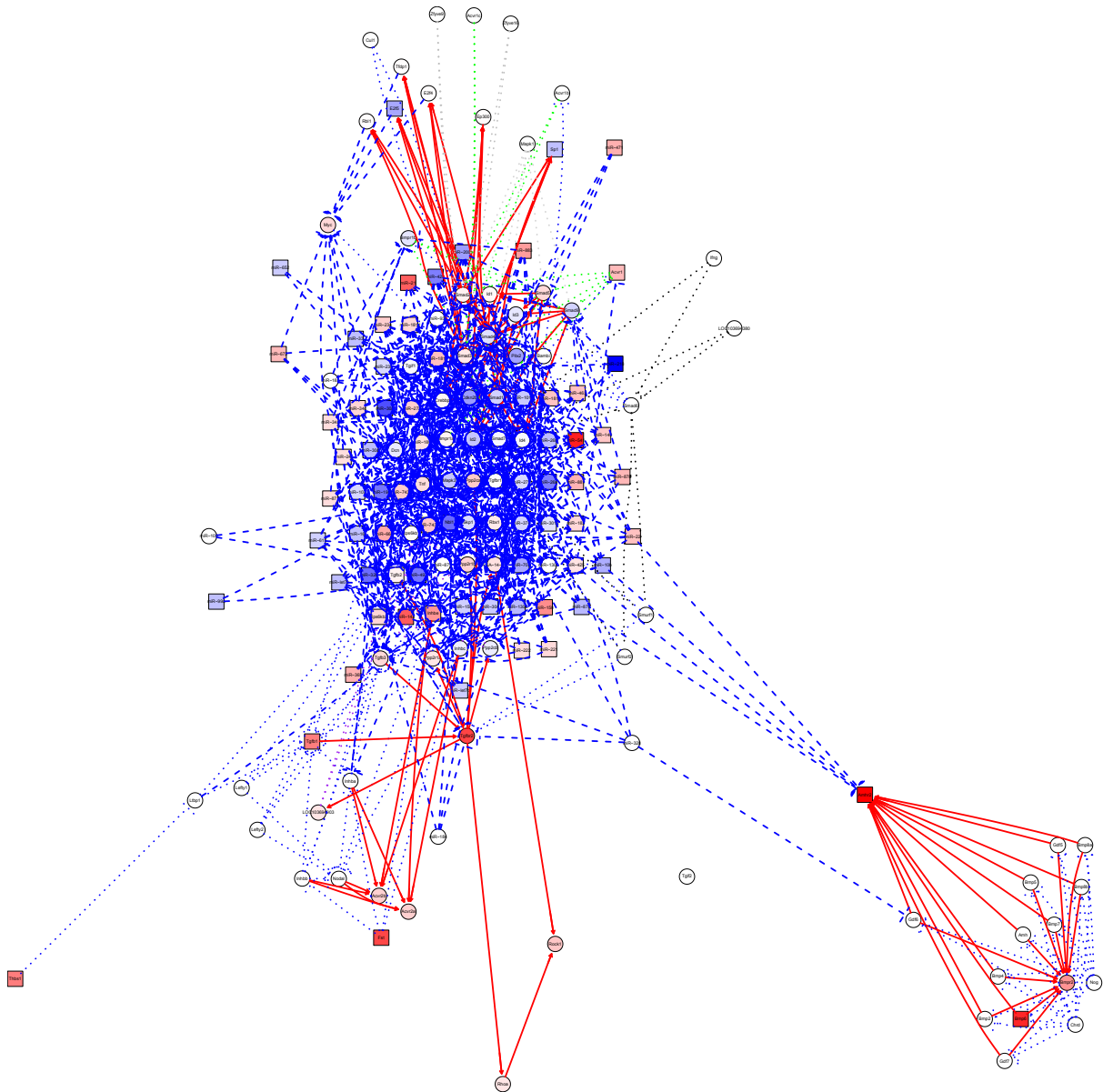


**Figure 5-7 Rat TGF $\beta$  signalling pathway (KEGG ID: 04350) augmented with miRNA-gene interactions.**

Arrangement with the fdp algorithm results in a custom network which highlights pathway topology. BMP cytokines are clustered in the lower right of the network and are not influenced by miRNA expression levels. Rho signalling members which are located to the left of this group are also not influenced by miRNA levels. The miRNA were pre-filtered for those that were significantly dysregulated and both miRNA and mRNA DGE data were rendered to the network with red nodes being up regulated and blue nodes being downregulated. *~//Results3\_supp//Figure7\_supp;*  
*~//Results3\_supp//ROntoTools\_paths\_naive//PTC*

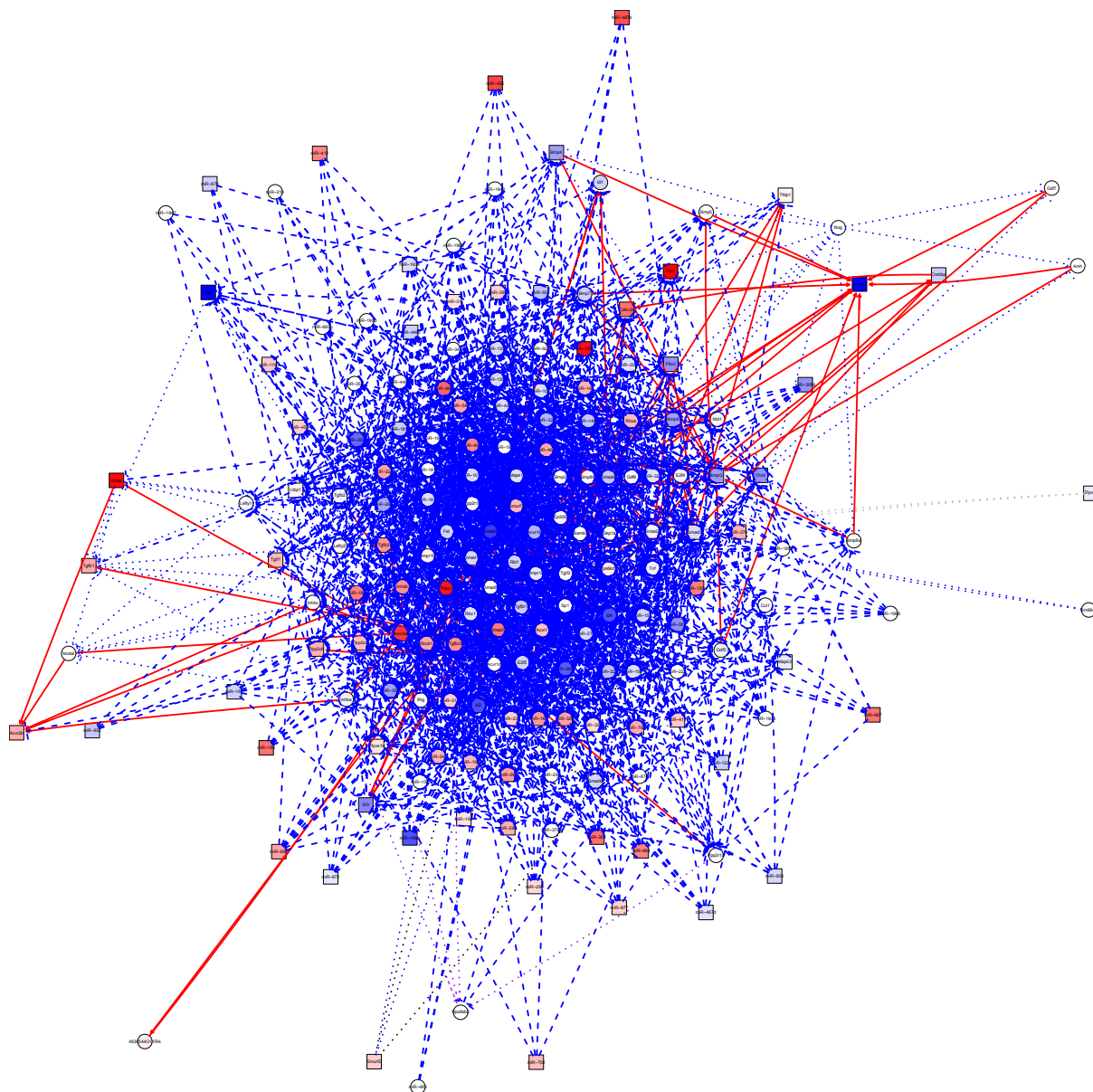


**Figure 5-8 Mouse TGF $\beta$  signalling pathway (KEGG ID: 04350) augmented with predicted miRNA-gene interactions.**

The increased genome annotation and miRNA identification in *M.musculus* result in much more complex networks from the MC datasets than that seen in PTC datasets. While this hinders readability of hardcopies, these pathways are digitally browseable either programmatically or, if exported from R as pdf files, with a standard pdf viewer. Regardless, this network reflects the true nature of miRNA-mediated gene regulation and highlights the need for discriminate data filtering.

*~//Results3\_supp//Figure8\_supp; ~//Results3\_supp//ROntoTools\_paths\_naive//MC*

### 5.3.2. Biased augmentation reveals novel roles for established and unestablished DN-associated miRNA

The high level of complexity inherent in miRNA integrated pathways such as that above (see Figure 5-9) can be somewhat reduced by filtering the input miRNA target lists beyond those that are merely significantly dysregulated. To this end, miRNA-target interaction lists were filtered for miRNA which have an established role in DN (Table 5-2) and, as expected, pathway complexity was greatly reduced (Figure 5-9). An additional benefit of biased pre-filtering is that novel miRNA-target interactions, such as that between miR-30-family members and TGF $\beta$ RI or false-hit predictions such as that between miR-21 and TGF $\beta$ RI immediately become apparent without further *in silico* interrogation. Furthermore, by utilising this biased approach, the potential impact of specific miRNA, or groups of miRNA on the global transcriptional landscape can be determined.

Biased pathway integration and subsequent IFA analysis on PTC data indicated that the scores of a number of top ranking pathways in the naïve approach are dependent upon novel miRNA-target interactions (Table 5-7). The Hippo signalling, JAK-STAT signalling and the TGF $\beta$  signalling pathways were all absent from the top 20 significantly perturbed pathways following integration of known DN-relevant miRNA. Conversely, several pathways appear amongst the top ranking pathways including ECM-receptor interaction, the complement and coagulation cascade and a number of immune/inflammatory pathways which were previously poorly ranked. Collectively, these data indicate that in PTC, novel interactions between unidentified miRNA and targets contributed to the previously high ranking of some pathways while those that have ranked highly in the biased approach do so because of novel interactions between known DN-associated miRNA and known/unknown mRNA targets.

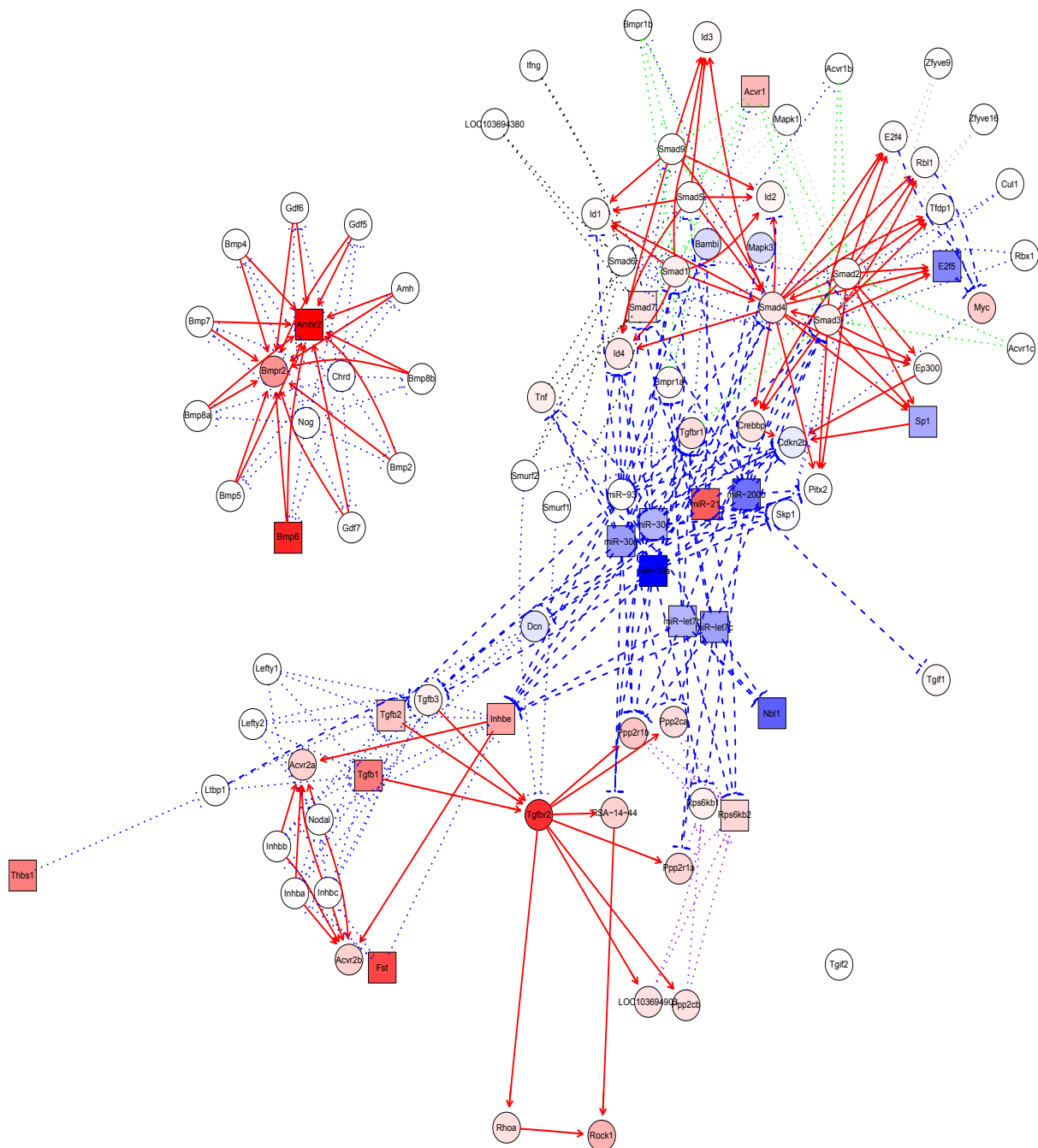


**Figure 5-9 Rat TGF $\beta$  signalling pathway (KEGG ID: 04350) augmented with predicted miRNA-gene interactions for DN-associated miRNA.**

Pre-filtering greatly reduces pathway complexity and improves readability. Although power is lost in terms of visually mining for novel miRNA important for any given pathway, it can be seen here that the downregulated miR-30-family targets potentially upregulate TGF $\beta$ RI. Conversely, miR-21 is upregulated and targets TGF $\beta$ RI and therefore, at least in this experiment, represents a false-hit. miRNA were pre-filtered for those that were significantly dysregulated. Both miRNA and mRNA DGE data were rendered to the pathway with red being upregulated and blue being downregulated.

*~/Results3\_supp//Figure9\_supp; ~/Results3\_supp//ROntoTools\_paths\_bias//PTC*

**Table 5-7 Top 10 results from impact factor analysis of rat KEGG pathways augmented with DN-associated miRNA**

~//Results3\_supp//Table7\_supp

pathID	pathNames	pPert	pORA	pComb	pPert.fdr	pORA.fdr	pComb.fdr
path:rno04610	Complement and coagulation cascades	9.95E-03	2.98E-07	1.93E-07	4.03E-02	1.71E-05	2.36E-05
path:rno04512	ECM-receptor interaction	1.49E-02	1.09E-08	2.84E-07	4.06E-02	1.88E-06	2.36E-05
path:rno05323	Rheumatoid arthritis	3.48E-02	1.90E-07	6.33E-07	5.35E-02	1.63E-05	3.50E-05
path:rno04060	Cytokine-cytokine receptor interaction	4.98E-03	2.07E-05	1.76E-06	4.03E-02	4.45E-04	5.40E-05
path:rno04151	PI3K-Akt signaling pathway	9.95E-03	1.11E-05	1.88E-06	4.03E-02	3.18E-04	5.40E-05
path:rno05150	Staphylococcus aureus infection	5.47E-02	2.10E-06	1.95E-06	6.27E-02	9.03E-05	5.40E-05
path:rno04510	Focal adhesion	4.98E-03	5.09E-05	4.10E-06	4.03E-02	6.26E-04	9.73E-05
path:rno04115	p53 signaling pathway	1.49E-02	3.10E-05	7.21E-06	4.06E-02	4.89E-04	1.50E-04
path:rno05321	Inflammatory bowel disease (IBD)	4.98E-03	1.21E-04	9.21E-06	4.03E-02	1.04E-03	1.70E-04
path:rno05320	Autoimmune thyroid disease	7.96E-02	1.11E-05	1.32E-05	8.42E-02	3.18E-04	2.16E-04

When performing the same analyses on MC datasets, colorectal cancer, leukocyte transendothelial migration and Ras signalling pathways were all uniquely highly perturbed in the biased IFA compared to both biased PTC and naïve MC and PTC experiments (Table 5-8). These pathways may represent highly novel roles for the tested ‘nephropathic’ miRNA with the interactions in these pathways requiring further investigation. Conversely, focal adhesion, PI3K-AKT signalling and cytokine-cytokine receptor interaction pathways all remained in the top most perturbed pathways following miRNA data trimming. These pathways also ranked highly in both naïve and biased IFA on PTC data indicating that these pathways are likely to represent core TGF $\beta$ -mediating pathways. Furthermore, the miRNA tested in the biased approach play an important role in propagating the effects of TGF $\beta$  on these pathways.

**Table 5-8 Top 10 results from impact factor analysis of mouse KEGG pathways augmented with DN-associated miRNA**

~//Results3\_supp//Table8\_supp

pathID	pathNames	pPert	pORA	pComb	pPert.fdr	pORA.fdr	pComb.fdr
path:mmu04510	Focal adhesion	4.98E-03	6.12E-09	1.00E-07	7.67E-03	5.38E-07	9.56E-06
path:mmu04151	PI3K-Akt signaling pathway	4.98E-03	1.71E-06	1.66E-07	7.67E-03	7.87E-05	9.56E-06
path:mmu04360	Axon guidance	4.98E-03	1.79E-06	1.74E-07	7.67E-03	7.87E-05	9.56E-06
path:mmu05205	Proteoglycans in cancer	4.98E-03	3.23E-06	3.05E-07	7.67E-03	1.14E-04	1.26E-05
path:mmu04060	Cytokine-cytokine receptor interaction	4.98E-03	1.27E-05	1.11E-06	7.67E-03	3.72E-04	3.66E-05
path:mmu04014	Ras signaling pathway	4.98E-03	3.95E-05	3.23E-06	7.67E-03	7.73E-04	8.89E-05
path:mmu04141	Protein processing in endoplasmic reticulum	4.98E-03	4.74E-05	3.83E-06	7.67E-03	8.34E-04	9.04E-05
path:mmu04512	ECM-receptor interaction	4.98E-03	1.98E-04	1.46E-05	7.67E-03	2.90E-03	3.01E-04
path:mmu04670	Leukocyte transendothelial migration	4.98E-03	2.44E-04	1.77E-05	7.67E-03	3.30E-03	3.25E-04
path:mmu05210	Colorectal cancer	1.49E-02	1.15E-04	2.45E-05	1.66E-02	1.84E-03	4.04E-04

However, as demonstrated with *gage* analysis, although TGF $\beta$  may utilise common pathways in disparate cell types, the ways in which these pathways are utilised may differ significantly. This is particularly prominent here and is highlighted by the vastly different network topologies obtained for the same KEGG pathway when integrating data from differing cell types under identical conditions (Figure 5-10a, Figure 5-10b).

IFA demonstrates, as have other analyses on miRNA or mRNA alone, that TGF $\beta$  acts on a central set of pathways and processes in PTC and MC. Encouragingly, cell specificity in the actions of TGF $\beta$  which were demonstrated through the various analyses share some degree of congruency even with the integration of miRNA data with mRNA data. The enormous complexity of the resulting augmented networks can be reduced through reduction of the number of inputs but this creates a biased, artificial environment. This bias is especially pronounced when using analyses such as IFA which takes into consideration many more factors than traditional ORA or functional class scoring (FCS) analysis (229). Regardless, these simplified networks can be viewed as standalone objects which may be used for rapidly assessing the potential validity of predicted miRNA-gene interactions.

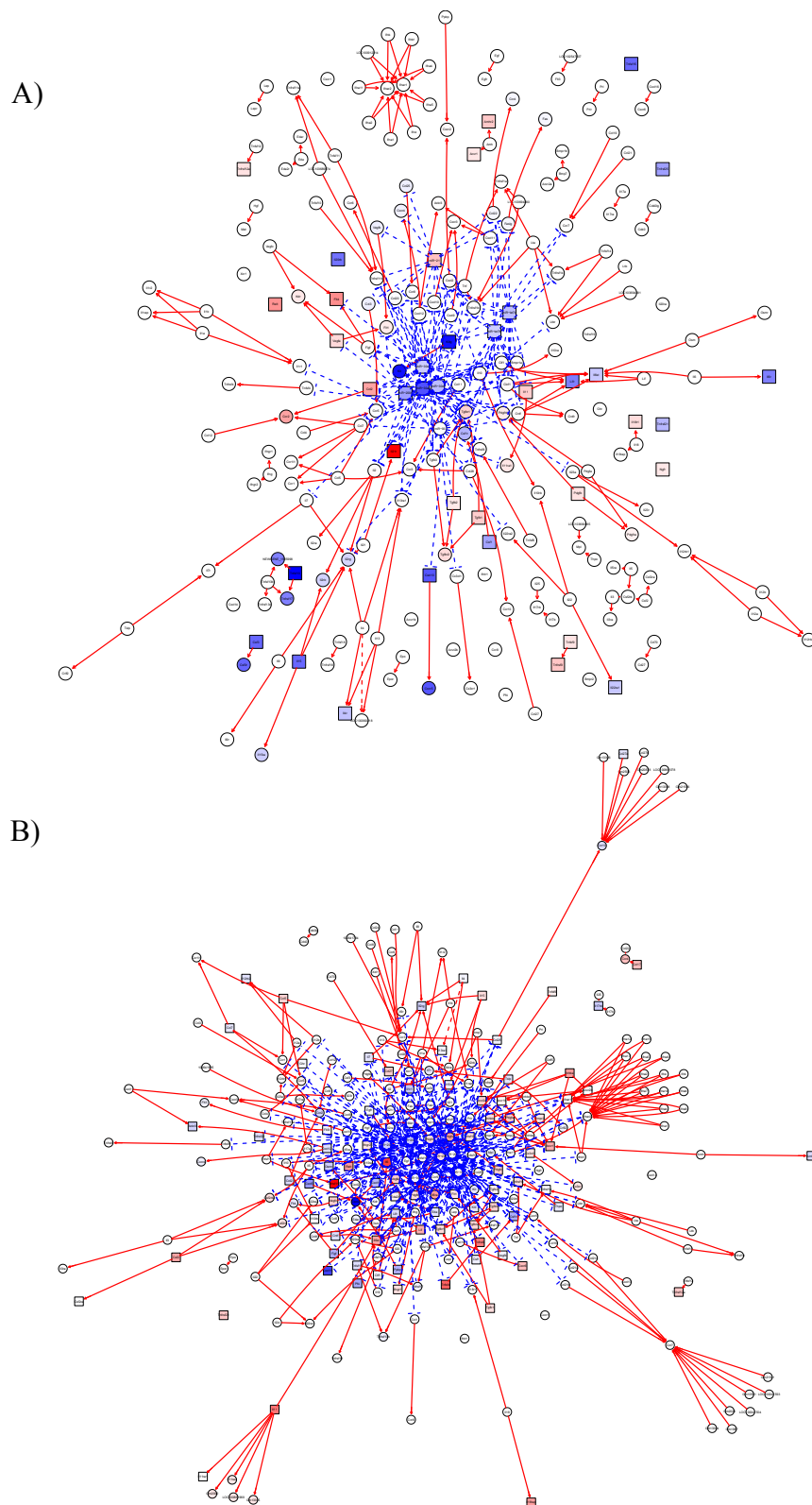


**Figure 5-10 TGF $\beta$  induces specific pathway topologies in PTC and MC.**

Following integration of DN-related miRNA, the cytokine-cytokine receptor pathway (KEGG ID: 04060) takes on specific topologies in (A) PTC and (B) MC in response to TGF $\beta$  treatment. The pathways highlight the cell specific nature in which TGF $\beta$  may affect the same signalling pathway through miRNA dysregulation. *~//Results3\_supp//Figure10\_supp*

## 5.4. Discussion

This chapter has explored and presented the effects of TGF $\beta$ -mediated miRNA dysregulation on the global transcriptional landscape in both PTC and MC. As with the *gag*e experiments presented in the previous chapter, the TGF $\beta$ -mediated miRNA transcriptome impacts upon signalling topography in both a general and a cell specific manner. Furthermore, a subset of miRNA known to be involved in DN were seen to impact upon pathways not previously identified using the global miRNA population. These studies not only highlight the impact on TGF $\beta$ -mediated miRNA dysregulation but also provide a means for rapidly identifying novel miRNA-target interactions in experimental datasets.

An emerging aspect of TGF $\beta$  biology is its role in dysregulation of a growing number of miRNA (230, 231). These small non-coding RNA post-transcriptionally regulate gene expression through targeting of 7 nucleotide regions within the 3' UTR of mRNA transcripts (232). There is considerable redundancy in miRNA-mRNA interactions with a single mRNA being targeted by multiple miRNA. miRNA are also highly promiscuous with single miRNA often having hundreds of mRNA targets. This creates an immensely complex regulatory network that acts to fine tune gene expression. Despite the redundancy and promiscuity of miRNA, they have emerged to be important players in the development and progression of a number of pathologies including DN (233). There has been little progress in system biology approaches in regard to miRNA networks and the roles that they play in disease. Indeed, much of the literature is focused on single miRNA-mRNA interactions and the downstream processes that these interactions impact upon.

In this study, two variations of a novel approach were taken in an attempt to bridge the information gap between mRNA and miRNA dysregulation. Both variations involved augmentation of KEGG signalling pathways with predicted miRNA-mRNA interactions. One approach took a semi-naive approach where potential interactions were filtered for miRNA that were significantly altered in the DGE datasets. The other approach took a biased approach utilising only interactions of a set of miRNA known to be important in DN. Augmented pathways were then integrated with DGE data for both miRNA and mRNA. They were then tested for biological relevance through IFA. This analytical method is superior to current systems biology methods which are primarily focused on either overrepresentation of gene ontology terms or on ranked overrepresentation of genes amongst all other genes in a pathway (229, 234). The strength of IFA is that it incorporates classical overrepresentation

techniques with gene-product and gene-gene interaction information and therefore provides a more realistic measure of potential biological significance.

The statistical results gained through IFA are vastly different to those obtained through more traditional pathway analysis methods utilising mRNA DGE data alone due to both the testing methods and the integration of miRNA data. *ROntoTools* utilises a novel approach to pathway analysis based upon the concept of IFA which is superior to traditional pathway analysis methods which rely on over representation of particular genes and gene ontology terms (229, 235, 236). Instead, IFA incorporates classical overrepresentation techniques with gene-product and gene-gene interaction and interaction type, expression data and DGE statistical information therefore providing a more realistic measure of potential biological significance.

IFA is centred on computation of an impact factor which incorporates a calculated perturbation factor (Pert) (234). Pert values incorporate DGE data for individual genes and the entire dataset, ORA statistics, the type of interactions between genes and also the  $p$ -value of differentially expressed genes. Pert scores are then used to generate an accumulated per gene perturbation factor value which is utilised to generate a  $p$ -value for pathway perturbation (pPert) (229). Finally,  $p$ -values of ORA (pORA) and Pert are combined to give a representation of a specific pathway being involved in a condition (pComb), or in the case of this study, a treatment response phenotype, above all other analysed pathways.

Both naïve and biased approaches to IFA yielded a subset of signalling pathways which likely represent a central mechanism of TGF $\beta$  induced cellular pathology in PTC and MC including PI3K-AKT signalling, cytokine-cytokine interaction and focal adhesion pathways. Indeed, TGF $\beta$  is known to regulate PI3K-AKT signalling leading to epithelial-mesenchymal transition related fibrotic signalling and also tubular hypertrophy as seen in early DN (126, 237). In MC, PI3K-AKT signalling can induce oxidative stress through decreased SOD2 expression and increased cell survival via downregulation of BCL-2 interacting mediator of cell death (BIM), both of which are important in glomerulosclerosis (238). Several cytokine families play various roles in the development and progression of DN (135, 239). While the links between TGF $\beta$  and some of these cytokines is known, inspection of the augmented cytokine-cytokine receptor interaction pathway reveals that TGF $\beta$  connects almost all mapped cytokines and their receptors with one another through targeting miRNA. This demonstrates a previously unrecognised level of control exerted by TGF $\beta$  over cellular physiology with some of these interactions, such as those between miR-30 family members

and interleukin 21 receptor (IL21R) or miR-let7 family members and interleukin 11 (IL-11), not having been described in DN. Finally, loss of focal adhesions is required for cell motility in PTC and MC and also leads to loss of contractile functions in MC in response to vasoconstrictors (240, 241). miR-200 and miR-30 families are predicted to target SRC homology 2 domain containing transforming protein 1 (SHC1) with their inverse expression in these datasets potentially indicating a novel method whereby TGF $\beta$  controls focal adhesion and subsequently cell proliferation and migration (242).

Pathways which were perturbed in PTC but not MC include p53 and JAK-STAT signalling pathways which are important in tubular necrosis and induction of EMT respectively (243, 244). Furthermore, tubular cell senescence is known to be promoted by the p53 pathway, specifically by cyclin dependent kinase inhibitor 1a (CDKN1A) in response to high glucose and may be further induced by TGF $\beta$ -mediated downregulation of miR-374 which directly targets CDKN1A (245). Conversely, JAK-STAT signalling may be increased via derepression of interleukin 23 alpha subunit (IL-23a) through downregulation of miR-30d. The p53 pathway was identified by both semi-naïve and biased approaches to IFA indicating that known diabetic miRNA may play a major role in regulating flux through this pathway. Furthermore, JAK-STAT signalling appears to be mostly regulated by novel miRNA-gene interactions as it was not ranked highly in the biased analysis.

Pathways uniquely disturbed in MC include PPAR and wingless-type MMTV integration site family (WNT) signalling pathways. PPAR $\gamma$  agonists have been shown to inhibit TGF $\beta$ -induced FN1 expression in mesangial cells therefore reducing glomerular sclerotic injury (246). Inspection of the augmented PPAR network reveals that miR-1938 is upregulated in response to TGF $\beta$  and directly targets, and potentially downregulates, solute carrier family 27 member 1 (SLC27A1), a membrane bound fatty acid transporter upstream of PPAR $\gamma$ . This novel interaction highlights a potential miRNA-mediated mechanism by which TGF $\beta$  induces FN1 expression in MC through repression of PPAR $\gamma$  signalling. WNT4A and WNT5A serve to protect mesangial cells from glycogen synthase kinase 3  $\beta$  (GSK3 $\beta$ ) mediated apoptosis yet are downregulated by high glucose (247). In this dataset, no miRNA are predicted to target WNT4A or WNT5A. However, frizzled class receptor 1 (FZD1) and FZD7 are potentially downregulated by miR-135a/b and miR-184 respectively which may act to inhibit WNT signalling (248). It is evident that IFA performed on augmented pathways not only provides valuable data on the genome wide effects of TGF $\beta$  on both mRNA and miRNA but

also represents a convenient method whereby novel miRNA-gene interactions can be quickly assessed.

The differing results between GAGE and IFA approaches are partially attributable to the incorporation of miRNA data. Given that miRNA expression, to an extent, is cell-type specific, it is no surprise that the detected miRNA populations with PTC and MC differ considerably. Regardless, there is still considerable congruency between the two disparate cell types in regard to miRNA expression. This is likely to contribute to the similarities observed in IFA. Likewise, the differences observed in those miRNA which are considered to be important in DN may contribute greatly to the differences seen between the cell types in the biased IFA approach. However, the lack of concordance between PTC and MC in regard to DN related miRNA is rather unexpected given the established roles that these miRNA play in the pathogenesis of DN (213, 220, 233, 249-252). Much of the evidence for these miRNA in DN has been garnered from *in vivo* studies. Furthermore, given that the bulk of the renal cortex is comprised of tubular regions this may explain, at least partly, some of the observed differences in this subset of miRNA.

An underlying concern in miRNA research is the accuracy of miRNA-mRNA interaction prediction algorithms and this is discussed further in Chapter 7. However, it should be noted here that algorithm accuracy can help clarify certain experimental phenomena such as that observed in MC which tended to increase miRNA expression without a reciprocal change in mRNA populations. This was not observed under identical experimental conditions in PTC and may therefore represent fundamental differences in species or cell specific RNAi machinery or possibly species specific polymorphisms in miRNA target sites. Prediction algorithm accuracy becomes important here as the degree of complementarity in miRNA-mRNA interactions determines both the mechanism of translational repression and the fate of the mRNA molecule itself (253, 254).

Both the algorithms and the miRNA-mRNA interactions themselves may be experimentally validated through the use of modified RNA-seq protocols such as CLIP-seq (also termed HITS-CLIP) or CLASH (255, 256). These protocols are similar to ChIP in that they required immunoprecipitation of protein-nucleic acid complexes (257). However, prior to this, RNA-RNA interactions are UV-crosslinked thus affording isolation of 'active' RNA-RNA interactions. There are a number of differences between the protocols which are beyond the scope of this discussion. Regardless, keeping in mind the reasons for seeking out such alternative protocols, CLASH would prove the superior option. This is due to CLASH involving 5'-3' ligation of cross linked miRNA-mRNA molecules prior to sequencing. This

affords miRNA-target interactions to be read as a single hybrid RNA molecule (256). When coupled with Argonaute immunoprecipitation, this would provide a snap-shot of specific, and active, miRNA-mRNA interactions.

There is a distinct lack of tools available for the integrative analysis of mRNA and miRNA RNA-seq or microarray data. This analytical void is even more distinct when attempting to undertake global or systems based approaches to integrative analysis of miRNA upon canonical signalling pathways. This chapter has presented a novel approach to integration and analysis of miRNA- and mRNA-seq datasets from two important renal cell types. The IFA method has been utilised in both a semi-naïve and biased approach, both of which have led to results including both novel and literature supported findings, thus adding to the validity of the approach. Both the IFA approaches taken and the results obtained from such approaches provide an analytical framework for future studies and for investigation of novel miRNA-target interactions while also filling a gap in the analytical tools available for assessment of global signalling network disruption. Furthermore, the data presented have provided important insight into the actions of TGF $\beta$  in PTC and MC and the ways in which it utilises miRNA to influence the global transcriptional landscape.

## **6. Results IV – miR-21 regulates mitochondrial function by targeting of ACAT1 and AK2**

### **6.1. Introduction**

Diabetic nephropathy progresses as a result of the cumulative dysfunction of a number of cell types in response to both hyperglycaemia and circulating factors secreted from other affected tissues. PTC are particularly important in DN as they play a central role in the development of tubulointerstitial fibrosis through both synthesis of ECM proteins and also via recruitment and transdifferentiation of mesenchymal stem cells (52, 54). PTC also promote renal inflammation through recruitment and activation of macrophages and other leukocytes which produce both ROS and inflammatory cytokines (97).

Mitochondria, a major source of ROS, have gained increasing attention from the research community. PTC are particularly prone to mitochondrial dysfunction for two main reasons; 1) they require energy for glucose reabsorption and which occurs in an entirely insulin independent manner and 2) the way in which they take up glucose requires active maintenance of artificial concentration gradients (35, 37). Therefore, in hyperglycaemic conditions PTC not only are exposed to an intracellular high glucose environment but they expend considerable amounts of energy in order to arrive at this state. As with many aspects of DN, this can result in a feed-forward loop with increasing glucose uptake requiring increased mitochondrial activity, producing increasing ROS leading to mitochondrial DNA damage and subsequently faulty ETC machinery leading to further ROS production (124).

Although many of these processes are mediated by TGF $\beta$ , microRNA are becoming increasingly recognised as mediators of cellular pathology in PTC (249, 258, 259). However, the role of TGF $\beta$ -mediated miRNA in the mitochondrial dysfunction observed in PTC in DN has gained little attention. To this end, this section explores the role of a known fibrotic TGF $\beta$ -regulated miRNA, miR-21, in mitochondrial dysfunction. Indeed, miR-21 appears to induce a mitochondrial phenotype which mimics that of TGF $\beta$  indicating that this miRNA may be involved in the propagation of TGF $\beta$ -mediated mitochondrial dysfunction. Furthermore, novel targets of miR-21 are identified and validated as direct targets and are also found to mimic the phenotype of TGF $\beta$  and miR-21 on mitochondria. Importantly, repression of these targets, acetyl-CoA acetyltransferase 1 (ACAT1) and adenylate kinase 2

(AK2), induces changes in important fibrotic genes and growth factors suggesting that miR-21-mediated repression of ACAT1 and AK2 may be a contributing factor to the fibrotic phenotype of PTC induced by TGF $\beta$ .

## 6.2. miR-21 alters mitochondrial function and morphology

Mitochondrial dysfunction is increasingly being recognised as an important player in DN pathophysiology. However the mechanisms responsible for this dysfunction and in what way they contribute to cellular pathology is still under investigation. TGF $\beta$  is known to be important in mitochondrial health and induces mitochondrial superoxide formation, an important mediator in tubulointerstitial fibrosis and DN in general. As miR-21 is heavily involved in propagation of fibrotic signals downstream of TGF $\beta$ , it stands to reason that miR-21 may also be involved in mediating the effects of TGF $\beta$  on mitochondria.

Mitochondrial superoxide content was assessed by way of fluorescence-activated cell sorting (FACS) analysis of MitoSox stained cells. Mitochondrial superoxide production was significantly increased by TGF $\beta$  with a non-significant increase induced by exogenous miR-21 (Figure 6-1a). As seen in chapter 3, exogenous miR-21 expression augments the effects of TGF $\beta$  on mitochondrial superoxide content. The increased level of superoxide production may indicate increased mitochondrial activity or, conversely, blockade in the electron transport chain. Regardless, further mitochondrial and cellular parameters may be altered either as a result of increased ROS production or possibly propagate increased ROS.

Mitochondrial membrane potential was measured via FACS analysis of cells stained with the potentiometric dye JC-1. This stain undergoes a shift in the emission maxima from 529nm to 590nm as it aggregates in the mitochondria in a membrane potential dependent manner. Increases in mitochondrial potential are indicated by an increase in the green:red ratio. The mitochondrial membrane potential tended increase with TGF $\beta$ -treatment, albeit this change did not reach statistical significance (Figure 6-1b). However, miR-21 alone significantly increased membrane potential above baseline levels with the combination of miR-21 and TGF $\beta$  having no significantly greater effect than miR-21 alone.

Production of ATP via oxidative phosphorylation is membrane potential dependent. Hence, changes in membrane potential may lead to changes in cellular ATP levels. Indeed, cellular ATP content was significantly reduced by both TGF $\beta$  treatment and exogenous miR-21 expression (Figure 6-1c). The combination of miR-21 and TGF $\beta$  did not result in reduction in

ATP levels beyond that of TGF $\beta$  alone. Collectively, these data indicate that miR-21-mediated gene dysregulation may play a role in TGF $\beta$ -mediated mitochondrial dysfunction in PTC.

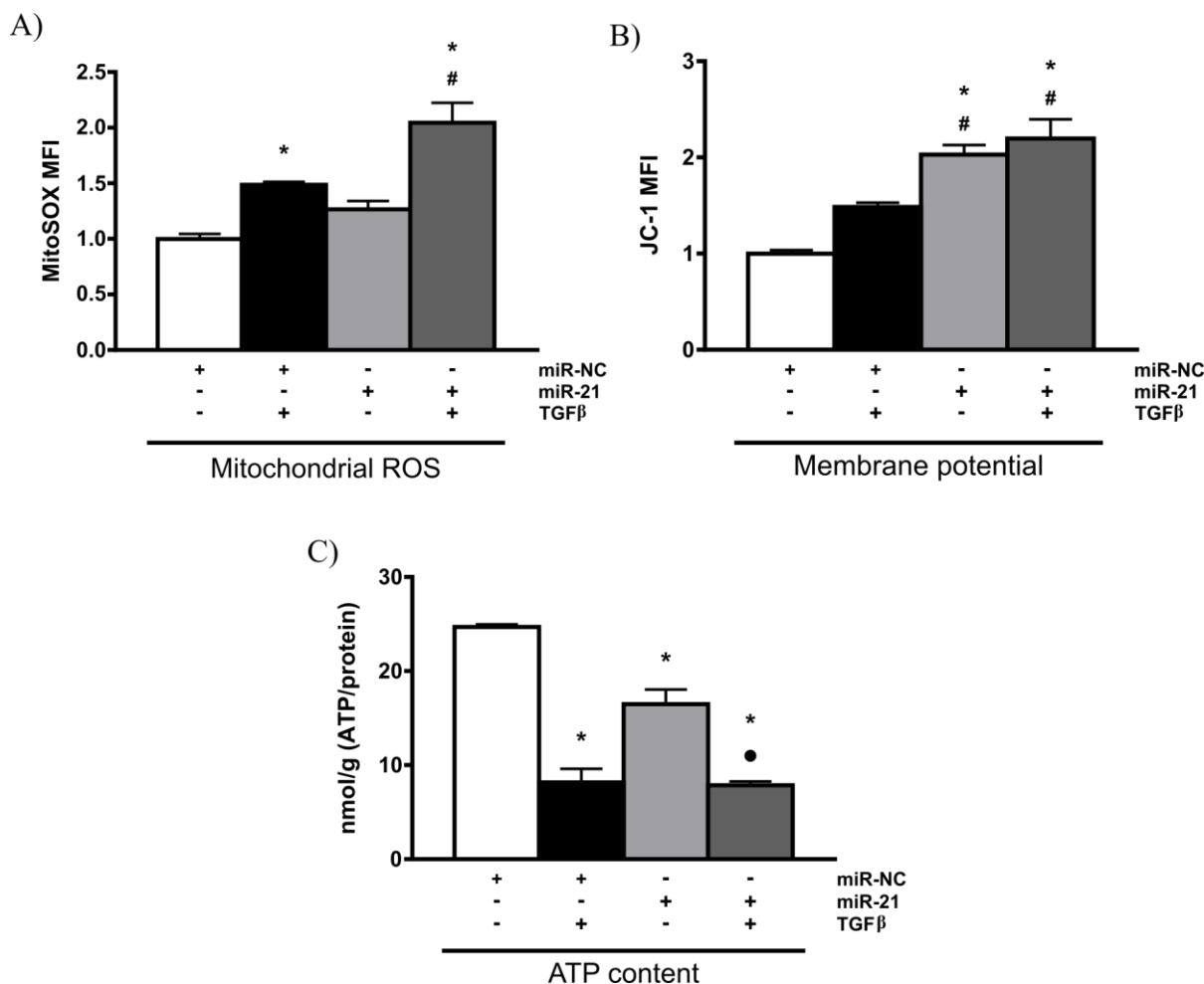


**Figure 6-1 TGF $\beta$  and miR-21 impact important mitochondrial parameters.**

A) Mitochondrial superoxide increases with TGF $\beta$  treatment and this increase is augmented by the exogenous miR-21. B) miR-21 increases mitochondrial membrane potential whilst TGF $\beta$  induces a trend to increase membrane potential. C) Both TGF $\beta$  and miR-21 decrease cellular ATP content. All data are Mean+SEM, N=6 per group, Tukey One-way ANOVA; \* $p < 0.05$ , Untreated vs. All; #  $p < 0.05$ , All vs. TGF $\beta$ ; •  $p < 0.05$ , miR-21 vs. miR-21 + TGF $\beta$ .

Alterations in basic mitochondrial parameters, as seen above (Figure 6-1) are likely to impact upon cellular respiration. The oxidative respiration capacity of PTC treated with TGF $\beta$  or miR-21 or miR-21 and TGF $\beta$  in combination was assessed via utilisation of the *Seahorse Bioanalyser* platform. This platform measures cellular oxygen consumption at both resting

states and after in assay delivery of oligomycin (ATP synthase blocker), FCCP (inner mitochondrial membrane proton carrier), antimycin A (complex III blocker) and rotenone (complex I blocker) injected at each point as indicated in Figure 6-2a. Measurement of oxygen consumption following each injection allows determination of basal mitochondrial respiration (Figure 6-2b), ATP production required for normal cellular activity (Figure 6-2c), proton leakage across the inner mitochondrial membrane (Figure 6-2d), maximal respirative capacity (Figure 6-2e) and respirative capacity beyond resting levels (Figure 6-2f).

Many of these parameters, including basal respiration, proton leak, maximal respiration and spare respiratory capacity were nonsignificantly increased by either TGF $\beta$  or miR-21 with ATP production only being increased by miR-21. Furthermore, combination treatment with miR-21 and TGF $\beta$  resulted in significant increases in basal respiration, maximal respiration, and spare respiratory capacity beyond that of untreated cells. This indicates that, as with TGF $\beta$ -mediated fibrotic gene expression, miR-21 may be contributing to mitochondrial dysfunction in PTC downstream of TGF $\beta$ .

Mitochondrial morphology is generally considered a function of mitochondrial health. Mitochondria typically exist in dynamic tubular networks and undergo fragmentation as a result of pathological cellular stress. PTC mitochondria are seen to possess typical mitochondrial morphology in healthy cells (Figure 6-3a, upper left panel). However, upon TGF $\beta$  treatment or exogenous miR-21 expression, the mitochondrial network is seen to break down with mitochondria taking on a fragmented appearance (Figure 6-3a, upper right and lower left panels). Exogenous miR-21 in combination with TGF $\beta$  treatment induces mitochondrial morphology that does not depart greatly from that induced by miR-21 or TGF $\beta$  alone (Figure 6-2a, lower right panel). Interestingly, these morphological changes were not associated with changes in mitochondrial content/mass as indicated by FACS analysis of cells stained with MitoTracker Green (Figure 6-3b). These changes may be a passive response to the internal changes described above or may be actively induced as a result of TGF $\beta$ /miR-21 induced changes in the mitochondrial dynamics machinery.

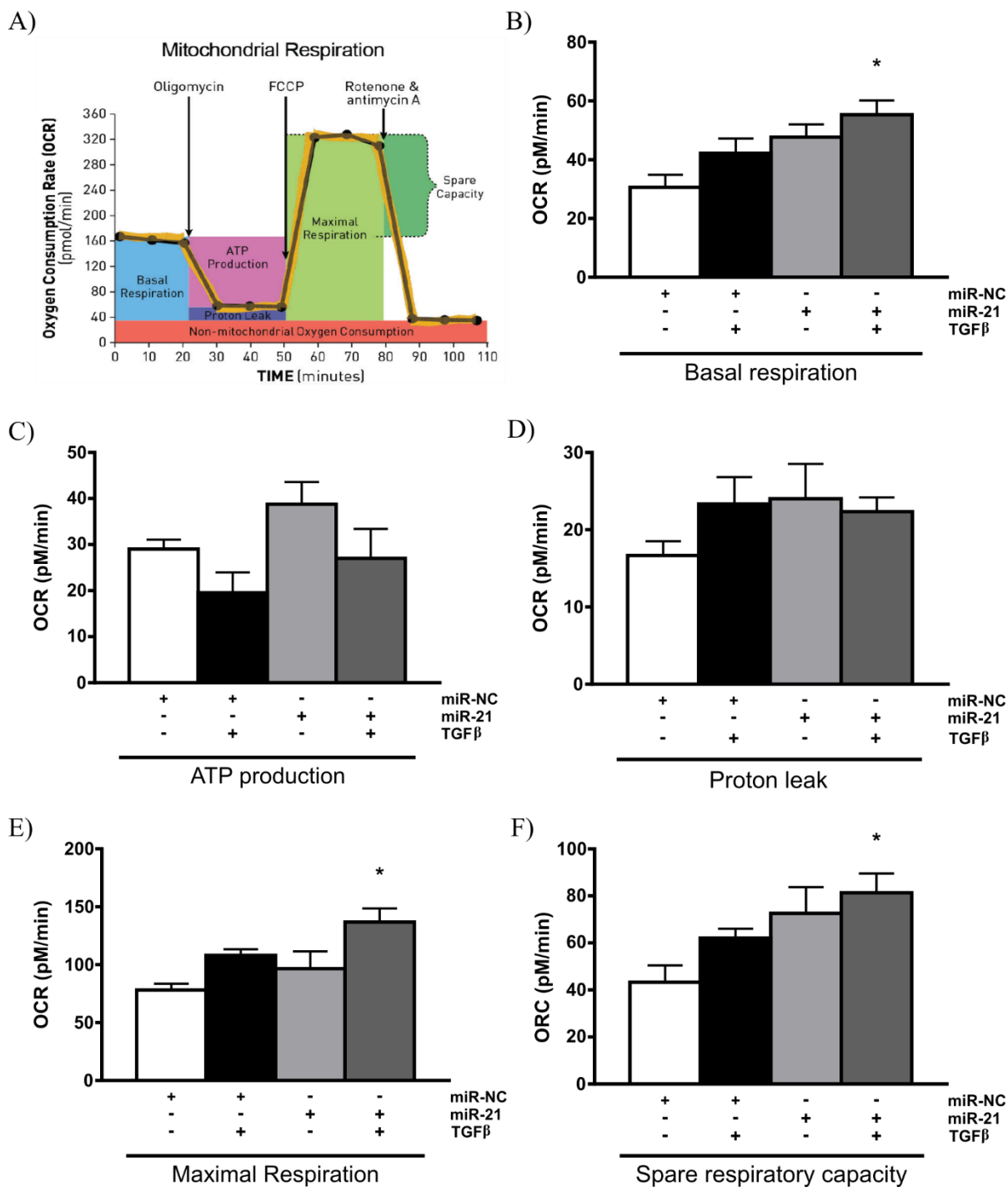


**Figure 6-2 Mitochondrial respiration parameters under TGFβ or miR-21 are mostly unaffected.**

A) Various compounds are delivered in assay and provide data about a number of aspects of mitochondrial respiration. Although mostly nonsignificant, miR-21 and TGFβ trended to increase (B) basal respiration, (C) ATP production, (D) proton leakage, and (E) maximal respiration and (F) spare respiratory capacity. The combination of miR-21 and TGFβ resulted in significant increases in basal respiration (B), maximal respiration (E) and spare respiratory capacity (F). All data are Mean+SEM, N=6 per group, Tukey One-way ANOVA; \* $p < 0.05$ , Untreated vs. All.

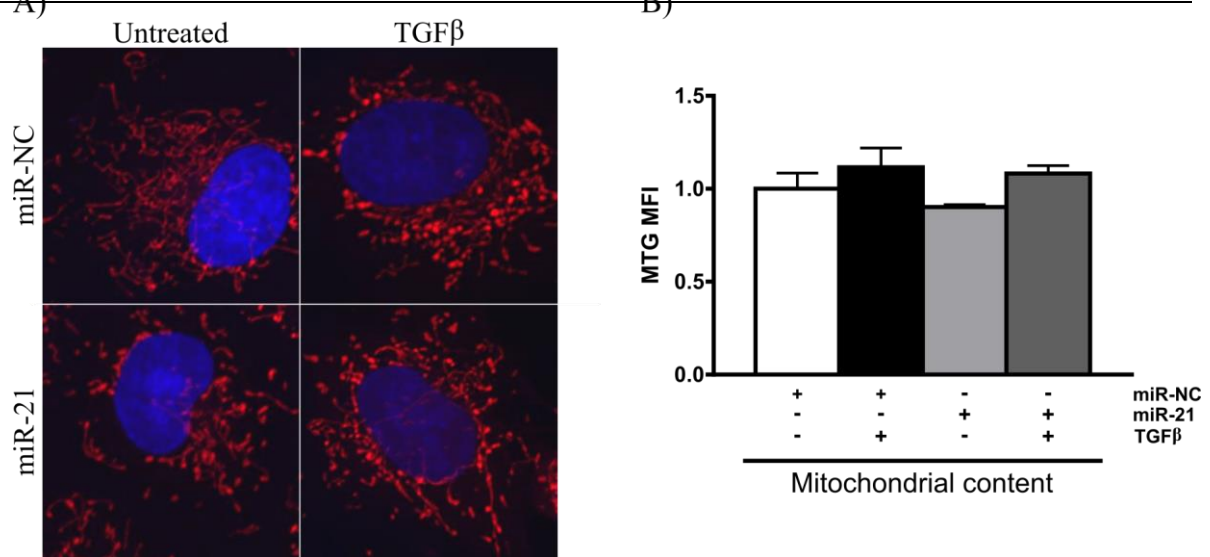


**Figure 6-3 miR-21 and TGFβ induce changes in mitochondrial morphology but not cellular mitochondrial content.**

A) Mitochondrial fragmentation is induced in PTC following treatment with either TGFβ or miR-21.  
 B) Mitochondrial fragmentation does not result in changes in cellular mitochondrial content/mass as indicated by FACS analysis of cells stained with MitoTracker Green.

Despite the increased fragmented mitochondrial phenotype induced by miR-21 and TGFβ, dynamin-related protein 1 (DRP1), a mitochondrial fission mediator, is significantly downregulated by miR-21 (Figure 6-4a, Figure 6-4c). TGFβ partially alleviated miR-21 mediated downregulation of DRP1 protein levels. Conversely, optic atrophy 1 (OPA1), a mitochondrial inner membrane protein involved in mitochondrial fusion, was non-significantly down regulated by either miR-21 or by combination treatment with miR-21 and TGFβ (Figure 6-4b, Figure 6-4d). However, mitofusin 2 (MFN2), another mitochondrial fusion protein was significantly downregulated by both miR-21 and TGFβ treatments with the combination of the two resulting in downregulation no greater than that seen with miR-21 or TGFβ alone (Figure 6-4b, Figure 6-4e). These changes in mitochondrial dynamics machinery do not clearly indicate a shift towards an increase in active mitochondrial fission. However, these changes may result in an inability to efficiently undergo fusion which may result in the observed mitochondrial morphological phenotype through spontaneous fission.

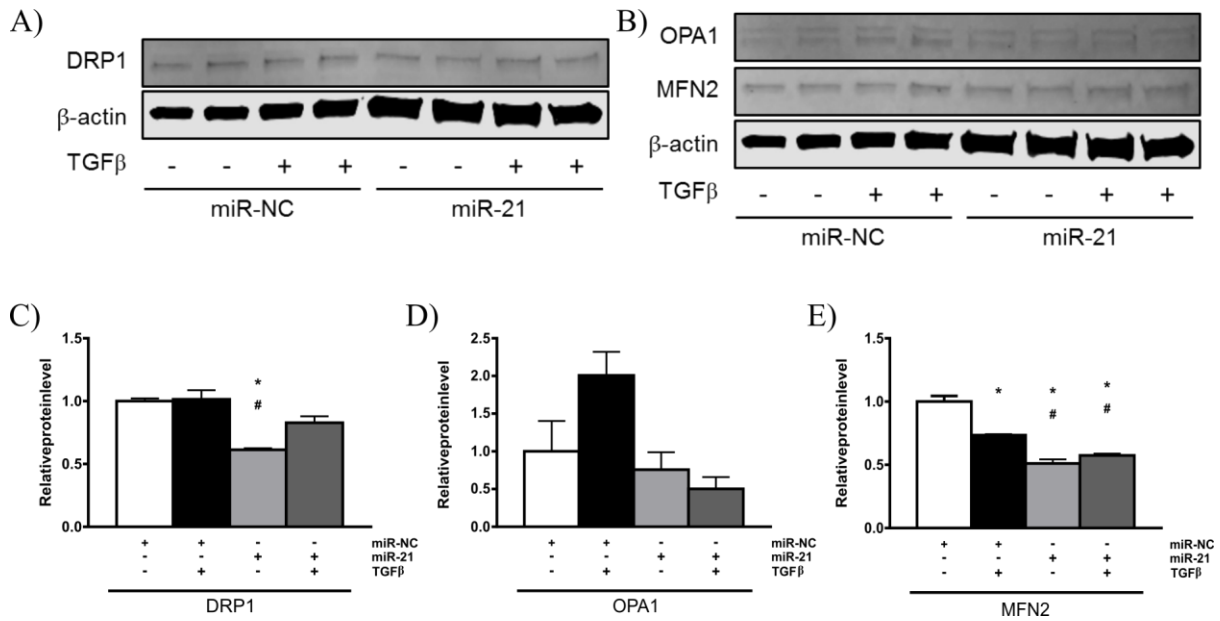


**Figure 6-4 miR-21 alters protein levels of mitochondrial dynamics machinery.**

Both (A, C) the mitochondrial fission protein DRP1 and (B, E) the mitochondrial fusion protein MFN2 were significantly decreased by miR-21 with MFN2 also being decreased by TGFβ treatment. (B, D) OPA1, which is also a mitochondrial fusion protein, was not significantly altered despite considerable positive dysregulation by TGFβ and negative dysregulation by combination treatment with miR-21 and TGFβ. All data are Mean+SEM, N=6 per group, Tukey One-way ANOVA; \* $p < 0.05$ , Untreated vs. All; #  $p < 0.05$ , All vs. TGFβ.

### 6.3. Integrative analysis of RNA-seq data and public databases identifies novel, mitochondrially relevant targets of miR-21

#### 6.3.1. Identification of novel mitochondrially associated miR-21 targets

mRNA-seq data from PTC was utilised to mine for novel miR-21 targets. Potential miR-21 targets containing putative and non-canonical miR-21 binding sites were retrieved from the rat databases at *microRNA.org* as performed in previous experiments. This list was used to subset the mRNA-seq dataset thereby yielding expression data for miR-21 targets which were detected in the mRNA-seq experiment. 477 of the 994 predicted miR-21 targets were detected in the dataset with 63 being significantly upregulated and 60 being significantly downregulated (Figure 6-5a). Given that miR-21 is 2.8-fold upregulated in the miRNA-seq

data, more downregulated targets may be expected. However these data illustrate the many-to-one relationship between miRNA and mRNA.

Similar data manipulations can be performed utilising MitoCarta, a curated online repository of mitochondrially expressed and mitochondrially associated genes and gene products. Using this database to subset the mRNA-seq data provides DGE data for mitochondrial genes which were detected in the PTC dataset. Of the 1098 MitoCarta genes, 679 were detected with 54 being significantly upregulated and 80 being significantly downregulated (Figure 6-5b). Combining these previous two outputs provides a list of mRNA genes which are targeted by miR-21, are mitochondrially expressed/associated and are detected in the PTC mRNA-seq dataset (Figure 6-5c). The resultant output consists of 37 mRNA of which only 3 are significantly upregulated and 4 are significantly downregulated (Table 6-1). These significantly downregulated genes were selected for further study while upregulated genes were discarded as their expression levels indicate miR-21 plays a minor role in their regulation.

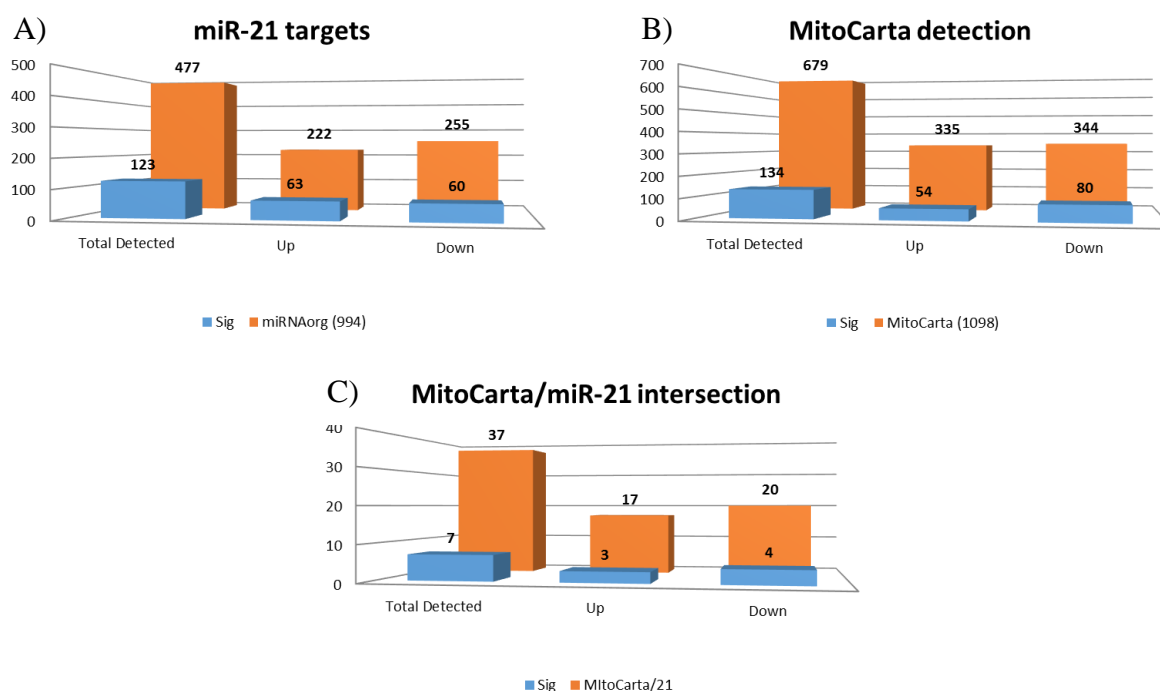


**Figure 6-5 Summary data from integration of mRNA-seq data with various resources.**

Reported here are the total number of genes returned from integration of PTC mRNA-seq data with (A) miR-21 predicted target lists from *microRNA.org*, (B) MitoCarta listed mitochondrially expressed/associated genes and (C) the integration of results from (A) and (B). Each plot breaks down directionality and significance tally for each analysis. [~/Results4\\_supp/Figure5\\_supp](#)

**Table 6-1 Significantly dysregulated genes identified following integration of PTC DGE data with MitoCarta and *microRNA.org* miR-21-target list.**

Genes selected for further study are bolded.

Ensembl.Gene.ID	ID	logFC	PValue	adj.p.value
<b>ENSRNOG00000007862</b>	<b>ACAT1</b>	<b>-0.763</b>	<b>1.15E-07</b>	<b>2.31E-06</b>
<b>ENSRNOG00000000122</b>	<b>AK2</b>	<b>-0.683</b>	<b>1.11E-06</b>	<b>1.84E-05</b>
ENSRNOG000000038001	SLC25A1	0.551	2.86E-03	1.69E-02
<b>ENSRNOG00000014338</b>	<b>SLC25A25</b>	<b>-0.603</b>	<b>1.95E-04</b>	<b>1.78E-03</b>
<b>ENSRNOG00000009088</b>	<b>TXNRD1</b>	<b>-0.452</b>	<b>1.71E-04</b>	<b>1.59E-03</b>
ENSRNOG000000045605	UXS1	0.435	1.38E-03	9.33E-03

### 6.3.2. AK2 and ACAT1 are downregulated *in vitro* and *in vivo*

Expression levels of the genes identified in the *in silico* experiments above were validated via qRT-PCR in PTC and in two experimental models of kidney disease. In PTC, TGF $\beta$  significantly reduced qRT-PCR detectable levels of mRNA for ACAT1, AK2, thioredoxin reductase 1 (TXNRD1), solute carrier family 25 member 25 (SLC25A25) albeit to a much lesser extent than that observed in the mRNA-seq dataset (Figure 6-6a-d). Repression of these genes by miR-21 was significantly greater than that by TGF $\beta$  which indicates that these mRNA are likely to be targets of miR-21. Finally, although the combination of miR-21 and TGF $\beta$  repressed the identified mRNA greater than TGF $\beta$  alone, the repressive effect of TGF $\beta$  and miR-21 on these targets was not additive.

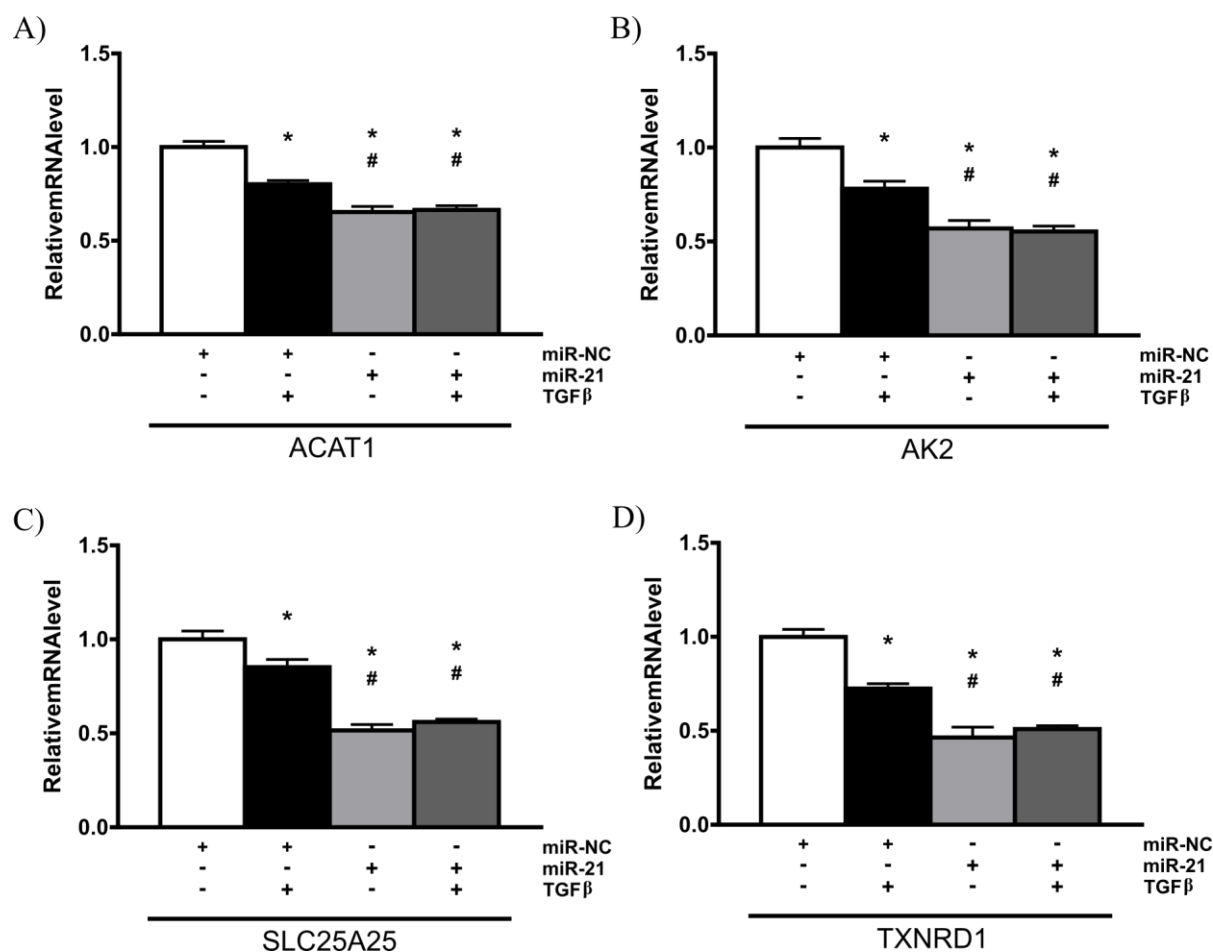


**Figure 6-6 Mitochondrially associated genes are downregulated by both TGFβ and miR-21.**

(A) ACAT1, (B) AK2, (C) SLC25A25 and (D) TXNRD1 were downregulated by TGFβ confirming mRNA-seq data. miR-21 significantly downregulated these genes greater than TGFβ alone confirming they may be miR-21 targets. All data are Mean+SEM, N=6 per group, Tukey One-way ANOVA; \* $p < 0.05$ , Untreated vs. All; #  $p < 0.05$ , All vs. TGFβ.

Gene expression was also measured in renal cortices from two experimental models of diabetes, namely streptozotocin (STZ) induced diabetic C57BL/6 mice and STZ induced diabetic uninephrectomised (UNx) Sprague Dawley rats. In diabetic mice, both ACAT1 and AK2 were significantly lower in diabetic compared to control mice. However, SLC25A25 and TXNRD1 gene expression were unaltered (Figure 6-7a, Figure 6-7b). In UNx rats, a similar pattern of expression was observed with ACAT1 and AK2 being downregulated in diabetic animals when compared to controls while SLC25A25 and TXNRD1 mRNA levels were unaltered (Figure 6-7c, Figure 6-7d). With ACAT1 and AK2 being dysregulated in experimental diabetes, these genes were selected for further study.

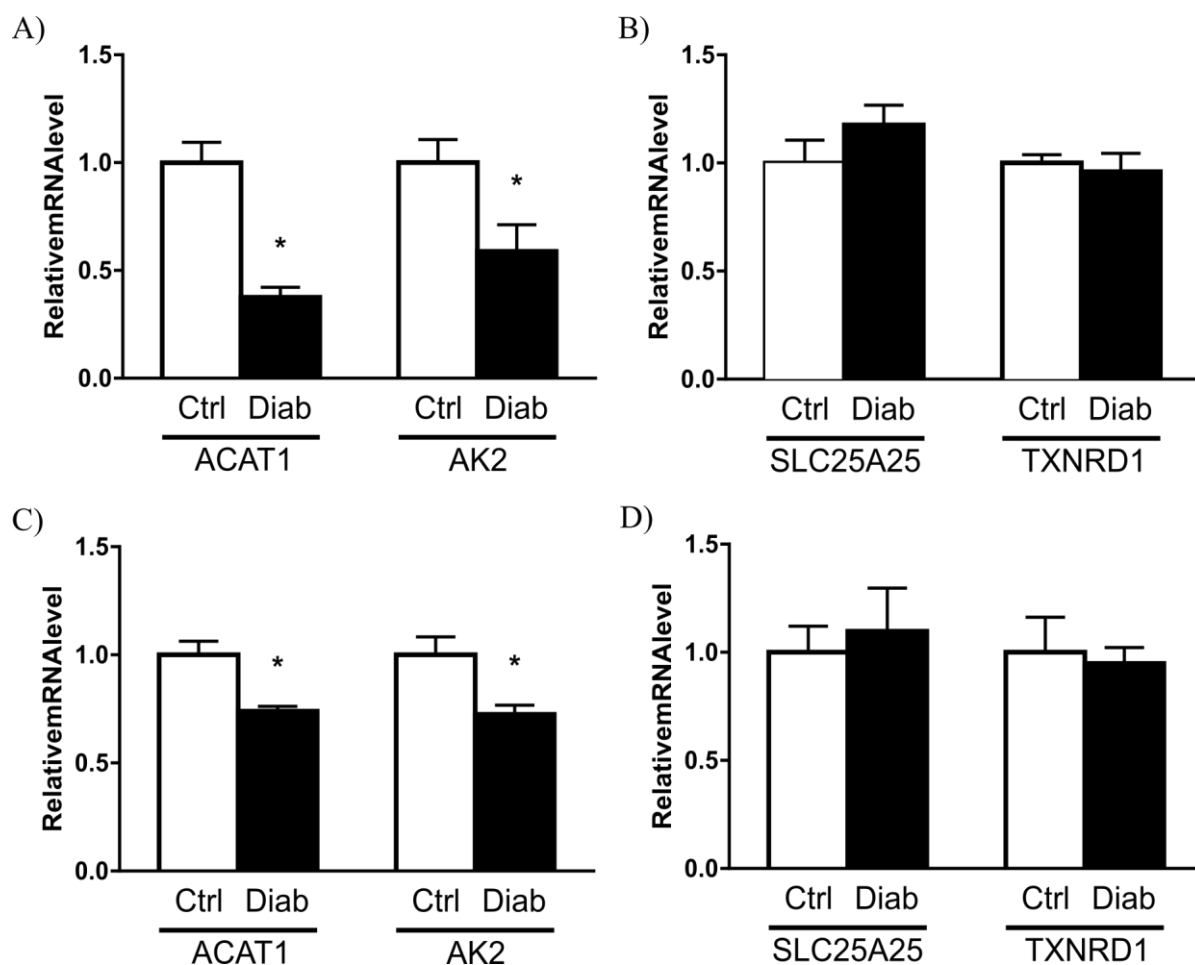


**Figure 6-7 ACAT1 and AK2 mRNA levels are decreased in experimental diabetic models.**

A) Both gene expression of ACAT1 and AK2 were decreased in STZ induced diabetic C57BL/6 mice while (B) SLC25A25 and TXNRD1 were unaltered. C) UNx diabetic rats also displayed decreased ACAT1 and AK2 mRNA levels compared to controls with (D) SLC25A25 and TXNRD1 being unchanged. All data are Mean+SEM, N=8 per group, Tukey One-way ANOVA; \* $p < 0.05$ , Control vs. Diabetic.

## 6.4. Repression of ACAT1 and AK2 is associated with changes in mitochondrial function

### 6.4.1. ACAT1 and AK2 are targeted and repressed by miR-21

Direct targeting of ACAT1 and AK2 mRNA by miR-21 was confirmed following validation of downregulation of these genes *in vitro* and *in vivo* via luciferase expression vectors containing wild-type and mutant 3' UTR sequences from ACAT1 and AK2 mRNA.

Conventionally only the miRNA seed region, that is, the region targeted by the canonical binding region of a miRNA, is mutated in such vectors. However, miR-21 targeting of these mRNA is predicted to occur by non-canonical targeting and is supplemented heavily by 3' binding of miR-21 to the target mRNA (Figure 6-8a). As such, the entire 22 nucleotide region spanned by miR-21 was mutated in these experiments by replacing the sequence with the direct complement of the original binding site.

Luciferase expression from ACAT1 wild-type 3' UTR vector was reduced by miR-21 (Figure 6-8b). Mutation of the miR-21 target site resulted in luciferase expression which was significantly greater than that seen with the wild-type 3' UTR vector. This is likely due to prohibition of binding by endogenous miR-21. However, despite target site mutation, luciferase expression was still decreased by exogenous miR-21 although this decrease was not significantly lower than expression from the wild-type vector under baseline conditions. A similar pattern was observed with the AK2 3' UTR vector with miR-21 decreasing expression of the wild-type vector and site mutation alleviating repression due to endogenous miR-21 (Figure 6-8c). The decreases observed in the mutant 3' UTR vectors induced by exogenous miR-21 may be due to miR-21 mediated dysregulation of the transcriptional machinery required for the cytomegalovirus (CMV) promoter. However this postulate requires further investigation.

In order to determine if targeting of ACAT1 and AK2 3' UTR is biologically relevant, protein levels of both ACAT1 and AK2 were measured via western blot. Exogenous miR-21 resulted in significant decreases in protein levels of both ACAT1 and AK2 (Figure 6-9a-d). Combination treatment with miR-21 and TGF $\beta$  did not result in greater repression of ACAT1 or AK2 than that by miR-21 alone. Only ACAT1 protein was decreased significantly by TGF $\beta$  alone. Collectively, these data confirm that miR-21 mediates downregulation of ACAT1 and AK2 protein expression downstream of TGF $\beta$ .



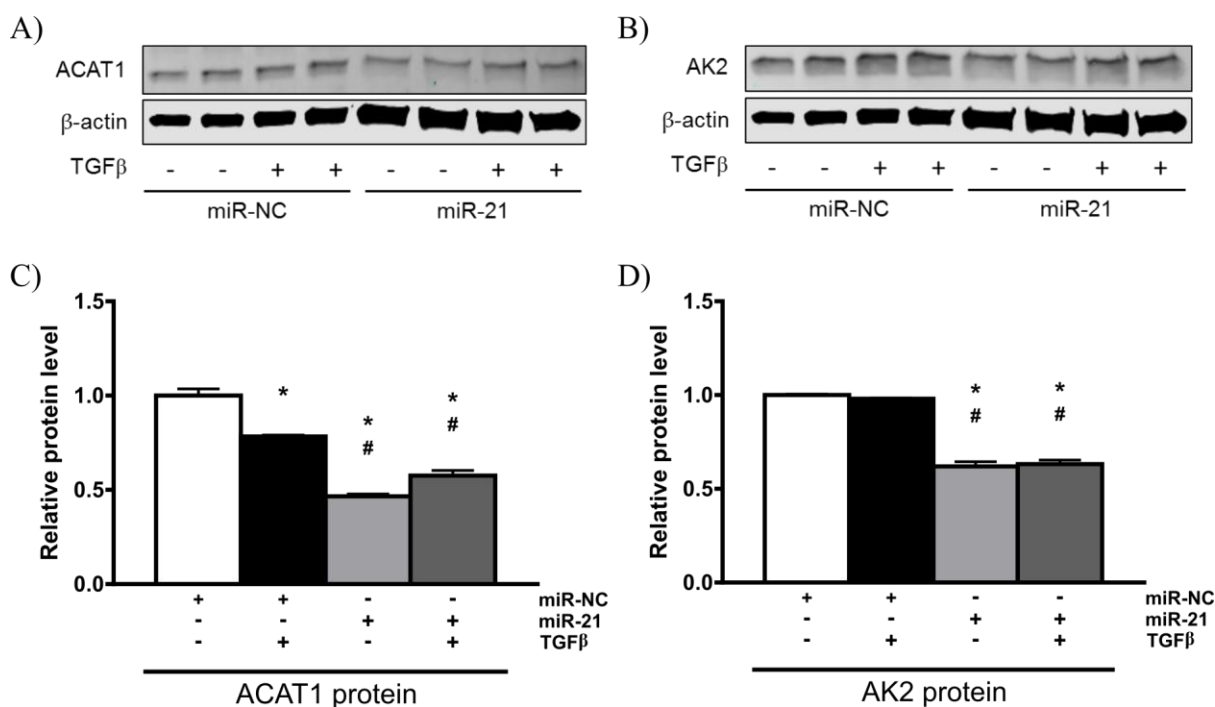


**Figure 6-9 Protein levels of ACAT1 and AK2 are decreased by miR-21.**

Exogenous expression of miR-21 significantly reduced (A,C) ACAT1 and (B,D) AK2 protein levels as detected by western blot analysis. Combination treatment with both miR-21 and TGFβ did not result in repression beyond that of miR-21 alone. All data are Mean+SEM, N=6 per group, Tukey One-way ANOVA; \* $p < 0.05$ , Untreated vs. All; #  $p < 0.05$ , All vs. TGFβ.

#### 6.4.2. siRNA-mediated repression of ACAT1 and AK2 alter mitochondrial function

##### similarly to miR-21

Short interfering RNA (siRNA) were utilised to determine what role, if any, miR-21 mediated targeting of ACAT1 and AK2 plays in mediating the effect of miR-21/TGFβ on mitochondrial function. Confirming effective targeting of siRNA against either ACAT1 or AK2, qRT-PCR detection of ACAT1 mRNA was decreased ~35% whilst AK2 mRNA levels were decreased ~30% (Figure 6-10a). At the protein level, siRNA-mediated repression of ACAT1 expression reduced detectable protein levels by 99% (Figure 6-10b, Figure 6-10d). AK2 protein levels were also reduced by 90% following siRNA delivery (Figure 6-10c, Figure 6-10e). Repression was increased to 95% with TGFβ treatment following siRNA transfection. These siRNA were subsequently utilised in an attempt to mimic the effects of miR-21/TGFβ on mitochondrial morphology and function.

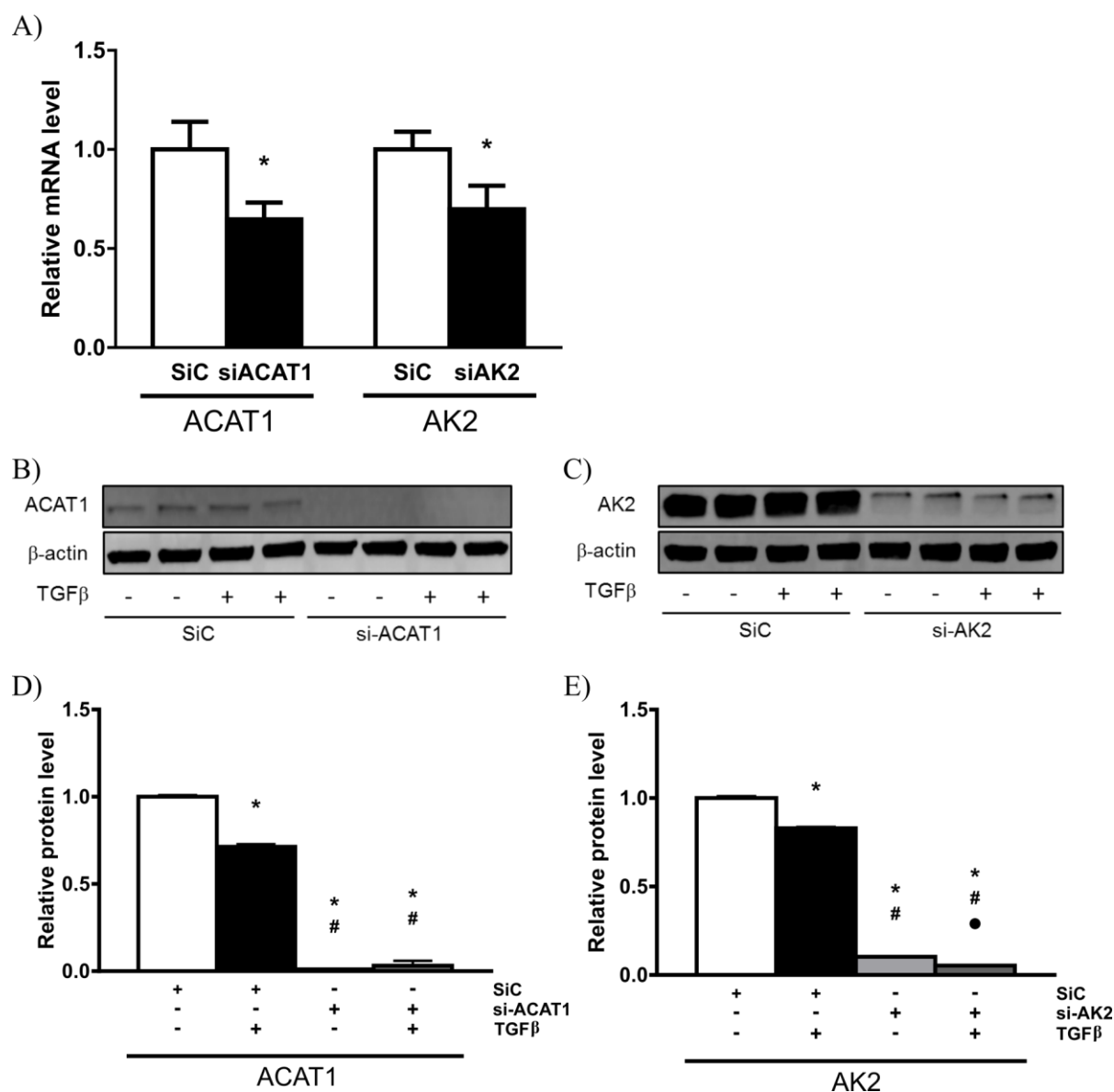


**Figure 6-10 siRNA sufficiently represses ACAT1 and AK2 gene expression.**

A) ACAT1 and AK2 mRNA levels are decreased by anti-ACAT1 and anti-AK2 siRNA respectively. C, E) ACAT1 protein levels are virtually undetectable following anti-ACAT1 siRNA treatment of PTC. D, F) anti-AK2 siRNA suppressed AK2 protein levels by 90% and was further suppressed by TGF $\beta$  treatment. All data are Mean+SEM, N=6 per group, Tukey One-way ANOVA; \* $p < 0.05$ , Untreated vs. All; #  $p < 0.05$ , All vs. TGF $\beta$ ; ●  $p < 0.05$ , target siRNA vs. target siRNA + TGF $\beta$ .

Mitochondrial superoxide content was significantly increased by siRNA-mediated repression of ACAT1 (Figure 6-11a). Anti-AK2 siRNA also significantly increased MitoSox staining in PTCs which mimics, albeit at a higher magnitude, the effects of miR-21/TGF $\beta$  on mitochondrial ROS production. Furthermore, induction of mitochondrial ROS by anti-AK2 siRNA was significantly greater than that induced by anti-ACAT1 siRNA. These findings suggest that AK2 may play a larger role in mitochondrial oxidative stress than ACAT1. The mitochondrial membrane potential was also increased by both anti-AK2 and anti-ACAT1 siRNAs. However, the change induced by siRNA-mediated repression of ACAT1 was not statistically significant (Figure 6-11b). The observed changes in mitochondrial membrane potential are approximately half that induced by the combination of exogenous miR-21 expression and TGF $\beta$  expression (Figure 6-1b) indicating that these genes may play a minor role in TGF $\beta$ -mediated regulation of mitochondrial membrane potential.

Despite the modest alterations in mitochondrial membrane potential, cellular ATP content was reduced by ~50% by anti-ACAT1 siRNA and ~20% by anti-AK2 siRNA. This implies that these genes are involved in ATP production in PTCs (Figure 6-11c). Addition of TGF $\beta$  following siRNA delivery further decreased cellular ATP levels. However this reduction, although notable, was not significantly greater than that induced by TGF $\beta$  alone. Regardless, this further reduction in ATP levels is congruent with TGF $\beta$  regulating ATP production and/or consumption via additional mechanisms not related to ACAT1 or AK2.

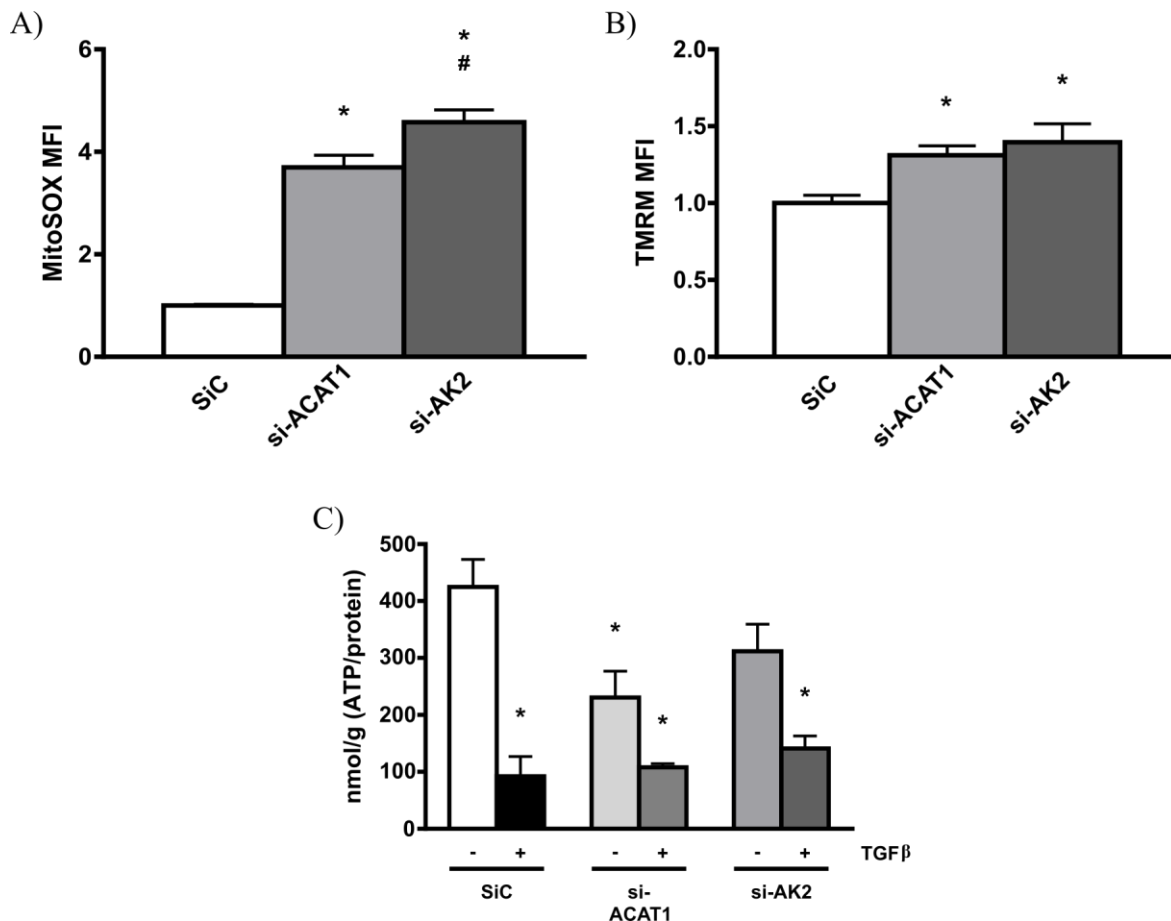


**Figure 6-11 Repression of ACAT1 or AK2 alter mitochondrial function.**

A) Mitochondrial superoxide content was increased by siRNA-mediated repression of ACAT1 or AK2. B) Although ACAT1 and AK2 repression increased mitochondrial membrane potential, only the increase induced by AK2 was statistically significant. C) siRNA against both ACAT1 and AK2 decreased cellular ATP content, albeit only the effect of ACAT1 siRNA was significant. TGF $\beta$  also significantly decreased ATP content with no additive effect observed from transfection of siRNA with TGF $\beta$  treatment. All data are Mean+SEM, N=6 per group, Tukey One-way ANOVA; \* $p < 0.05$ , Untreated vs. All; #  $p < 0.05$ , All vs. TGF $\beta$ .

### **6.5. Fibrotic effects of miR-21/TGF $\beta$ may be partially mediated through dysregulation of novel mitochondrially associated targets of miR-21**

Targeting of ACAT1 and AK2 3' UTRs leads to decreased protein expression of these genes and consequently alters a number of mitochondrial and cellular parameters often observed in *in vitro* and *in vivo* models of diabetic nephropathy. However, it is important to establish if these parameters are linked to the fibrotic phenotype induced by miR-21/TGF $\beta$  demonstrated in Chapter 3.

Genes which are commonly dysregulated by TGF $\beta$  were analysed by qRT-PCR in PTCs transfected with siRNA targeted against ACAT1 and AK2 mRNA. COLI mRNA was increased by both anti-ACAT1 and anti-AK2 siRNA, albeit upregulation by AK2 repression was non-significant (Figure 6-12a). Similar to the effect of miR-21 on TGF $\beta$ -induced expression of a number of fibrotic genes, repression of ACAT1 and AK2 by siRNA further increased the effect of TGF $\beta$  on COLI expression. Conversely, COLIV did not display the same pattern of dysregulation with only siRNA against ACAT1 and the combination of anti-AK2 siRNA and TGF $\beta$  resulting in significant upregulation of COLIV mRNA (Figure 6-12b). Although siRNA-mediated repression of ACAT1 or AK2 alone did not significantly induce FN1 expression, repression of these genes resulted in augmentation of TGF $\beta$ -mediated upregulation of FN1. However, the augmentation by anti-AK2 siRNA was not statistically significant (Figure 6-12c). Interestingly, TGF $\beta$ -induced MMP9 expression was also augmented by siRNA-mediated downregulation of ACAT1 and AK2 (Figure 6-12d). Anti-ACAT1 siRNA was also found to significantly upregulate matrix metalloproteinase 9 (MMP9) expression. Although this seems counter to the paradigm of decreased ECM turnover that is seen in DN, similar changes in MMP9 expression are induced in response to exogenous miR-21 expression and TGF $\beta$  treatment.

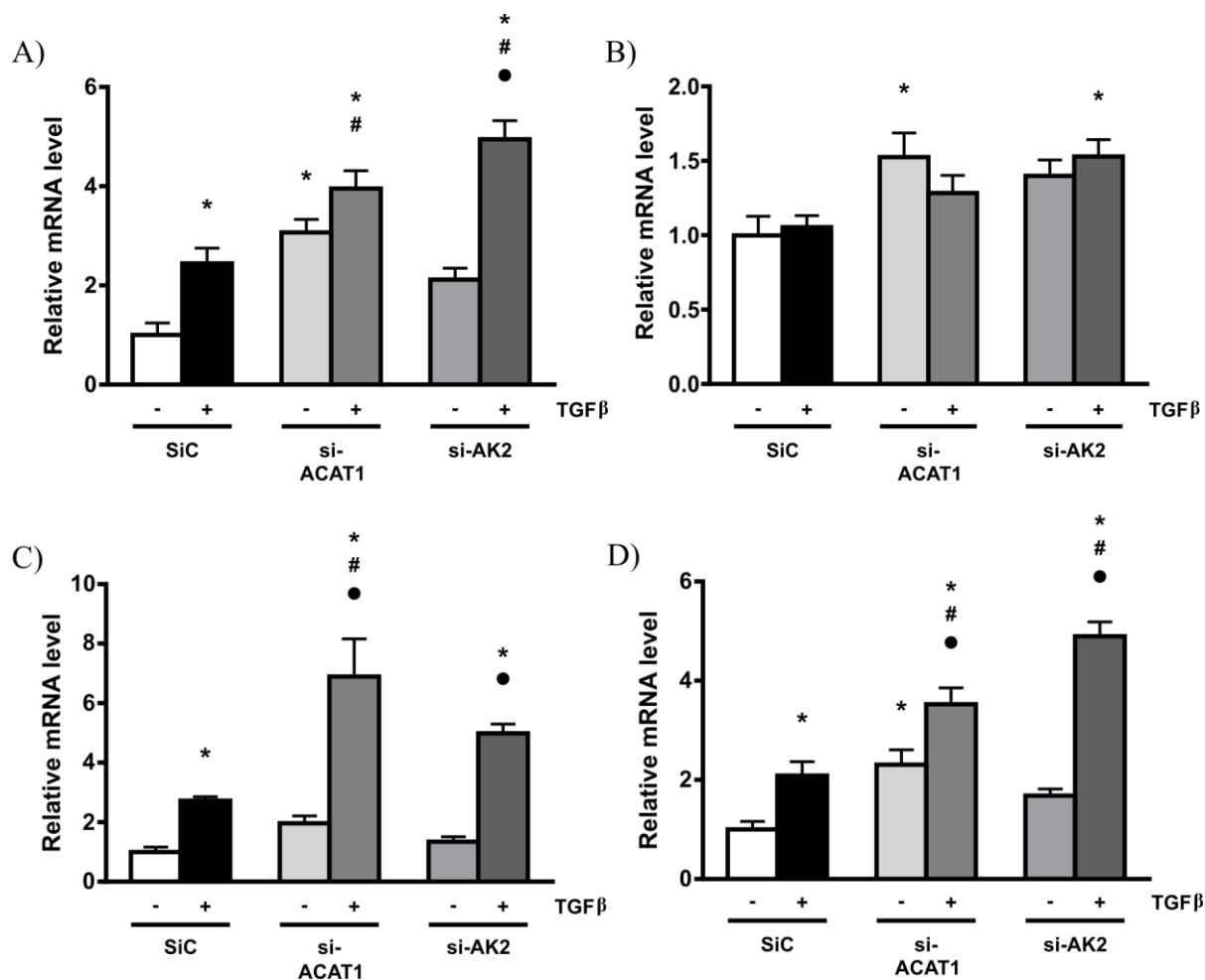


**Figure 6-12 ACAT1 and AK2 repression alter fibrotic gene expression.**

A) Anti-ACAT1 siRNA increases COL1 expression while both anti-ACAT1 and anti-AK2 siRNA augment TGF $\beta$ -mediated COL1 induction. B) COL1V is induced by anti-ACAT1 siRNA and TGF $\beta$  mediated induction is augmented by anti-AK2 siRNA. C) TGF $\beta$ -mediated induction of FN1 is augmented by anti-ACAT1 siRNA and nonsignificantly tended to be increased by anti-AK2 siRNA. D) Anti-ACAT1 siRNA increases MMP9 expression and siRNA against ACAT1 and AK2 increase the effect of TGF $\beta$  on MMP9 expression. All data are Mean+SEM, N=6 per group, Tukey One-way ANOVA; \* $p < 0.05$ , Untreated vs. All; #  $p < 0.05$ , All vs. TGF $\beta$ ; ●  $p < 0.05$ , target siRNA vs. target siRNA + TGF $\beta$ .

In addition to dysregulation of important ECM genes, repression of ACAT1 and AK2 also resulted in modulation of the effect of TGF $\beta$  on fibrotic growth factors typically upregulated in the diabetic kidney. Specifically, siRNA mediated repression of ACAT1 augmented TGF $\beta$ -induced upregulation of CTGF while ACAT1 repression alone led to a non-significant

increase in CTGF mRNA. Similarly, anti-AK2 siRNA further increased TGF $\beta$ -induced CTGF upregulation while AK2 repression alone induced CTGF mRNA levels by 70%. VEGF expression was induced by ACAT1 and AK2 repression by 2.5-fold and 2-fold respectively, although these changes were non-significant. Finally, siRNA mediated gene repression had no effect on TGF $\beta$  expression itself. However, AK2 siRNA augmented TGF $\beta$ -mediated self upregulation. These alterations to expression of fibrotic genes and factors demonstrate that the role of miR-21 in fibrotic outcomes in PTCs extends beyond canonical TGF $\beta$  signalling and mediates the fibrotic phenotype through targeting of mitochondrially associated genes.

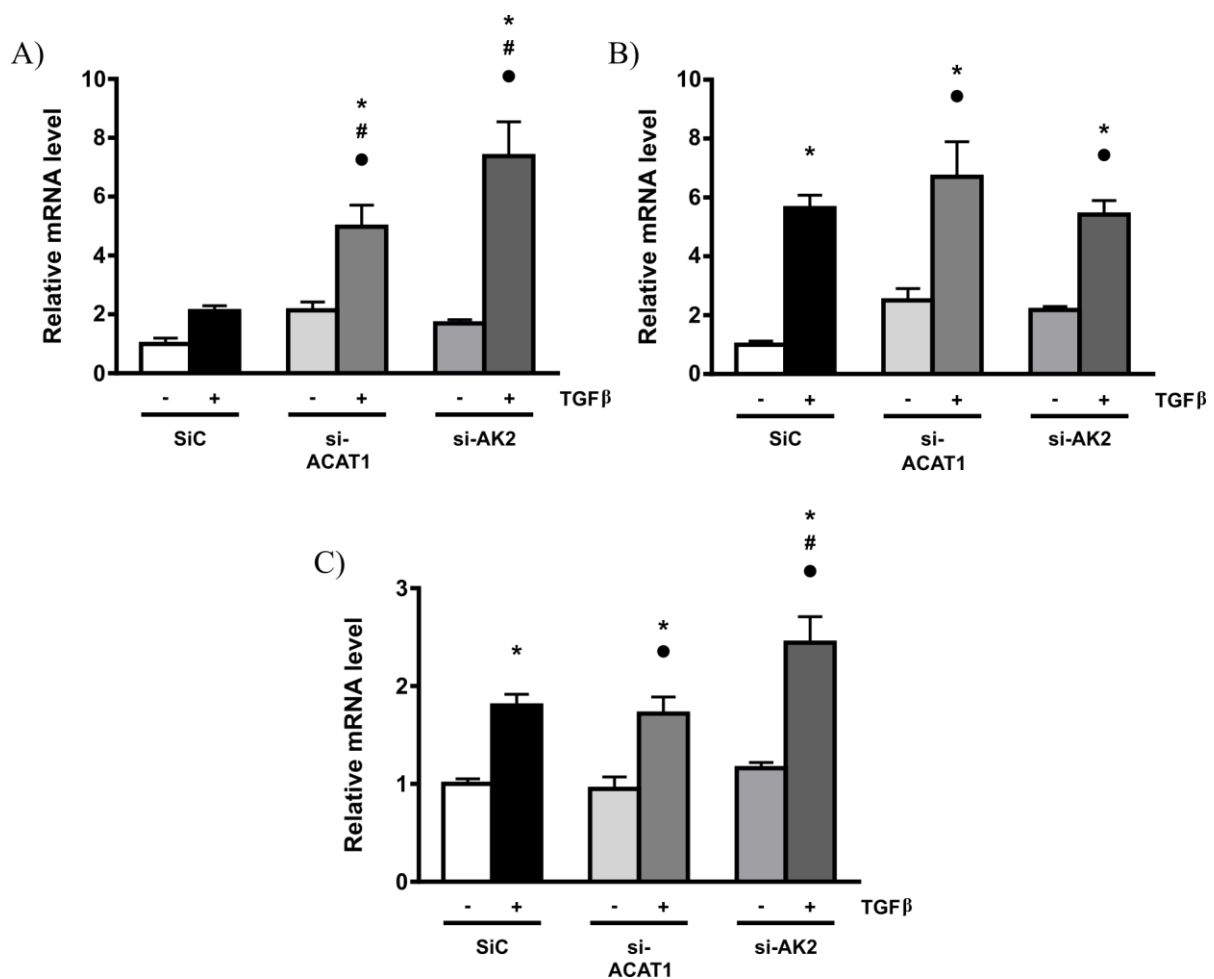


**Figure 6-13 ACAT1 and AK2 repression impact TGF $\beta$ -mediated expression of growth factors.**

A) CTGF induction by TGF $\beta$  is augmented by anti-ACAT1 and anti-AK2 siRNA. B) Although anti-ACAT1 siRNA and anti-AK2 siRNA trends an increase in VEGF expression, these were not found to be significant. C) TGF $\beta$ -mediated self-upregulation is enhanced by repression of AK2 via siRNA. All data are Mean+SEM, N=6 per group, Tukey One-way ANOVA; \* $p < 0.05$ , Untreated vs. All; #  $p < 0.05$ , All vs. TGF $\beta$ ; •  $p < 0.05$ , target siRNA vs. target siRNA + TGF $\beta$ .

Although gene expression changes induced by ACAT1 or AK2 repression do not mirror those of miR-21 completely, there is sufficient congruency to indicate that, at least in part, miR-21 mediates its fibrotic effects through direct targeting and repression of ACAT1 and AK2. Given that miR-21 is upregulated by TGF $\beta$ , this represents a previously unrecognised function of miR-21 in mediating the effects of TGF $\beta$  in PTC. Furthermore, similarities between the mitochondrial parameters under miR-21 treatment and ACAT1 or AK2 further indicate that miR-21 may play a much broader role in PTC pathophysiology outside of its conventional role in fibrosis and EMT-like processes. As such, this study presents data which expands our understanding of miR-21 in PTC and potentially adds weight to the importance of mitochondrial health in renal pathobiology.

## 6.6. Discussion

This study demonstrates a novel mechanism for the fibrotic phenotype exhibited by PTC in response to TGF $\beta$ . These results extend the mechanistic framework of the role of miR-21 in TGF $\beta$ -regulated PTC biology by highlighting changes in mitochondrial morphology and function induced by TGF $\beta$  and miR-21. Furthermore, these changes are proposed to occur downstream of TGF $\beta$  via miR-21-mediated repression of two mitochondrially associated genes, namely, ACAT1 and AK2. Finally, repression of these genes has been linked to fibrotic gene expression in PTC thereby demonstrating the importance of mitochondrial function in relation to PTC pathophysiology.

Mitochondrial dysfunction has been linked to various renal pathologies including diabetic nephropathy (176, 260, 261). Aspects of mitochondrial biology encompassing oxidative phosphorylation, biogenesis and dynamics are regulated by a number of pathways and factors which are impacted directly or indirectly by the central feature of diabetes mellitus, systemic hyperglycaemia (52, 104, 118, 262). Recently, microRNAs have been implicated as regulators of various mitochondrial processes including ATP production, mitochondrial metabolism, ROS production, mitochondrial dynamics, mitophagy and mitochondria-induced apoptosis (147, 149, 263). To date, microRNA mediated mitochondrial dysfunction has been reported in a number tissues and cell types but this interface has remained largely unexplored in diabetic nephropathy.

Mitochondrial superoxide production is a major source of cellular oxidative stress and is the central tenet of Brownlee's unifying hypothesis for the development of diabetic

complications (264). Systemic hyperglycaemia results in increased levels of intra-cellular glucose in a number of cell types, including PTCs, which are unable to efficiently control glucose uptake due to expression of the insulin-independent glucose cotransporter SGLT1/2 (35, 126). Increased intra-cellular glucose directly increases citric acid cycle activity via increased pyruvate generation consequently increasing electron transport chain electron donors such as NADH and FADH and therefore ETC activity (107, 111). Essentially, the sole purpose of the ETC is to establish a proton gradient which is in turn the driving force behind ATP synthesis via ATP synthase. Korshunov *et al* reported that if this proton gradient reaches a critical level, complex III becomes blocked leading to electron build-up within the ETC (265). Excess electrons are passed to molecular oxygen by coenzyme Q thereby increasing superoxide production. Superoxide production therefore is directly linked with the mitochondrial membrane potential.

In the present study, mitochondrial superoxide content increased in response to TGF $\beta$  treatment of PTCs with the addition of miR-21 further elevating superoxide production. In accordance with the findings of Korshunov, mitochondrial membrane potential was also increased by these treatments with miR-21 alone also increasing the mitochondrial membrane potential. These findings mirror those of Das *et al.* where miR-181c was overexpressed in Sprague-Dawley rats by way of intravenously delivered liposomal nanoparticles (266). That study reported reduction of the complex IV cytochrome C oxidase (COX) enzymes COX1, COX2 and COX3, in cardiomyocyte mitochondria after 3 weeks, which led to complex IV remodelling presumably as a result of direct downregulation of COX1 by miR-181c (267).

In the PTC mRNA-seq dataset utilised in this study, COX1, COX2 and COX3 were all non-significantly downregulated by TGF $\beta$ . Furthermore, miRNA-seq data from TGF $\beta$  treated PTC indicate that miR-181c was unchanged in PTCs following TGF $\beta$  treatment. In the present study, the observed changes in PTC mitochondrial membrane potential and mitochondrial superoxide production are proposed to occur via direct targeting of novel miR-21 targets identified in the present study, ACAT1 and AK2.

TGF $\beta$  has also been implicated in oxidative stress and alteration of mitochondrial membrane potential in pulmonary fibroblasts from subjects with idiopathic pulmonary fibrosis (268). In that study, TGF $\beta$  induced reactive oxygen species production via upregulation of NOX4 and induced fibroblast to myofibroblast transdifferentiation. Furthermore, TGF $\beta$  reduced complex IV activity in senescent mink lung epithelial cells via an unknown mechanism (193). Reduced complex IV activity was associated with increased ROS production and a sustained decrease in the mitochondrial membrane potential as opposed to the increased membrane

potential observed in the present study. Furthermore, although not reported by Yoon *et al.*, reduction in complex IV activity may also lead to decreased ATP production or decreased total ATP content and may therefore contribute to the phenotype observed in the present study.

TGF $\beta$ -mediated ROS production may also induce miR-21 expression. In gastric cancer, Tu *et al.* reported that oxidative stress upregulates miR-21 leading to decreased programmed cell death 4 (PDCD4) expression with an associated increase in metastasis (178). Oxidative stress also upregulates miR-21 via NF $\kappa$ B in cardiomyocytes (269). However, this mechanism appears not to be relevant to PTC since NF $\kappa$ B was downregulated in the mRNA-seq dataset. Conversely, miR-21 itself may upregulate ROS production via downregulation of SOD2 in angiogenic progenitor cells from subjects with coronary artery disease (270). Furthermore, Leissner *et al.* reported miR-21-dependent decreases in sprouty RTK signalling antagonist 2 (SPRY2) which also increased ROS production via ERK/MAPK pathway activation. Although SOD2 was unchanged in the mRNA-seq dataset, SPRY2 was significantly downregulated in the mRNA-seq data and thereby presents an alternative mechanism for increased ROS and mitochondrial membrane potential in the above experiments.

The findings of the present study are consistent with the view that TGF $\beta$ -mediated upregulation of miR-21 decreases ACAT1 and AK2 expression and this effect contributes to the dysfunctional mitochondrial phenotype observed under TGF $\beta$ -treatment. Both ACAT1 and AK2 mRNA and protein levels were downregulated by TGF $\beta$  and miR-21 in PTCs. This downregulation was shown to occur as a result of direct interaction of miR-21 with the 3'UTR region of mRNA for these genes, as reflected by the findings from the luciferase reporter assays containing either wild-type or mutant predicted target sites as derived from *microRNA.org*. Repression of these genes utilising siRNA, in the absence of exogenous miR-21, mimicked the effects of miR-21/TGF $\beta$  on mitochondrial membrane potential and mitochondrial superoxide content. These findings highlight a novel mechanism by which TGF $\beta$ /miR-21 contribute to mitochondrial superoxide production and increased mitochondrial membrane potential.

Neither ACAT1 nor AK2 are directly involved in ROS metabolism or mitochondrial membrane potential but rather influence the availability of substrates required for cellular metabolism. ACAT1 classically carries out interconversion of acetyl-CoA and acetoacetyl-CoA with acetyl-CoA being primarily utilised by the TCA cycle and acetoacetyl-CoA, in conjunction with acetyl-CoA being utilised to form HMG-CoA (271, 272). Therefore, reduction in ACAT1 levels may lead to a reduction in the acetyl-CoA pool. However, in the

intracellular hyperglycaemic environment, there is no real shortage of the metabolic acetyl-CoA precursor, glucose derived pyruvate. However, ACAT1 depletion may influence cellular metabolism via its recently discovered role as an acetyl-transferase.

The role of ACAT1 in acetyl-CoA substrate availability is extended beyond acetyl-CoA and acetoacetyl-CoA interconversion via its acetyl-transferase activity. ACAT1 may acetylate and inactivate pyruvate dehydrogenase phosphatase 1 (PDP1) which is the primary activator of the PDC (273). Indeed, in H1299 lung cancer cells, ACAT1 was found to acetylate not only PDP1 but also pyruvate dehydrogenase alpha 1 (PDHA1), an essential component of PDC. ACAT1 mediated acetylation resulted in decreased PDP1 activity thereby decreasing PDC dephosphorylation and activation. PDC activity was also decreased by acetylation of PDHA1. Therefore, miR-21-mediated downregulation of ACAT1 may lead to derepression of acetyl-CoA production from pyruvate through derepression of PDP1 and PDHA1 activity.

Derepression of PDC activity may explain, at least in part, miR-21 induced increases in ROS production and mitochondrial membrane potential. Glycolysis, the TCA cycle and the ETC are all primarily allosterically regulated. In hyperglycaemic conditions, the intracellular environment within PTC will also become hyperglycaemic due to the activity of SGLT2 thereby providing ample glucose for glycolysis (105). This subsequently increases acetyl-CoA availability and therefore activity within the TCA cycle which in turn produces increasing levels of the electron donors NADH and FADH<sub>2</sub>. Increased electron donor availability invariably results in increased ETC activity and electron leakage in addition to partial reduction of molecular oxygen, both of which result in formation of superoxide and other reactive oxygen species (117, 274).

Elevated ETC activity also increases the mitochondrial membrane potential due to increased proton pumping associated with electron donor oxidisation. As mentioned previously, excessive mitochondrial membrane potential can lead to stalling of the ETC due to voltage-mediated repression of complex III with electrons essentially stockpiling within the ETC (265). With continued ETC activity this inevitably further increases mitochondrial membrane potential and ROS production. At this point uncoupling proteins such as UCP2 should be increased to aid in dissipation of the excess membrane potential (121). However, there was no such upregulation in the mRNA-seq dataset. Conversely, the proton gradient may be dissipated via ATP synthase activity but this may be hindered by substrate availability or ATP synthase functionality.

AK2 mediates the interconversion of ATP and ADP yielding two ADP for every ATP and therefore plays an important role in substrate availability within the mitochondria (275).

Indeed, AK2 depletion in 3T3 adipocytes resulted in decreased ATP content during differentiation (276). Furthermore, AK2 repression also resulted in increased ROS production in hematopoietic stem cells (277). The data support the findings of the present study and the notion that miR-21 mediated repression of AK2 may contribute to ETC stalling due to excessive membrane potential resulting from blockade of ATP production. Alternatively, ATP synthase may be dysfunctional, incorrectly assembled or present at lower concentration due to TGF $\beta$ -mediated repression of ATPAF1, an assembly factor for the F<sub>1</sub> subunit of ATP synthase (278). This mRNA is not listed for *R.norvegicus* in *microRNA.org* and was therefore not identified in the *in silico* experiments. However, the sequence is listed for both *M.musculus* and *H.sapiens* and contains two miR-21 binding sites in the 3'UTR for these species and is also significantly downregulated by TGF $\beta$  in the mRNA-seq dataset. This miR-21 target, although not investigated, represents another mechanism whereby miR-21 may alter mitochondrial metabolism.

Recently, Gomez *et al.* reported that repression of miR-21 may prevent progression of Alport nephropathy (AN) by modulating activity within metabolic pathways, specifically FA metabolism (176). That study utilised a COL4A3<sup>-/-</sup> knockout mouse model which displays many of the characteristics of AN, many of which are shared with DN. Delivery of anti-miR-21 oligonucleotides prevented tubular atrophy, podocytes loss, glomerulosclerosis and improved urinary albumin:creatinine ratio and interstitial inflammation. These results provide evidence of utility of both miRNA therapeutics and miR-21 itself as a therapeutic target. Improvements in renal pathology and function were seen to occur with enrichment of the PPAR $\alpha$  signalling pathway as a direct result of derepression of PPAR $\alpha$ , a direct target of miR-21.

In addition to PPAR $\alpha$  restoration, a number of  $\beta$ -oxidation pathway members including acyl-CoA dehydrogenase C-4 To C-12 straight chain (ACADM) and carnitine palmitoyltransferase 1 (CPT1) were also restored by miR-21 inhibition (176). Each of these genes were downregulated by TGF $\beta$  in the PTC mRNA-seq dataset. The authors also reported restoration of ACAT1 under miR-21 repression as support for increased  $\beta$ -oxidation. However, these investigations did not report any changes in PDP1 or PDHA1 acetylation levels. Regardless, there is compelling evidence that miR-21 is involved in mitochondrial function and metabolism.

The level of the mitochondrial biogenesis mediator, PGC1 $\alpha$ , was maintained following TGF $\beta$  treatment in miR-21 deficient PTC leading to improvements in mitochondrial content and protection of ATP levels against TGF $\beta$ -mediated downregulation (176). Mitochondrial

superoxide content was also lower in mitochondria from anti-miR-21 treated mice compared to controls which was attributed to restoration of MPV17 mitochondrial membrane protein-like (MPV17L) levels. These findings lend weight to the involvement of miR-21 in mitochondrial function, in particular ATP production and superoxide content. However, it is interesting to note that the present study found no difference in mitochondrial content following TGF $\beta$  or miR-21 treatment nor was there any alteration in MPV17L or SOD2 levels in the mRNA-seq dataset.

Aside from regulation of  $\beta$ -oxidation, a final alternative to the phenotype observed in this section centres upon mitophagy. Indeed, the fragmented mitochondrial morphology seen under TGF $\beta$  treatment or exogenous miR-21 expression may be indicative of increased mitophagy or failure of mitophagy to completely degrade dysfunctional mitochondria (279). Mitophagy may be activated by excessive mitochondria ROS such as that produced during hyperglycaemia in PTC. However, essential members of the mitophagy pathway including microtubule-associated protein 1 light chain 3 (LC3) and beclin 1 (BECN) were unchanged or were downregulated such as B-cell CCL/lymphoma 2 (BCL2). Interestingly, the proapoptotic BCL2-associated X protein (BAX) and BCL2-antagonist/killer 2 (BAK) were upregulated indicating that the mitochondrial morphology seen in this study may be the result of apoptotic processes (280). However, the observation that membrane potential was not only maintained but actually increased indicates that both the inner and outer mitochondrial membranes are intact thereby ruling out apoptosis-mediated mitochondrial fragmentation.

Further investigation is required to clarify the exact role of miR-21-mediated regulation of ACAT1 and AK2 in mitochondrial function. Interrogation of ETC complexes may shed light upon the source of increased super oxide content as may SOD activity assays. Dynamic, cell free ATP assays could assist in defining the nature of ATP depletion; specifically, is it a matter of impaired production or excessive consumption? Furthermore, inhibition of various members of the TCA cycle and ETC may confirm that increased electron donor production is a major mitigating factor in ACAT1-mediated mitochondrial dysfunction. Further investigation into mitophagy and apoptosis is also required especially when considering the antiapoptotic role of miR-21 in various cancers (175, 281-283). Finally, determination of the mechanisms by which repression of ACAT1 and AK2 lead to altered fibrotic gene and growth factor expression would also be of interest.

This section has presented data demonstrating the involvement of miR-21 in mitochondrial dysfunction through direct targeting of two novel mRNA genes, namely ACAT1 and AK2. Repression of these targets leads to increases in mitochondrial superoxide content, increased

mitochondrial membrane potential and decreased ATP content. Importantly, repression of these targets also increased expression, or augmented TGF $\beta$ -mediated expression of a number of important fibrotic genes and growth factors. Collectively, this work provides novel and important information on miR-21 in PTC pathology and more specifically how miR-21 mediates the effects of TGF $\beta$  through alteration of mitochondrial biology.

## 7. General Discussion

### 7.1. Introduction

Understanding the contribution and biology of any given cell type is paramount to the management and treatment of any given disease in any given tissue. This is especially true in the diabetic kidney where various cell types are directly susceptible to the hyperglycaemic conditions characteristic of the diabetic milieu. The role of primary cell types, specifically podocytes, MC and PTC, is further complicated by the retrograde and anterograde communication among these cells and the structural components of the nephron. Although podocyte loss and damage are responsible for clinical manifestations of DN such as albuminuria, they are somewhat downstream from MC and PTC in regard to the progression of renal structural damage.

In regard to MC, haemodynamic factors secreted from both renal and non-renal cells impact on intra-glomerular pressure by inducing MC contraction and dilation which may impact upon endothelial cells and consequently podocytes (18). Circulating growth factors such as CTGF can also impact on MC leading to increased ECM deposition, again influencing the ability of MC to fine-tune intra-glomerular pressure. Other factors such as TGF $\beta$  are considerably more potent and, in addition to inducing other growth factors including CTGF and VEGF, can induce ECM upregulation and gross changes to cellular physiology (59). Hyperglycaemia also upregulates TGF $\beta$  in MC, and combined with intracellular hyperglycaemia, results in increased ROS production which can go on to affect various cell types including podocytes (68).

Hyperglycaemia and TGF $\beta$  also impact upon PTC which play a central role in the development of interstitial fibrosis and are also implicated in glomerular injury. The role of PTC in glomerulosclerosis relates to increased Na<sup>+</sup> reabsorption which occurs as a consequence of increased glucose reabsorption. This leads to decreased Na<sup>+</sup> delivery to the macula densa (126). Ultimately this influences tubuloglomerular feedback and results in increased intra-glomerular pressure which promotes glomerular injury. Increased glucose reabsorption, intracellular hyperglycaemia and TGF $\beta$  all increase ROS production in PTC which has consequences for PTC themselves and also enhances interstitial inflammation by recruiting and activating leukocytes and macrophages (35, 97). TGF $\beta$  also induces an EMT-like phenotype in PTC resulting in increased ECM synthesis and induction of

transdifferentiation of bone-marrow derived mesenchymal stem cells to myofibroblasts thereby leading to further ECM production (52).

An underlying factor in the TGF $\beta$ -induced phenotype of both MC and PTC is dysregulation of miRNA (284). These small, non-coding RNA are implicated in a vast array of diseases and cell types not least of all in DN, specifically including MC and PTC (233, 285). Given the miRNA-mRNA interaction occurs via a small 7-8 nucleotide seed sequence, it is not surprising that a single miRNA may have hundreds of targets and a single mRNA may have tens of miRNA targeting it (232). This creates immense regulatory networks many magnitudes of complexity greater than what had previously been recognised in regard to genetic regulation. When considering the wide-reaching effects of TGF $\beta$ , it is important to consider miRNA dysregulation and given that miRNA often exhibit cell specific expression profiles, it becomes apparent that despite the immense progress made towards understanding the cellular contribution towards DN there is still much to decipher.

The collection of studies presented here have highlighted the wide reaching effects of TGF $\beta$  (chapter 4) and the impact of TGF $\beta$ -mediated miRNA dysregulation (chapter 5) not just at the global level in MC and PTC but also at the gene level in regard to PTC. Furthermore, the role of miR-21 in TGF $\beta$ -mediated fibrotic signalling (chapter 3) and TGF $\beta$ -mediated mitochondrial dysfunction has also been explored (chapter 6). Indeed, PTC and MC display remarkable similarity in terms of their response to TGF $\beta$  while also maintaining a degree of cell specificity. In regard to mRNA-seq data, cellular responses to TGF $\beta$  were determined through both 'classic' gene ontology term enrichment in addition to a derivation of gene-set enrichment analysis, namely GAGE, providing a thorough cross-sectional approach in delineating the transcriptional landscape induced by TGF $\beta$  (chapter 4). Conversely, the effect of TGF $\beta$  on miRNA expression and its impact upon the transcriptional and signalling landscape in PTC and MC was ascertained through utilisation of the Pathway-Express algorithm from Onto-Tools (chapter 5).

## **7.2. GAGE-mediated analysis of the TGF $\beta$ -induced transcriptional landscape**

Gene set analysis is widely used in bioinformatics as a means to garner information from the bulk data acquired from either microarray or RNA-seq experiments. However, classic gene set analysis such as GSEA has a number of shortcomings which limit the power of such analyses (286, 287). One such shortfall of GSEA is that it does not consider the sign of

dysregulation, just that a gene is dysregulated and the statistical ranking of such dysregulation. GAGE attempts to rectify this by utilising gene fold-change data in addition to gene dysregulation  $p$ -values when testing gene sets (163). This enables reporting of gene sets that may be enriched for downregulated or upregulated genes rather than a gene set being enriched *per se*. GAGE also employs parametric gene randomization processes similar to that utilised by the PAGE algorithms which not only increases computational efficiency but also affords greater statistical sensitivity, which, coupled with directional enrichment scores as highlighted above, increase the likelihood of obtaining biological relevant data from GAGE based experiments.

The implementation of GAGE in *R* allows utilisation of not only conventional gene ontology terms but also KEGG pathways (chapter 4). Furthermore, KEGG pathways may also be rendered with mRNA-seq data allowing visualisation of GAGE results while subsequent analyses can highlight genes that are essential to the enrichment score of a given gene set. Essential genes are those that are not only enriched above background noise in the entire data set but are also above the noise contained within the resident gene set itself (163). Given that gene ontology terms are based upon discrete molecular functions, biological processes or cellular compartmentalisation, post-hoc analysis for essential gene detection is considered unnecessary as the purpose of gene ontology analysis is to view enrichment in cellular processes as a whole rather than at the gene level. Regardless, supplementary testing, in addition to the visualisation capabilities of the *gage* package allows rapid interpretation of test results especially when comparing results from differing cell lines as has been the case here.

Comparative analysis of differing cell types under identical conditions highlights and clarifies cellular biology in the said conditions. In the case of chapter 4, this pertains to PTC and MC treated with TGF $\beta$  in high glucose conditions with the ensuing results highlighting the way in which TGF $\beta$  alters the physiology of these cells types in an *in vitro* model of chronic hyperglycaemia. Some of the more prominent findings in this chapter pertain to unique pathway topologies between cell types even when the pathways are both significantly enriched in any given direction. For example, although the focal adhesion and ECM-receptor interaction pathways were positively enriched in both PTC and MC, the genes which were identified as being essential to enrichment of these pathways were different. In particular, FN1 was not considered to be essential to focal adhesion enrichment while differing actin isoforms were identified as essential in PTC and MC and COL5A2 was inversely expressed between the cell types while also being considered essential.

Given the importance of FN1, collagens and actins to tubulointerstitial fibrosis and glomerulosclerosis one would expect these genes to be similarly dysregulated by TGF $\beta$  (42, 62). However, upon inspection of the rendered focal adhesion KEGG pathway it can be seen that the majority of member genes are grossly dysregulated in both cell types thereby increasing ‘competition’ for statistical validity which will impact upon essential gene lists (chapter 4). This does not negate the biological significance of non-essential genes nor does extreme statistical significance necessarily preclude biological significance. Hence *in silico* experiments such as those conducted in chapters 4-6 should be validated by molecular studies. Although only those in chapter 6 were supplemented with molecular studies, it should be noted that the data contained within chapters 4-5 constitute a substantial body of work from which further studies may be launched.

This is particularly true when observing pathways and gene ontology terms which were uniquely enriched in either PTC or MC (chapter 4). For example, there are a considerable number of MC specific pathways pertaining to muscle and vascular contraction. Indeed, these findings may provide novel targets for development of mice with hyper or hypo glomerular contractility. This may allow investigation of approaches to modulate intraglomerular pressure and how it affects glomerulosclerosis. For example, it is likely that strategies which modulate PCT sodium reabsorption leading to altered macula densa and juxtaglomerular apparatus activity will ultimately influence intraglomerular pressure and its effects on glomerular ultrastructure. Likewise, essential genes identified in the oxidative phosphorylation pathway in PTC may be utilised for supplementary studies to those conducted in chapter 6 or genes identified in the collecting duct acid secretion pathway may be utilised for *in vivo* studies into the role of renal bicarbonate reabsorption in influencing acid/base balance in diabetes.

### **7.3. Impact factor analysis of TGF $\beta$ -mediated miRNA dysregulation of signalling topology**

The second series of *in silico* experiments in this study utilised a number of *R* packages to integrate miRNA-seq and mRNA-seq data into KEGG pathways (chapter 5). The resulting augmented networks were tested with an *R* port of Onto-Tools’ Pathway-Express (PE) algorithm which aims to find the most perturbed pathways within a data set. At its core, PE is a gene set analysis algorithm. However, unlike GSEA, PAGE or even GAGE, the interactions

between member genes, the type of interactions between member genes, the location of a member gene in the gene set topology and also the extent to which member genes are dysregulated are all taken into account by PE (229, 234). This makes PE an ideal algorithm for testing custom networks generated by augmentation of miRNA-target lists with KEGG signalling pathways.

Generation of the custom networks requires miRNA-target lists. The present study utilised a machine learning adaptation of the miRanda algorithm provided by *microRNA.org* which searches for canonical 7-8 nucleotide seed regions in 3' UTR. The algorithm also finds a variety of non-canonical seed regions with mismatch bulges and point mutations in either the miRNA or mRNA. This is important as miRNA-mRNA interactions have been found to occur via all types of noncanonical interactions (288). This makes *miRanda-SVR* superior to other algorithms such as *miRTar*, which only searches for canonical sites or *TargetScan*, whose noncanonical site identification is limited to base mismatches. However, the sensitivity of *miRanda-SVR* results in immense data complexity with 586,000 and 1.4 million miRNA-mRNA interactions being predicted in rat and mouse genomes respectively. The lists were reduced significantly when double filtered for miRNA which were both detected in the dataset and also significantly dysregulated and were even further reduced when filtered for DN-related miRNA. Both naïve and biased lists may have been further reduced by filtering interactions for those whose miRNA and mRNA were inversely expressed. While this may have increased the degree of biological significance of these networks this would have lost the important feature of being able to identify false positives generated by the miRNA-target interaction algorithms (chapter 5).

Prediction algorithms, regardless of complexity, have only limited accuracy. Conventional miRNA research involves identification of a gene of interest and investigating miRNA that may target it on a case-by-case basis. However, by integrating mRNA and miRNA DGE data along with miRNA-target interaction prediction into readily available curated pathways such as those available from KEGG, the process becomes somewhat streamlined. The obvious drawback to this approach is that any networks obtained are only applicable to that particular cell or tissue type in whatever conditions the samples were obtained from. Furthermore, false-positives interactions such as those observed between miR-21 and TGF $\beta$ RI in the TGF $\beta$  signalling network do not necessarily exclude the likelihood of a positive interaction between these two RNA but rather that the expression levels of TGF $\beta$ RI are controlled by other factors such as let-7b/c (221, 259). Indeed, miR-21-mediated repression of TGF $\beta$ RI may

occur in PTC in renal pathologies other than DN or even in other cell types entirely although this is yet to be demonstrated.

Aside from ready validation of a large number of miRNA-mRNA interactions in the given model, the resultant networks generated by *miRIntegrator* and perturbation scores from *ROntoTools* provide a useful platform for the development or investigation of novel therapies against, in this case, DN (chapter 5). More specifically, this could lead to future progress in identifying therapies to combat PTC mediated TIF or MC mediated GS. Both PTC and MC exhibit distinct cellular physiology and serve highly specialised roles within the kidney. Thus, by extension, PTC and MC contribute heavily to the processes of TIF and GS respectively (28, 54, 88, 289). Furthermore, evidence is mounting that pathological changes in one cell type will lead to pathological changes in the other resulting in the familiar progressive and unrelenting nature of DN. Additionally, given the cell specific nature of miRNA profiles and the often cell specific ways in which miRNA impact upon gene expression levels, it is paramount that not just tissue specific therapies but cell specific therapies are developed in order to interrupt the cycle leading to increasing functional and structural damage in the diabetic kidney.

In addition to TGF $\beta$ RI being targeted by let-7b/c and possibly miR-21, the miR-30 family of miRNA are also predicted to target the 3' UTR of the TGF $\beta$ RI mRNA (chapter 5). A number of the miR-30 family members including miR-30a, miR-30d and miR-30e were all downregulated in PTC with an associated increase in TGF $\beta$ RI expression. However in MC, only miR-30c was downregulated. Furthermore, although the TGF $\beta$  pathway plays an important role in MC pathology in DN, TGF $\beta$ RI was actually downregulated. Therefore, delivery of miR-30 family members to the diabetic kidney may confer a more profound effect upon PTC than in MC through repression of TGF $\beta$ RI expression. miRNA mediated gene repression is considered a 'soft' approach when compared to siRNA or enzymatic inhibition and as such, some degree of TGF $\beta$ RI expression would remain regardless of the concentrations of miRNA delivered. This is likely to be a better approach considering the adverse side effects observed in the case of complete ablation of TGF $\beta$ -mediated signalling (290, 291).

#### 7.4. The link between miR-21, TGF $\beta$ and tubulointerstitial fibrosis

Aside from development of *in silico* protocols for the comparative and integrative analysis of mRNA and miRNA datasets, the studies presented here have also explored the role of miR-21 in PTC in both fibrotic signalling (chapter 3). Recently, miR-21 has emerged as an important player in various epithelial cancers through modulation of the EMT phenotype required for metastasis and also in organ fibrosis including lung, heart and kidney through targeting of a number of mRNA (174, 250, 291-293). The initial miR-21 studies presented here focused on resolution of the link between miR-21 and DN in addition to delineating the contribution of miR-21 mediated repression of SAMD7 and PTEN to fibrotic signalling in PTC (chapter 3). Subsequent miR-21 studies explored novel miR-21 targets and their role in mitochondrial dysfunction (chapter 6).

miR-21 has been implicated in a number of experimental fibrotic models including heart, lung and kidney through targeting of SPRY1, SMAD7 and PTEN (294). Despite this, there is little evidence of a role for miR-21 in human renal pathologies, least of all DN. Recently, miR-21 was found to be increased in glomerular fractions from American-Indian subjects with early DN (295). This contrasts with the results presented here which demonstrate increased miR-21 expression in laser-capture microdissected tubules compared to glomeruli in human renal biopsies from subjects with varying degrees of DN-associated fibrosis when compared to control subjects (chapter 3).

The laser capture microdissected biopsy data is supported by *in situ* staining for miR-21 in human renal biopsies which indicate increased staining in tubular regions with increasing fibrosis but not in the glomeruli (chapter 3). Furthermore, miR-21 levels were correlated with a decline in renal function and were also associated with increasing renal fibrosis. It is therefore interesting to speculate that the increased glomerular levels of miR-21 reported by Lai *et al* (295) may be a feature of early DN which is then lost as the disease progresses with miR-21 increasing in the tubular fractions at a stage reflecting the period between the Lai study and that presented here. Indeed, a larger cohort of renal biopsies from a large range of subjects with varying degrees of severity of DN would be critical to resolving this issue.

There is also a lack of any studies aiming to delineate the relative contribution of various miR-21 targets with any given pathological setting. A considerable number of targets have been validated for miR-21 including SPRY1, SMAD7, PDCD4, PTEN, TIMP3, BCL2 and IL-12A which have all been shown to play a role in either EMT-dependant cancer metastasis, cell survival or various fibrotic pathologies (281, 295-300). However, despite the growing list

of validated miR-21 targets, there have yet to be any studies which explore the relative contribution of multiple targets to any given phenotype. The present study has explored miR-21-mediated regulation of two of the above targets, namely SMAD7 and PTEN, in respect to their contribution to fibrotic signalling in PTC.

This study revealed, in the case of COL1 and FN1, that the effect of miR-21 acting downstream of TGF $\beta$ , is dependent upon coordinated repression of both SMAD7 and PTEN (chapter 3). This ultimately leads to increased flux through the TGF $\beta$ -mediated SMAD3- and PI3K-dependent signalling pathways. This work can evidently be extended to include other miR-21 targets. However, the probability of high level cytotoxicity resulting from multiple treatments is very real and therefore this line of inquiry may be limited. Alternatively, a panel of experiments simultaneously targeting no more than three pathways at a time may be more amendable to investigation of the regulation of TGF $\beta$ -mediated fibrosis and EMT-related events by multiple miR-21 targets. Furthermore, validation of the pathway interrogation experiments *in vivo* would also be desirable. This particular area of research was not explored due to time constraints but clearly warrants further investigation.

### **7.5. The link between miR-21, TGF $\beta$ and mitochondrial dysfunction**

In addition to the induction of fibrosis, TGF $\beta$  has also been implicated in mitochondrial dysfunction which itself has been linked to fibrosis (97, 144). Given the wide-reaching effects of miRNA in general and the already demonstrated fibrotic role of miR-21 downstream of TGF $\beta$ , it stands to reason that miR-21 may be involved in mitochondrial dysfunction and more specifically mitochondrially-mediated fibrotic gene expression. Indeed, miR-21 increased mitochondrial ROS and membrane potential while also decreasing cellular ATP content (chapter 6), an effect similar to that reported with TGF $\beta$ . Importantly, as with ECM gene expression in the initial miR-21 studies, the effect of TGF $\beta$  was compounded by miR-21 indicating that miR-21 may be mediating the effects of TGF $\beta$  upon mitochondria (chapter 6).

Following a series of *in silico* experiments utilising PTC mRNA and miRNA DGE data, miR-21-target prediction lists and the MitoCarta database, a number of mitochondrially associated genes were identified which were both dysregulated in the RNA-seq data and are also predicted targets of miR-21 (chapter 6). Despite SLC25A25, TXNRD1, ACAT1 and AK2 all being decreased by miR-21 or TGF $\beta$  in PTC *in vitro*, only ACAT1 and AK2 were

decreased in renal cortices from experimental models of diabetic kidney disease. Therefore, dysregulation of SLC25A25 and TXNRD1 as detected by NGS or qRT-PCR may be artefacts of the *in vitro* environment and not necessarily a reflection of natural gene expression patterns. Changes in SLC25a25 and TXNRD1 may also be masked in the renal cortex due to changes in gene expression in non-PTC populations. Indeed, isolation of tubules from renal cortices would clarify this matter. Both ACAT1 and AK2 were validated as *bona fide* targets of miR-21 through 3' UTR assays and western blot protein analysis which are the generally used approach to confirm repressive interaction between a miRNA and mRNA. However, in this case, instead of merely mutating the 8 nucleotide seed region in the 3' UTR, a 22 nucleotide sequence required mutation due to substantial supplementary binding of the miRNA 3' regions to the mRNA sequence.

Subsequent experiments involved utilisation of siRNA targeted against either AK2 or ACAT1 (chapter 6). These studies revealed that repression of these targets has similar consequences to mitochondrial function as either miR-21 or TGF $\beta$  treatment. Interestingly, repression of these genes also altered expression of a number of fibrotic genes and growth factors thereby not only strengthening the link between mitochondrial function and fibrotic signalling in PTC but also that this process may be in part propagated by miR-21-mediated repression of ACAT1 and AK2, downstream of TGF $\beta$ . Although there is considerable evidence in this series of experiments to support this postulate there are a number of lines of enquiry which should ideally be followed in later experiments to support and clarify the role of these genes in mediating the effects of miR-21 downstream of TGF $\beta$ .

Given that miR-21 targets both ACAT1 and AK2, co-transfection of siRNA against ACAT1 and AK2 may more accurately reflect the effect of miR-21 overexpression. However, as demonstrated in chapter 6, both ACAT1 and AK2 expression were almost completely abrogated with minimal siRNA concentrations. Considering this alongside the 'soft' repression induced by miRNA as discussed previously, it may be difficult to approach a somewhat more natural replication of the miR-21-induced translational landscape. An alternative, and somewhat more practical approach may be restoration of ACAT1 and AK2, both individually and concurrently, through delivery of expression vectors. One would expect that cells transfected with either one or both of these expression vectors would retain some degree of normality even in the presence of exogenous miR-21 or TGF $\beta$ .

Previous evidence for both ACAT1 and AK2 in regard to the measured parameters is lacking and not just in a diabetic setting. As such, the way in which these genes contribute to the observed phenotype is not entirely elucidated. However, ACAT1 deficiency results in

defective isoleucine and ketone catabolism leading to intermittent ketoacidotic episodes (192). It is therefore interesting to speculate that periodic elevation of miR-21 may contribute to disturbed acid/base balance as has been experienced by diabetic subjects. Nevertheless, since management of ACAT1 deficiency is simple and the condition is a rare hereditary in-born error of metabolism, little research has been published in regard to its effects on mitochondrial dysfunction (301, 302). Conversely, AK2 deficiency has been implicated in reticular digenesis, a rare form of combined immunodeficiency characterised by almost complete lymphocyte depletion. This condition results in chronic sepsis and death within days of birth if left untreated (303). The clinical condition arises as a result of energy-depletion induced failure of lymphocyte development and as such the role of AK2 in mitochondrial biology has attracted considerably more attention than ACAT1. Indeed, AK2 depletion induces decreased ATP content and increased ROS production in 3T3 adipocytes and hematopoietic stem cells respectively (276, 277). Therefore, the role of AK2 in TGF $\beta$ -induced miR-21-dependant mitochondrial dysfunction is consistent with the current literature whereas ACAT1 has yet to be studied as extensively as AK2.

As ACAT1 and AK2 have garnered little attention in DN research, the proposed interactions and resultant phenotypes present a highly novel mechanism by which mitochondrial function may be altered. Furthermore, these interactions may directly contribute to the development and progression of tubulointerstitial fibrosis in DN. Therefore, it is paramount that future studies be directed towards validation of these findings *in vivo* in appropriate experimental models of diabetic nephropathy. Additionally, clarification of the mechanisms by which repression of these genes contributes to the miR-21 induced phenotype is also required. Importantly, in light of the study by Gomez *et al.* linking miR-21 to PPAR $\alpha$  and  $\beta$ -oxidation, delineation of the role of miR-21-mediated repression of ACAT1 and AK2 from that of miR-21-mediated repression of PPAR $\alpha$  is also of importance when considering future experiments based upon this work (176).

## 7.6. Conclusion

Collectively, this thesis has demonstrated and explored the wide reaching effects of TGF $\beta$  upon both PTC and MC. The genome wide effect of TGF $\beta$ -mediated miRNA dysregulation of the cell wide signalling landscape has also been explored. miR-21 is highly dysregulated in PTC and its role in TGF $\beta$ -mediated fibrotic signalling has been clarified. This effect has been

clearly defined in regard to the relative contribution of SMAD7 and PTEN. The significance of miR-21 in human DN has also been demonstrated. Finally, the role of miR-21 in mitochondrial dysfunction in PTC is proposed to occur at least in part through ACAT1 and AK2. This work has added valuable knowledge to the growing recognition of the importance of miRNA in DN. Furthermore, the development of *in silico* pipelines may aid those who endeavour to undertake similar projects with the data garnered from such experiments providing an important reference for future investigations.

Although this thesis presents considerable data on the role of TGF $\beta$  and miRNA, in particular miR-21, in PTC and MC, the bulk of this data has been generated in both *in vitro* and *in silico* experiments. These types of investigations are important for increasing our understanding of cell, cytokine and RNAi biology. However, it is important that, where possible, these experiments be replicated *in vivo* utilising standard models for DN or by repeating analysis on *ex vivo* tissues from such models in order to validate the findings of the present studies.

In conclusion, the findings from this thesis are likely to aid in the development of future therapies focusing on retarding the development and progression of DN, not least of all in the rectification of mitochondrial dysfunction and preventing the relentless cycle of fibrotic tissue damage that ultimately results in renal failure.

## 8. Reference List

1. Zimmet P. Diabetes Mellitus-One of Australia's top six health priorities. Retrieved March [Internet]. 2008; 25:[2010 p.].
2. IDF. IDF Diabetes Atlas, 7 ed. 7 ed. Brussels, Belgium: International Diabetes Federation; 2015.
3. Brownlee M. The pathobiology of diabetic complications. *Diabetes*. 2005;54(6):1615.
4. Joslin EP, Kahn CR. *Joslin's diabetes mellitus*: Lippincott Williams & Wilkins; 2005.
5. Scheen AJ. Pathophysiology of type 2 diabetes. *Acta Clin Belg*. 2003;58(6):335-41. Epub 2004/04/08.
6. Webbie K, O'Brian K. Use of medicines by Australians with diabetes. In: AIHW, editor. Canberra: AIHW; 2006.
7. AIHW. Diabetes: Australian facts 2008. In: AIHW, editor. CVD 40 ed. Canberra: AIHW; 2008.
8. Brownlee M. Biochemistry and molecular cell biology of diabetic complications. *Nature*. 2001;414(6865):813-20.
9. Grace BS, Clayton P, McDonald SP. Increases in renal replacement therapy in Australia and New Zealand: understanding trends in diabetic nephropathy. *Nephrology (Carlton)*. 2012;17(1):76-84. Epub 2011/08/23.
10. Forbes J, Fukami K, Cooper M. Diabetic nephropathy: where hemodynamics meets metabolism. *Experimental and Clinical Endocrinology and Diabetes*. 2007;115(2):69-84.
11. Holt TA, Kumar S. *ABC of Diabetes*: BMJ Books; 2009.
12. Schena FP, Gesualdo L. Pathogenetic Mechanisms of Diabetic Nephropathy. *Journal of the American Society of Nephrology*. 2005;16(3 suppl 1):S30-S3.
13. Kriz W, Elger M. CHAPTER 1 - Renal Anatomy. In: Feehally JFJJ, editor. *Comprehensive Clinical Nephrology (Fourth Edition)*. Philadelphia: Mosby; 2010. p. 3-14.
14. Shirley DG, Unwin RJ. CHAPTER 2 - Renal Physiology. In: Feehally JFJJ, editor. *Comprehensive Clinical Nephrology (Fourth Edition)*. Philadelphia: Mosby; 2010. p. 15-28.
15. Li JJ, Kwak SJ, Jung DS, Kim JJ, Yoo TH, Ryu DR, et al. Podocyte biology in diabetic nephropathy. *Kidney Int Suppl*. 2007(106):S36-42. Epub 2007/08/04.
16. Brosius FC, Coward RJ. Podocytes, signaling pathways, and vascular factors in diabetic kidney disease. *Adv Chronic Kidney Dis*. 2014;21(3):304-10. Epub 2014/05/02.
17. Davies M. The mesangial cell: A tissue culture view. *Kidney Int*. 1994;45(2):320-7.

18. Schlöndorff D, Banas B. The Mesangial Cell Revisited: No Cell Is an Island. *J Am Soc Nephrol*. 2009;20(6):1179-87.
19. Kriz W, Elger M, Mundel P, Lemley KV. Structure-stabilizing forces in the glomerular tuft. *Journal of the American Society of Nephrology*. 1995;5(10):1731.
20. STOCKAND JD, SANSOM SC. Glomerular Mesangial Cells: Electrophysiology and Regulation of Contraction. *Physiological Reviews*. 1998;78(3):723-44.
21. Riser BL, Cortes P, Heilig C, Grondin J, Ladson-Wofford S, Patterson D, et al. Cyclic stretching force selectively up-regulates transforming growth factor-beta isoforms in cultured rat mesangial cells. *Am J Pathol*. 1996;148(6):1915-23. Epub 1996/06/01.
22. Gruden G, Thomas S, Burt D, Zhou W, Chusney G, Gnudi L, et al. Interaction of angiotensin II and mechanical stretch on vascular endothelial growth factor production by human mesangial cells. *J Am Soc Nephrol*. 1999;10(4):730-7. Epub 1999/04/15.
23. Riser BL, Denichilo M, Cortes P, Baker C, Grondin JM, Yee J, et al. Regulation of connective tissue growth factor activity in cultured rat mesangial cells and its expression in experimental diabetic glomerulosclerosis. *J Am Soc Nephrol*. 2000;11(1):25-38. Epub 2000/01/05.
24. Ingram AJ, James L, Ly H, Thai K, Scholey JW. Stretch activation of jun N-terminal kinase/stress-activated protein kinase in mesangial cells. *Kidney Int*. 2000;58(4):1431-9. Epub 2000/09/30.
25. Ingram AJ, Ly H, Thai K, Kang M, Scholey JW. Activation of mesangial cell signaling cascades in response to mechanical strain. *Kidney Int*. 1999;55(2):476-85. Epub 1999/02/13.
26. Krepinsky JC, Li Y, Chang Y, Liu L, Peng F, Wu D, et al. Akt mediates mechanical strain-induced collagen production by mesangial cells. *J Am Soc Nephrol*. 2005;16(6):1661-72. Epub 2005/04/09.
27. Wakisaka M, He Q, Spiro MJ, Spiro RG. Glucose entry into rat mesangial cells is mediated by both Na(+)-coupled and facilitative transporters. *Diabetologia*. 1995;38(3):291-7. Epub 1995/03/01.
28. Mahimainathan L, Das F, Venkatesan B, Choudhury GG. Mesangial cell hypertrophy by high glucose is mediated by downregulation of the tumor suppressor PTEN. *Diabetes*. 2006;55(7):2115-25. Epub 2006/06/29.
29. Heilig CW, Liu Y, England RL, Freytag SO, Gilbert JD, Heilig KO, et al. D-glucose stimulates mesangial cell GLUT1 expression and basal and IGF-I-sensitive glucose uptake in

- rat mesangial cells: implications for diabetic nephropathy. *Diabetes*. 1997;46(6):1030-9. Epub 1997/06/01.
30. Inoki K, Haneda M, Maeda S, Koya D, Kikkawa R. TGF-beta 1 stimulates glucose uptake by enhancing GLUT1 expression in mesangial cells. *Kidney Int*. 1999;55(5):1704-12. Epub 1999/05/07.
31. Qian Y, Feldman E, Pennathur S, Kretzler M, Brosius FC. From Fibrosis to Sclerosis. *Diabetes*. 2008;57(6):1439-45.
32. Schiffer M, Bitzer M, Roberts ISD, Kopp JB, ten Dijke P, Mundel P, et al. Apoptosis in podocytes induced by TGF- $\beta$  and Smad7. *J Clin Invest*. 2001;108(6):807-16.
33. Yokoi H, Mukoyama M, Mori K, Kasahara M, Suganami T, Sawai K, et al. Overexpression of connective tissue growth factor in podocytes worsens diabetic nephropathy in mice. *Kidney Int*. 2008;73(4):446-55. Epub 2007/12/14.
34. Hall JE, Guyton AC. *Textbook of medical physiology*: Saunders London; 2011.
35. Vallon V, Platt KA, Cunard R, Schroth J, Whaley J, Thomson SC, et al. SGLT2 Mediates Glucose Reabsorption in the Early Proximal Tubule. *Journal of the American Society of Nephrology : JASN*. 2011;22(1):104-12.
36. Schnerman J, Briggs JP. *Function of the Juxtaglomerular Apparatus: control of glomerular hemodynamics and renin secretion*. Burlington, MA: Elsevier Academic Press; 2008. 589-626 p.
37. Leyssac PP, Karlsen FM, Skott O. Role of proximal tubular reabsorption for the intrarenal control of GFR. *Kidney Int Suppl*. 1991;32:S132-5. Epub 1991/06/01.
38. Lam S, Verhagen NAM, Strutz F, Van Der Pijl JW, Daha MR, Van Kooten C. Glucose-induced fibronectin and collagen type III expression in renal fibroblasts can occur independent of TGF- $\beta$ 1. *Kidney Int*. 2003;63(3):878-88.
39. Rocco MV, Chen Y, Goldfarb S, Ziyadeh FN. Elevated glucose stimulates TGF- $\beta$  gene expression and bioactivity in proximal tubule. *Kidney Int*. 1992;41(1):107-14.
40. Kobayashi T, Inoue T, Okada H, Kikuta T, Kanno Y, Nishida T, et al. Connective tissue growth factor mediates the profibrotic effects of transforming growth factor-beta produced by tubular epithelial cells in response to high glucose. *Clin Exp Nephrol*. 2005;9(2):114-21. Epub 2005/06/28.
41. Kim BS, Chen J, Weinstein T, Noiri E, Goligorsky MS. VEGF expression in hypoxia and hyperglycemia: reciprocal effect on branching angiogenesis in epithelial-endothelial co-cultures. *J Am Soc Nephrol*. 2002;13(8):2027-36. Epub 2002/07/26.

42. Zeisberg M, Neilson EG. Mechanisms of Tubulointerstitial Fibrosis. *J Am Soc Nephrol*. 2010;21(11):1819-34.
43. Yuan Q, Wang R, Peng Y, Fu X, Wang W, Wang L, et al. Fluorofenidone attenuates tubulointerstitial fibrosis by inhibiting TGF- $\beta$ 1-induced fibroblast activation. *Am J Nephrol*. 2011;34(2):181-94. Epub 2011/07/28.
44. Simonson M. Phenotypic transitions and fibrosis in diabetic nephropathy. *Kidney International*. 2007;71(9):846-54.
45. Thompson EW, Newgreen DF. Carcinoma Invasion and Metastasis: A Role for Epithelial-Mesenchymal Transition? *Cancer Res*. 2005;65(14):5991-5.
46. Iwano M, Plieth D, Danoff TM, Xue C, Okada H, Neilson EG. Evidence that fibroblasts derive from epithelium during tissue fibrosis. *J Clin Invest*. 2002;110(3):341-50. Epub 2002/08/07.
47. Humphreys BD, Lin SL, Kobayashi A, Hudson TE, Nowlin BT, Bonventre JV, et al. Fate tracing reveals the pericyte and not epithelial origin of myofibroblasts in kidney fibrosis. *Am J Pathol*. 2010;176(1):85-97. Epub 2009/12/17.
48. LeBleu VS, Taduri G, O'Connell J, Teng Y, Cooke VG, Woda C, et al. Origin and Function of Myofibroblasts in Kidney Fibrosis. *Nat Med*. 2013;19(8):1047-53.
49. Carew RM, Wang B, Kantharidis P. The role of EMT in renal fibrosis. *Cell Tissue Res*. 2012;347(1):103-16.
50. Kriz W, Kaissling B, Le Hir M. Epithelial-mesenchymal transition (EMT) in kidney fibrosis: fact or fantasy? *J Clin Invest*. 121(2):468-74.
51. Fragiadaki M, Mason RM. Epithelial-mesenchymal transition in renal fibrosis – evidence for and against. *Int J Exp Pathol*. 2011;92(3):143-50.
52. Grande MT, Sanchez-Laorden B, Lopez-Blau C, De Frutos CA, Boutet A, Arevalo M, et al. Snail1-induced partial epithelial-to-mesenchymal transition drives renal fibrosis in mice and can be targeted to reverse established disease. *Nat Med*. 2015;21(9):989-97.
53. Grgic I, Campanholle G, Bijol V, Wang C, Sabbisetti VS, Ichimura T, et al. Targeted proximal tubule injury triggers interstitial fibrosis and glomerulosclerosis. *Kidney Int*. 2012;82(2):172-83.
54. Bonventre JV. Primary proximal tubule injury leads to epithelial cell cycle arrest, fibrosis, vascular rarefaction, and glomerulosclerosis. *Kidney inter, Suppl*. 2014;4(1):39-44.
55. Goldin A, Beckman JA, Schmidt AM, Creager MA. Advanced Glycation End Products: Sparking the Development of Diabetic Vascular Injury. *Circulation*. 2006;114(6):597-605.

56. Thannickal VJ, Fanburg BL. Reactive oxygen species in cell signaling. *Am J Physiol Lung Cell Mol Physiol*. 2000;279(6):L1005-28. Epub 2000/11/15.
57. King GL. The role of inflammatory cytokines in diabetes and its complications. *J Periodontol*. 2008;79(8 Suppl):1527-34. Epub 2008/09/04.
58. Chiarelli F, Santilli F, Mohn A. Role of growth factors in the development of diabetic complications. *Horm Res*. 2000;53(2):53-67. Epub 2000/09/06.
59. Ziyadeh FN. Mediators of Diabetic Renal Disease: The Case for TGF- $\beta$  as the Major Mediator. *Journal of the American Society of Nephrology*. 2004;15(1 suppl):S55-S7.
60. Tervaert TWC, Mooyaart AL, Amann K, Cohen AH, Cook HT, Drachenberg CB, et al. Pathologic Classification of Diabetic Nephropathy. *Journal of the American Society of Nephrology*. 2010;21(4):556-63.
61. Maezawa Y, Takemoto M, Yokote K. Cell biology of diabetic nephropathy: Roles of endothelial cells, tubulointerstitial cells and podocytes. *Journal of diabetes investigation*. 2015;6(1):3-15.
62. Qian Y, Feldman E, Pennathur S, Kretzler M, Brosius FC. Mechanisms of Glomerulosclerosis in Diabetic Nephropathy. *Diabetes*. 2008;57(6):1439-45.
63. Tamaki K, Okuda S, Ando T, Iwamoto T, Nakayama M, Fujishima M. TGF- $\beta$ 1 in glomerulosclerosis and interstitial fibrosis of adriamycin nephropathy. *Kidney Int*. 1994;45(2):525-36. Epub 1994/02/01.
64. Kamata T, Muso E, Yashiro M, Kawamura T, Oyama A, Matsushima H, et al. Up-regulation of glomerular extracellular matrix and transforming growth factor- $\beta$  expression in RF/J mice. *Kidney Int*. 1999;55(3):864-76. Epub 1999/02/23.
65. Schnaper HW, Hayashida T, Hubchak SC, Poncelet AC. TGF- $\beta$  signal transduction and mesangial cell fibrogenesis. *Am J Physiol Renal Physiol*. 2003;284(2):F243-52. Epub 2003/01/17.
66. Herman-Edelstein M, Thomas MC, Thallas-Bonke V, Saleem M, Cooper ME, Kantharidis P. Dedifferentiation of Immortalized Human Podocytes in Response to Transforming Growth Factor- $\beta$ : A Model for Diabetic Podocytopathy. *Diabetes*. 2011;60(6):1779-88.
67. Schiffer M, Bitzer M, Roberts ISD, Kopp JB, Dijke P, Mundel P, et al. Apoptosis in podocytes induced by TGF-beta and Smad7. *Journal of Clinical Investigation*. 2001;108(6):807-16.

68. Das R, Xu S, Quan X, Nguyen TT, Kong ID, Chung CH, et al. Upregulation of mitochondrial Nox4 mediates TGF- $\beta$ -induced apoptosis in cultured mouse podocytes. *Am J Physiol Renal Physiol*. 2014;306(2):F155-67. Epub 2013/11/22.
69. Datta K, Li J, Karumanchi SA, Wang E, Rondeau E, Mukhopadhyay D. Regulation of vascular permeability factor/vascular endothelial growth factor (VPF/VEGF-A) expression in podocytes. *Kidney Int*. 2004;66(4):1471-8.
70. Gerber H-P, McMurtrey A, Kowalski J, Yan M, Keyt BA, Dixit V, et al. Vascular Endothelial Growth Factor Regulates Endothelial Cell Survival through the Phosphatidylinositol 3'-Kinase/Akt Signal Transduction Pathway: REQUIREMENT FOR Flk-1/KDR ACTIVATION. *J Biol Chem*. 1998;273(46):30336-43.
71. Li Y, Kang YS, Dai C, Kiss LP, Wen X, Liu Y. Epithelial-to-mesenchymal transition is a potential pathway leading to podocyte dysfunction and proteinuria. *Am J Pathol*. 2008;172(2):299-308. Epub 2008/01/19.
72. Sam R, Wanna L, Gudehithlu KP, Garber SL, Dunea G, Arruda JAL, et al. Glomerular epithelial cells transform to myofibroblasts: early but not late removal of TGF- $\beta$ 1 reverses transformation. *Translational Research*. 2006;148(3):142-8.
73. Zeisberg EM, Potenta SE, Sugimoto H, Zeisberg M, Kalluri R. Fibroblasts in Kidney Fibrosis Emerge via Endothelial-to-Mesenchymal Transition. *J Am Soc Nephrol*. 2008;19(12):2282-7.
74. Wolf G, Schroeder R, Zahner G, Stahl RA, Shankland SJ. High glucose-induced hypertrophy of mesangial cells requires p27(Kip1), an inhibitor of cyclin-dependent kinases. *Am J Pathol*. 2001;158(3):1091-100. Epub 2001/03/10.
75. Monkawa T, Hiromura K, Wolf G, Shankland SJ. The Hypertrophic Effect of Transforming Growth Factor- $\beta$  is Reduced in the Absence of Cyclin-Dependent Kinase-Inhibitors p21 and p27. *J Am Soc Nephrol*. 2002;13(5):1172-8.
76. Cortes P, Zhao X, Riser BL, Narins RG. Role of glomerular mechanical strain in the pathogenesis of diabetic nephropathy. *Kidney Int*. 1997;51(1):57-68.
77. Eddy AA. Overview of the cellular and molecular basis of kidney fibrosis. *Kidney International Supplements*. 2014;4(1):2-8.
78. Liu Y. Cellular and molecular mechanisms of renal fibrosis. *Nat Rev Nephrol*. 2011;7(12):684-96.
79. Christ M, McCartney-Francis NL, Kulkarni AB, Ward JM, Mizel DE, Mackall CL, et al. Immune dysregulation in TGF- $\beta$ 1-deficient mice. *J Immunol*. 1994;153(5):1936-46.

80. Sanjabi S, Zenewicz LA, Kamanaka M, Flavell RA. Anti- and Pro-inflammatory Roles of TGF- $\beta$ , IL-10, and IL-22 In Immunity and Autoimmunity. *Curr Opin Pharmacol*. 2009;9(4):447-53.
81. Huang HC, Preisig PA. G1 kinases and transforming growth factor-beta signaling are associated with a growth pattern switch in diabetes-induced renal growth. *Kidney Int*. 2000;58(1):162-72. Epub 2000/07/08.
82. Deng A, Munger KA, Valdivielso JM, Satriano J, Lortie M, Blantz RC, et al. Increased expression of ornithine decarboxylase in distal tubules of early diabetic rat kidneys: are polyamines paracrine hypertrophic factors? *Diabetes*. 2003;52(5):1235-9. Epub 2003/04/30.
83. Fujita H, Omori S, Ishikura K, Hida M, Awazu M. ERK and p38 mediate high-glucose-induced hypertrophy and TGF- $\beta$  expression in renal tubular cells. *Am J Physiol Renal Physiol*. 2004;286(1):F120-6. Epub 2003/09/04.
84. Meier M, Park JK, Overheu D, Kirsch T, Lindschau C, Gueler F, et al. Deletion of protein kinase C-beta isoform in vivo reduces renal hypertrophy but not albuminuria in the streptozotocin-induced diabetic mouse model. *Diabetes*. 2007;56(2):346-54. Epub 2007/01/30.
85. Chen S, Hoffman BB, Lee JS, Kasama Y, Jim B, Kopp JB, et al. Cultured tubule cells from TGF-beta1 null mice exhibit impaired hypertrophy and fibronectin expression in high glucose. *Kidney Int*. 2004;65(4):1191-204. Epub 2004/04/17.
86. Feehally J, Floege J, Johnson RJ. *Comprehensive clinical nephrology*. Journal of Renal Care. 2008.
87. Sharma K, Ziyadeh FN. Hyperglycemia and diabetic kidney disease. The case for transforming growth factor-beta as a key mediator. *Diabetes*. 1995;44(10):1139-46. Epub 1995/10/01.
88. Lee HS, Song CY. Differential role of mesangial cells and podocytes in TGF-beta-induced mesangial matrix synthesis in chronic glomerular disease. *Histol Histopathol*. 2009;24(7):901-8. Epub 2009/05/29.
89. Zeisberg M, Hanai J, Sugimoto H, Mammoto T, Charytan D, Strutz F, et al. BMP-7 counteracts TGF-1-induced epithelial-to-mesenchymal transition and reverses chronic renal injury. *Nature Medicine*. 2003;9(7):964-8.
90. Lan R, Geng H, Polichnowski AJ, Singha PK, Saikumar P, McEwen DG, et al. PTEN loss defines a TGF- $\beta$ -induced tubule phenotype of failed differentiation and JNK signaling during renal fibrosis. *Am J Physiol Renal Physiol*. 2012;302(9):F1210-23. Epub 2012/02/04.

91. Phanish MK, Heidebrecht F, Nabi ME, Shah N, Niculescu-Duvaz I, Dockrell ME. The Regulation of TGF $\beta$ 1 Induced Fibronectin EDA Exon Alternative Splicing in Human Renal Proximal Tubule Epithelial Cells. *J Cell Physiol*. 2015;230(2):286-95. Epub 2014/06/26.
92. Kohan M, Muro AF, White ES, Berkman N. EDA-containing cellular fibronectin induces fibroblast differentiation through binding to  $\alpha$ 4 $\beta$ 7 integrin receptor and MAPK/Erk 1/2-dependent signaling. *FASEB J*. 2010;24(11):4503-12. Epub 2010/07/21.
93. Serini G, Bochaton-Piallat M-L, Ropraz P, Geinoz A, Borsi L, Zardi L, et al. The Fibronectin Domain ED-A Is Crucial for Myofibroblastic Phenotype Induction by Transforming Growth Factor- $\beta$ 1. *J Cell Biol*. 1998;142(3):873-81.
94. Qi W, Chen X, Polhill TS, Sumual S, Twigg S, Gilbert RE, et al. TGF- $\beta$ 1 induces IL-8 and MCP-1 through a connective tissue growth factor-independent pathway. *Am J Physiol Renal Physiol*. 2006;290(3):F703-9. Epub 2005/10/06.
95. Kanasaki K, Taduri G, Koya D. Diabetic nephropathy: the role of inflammation in fibroblast activation and kidney fibrosis. *Front Endocrinol*. 2013;4:7.
96. Dienz O, Rincon M. The effects of IL-6 on CD4 T cell responses. *Clin Immunol*. 2009;130(1):27-33.
97. Gentle ME, Shi S, Daehn I, Zhang T, Qi H, Yu L, et al. Epithelial cell TGF $\beta$  signaling induces acute tubular injury and interstitial inflammation. *J Am Soc Nephrol*. 2013;24(5):787-99. Epub 2013/03/30.
98. Massagué J. TGF $\beta$  in Cancer. *Cell*. 2008;134(2):215-30.
99. Padua D, Massague J. Roles of TGF $\beta$  in metastasis. *Cell Res*. 2009;19(1):89-102.
100. Lebrun J-J. The Dual Role of TGF in Human Cancer: From Tumor Suppression to Cancer Metastasis. *ISRN Molecular Biology*. 2012;2012:28.
101. Zeisberg M, Hanai J, Sugimoto H, Mammoto T, Charytan D, Strutz F, et al. BMP-7 counteracts TGF- $\beta$ 1-induced epithelial-to-mesenchymal transition and reverses chronic renal injury. *Nat Med*. 2003;9(7):964-8.
102. Wang S, Hirschberg R. BMP7 antagonizes TGF- $\beta$  -dependent fibrogenesis in mesangial cells. *Am J Physiol Renal Physiol*. 2003;284(5):F1006-13.
103. Luo DD, Phillips A, Fraser D. Bone morphogenetic protein-7 inhibits proximal tubular epithelial cell Smad3 signaling via increased SnoN expression. *Am J Pathol*. 2010;176(3):1139-47.
104. Crescenzo R, Bianco F, Mazzoli A, Giacco A, Liverini G, Iossa S. Mitochondrial efficiency and insulin resistance. *Front Physiol*. 2014;5:512.

105. Vallon V, Platt KA, Cunard R, Schroth J, Whaley J, Thomson SC, et al. SGLT2 mediates glucose reabsorption in the early proximal tubule. *J Am Soc Nephrol*. 2011;22(1):104-12. Epub 2010/07/10.
106. Balen D, Ljubojevic M, Breljak D, Brzica H, Zlender V, Koepsell H, et al. Revised immunolocalization of the Na<sup>+</sup>-D-glucose cotransporter SGLT1 in rat organs with an improved antibody. *Am J Physiol Cell Physiol*. 2008;295(2):C475-89. Epub 2008/06/06.
107. Scrutton MC, Utter MF. The regulation of glycolysis and gluconeogenesis in animal tissues. *Annu Rev Biochem*. 1968;37(1):249-302.
108. Spector AA. Plasma lipid transport. *Clin Physiol Biochem*. 1984;2(2-3):123-34. Epub 1984/01/01.
109. Christensen EI, Gburek J. Protein reabsorption in renal proximal tubule-function and dysfunction in kidney pathophysiology. *Pediatr Nephrol*. 2004;19(7):714-21. Epub 2004/05/18.
110. Brière J-J, Favier J, Gimenez-Roqueplo A-P, Rustin P. Tricarboxylic acid cycle dysfunction as a cause of human diseases and tumor formation. *Am J Physiol Cell Physiol*. 2006;291(6):C1114-C20.
111. Brand Martin D, Nicholls David G. Assessing mitochondrial dysfunction in cells. *Biochem J*. 2011;435(Pt 2):297-312.
112. Hosler JP, Ferguson-Miller S, Mills DA. Energy transduction: proton transfer through the respiratory complexes. *Annu Rev Biochem*. 2006;75:165-87. Epub 2006/06/08.
113. Lenaz G, Fato R, Genova ML, Bergamini C, Bianchi C, Biondi A. Mitochondrial Complex I: structural and functional aspects. *Biochim Biophys Acta*. 2006;1757(9-10):1406-20. Epub 2006/07/11.
114. Yankovskaya V, Horsefield R, Tornroth S, Luna-Chavez C, Miyoshi H, Leger C, et al. Architecture of succinate dehydrogenase and reactive oxygen species generation. *Science*. 2003;299(5607):700-4. Epub 2003/02/01.
115. Quinlan CL, Orr AL, Perevoshchikova IV, Treberg JR, Ackrell BA, Brand MD. Mitochondrial complex II can generate reactive oxygen species at high rates in both the forward and reverse reactions. *J Biol Chem*. 2012;287(32):27255-64. Epub 2012/06/13.
116. Liu Y, Fiskum G, Schubert D. Generation of reactive oxygen species by the mitochondrial electron transport chain. *J Neurochem*. 2002;80(5):780-7. Epub 2002/04/12.
117. Jastroch M, Divakaruni AS, Mookerjee S, Treberg JR, Brand MD. Mitochondrial proton and electron leaks. *Essays Biochem*. 2010;47:53-67.

118. Gredilla R, Phaneuf S, Selman C, Kendaiah S, Leeuwenburgh C, Barja G. Short-term caloric restriction and sites of oxygen radical generation in kidney and skeletal muscle mitochondria. *Ann N Y Acad Sci.* 2004;1019:333-42. Epub 2004/07/13.
119. Poburko D, Santo-Domingo J, Demaurex N. Dynamic Regulation of the Mitochondrial Proton Gradient during Cytosolic Calcium Elevations. *J Biol Chem.* 2011;286(13):11672-84.
120. Boyer PD. The ATP synthase--a splendid molecular machine. *Annu Rev Biochem.* 1997;66:717-49. Epub 1997/01/01.
121. Rousset S, Alves-Guerra M-C, Mozo J, Miroux B, Cassard-Doulicier A-M, Bouillaud F, et al. The Biology of Mitochondrial Uncoupling Proteins. *Diabetes.* 2004;53(suppl 1):S130-S5.
122. Tsuchiya K, Wang W, Giebisch G, Welling PA. ATP is a coupling modulator of parallel Na,K-ATPase-K-channel activity in the renal proximal tubule. *Proc Natl Acad Sci U S A.* 1992;89(14):6418-22.
123. Wang X, Armando I, Upadhyay K, Pascua A, Jose PA. The regulation of proximal tubular salt transport in hypertension: an update. *Curr Opin Nephrol Hypertens.* 2009;18(5):412-20. Epub 2009/08/06.
124. Higgins GC, Coughlan MT. Mitochondrial dysfunction and mitophagy: the beginning and end to diabetic nephropathy? *Br J Pharmacol.* 2014;171(8):1917-42. Epub 2014/04/12.
125. Czajka A, Ajaz S, Gnudi L, Parsade CK, Jones P, Reid F, et al. Altered Mitochondrial Function, Mitochondrial DNA and Reduced Metabolic Flexibility in Patients With Diabetic Nephropathy. *EBioMedicine.* 2015;2(6):499-512.
126. Vallon V. The proximal tubule in the pathophysiology of the diabetic kidney. *American Journal of Physiology - Regulatory, Integrative and Comparative Physiology.* 2011;300(5):R1009-R22.
127. Sedeek M, Nasrallah R, Touyz RM, Hébert RL. NADPH Oxidases, Reactive Oxygen Species, and the Kidney: Friend and Foe. *J Am Soc Nephrol.* 2013;24(10):1512-8.
128. Bretón-Romero R, Lamas S. Hydrogen peroxide signaling in vascular endothelial cells. *Redox Biology.* 2014;2:529-34.
129. Guo S, Chen X. The human Nox4: gene, structure, physiological function and pathological significance. *J Drug Target.* 2015;23(10):888-96. Epub 2015/05/08.
130. Nisimoto Y, Diebold BA, Cosentino-Gomes D, Lambeth JD. Nox4: a hydrogen peroxide-generating oxygen sensor. *Biochemistry.* 2014;53(31):5111-20. Epub 2014/07/26.

131. Carmona-Cuenca I, Roncero C, Sancho P, Caja L, Fausto N, Fernandez M, et al. Upregulation of the NADPH oxidase NOX4 by TGF- $\beta$  in hepatocytes is required for its pro-apoptotic activity. *J Hepatol.* 2008;49(6):965-76. Epub 2008/10/11.
132. Griendling KK, Sorescu D, Ushio-Fukai M. NAD(P)H oxidase: role in cardiovascular biology and disease. *Circ Res.* 2000;86(5):494-501. Epub 2000/03/17.
133. Amara N, Goven D, Prost F, Muloway R, Crestani B, Boczkowski J. NOX4/NADPH oxidase expression is increased in pulmonary fibroblasts from patients with idiopathic pulmonary fibrosis and mediates TGF $\beta$ 1-induced fibroblast differentiation into myofibroblasts. *Thorax.* 2010;65(8):733-8. Epub 2010/08/06.
134. Heid ME, Keyel PA, Kanga C, Shiva S, Watkins SC, Salter RD. Mitochondrial reactive oxygen species induces NLRP3-dependent lysosomal damage and inflammasome activation. *J Immunol.* 2013;191(10):5230-8. Epub 2013/10/04.
135. Navarro-González JF, Mora-Fernández C. The Role of Inflammatory Cytokines in Diabetic Nephropathy. *Journal of the American Society of Nephrology.* 2008;19(3):433-42.
136. Brezniceanu M-L, Liu F, Wei C-C, Chénier I, Godin N, Zhang S-L, et al. Attenuation of Interstitial Fibrosis and Tubular Apoptosis in db/db Transgenic Mice Overexpressing Catalase in Renal Proximal Tubular Cells. *Diabetes.* 2008;57(2):451-9.
137. Brezniceanu ML, Lau CJ, Godin N, Chenier I, Duclos A, Ethier J, et al. Reactive oxygen species promote caspase-12 expression and tubular apoptosis in diabetic nephropathy. *J Am Soc Nephrol.* 2010;21(6):943-54. Epub 2010/03/20.
138. Estaquier J, Vallette F, Vayssiere JL, Mignotte B. The mitochondrial pathways of apoptosis. *Adv Exp Med Biol.* 2012;942:157-83. Epub 2012/03/09.
139. Stukalin EB, Kolomeisky AB. ATP Hydrolysis Stimulates Large Length Fluctuations in Single Actin Filaments. *Biophys J.* 2006;90(8):2673-85.
140. Acloque H, Adams MS, Fishwick K, Bronner-Fraser M, Nieto MA. Epithelial-mesenchymal transitions: the importance of changing cell state in development and disease. *The Journal of clinical investigation.* 2009;119(6):1438.
141. Hollenberg NK, Stevanovic R, Agarwal A, Lansang MC, Price DA, Laffel LM, et al. Plasma aldosterone concentration in the patient with diabetes mellitus. *Kidney Int.* 2004;65(4):1435-9. Epub 2004/04/17.
142. Yuan Y, Chen Y, Zhang P, Huang S, Zhu C, Ding G, et al. Mitochondrial dysfunction accounts for aldosterone-induced epithelial-to-mesenchymal transition of renal proximal tubular epithelial cells. *Free Radic Biol Med.* 2012;53(1):30-43.

143. Pang L, Qiu T, Cao X, Wan M. Apoptotic role of TGF- $\beta$  mediated by Smad4 mitochondria translocation and cytochrome c oxidase subunit II interaction. *Exp Cell Res*. 2011;317(11):1608-20. Epub 2011/02/18.
144. Abe Y, Sakairi T, Beeson C, Kopp JB. TGF- $\beta$ 1 stimulates mitochondrial oxidative phosphorylation and generation of reactive oxygen species in cultured mouse podocytes, mediated in part by the mTOR pathway. *Am J Physiol Renal Physiol*. 2013;305(10):F1477-90. Epub 2013/09/21.
145. Jain M, Rivera S, Monclus EA, Synenki L, Zirk A, Eisenbart J, et al. Mitochondrial Reactive Oxygen Species Regulate Transforming Growth Factor- $\beta$  Signaling. *J Biol Chem*. 2013;288(2):770-7.
146. Patel AS, Song JW, Chu SG, Mizumura K, Osorio JC, Shi Y, et al. Epithelial Cell Mitochondrial Dysfunction and PINK1 Are Induced by Transforming Growth Factor- $\beta$ 1 in Pulmonary Fibrosis. *PLoS One*. 2015;10(3):e0121246.
147. Das S, Ferlito M, Kent OA, Fox-Talbot K, Wang R, Liu D, et al. Nuclear miRNA regulates the mitochondrial genome in the heart. *Circ Res*. 2012;110(12):1596-603. Epub 2012/04/21.
148. Colleoni F, Padmanabhan N, Yung HW, Watson ED, Cetin I, Tissot van Patot MC, et al. Suppression of mitochondrial electron transport chain function in the hypoxic human placenta: a role for miRNA-210 and protein synthesis inhibition. *PLoS One*. 2013;8(1):e55194. Epub 2013/02/06.
149. Baseler WA, Thapa D, Jagannathan R, Dabkowski ER, Croston TL, Hollander JM. miR-141 as a regulator of the mitochondrial phosphate carrier (Slc25a3) in the type 1 diabetic heart. *Am J Physiol Cell Physiol*. 2012;303(12):C1244-51. Epub 2012/10/05.
150. Ye Q, Zhao X, Xu K, Li Q, Cheng J, Gao Y, et al. Polymorphisms in lipid metabolism related miRNA binding sites and risk of metabolic syndrome. *Gene*. 2013;528(2):132-8. Epub 2013/08/06.
151. Civelek M, Hagopian R, Pan C, Che N, Yang WP, Kayne PS, et al. Genetic regulation of human adipose microRNA expression and its consequences for metabolic traits. *Hum Mol Genet*. 2013;22(15):3023-37. Epub 2013/04/09.
152. Mohamed JS, Hajira A, Pardo PS, Boriek AM. MicroRNA-149 inhibits PARP-2 and promotes mitochondrial biogenesis via SIRT-1/PGC-1 $\alpha$  network in skeletal muscle. *Diabetes*. 2014;63(5):1546-59. Epub 2014/04/24.

153. Fu Y, Zhang Y, Wang Z, Wang L, Wei X, Zhang B, et al. Regulation of NADPH oxidase activity is associated with miRNA-25-mediated NOX4 expression in experimental diabetic nephropathy. *Am J Nephrol*. 2010;32(6):581-9. Epub 2010/11/13.
154. Lee EA, Seo JY, Jiang Z, Yu MR, Kwon MK, Ha H, et al. Reactive oxygen species mediate high glucose-induced plasminogen activator inhibitor-1 up-regulation in mesangial cells and in diabetic kidney. *Kidney Int*. 2005;67(5):1762-71.
155. Jiang L, Qiu W, Zhou Y, Wen P, Fang L, Cao H, et al. A microRNA-30e/mitochondrial uncoupling protein 2 axis mediates TGF- $\beta$ 1-induced tubular epithelial cell extracellular matrix production and kidney fibrosis. *Kidney Int*. 2013;84(2):285-96.
156. Schulze-Lohoff E, Hugo C, Rost S, Arnold S, Gruber A, Brüne B, et al. Extracellular ATP causes apoptosis and necrosis of cultured mesangial cells via P2Z/P2X7 receptors. *American Journal of Physiology - Renal Physiology*. 1998;275(6):F962-F71.
157. Dheda K, Huggett JF, Bustin SA, Johnson MA, Rook G, Zumla A. Validation of housekeeping genes for normalizing RNA expression in real-time PCR. *Biotechniques*. 2004;37(1):112-4.
158. Dobin A, Davis CA, Schlesinger F, Drenkow J, Zaleski C, Jha S, et al. STAR: ultrafast universal RNA-seq aligner. *Bioinformatics*. 2013;29(1):15-21.
159. Liao Y, Smyth GK, Shi W. featureCounts: an efficient general purpose program for assigning sequence reads to genomic features. *Bioinformatics*. 2014;30(7):923-30.
160. Robinson MD, McCarthy DJ, Smyth GK. edgeR: a Bioconductor package for differential expression analysis of digital gene expression data. *Bioinformatics*. 2010;26:139-40.
161. Team RC. R: A language and environment for statistical computing. R Foundation for Statistical Computing, Vienna, Austria. URL <http://www.R-project.org/>. 2015.
162. Wickham H, Francois R. dplyr: A Grammar of Data Manipulation. 2015; R package version 0.4.2:[Available from: <http://CRAN.R-project.org/package=dplyr>].
163. Luo W, Friedman MS, Shedden K, Hankenson KD, Woolf PJ. GAGE: generally applicable gene set enrichment for pathway analysis. *BMC Bioinformatics*. 2009;10(161):1471-2105.
164. Luo W. gageData: Auxillary data for gage package. 2013; R package version 2.6.0:[Available from: <http://bioconductor.org/packages/release/data/experiment/html/gageData.html>].

165. Diaz D, Draghici S. mirIntegrator: Integrating microRNA expression into signalling pathways for pathway analysis. 2015; R package version 1.1.0:[Available from: <http://vortex.cs.wayne.edu/>].
166. Carlson M. org.Mm.eg.db: Genome wide annotation for Mouse. 2015; R package version 3.1.2:[Available from: <http://bioconductor.org/packages/release/data/annotation/html/org.Mm.eg.db.html>].
167. Carlson M. org.Rn.eg.db: Genome wide annotation for Rat. 2015; R package version 3.1.2:[Available from: <http://bioconductor.org/packages/release/data/annotation/html/org.Rn.eg.db.html>].
168. Luo W, Brouwer C. Pathview: an R/Bioconductor package for pathway-based data integration and visualization. *Bioinformatics*. 2013.
169. Wickham H. The Split-Apply-Combine Strategy for Data Analysis. *J Stat Softw*. 2011;40(1):29. Epub 2011-04-07.
170. Voichita C, Draghici S. ROntoTools: R Onto-Tools suite. 2015; R package version 1.9.1:[Available from: <https://www.bioconductor.org/packages/release/bioc/html/ROntoTools.html>].
171. Gagolewski M, Tartanus B. R package stringi: Character string processing facilities. 2015; R package version 0.5-5:[Available from: <http://stringi.rexamine.com/>].
172. Dronavalli S, Duka I, Bakris GL. The pathogenesis of diabetic nephropathy. *Nat Clin Pract End Met*. 2008;4(8):444-52.
173. Wang J, Gao Y, Ma M, Li M, Zou D, Yang J, et al. Effect of miR-21 on Renal Fibrosis by Regulating MMP-9 and TIMP1 in kk-ay Diabetic Nephropathy Mice. *Cell Biochem Biophys*. 2013:1-10.
174. Liu G, Friggeri A, Yang Y, Milosevic J, Ding Q, Thannickal VJ, et al. miR-21 mediates fibrogenic activation of pulmonary fibroblasts and lung fibrosis. *J Exp Med*. 2010;207(8):1589-97.
175. Cottonham CL, Kaneko S, Xu L. miR-21 and miR-31 converge on TIAM1 to regulate migration and invasion of colon carcinoma cells. *Journal of Biological Chemistry*. 2010;285(46):35293.
176. Gomez IG, MacKenna DA, Johnson BG, Kaimal V, Roach AM, Ren S, et al. Anti-microRNA-21 oligonucleotides prevent Alport nephropathy progression by stimulating metabolic pathways. *The Journal of Clinical Investigation*. 2015;125(1):141-56.

177. Glowacki F, Savary G, Gnemmi V, Buob D, Van der Hauwaert C, Lo-Guidice JM, et al. Increased circulating miR-21 levels are associated with kidney fibrosis. *PLoS ONE*. 2013;8(2):e58014. Epub 2013/03/08.
178. Tu H, Sun H, Lin Y, Ding J, Nan K, Li Z, et al. Oxidative stress upregulates PDCD4 expression in patients with gastric cancer via miR-21. *Curr Pharm Des*. 2014;20(11):1917-23.
179. Akhurst RJ, Hata A. Targeting the TGF[ $\beta$ ] signalling pathway in disease. *Nat Rev Drug Discov*. 2012;11(10):790-811.
180. McCarthy DJ, Chen Y, Smyth GK. Differential expression analysis of multifactor RNA-Seq experiments with respect to biological variation. *Nucleic Acids Research*. 2012.
181. Weiner ID, Mitch WE, Sands JM. Urea and Ammonia Metabolism and the Control of Renal Nitrogen Excretion. *Clinical Journal of the American Society of Nephrology*. 2014.
182. Wolf G. Molecular Mechanisms of Diabetic Mesangial Cell Hypertrophy: A Proliferation of Novel Factors. *Journal of the American Society of Nephrology*. 2002;13(10):2611-3.
183. Pohlers D, Brenmoehl J, Löffler I, Müller CK, Leipner C, Schultze-Mosgau S, et al. TGF- $\beta$  and fibrosis in different organs — molecular pathway imprints. *Biochimica et Biophysica Acta (BBA) - Molecular Basis of Disease*. 2009;1792(8):746-56.
184. Gérard C, Goldbeter A. The balance between cell cycle arrest and cell proliferation: control by the extracellular matrix and by contact inhibition. *Interface Focus*. 2014;4(3).
185. Dalla Vestra M, Saller A, Mauer M, Fioretto P. Role of mesangial expansion in the pathogenesis of diabetic nephropathy. *Journal of nephrology*. 2001;14:S51.
186. Patel K, Harding P, Haney LB, Glass WF, 2nd. Regulation of the mesangial cell myofibroblast phenotype by actin polymerization. *J Cell Physiol*. 2003;195(3):435-45.
187. Boron WF. Acid-Base Transport by the Renal Proximal Tubule. *Journal of the American Society of Nephrology*. 2006;17(9):2368-82.
188. Buschhausen L, Seibold S, Gross O, Matthaeus T, Weber M, Schulze-Lohoff E. Regulation of mesangial cell function by vasodilatory signaling molecules. *Cardiovasc Res*. 2001;51(3):463-9.
189. Dalla Vestra M, Saller A, Mauer M, Fioretto P. Role of mesangial expansion in the pathogenesis of diabetic nephropathy. *J Nephrol*. 2001;14(4):S51-7.
190. Zeisberg M, Duffield JS. Resolved: EMT Produces Fibroblasts in the Kidney. *Journal of the American Society of Nephrology*. 2010;21(8):1247-53.
191. Zoja C, Morigi M, Remuzzi G. Proteinuria and Phenotypic Change of Proximal Tubular Cells. *Journal of the American Society of Nephrology*. 2003;14(suppl 1):S36-S41.

192. Kim S-Y, Volsky DJ. PAGE: Parametric Analysis of Gene Set Enrichment. *BMC Bioinformatics*. 2005;6:144-.
193. Yoon YS, Lee JH, Hwang SC, Choi KS, Yoon G. TGF beta1 induces prolonged mitochondrial ROS generation through decreased complex IV activity with senescent arrest in Mv1Lu cells. *Oncogene*. 2005;24(11):1895-903.
194. Noris M, Remuzzi G. Overview of Complement Activation and Regulation. *Seminars in Nephrology*. 2013;33(6):479-92.
195. Mudaliar H, Pollock C, Komala MG, Chadban S, Wu H, Panchapakesan U. The role of Toll-like receptor proteins (TLR) 2 and 4 in mediating inflammation in proximal tubules. *Am J Physiol Renal Physiol*. 2013;305(2):10.
196. Lamouille S, Xu J, Derynck R. Molecular mechanisms of epithelial–mesenchymal transition. *Nat Rev Mol Cell Biol*. 2014;15(3):178-96.
197. Simonson MS. Phenotypic transitions and fibrosis in diabetic nephropathy. *Kidney Int*. 2007;71(9):846-54.
198. Ghayur MN, Krepinsky JC, Janssen LJ. Contractility of the renal glomerulus and mesangial cells: Lingering doubts and strategies for the future. *Medical hypotheses and research: MHR*. 2008;4(1):1.
199. Endlich N, Endlich K. The challenge and response of podocytes to glomerular hypertension. *Semin Nephrol*. 2012;32(4):327-41.
200. Lee LK, Meyer TW, Pollock AS, Lovett DH. Endothelial cell injury initiates glomerular sclerosis in the rat remnant kidney. *Journal of Clinical Investigation*. 1995;96(2):953-64.
201. Bell SP, Dutta A. DNA replication in eukaryotic cells. *Annual review of biochemistry*. 2002;71(1):333-74.
202. Martinez E. Multi-protein complexes in eukaryotic gene transcription. *Plant molecular biology*. 2002;50(6):925-47.
203. Nouws J, Nijtmans LG, Smeitink JA, Vogel RO. Assembly factors as a new class of disease genes for mitochondrial complex I deficiency: cause, pathology and treatment options. *Brain*. 2012;135(Pt 1):12-22.
204. Murphy Michael P. How mitochondria produce reactive oxygen species. *Biochemical Journal*. 2009;417(Pt 1):1-13.
205. Liang J, Slingerland JM. Multiple roles of the PI3K/PKB (Akt) pathway in cell cycle progression. *Cell Cycle*. 2003;2(4):339-45.

206. Shaw PH. The role of p53 in cell cycle regulation. *Pathol Res Pract*. 1996;192(7):669-75.
207. Johnson RJ, Floege J, Yoshimura A, Iida H, Couser WG, Alpers CE. The activated mesangial cell: a glomerular "myofibroblast"? *J Am Soc Nephrol*. 1992;2(10 Suppl):S190-7.
208. Curthoys NP, Moe OW. Proximal Tubule Function and Response to Acidosis. *Clinical Journal of the American Society of Nephrology*. 2014;9(9):1627-38.
209. Brennan EP, Morine MJ, Walsh DW, Roxburgh SA, Lindenmeyer MT, Brazil DP, et al. Next-generation sequencing identifies TGF-beta1-associated gene expression profiles in renal epithelial cells reiterated in human diabetic nephropathy. *Biochim Biophys Acta*. 2012;1822(4):589-99. Epub 2012/01/24.
210. Thannickal VJ, Lee DY, White ES, Cui Z, Larios JM, Chacon R, et al. Myofibroblast Differentiation by Transforming Growth Factor- $\beta$ 1 Is Dependent on Cell Adhesion and Integrin Signaling via Focal Adhesion Kinase. *Journal of Biological Chemistry*. 2003;278(14):12384-9.
211. Dong C, Gongora R, Sosulski ML, Luo F, Sanchez CG. Regulation of transforming growth factor-beta1 (TGF- $\beta$ 1)-induced pro-fibrotic activities by circadian clock gene BMAL1. *Respiratory Research*. 2016;17(1):1-17.
212. D'Souza RC, Knittle AM, Nagaraj N, van Dinther M, Choudhary C, ten Dijke P, et al. Time-resolved dissection of early phosphoproteome and ensuing proteome changes in response to TGF- $\beta$ . *Sci Signal*. 2014;7(335):2004856.
213. McClelland A, Hagiwara S, Kantharidis P. Where are we in diabetic nephropathy: microRNAs and biomarkers? *Curr Opin Nephrol Hypertens*. 2014;23(1):80-6.
214. Uchino K, Takeshita F, Takahashi R-u, Kosaka N, Fujiwara K, Naruoka H, et al. Therapeutic Effects of MicroRNA-582-5p and -3p on the Inhibition of Bladder Cancer Progression. *Mol Ther*. 2013.
215. Aure MR, Jernstrom S, Krohn M, Vollan HK, Due EU, Rodland E, et al. Integrated analysis reveals microRNA networks coordinately expressed with key proteins in breast cancer. *Genome Med*. 2015;7(1):21. Epub 2015/04/16.
216. Xu YY, Wu HJ, Ma HD, Xu LP, Huo Y, Yin LR. MicroRNA-503 suppresses proliferation and cell-cycle progression of endometrioid endometrial cancer by negatively regulating cyclin D1. *FEBS J*. 2013;280(16):3768-79. Epub 2013/06/05.
217. Ambros V, Bartel B, Bartel DP, Burge CB, Carrington JC, Chen X, et al. A uniform system for microRNA annotation. *RNA*. 2003;9(3):277-9.

218. Bartel D. MicroRNAs: genomics, biogenesis, mechanism, and function. *Cell*. 2004;116(2):281 - 97.
219. Babak T, Zhang WEN, Morris Q, Blencowe BJ, Hughes TR. Probing microRNAs with microarrays: Tissue specificity and functional inference. *RNA*. 2004;10(11):1813-9.
220. McClelland AD, Herman-Edelstein M, Komers R, Jha JC, Winbanks CE, Hagiwara S, et al. miR-21 promotes renal fibrosis in diabetic nephropathy by targeting PTEN and SMAD7. *Clin Sci*. 2015;28.
221. Wang B, Jha JC, Hagiwara S, McClelland AD, Jandeleit-Dahm K, Thomas MC, et al. Transforming growth factor- $\beta$ 1-mediated renal fibrosis is dependent on the regulation of transforming growth factor receptor 1 expression by let-7b. *Kidney Int*. 2014;85(2):352-61. Epub 2013/10/04.
222. Wang B, Komers R, Carew R, Winbanks CE, Xu B, Herman-Edelstein M, et al. Suppression of microRNA-29 expression by TGF- $\beta$ 1 promotes collagen expression and renal fibrosis. *Journal of the American Society of Nephrology*. 2012;23(2):252-65.
223. Diaz D, Draghici S. mirIntegrator: Integrating microRNA expression into signaling pathways for pathway analysis. 2015; R package version 0.99.5:[Available from: <http://vortex.cs.wayne.edu/>].
224. Nakajima H, Takenaka M, Kaimori J-Y, Hamano T, Iwatani H, Sugaya T, et al. Activation of the Signal Transducer and Activator of Transcription Signaling Pathway in Renal Proximal Tubular Cells by Albumin. *Journal of the American Society of Nephrology*. 2004;15(2):276-85.
225. Gould SE, Day M, Jones SS, Dorai H. BMP-7 regulates chemokine, cytokine, and hemodynamic gene expression in proximal tubule cells. *Kidney Int*. 2002;61(1):51-60.
226. Chen J, Harris RC. Interaction of the EGF Receptor and the Hippo Pathway in the Diabetic Kidney. *J Am Soc Nephrol*. 2015;9:2015040415.
227. Gentleman R, Whalen E, Huber W, Falcon S. graph: A package to handle graph data structures. 2015; R package version 1.47.2:[Available from: <https://www.bioconductor.org/packages/release/bioc/html/graph.html>].
228. Hansen KD, Gentry J, Long L, Gentleman R, Falcon S, Hahne F, et al. Rgraphviz: Provides plotting capabilities for R graph objects. 2015; R package version 2.13.0:[Available from: <http://bioconductor.org/packages/release/bioc/html/Rgraphviz.html>].
229. Voichita C, Donato M, Draghici S, editors. Incorporating Gene Significance in the Impact Analysis of Signaling Pathways. *Machine Learning and Applications (ICMLA), 2012 11th International Conference on; 2012 12-15 Dec. 2012*.

230. Butz H, Racz K, Hunyady L, Patocs A. Crosstalk between TGF-beta signaling and the microRNA machinery. *Trends Pharmacol Sci.* 2012;33(7):382-93.
231. Kato M. TGF-[beta]-induced signaling circuit loops mediated by microRNAs as new therapeutic targets for renal fibrosis[quest]. *Kidney Int.* 2013;84(6):1067-9.
232. Lewis BP, Burge CB, Bartel DP. Conserved Seed Pairing, Often Flanked by Adenosines, Indicates that Thousands of Human Genes are MicroRNA Targets. *Cell.* 2005;120(1):15-20.
233. McClelland AD, Kantharidis P. microRNA in the development of diabetic complications. *Clinical Science.* 2014;126(2):95-110.
234. Tarca AL, Draghici S, Khatri P, Hassan SS, Mittal P, Kim J-s, et al. A novel signaling pathway impact analysis. *Bioinformatics.* 2009;25(1):75-82.
235. Subramanian A, Tamayo P, Mootha VK, Mukherjee S, Ebert BL, Gillette MA, et al. Gene set enrichment analysis: A knowledge-based approach for interpreting genome-wide expression profiles. *Proceedings of the National Academy of Sciences.* 2005;102(43):15545-50.
236. Drăghici S, Khatri P, Martins RP, Ostermeier GC, Krawetz SA. Global functional profiling of gene expression. *Genomics.* 2003;81(2):98-104.
237. Bakin AV, Tomlinson AK, Bhowmick NA, Moses HL, Arteaga CL. Phosphatidylinositol 3-Kinase Function Is Required for Transforming Growth Factor  $\beta$ -mediated Epithelial to Mesenchymal Transition and Cell Migration. *Journal of Biological Chemistry.* 2000;275(47):36803-10.
238. Kato M, Yuan H, Xu Z-G, Lanting L, Li S-L, Wang M, et al. Role of the Akt/FoxO3a Pathway in TGF- $\beta$ 1-Mediated Mesangial Cell Dysfunction: A Novel Mechanism Related to Diabetic Kidney Disease. *Journal of the American Society of Nephrology.* 2006;17(12):3325-35.
239. Boor P, Ostendorf T, Floege J. PDGF and the progression of renal disease. *Nephrology Dialysis Transplantation.* 2014;29(suppl 1):i45-i54.
240. Mason RM. Connective tissue growth factor(CCN2), a pathogenic factor in diabetic nephropathy. What does it do? How does it do it? *Journal of Cell Communication and Signaling.* 2009;3(2):95-104.
241. Cao Y, Baig MR, Hamm LL, Wu K, Simon EE. Growth factors stimulate kidney proximal tubule cell migration independent of augmented tyrosine phosphorylation of focal adhesion kinase. *Biochem Biophys Res Commun.* 2005;328(2):560-6.
242. Giancotti FG, Ruoslahti E. Integrin Signaling. *Science.* 1999;285(5430):1028-33.

243. Zhang MZ, Zhang MY, Zhao S, Duan JZ, Zhang YQ, Zuo CX, et al. [Effect of JAK/STAT pathway activation on high glucose-induced transdifferentiation in renal proximal tubular epithelial cells]. *Zhongguo Yi Xue Ke Xue Yuan Xue Bao*. 2007;29(3):364-9.
244. Ying Y, Kim J, Westphal SN, Long KE, Padanilam BJ. Targeted deletion of p53 in the proximal tubule prevents ischemic renal injury. *J Am Soc Nephrol*. 2014;25(12):2707-16.
245. Kitada K, Nakano D, Ohsaki H, Hitomi H, Minamino T, Yatabe J, et al. Hyperglycemia causes cellular senescence via a SGLT2- and p21-dependent pathway in proximal tubules in the early stage of diabetic nephropathy. *Journal of diabetes and its complications*. 2014;28(5):604-11.
246. Guo B, Koya D, Isono M, Sugimoto T, Kashiwagi A, Haneda M. Peroxisome Proliferator-Activated Receptor- $\gamma$  Ligands Inhibit TGF- $\beta$ 1-Induced Fibronectin Expression in Glomerular Mesangial Cells. *Diabetes*. 2004;53(1):200-8.
247. Lin CL, Wang JY, Huang YT, Kuo YH, Surendran K, Wang FS. Wnt/beta-catenin signaling modulates survival of high glucose-stressed mesangial cells. *J Am Soc Nephrol*. 2006;17(10):2812-20.
248. Dijksterhuis JP, Petersen J, Schulte G. WNT/Frizzled signalling: receptor-ligand selectivity with focus on FZD-G protein signalling and its physiological relevance: IUPHAR Review 3. *Br J Pharmacol*. 2014;171(5):1195-209. Epub 2013/09/17.
249. Wang B, Koh P, Winbanks C, Coughlan MT, McClelland A, Watson A, et al. miR-200a Prevents Renal Fibrogenesis Through Repression of TGF- $\beta$ 2 Expression. *Diabetes*. 2011;60(1):280-7.
250. Patel V, Nouredine L. MicroRNAs and fibrosis. *Curr Opin Nephrol Hypertens*. 2012;21(4):410-6.
251. Fang Y, Yu X, Liu Y, Kriegel AJ, Heng Y, Xu X, et al. miR-29c is downregulated in renal interstitial fibrosis in humans and rats and restored by HIF $\alpha$  activation. *American Journal of Physiology - Renal Physiology*. 2013;304(10):F1274-F82.
252. Liu Y, Taylor NE, Lu L, Usa K, Cowley AW, Ferreri NR, et al. Renal medullary MicroRNAs in dahl salt-sensitive rats: MiR-29b regulates several collagens and related genes. *Hypertension*. 2010;55(4):974-82.
253. Carthew RW, Sontheimer EJ. Origins and mechanisms of miRNAs and siRNAs. *Cell*. 2009;136(4):642-55.
254. Fabian MR, Sonenberg N, Filipowicz W. Regulation of mRNA translation and stability by microRNAs. *Annual review of biochemistry*. 2010;79:351-79.

255. Chi SW, Zang JB, Mele A, Darnell RB. Ago HITS-CLIP decodes miRNA-mRNA interaction maps. *Nature*. 2009;460(7254):479-86.
256. Helwak A, Kudla G, Dudnakova T, Tollervey D. Mapping the Human miRNA Interactome by CLASH Reveals Frequent Noncanonical Binding. *Cell*. 2013;153(3):654-65.
257. Barski A, Cuddapah S, Cui K, Roh TY, Schones DE, Wang Z, et al. High-resolution profiling of histone methylations in the human genome. *Cell*. 2007;129(4):823-37.
258. Wang B, Komers R, Carew RM, Winbanks CE, Xu B, Herman-Edelstein M, et al. microRNA-29 is a regulator of collagen expression in renal fibrosis. *JASN*. 2011;in press.
259. Brennan EP, Nolan KA, Børgesen E, Gough OS, McEvoy CM, Docherty NG, et al. Lipoxins Attenuate Renal Fibrosis by Inducing let-7c and Suppressing TGFβ1. *Journal of the American Society of Nephrology*. 2013;24(4):627-37.
260. Douglas AP, Vance DR, Kenny EM, Morris DW, Maxwell AP, McKnight AJ. Next-generation sequencing of the mitochondrial genome and association with IgA nephropathy in a renal transplant population. *Sci Rep*. 2014;4:7379.
261. Hagiwara M, Yamagata K, Capaldi RA, Koyama A. Mitochondrial dysfunction in focal segmental glomerulosclerosis of puromycin aminonucleoside nephrosis. *Kidney Int*. 2006;69(7):1146-52. Epub 2006/04/13.
262. Parcellier A, Tintignac LA, Zhuravleva E, Hemmings BA. PKB and the mitochondria: AKTing on apoptosis. *Cellular Signalling*. 2008;20(1):21-30.
263. Gomez B, Jr., Robinson NC. Phospholipase digestion of bound cardiolipin reversibly inactivates bovine cytochrome bc1. *Biochemistry*. 1999;38(28):9031-8.
264. Brownlee M. The Pathobiology of Diabetic Complications: A Unifying Mechanism. *Diabetes*. 2005;54(6):1615-25.
265. Korshunov SS, Skulachev VP, Starkov AA. High protonic potential actuates a mechanism of production of reactive oxygen species in mitochondria. *FEBS Letters*. 1997;416(1):15-8.
266. Das S, Bedja D, Campbell N, Dunkerly B, Chenna V, Maitra A, et al. miR-181c Regulates the Mitochondrial Genome, Bioenergetics, and Propensity for Heart Failure *In Vivo*. *PLoS ONE*. 2014;9(5):e96820.
267. Das S, Ferlito M, Kent OA, Fox-Talbot K, Wang R, Liu D, et al. Nuclear miRNA Regulates the Mitochondrial Genome in the Heart. *Circulation research*. 2012;110(12):1596-603.
268. Amara N, Goven D, Prost F, Muloway R, Crestani B, Boczkowski J. NOX4/NADPH oxidase expression is increased in pulmonary fibroblasts from patients with idiopathic

- pulmonary fibrosis and mediates TGF- $\beta$ 1-induced fibroblast differentiation into myofibroblasts. *Thorax*. 2010;65(8):733-8.
269. Wei C, Li L, Kim IK, Sun P, Gupta S. NF- $\kappa$ B mediated miR-21 regulation in cardiomyocytes apoptosis under oxidative stress. *Free Radical Research*. 2014;48(3):282-91.
270. Fleissner F, Jazbutyte V, Fiedler J, Gupta SK, Yin X, Xu Q, et al. Short Communication: Asymmetric Dimethylarginine Impairs Angiogenic Progenitor Cell Function in Patients With Coronary Artery Disease Through a MicroRNA-21-Dependent Mechanism. *Circulation research*. 2010;107(1):138-43.
271. Fukao T, Kamijo K, Osumi T, Fujiki Y, Yamaguchi S, Orii T, et al. Molecular cloning and nucleotide sequence of cDNA encoding the entire precursor of rat mitochondrial acetoacetyl-CoA thiolase. *J Biochem*. 1989;106(2):197-204. Epub 1989/08/01.
272. Bergstrom JD, Wong GA, Edwards PA, Edmond J. The regulation of acetoacetyl-CoA synthetase activity by modulators of cholesterol synthesis in vivo and the utilization of acetoacetate for cholesterologenesis. *J Biol Chem*. 1984;259(23):14548-53. Epub 1984/12/10.
273. Fan J, Shan C, Kang H-B, Elf S, Xie J, Tucker M, et al. Tyr-phosphorylation of PDP1 toggles recruitment between ACAT1 and SIRT3 to regulate pyruvate dehydrogenase complex. *Molecular cell*. 2014;53(4):534-48.
274. Jastroch M, Divakaruni AS, Mookerjee S, Treberg JR, Brand MD. Mitochondrial proton and electron leaks. *Essays Biochem*. 2010;47:53-67. Epub 2010/06/11.
275. Hamada M, Sumida M, Okuda H, Watanabe T, Nojima M, Kuby SA. Adenosine triphosphate-adenosine-5'-monophosphate phosphotransferase from normal human liver mitochondria. Isolation, chemical properties, and immunochemical comparison with Duchenne dystrophic serum aberrant adenylate kinase. *J Biol Chem*. 1982;257(21):13120-8. Epub 1982/11/10.
276. Burkart A, Shi X, Chouinard M, Corvera S. Adenylate kinase 2 links mitochondrial energy metabolism to the induction of the unfolded protein response. *J Biol Chem*. 2011;286(6):4081-9. Epub 2010/09/30.
277. Six E, Lagresle-Peyrou C, Susini S, De Chappedelaine C, Sigrist N, Sadek H, et al. AK2 deficiency compromises the mitochondrial energy metabolism required for differentiation of human neutrophil and lymphoid lineages. *Cell Death Dis*. 2015;6:e1856.
278. Wang Z-G, White PS, Ackerman SH. Atp11p and Atp12p Are Assembly Factors for the F1-ATPase in Human Mitochondria. *J Biol Chem*. 2001;276(33):30773-8.

279. Frank M, Duvezin-Caubet S, Koob S, Occhipinti A, Jagasia R, Petcherski A, et al. Mitophagy is triggered by mild oxidative stress in a mitochondrial fission dependent manner. *Biochim Biophys Acta*. 2012;1823(12):2297-310.
280. Brooks C, Wei Q, Feng L, Dong G, Tao Y, Mei L, et al. Bak regulates mitochondrial morphology and pathology during apoptosis by interacting with mitofusins. *Proc Natl Acad Sci U S A*. 2007;104(28):11649-54.
281. Shi L, Chen J, Yang J, Pan T, Zhang S, Wang Z. MiR-21 protected human glioblastoma U87MG cells from chemotherapeutic drug temozolomide induced apoptosis by decreasing Bax/Bcl-2 ratio and caspase-3 activity. *Brain Res*. 2010;1352:255-64. Epub 2010/07/17.
282. Sayed D, He M, Hong C, Gao S, Rane S, Yang Z, et al. MicroRNA-21 Is a Downstream Effector of AKT That Mediates Its Antiapoptotic Effects via Suppression of Fas Ligand. *Journal of Biological Chemistry*. 2010;285(26):20281-90.
283. Han M, Liu M, Wang Y, Chen X, Xu J, Sun Y, et al. Antagonism of miR-21 Reverses Epithelial-Mesenchymal Transition and Cancer Stem Cell Phenotype through AKT/ERK1/2 Inactivation by Targeting PTEN. *PloS one*. 2012;7(6):e39520.
284. Kantharidis P, Wang B, Carew RM, Lan HY. Diabetes complications: The microRNA perspective. *Diabetes*. 2011;60(7):1832-7.
285. Ardekani AM, Naeini MM. The Role of MicroRNAs in Human Diseases. *Avicenna J Med Biotechnol*. 2010;2(4):161-79.
286. Rahmatallah Y, Emmert-Streib F, Glazko G. Gene set analysis approaches for RNA-seq data: performance evaluation and application guideline. *Brief Bioinform*. 2015.
287. Irizarry RA, Wang C, Zhou Y, Speed TP. Gene Set Enrichment Analysis Made Simple. *Stat Methods Med Res*. 2009;18(6):565-75.
288. Hausser J, Zavolan M. Identification and consequences of miRNA-target interactions - beyond repression of gene expression. *Nat Rev Genet*. 2014;15(9):599-612.
289. Morcos M, Sayed AAR, Bierhaus A, Yard B, Waldherr R, Merz W, et al. Activation of Tubular Epithelial Cells in Diabetic Nephropathy. *Diabetes*. 2002;51(12):3532-44.
290. Honjo Y, Bian Y, Kawakami K, Molinolo A, Longenecker G, Boppana R, et al. TGF- $\beta$  receptor I conditional knockout mice develop spontaneous squamous cell carcinoma. *Cell Cycle*. 2007;6(11):1360-6. Epub 2007/05/31.
291. Letterio JJ, Böttinger EP. TGF- $\beta$  Knockout and Dominant-Negative Receptor Transgenic Mice. *Miner Electrolyte Metab*. 1998;24(2-3):161-7.

292. Van Rooij E, Olson EN. Searching for miR-acles in cardiac fibrosis. *Circulation research*. 2009;104(2):138-40.
293. Godwin JG, Ge X, Stephan K, Jurisch A, Tullius SG, Iacomini J. Identification of a microRNA signature of renal ischemia reperfusion injury. *Proceedings of the National Academy of Sciences, USA*. 2010;107(32):14339-44.
294. Dey N, Das F, Mariappan MM, Mandal CC, Ghosh-Choudhury N, Kasinath BS, et al. MicroRNA-21 Orchestrates High Glucose-induced Signals to TOR Complex 1, Resulting in Renal Cell Pathology in Diabetes. *Journal of Biological Chemistry*. 2011;286(29):25586-603.
295. Lai JY, Luo J, O'Connor C, Jing X, Nair V, Ju W, et al. MicroRNA-21 in Glomerular Injury. *Journal of the American Society of Nephrology*. 2014.
296. Thum T, Gross C, Fiedler J, Fischer T, Kissler S, Bussen M, et al. MicroRNA-21 contributes to myocardial disease by stimulating MAP kinase signalling in fibroblasts. *Nature*. 2008;456(7224):980-4.
297. Li Q, Zhang D, Wang Y, Sun P, Hou X, Lerner J, et al. MiR-21/Smad 7 signaling determines TGF-beta1-induced CAF formation. *Sci Rep*. 2013;3(2038):2038. Epub 2013/06/21.
298. Wei J, Feng L, Li Z, Xu G, Fan X. MicroRNA-21 activates hepatic stellate cells via PTEN/Akt signaling. *Biomed Pharmacother*. 2013;67(5):387-92.
299. Song B, Wang C, Liu J, Wang X, Lv L, Wei L, et al. MicroRNA-21 regulates breast cancer invasion partly by targeting tissue inhibitor of metalloproteinase 3 expression. *J Exp Clin Cancer Res*. 2010;29:29. Epub 2010/03/30.
300. Lu TX, Munitz A, Rothenberg ME. MicroRNA-21 is up-regulated in allergic airway inflammation and regulates IL-12p35 expression. *J Immunol*. 2009;182(8):4994-5002. Epub 2009/04/04.
301. Fukao T, Yamaguchi S, Orii T, Hashimoto T. Molecular basis of  $\beta$ -ketothiolase deficiency: Mutations and polymorphisms in the human mitochondrial acetoacetyl-coenzyme a thiolase gene. *Hum Mutat*. 1995;5(2):113-20.
302. Fukao DT.  $\beta$ -ketothiolase deficiency. *Orphanet encyclopedia*; 2004; Available from: <https://www.orpha.net/data/patho/GB/uk-T2.pdf>.
303. Pannicke U, Honig M, Hess I, Friesen C, Holzmann K, Rump E-M, et al. Reticular dysgenesis (aleukocytosis) is caused by mutations in the gene encoding mitochondrial adenylate kinase 2. *Nat Genet*. 2009;41(1):101-5.